



**HAL**  
open science

## Nickel mediated negishi and oxidative couplings

Alexia Ohleier

► **To cite this version:**

Alexia Ohleier. Nickel mediated negishi and oxidative couplings. Coordination chemistry. Université Paul Sabatier - Toulouse III, 2017. English. NNT : 2017TOU30074 . tel-01831630

**HAL Id: tel-01831630**

**<https://theses.hal.science/tel-01831630v1>**

Submitted on 6 Jul 2018

**HAL** is a multi-disciplinary open access archive for the deposit and dissemination of scientific research documents, whether they are published or not. The documents may come from teaching and research institutions in France or abroad, or from public or private research centers.

L'archive ouverte pluridisciplinaire **HAL**, est destinée au dépôt et à la diffusion de documents scientifiques de niveau recherche, publiés ou non, émanant des établissements d'enseignement et de recherche français ou étrangers, des laboratoires publics ou privés.



# THÈSE

En vue de l'obtention du

## DOCTORAT DE L'UNIVERSITÉ DE TOULOUSE

Délivré par :

Université Toulouse 3 Paul Sabatier (UT3 Paul Sabatier)

---

**Présentée et soutenue par :**

**Alexia OHLEIER**

**le** mardi 14 mars 2017

**Titre :**

Nickel Mediated Negishi and Oxidative Couplings

---

**École doctorale et discipline ou spécialité :**

ED SDM : Chimie organométallique de coordination - CO 043

**Unité de recherche :**

Laboratoire Hétérochimie Fondamentale et Appliquée - UMR-CNRS 5069

**Directeur/trice(s) de Thèse :**

Nicolas MEZAILLES, Directeur de Recherche C.N.R.S. à Toulouse

Noel NEBRA MUNIZ, Chargé de Recherche C.N.R.S. à Toulouse

**Jury :**

Stéphane BELLEMIN-LAPONNAZ, Directeur de Recherche C.N.R.S. à Strasbourg

María Amor RODRIGUEZ IGLESIAS, Profesor Titular de Investigación à Sevilla

Sylviane SABO-ETIENNE, Directrice de Recherche C.N.R.S. à Toulouse





# THÈSE

En vue de l'obtention du

## DOCTORAT DE L'UNIVERSITÉ DE TOULOUSE

Délivré par :

Université Toulouse 3 Paul Sabatier (UT3 Paul Sabatier)

---

**Présentée et soutenue par :**

**Alexia OHLEIER**

**le** mardi 14 mars 2017

**Titre :**

Nickel Mediated Negishi and Oxidative Couplings

---

**École doctorale et discipline ou spécialité :**

ED SDM : Chimie organométallique de coordination - CO 043

**Unité de recherche :**

Laboratoire Hétérochimie Fondamentale et Appliquée - UMR-CNRS 5069

**Directeur/trice(s) de Thèse :**

Nicolas MEZAILLES, Directeur de Recherche C.N.R.S. à Toulouse

Noel NEBRA MUNIZ, Chargé de Recherche C.N.R.S. à Toulouse

**Jury :**

Stéphane BELLEMIN-LAPONNAZ, Directeur de Recherche C.N.R.S. à Strasbourg

María Amor RODRIGUEZ IGLESIAS, Profesor Titular de Investigación à Sevilla

Sylviane SABO-ETIENNE, Directrice de Recherche C.N.R.S. à Toulouse



*A ma famille*



*Les seules choses qui existent sont celles auxquelles,  
à un moment ou à un autre, on a décidé de croire.*

*Philippe Forest*





# Remerciements

Je remercie tout d'abord le directeur de recherche Stéphane Bellemin-Lapponnaz et la Dr. María Amor Rodríguez Iglesias d'avoir accepté de juger ce travail de recherche. Je remercie également la directrice de recherche Sylviane Sabo-Etienne pour sa participation au jury de thèse.

Je remercie Nicolas, qui m'a accueillie dans son équipe et m'a donné l'opportunité de préparer une thèse. Je tiens aussi à remercier Noël, qui avec Nicolas, a accepté de diriger cette thèse. A tous deux, ils ont grandement contribué à élargir mes connaissances théoriques en chimie organométallique et techniques au laboratoire. Je remercie également Marie, pour ses explications concises et ses bons conseils. C'était agréable de travailler dans un groupe avec des thématiques variées et une grande richesse d'idées nouvelles.

Je remercie la région Midi-Pyrénées d'avoir fourni le financement de cette thèse.

Je remercie Nathalie, Sonia et Rémi pour leur travail très rigoureux et les nombreuses structures RX résolues. Ensuite, je remercie Caroline Toppan, Pierre Lavedan, Marc Vedrenne et Stéphane Massou du service RMN pour la programmation et l'acquisition de nombreux spectres RMN ainsi que pour les simulations de spectres. De plus, je remercie Lionel Rechinat pour les mesures de RPE et Christian pour la spectrométrie de masse MALDI et ses conseils au sujet de l'utilisation de la GC-MS et du spectromètre IR. Je remercie également Isabelle pour son aide avec les boîtes à gants ainsi que pour ses connaissances et son équipement pour les réactions sous pression. Finalement, je remercie Dominique Stein pour la synthèse des précurseurs de carbènes.

Je tiens également à remercier Maryse et Sérah pour leur excellent travail administratif et Olivier pour s'assurer du bon fonctionnement du laboratoire avec bonne humeur.

Je remercie Benoît Champin, Paul-Louis Fabre, Olivier Reynes, David Lafarge et Emilie Beugin, que j'ai rencontré à l'IUT Mesures Physiques, et avec qui j'ai effectué le service d'enseignement dans de très bonnes conditions et dans une bonne ambiance.

Je remercie ensuite l'ensemble du personnel du LHFA, toujours très sympathique et avec qui il a été très agréable de travailler pendant trois ans. Je remercie Marta, Laura, Antonio, Tatsuya, Amos, Natalia, Isabel, Marianna, María, Abdallah, Raphaël, Morelia, Alfredo, Sytze, Franck, Nicolas, Alexandre, Julian, Noemi et Sophie pour de nombreux bons moments au laboratoire et parfois en ville.

Je remercie tout particulièrement les membres de l'équipe SHEN et surtout Koyel, Florian, Sébastien, Anthony, Sam, Pilár et Anthony (2) pour la bonne humeur, parfois légèrement bruyante au bureau, et des moments mémorables et inoubliables. Sans vous, je n'aurais pas survécu à ces trois années!

Je remercie également ma famille pour son soutien tout au long de mes études et de cette thèse.

---

# Table of Contents

Table of contents.....	I
List of abbreviations.....	VII
General remarks.....	1
<b>Nickel catalyzed Negishi cross coupling reactions</b>	
1 State of the art .....	7
1.1 Palladium catalyzed C <sub>sp2</sub> -C <sub>sp2</sub> Negishi Cross Couplings.....	7
1.1.1 Advantages of Negishi cross coupling reactions.....	7
1.1.2 Advances in palladium catalyzed C <sub>sp2</sub> -C <sub>sp2</sub> Negishi cross couplings.....	8
1.2 Nickel catalyzed C <sub>sp2</sub> -C <sub>sp2</sub> Negishi cross couplings.....	10
1.2.1 Advantages and challenges of nickel chemistry.....	10
1.2.2 Advances in nickel catalyzed C <sub>sp2</sub> -C <sub>sp2</sub> Negishi cross couplings.....	11
1.2.3 Mechanisms of nickel catalyzed Negishi cross-couplings.....	14
1.3 Research objectives.....	19
1.4 References.....	21
2 (Bis-phosphine)nickel-catalyzed Negishi cross coupling.....	25
2.1 Synthesis of precatalyst [(dcpp)nickel(toluene)] <b>II-4</b> .....	25
2.1.1 Synthesis of Ni(II) precursor [(dcpp)NiCl <sub>2</sub> ] <b>II-3</b> .....	25
2.1.2 Synthesis of Ni(0) complex [(dcpp)Ni(toluene)] <b>II-4</b> .....	26
2.2 Negishi cross coupling.....	29
2.2.1 Testing [(dcpp)Ni(toluene)] <b>II-4</b> in Negishi cross coupling.....	29
2.2.2 Reaction scope.....	30
2.3 Mechanistic investigations.....	32
2.3.1 Stoichiometric reactions.....	32
2.3.1.1 Oxidative addition.....	33
2.3.1.2 Transmetalation and reductive elimination.....	35
2.3.1.3 Synthesis and reactivity of Ni(I) complex [(dcpp)NiCl] <sub>2</sub> <b>II-16</b> .....	35
2.3.2 Catalytic activity of Ni(0), Ni(I) and Ni(II) precursors.....	38
2.3.3 Proposed catalytic cycle.....	40
2.4 DFT calculations.....	41

---

2.4.1 Coordination of chlorobenzene.....	42
2.4.2 Catalytic process.....	43
2.4.3 Product to reagent exchange.....	45
2.5 Conclusion and perspectives.....	47
2.6 Experimental part.....	49
2.6.1 General remarks.....	49
2.6.2 Synthesis of the dcpp ligand <b>II-1</b> .....	49
2.6.3 Synthesis of (dcpp)nickel complexes.....	50
2.6.3.1. Synthesis of [(dcpp)NiCl <sub>2</sub> ] <b>II-3</b> .....	50
2.6.3.2 Synthesis of [(dcpp)Ni(toluene)] <b>II-4</b> .....	50
2.6.3.3 Synthesis of [(dcpp)Ni(Ph)(Cl)] <b>II-14</b> .....	51
2.6.3.4 Synthesis of [(dcpp)NiCl] <sub>2</sub> <b>II-16</b> .....	52
2.6.4 Negishi cross coupling.....	52
2.6.4.1 Synthesis of PhZnCl.LiCl <b>II-8</b> .....	52
2.6.4.2 General procedure for Negishi cross coupling.....	52
2.7 References	54
 <b>Activation of CO<sub>2</sub> with chelating (bis-phosphine) nickel complexes</b>	
3 Functionalization of CO <sub>2</sub> towards acrylates.....	59
3.1 The economic challenges of CO <sub>2</sub> .....	59
3.1.1 CO <sub>2</sub> from waste to resource.....	59
3.1.2 Thermodynamic and kinetic stability of CO <sub>2</sub> .....	59
3.1.3 Industrial production of chemicals from CO <sub>2</sub> .....	60
3.1.4 Design of new reactions involving CO <sub>2</sub> .....	61
3.2. Towards the formation of acrylates from ethylene and CO <sub>2</sub> .....	62
3.2.1 Synthesis of nickelalactones.....	62
3.2.1.1 Oxidative coupling between ethylene and CO <sub>2</sub> .....	62
3.2.1.1 Alternative synthesis of nickelalactones.....	63
3.2.2 Stoichiometric production of acrylates .....	64
3.2.2.1 Theoretical investigations and first reports of β hydride elimi- nations.....	64
3.2.2.2 Cleavage of nickelalactones by strong electrophiles.....	66
3.2.2.3 Cleavage of nickelalactones by bases.....	71
3.2.3 Catalytic production of acrylates.....	72

## Table of Contents

3.3 Research objectives.....	74
3.4 References	78
4 Functionalization of CO <sub>2</sub> with boranes.....	83
4.1 Synthesis of [(dcpp)Ni(C <sub>2</sub> H <sub>4</sub> )] <b>IV-3</b> and [(dcpp)nickelalactone] <b>IV-4</b> .....	83
4.1.1 Synthesis of [(dcpp)Ni(C <sub>2</sub> H <sub>4</sub> )] <b>IV-3</b> .....	83
4.1.2 Synthesis of [(dcpp)nickelalactone] <b>IV-4</b> .....	84
4.2 Kinetic Study.....	86
4.3 Reactivity between [(dcpp)nickel]-complexes and boranes.....	91
4.3.1 Choosing an appropriate borane.....	91
4.3.2 Reactivity between [(dcpp)nickelalactone] <b>IV-4</b> and pinacolborane <b>IV-8</b> .....	92
4.4 Mechanistic investigations.....	97
4.4.1 Cleavage of [(dcpp)nickelalactone] <b>IV-4</b> through pinacolborane <b>IV-8</b> ...	97
4.4.2 Reduction of propanoic acid pinacolborane ester <b>IV-14</b> through a metal hydride.....	98
4.4.3 Reduction of propanoic acid pinacolborane ester through oxidative addition.....	100
4.4.4 Reduction of propanoic acid pinacolborane ester <b>IV-14</b> through Ni(I) intermediates .....	104
4.5 Stepwise catalytic cycle.....	106
4.6 Catalysis.....	107
4.7 Conclusion.....	112
4.8 Experimental part.....	114
4.8.1 General Remarks.....	114
4.8.2 Synthesis of organic products.....	114
4.8.2.1 Synthesis of the dcpp ligand <b>IV-1</b> .....	114
4.8.2.2 Synthesis of propoxypinacolborane <b>IV-11</b> .....	115
4.8.2.3 Synthesis of propanoic acid pinacolborane ester <b>IV-14</b> .....	115
4.8.3 Synthesis of [(dcpp)-nickel]-complexes.....	116
4.8.3.1 Synthesis of [(tmeda)nickelalactone] <b>IV-5</b> .....	116
4.8.3.2 Synthesis of [(dcpp)Ni(C <sub>2</sub> H <sub>4</sub> )] <b>IV-3</b> .....	117
4.8.3.3 Synthesis of (dcpp)nickelalactone <b>IV-4</b> .....	117
4.8.4 Description of typical reaction set-ups.....	119

---

4.8.4.1 Kinetic experiments.....	119
4.8.4.2 Reaction between [(dcpp)nickelalactone] <b>IV-4</b> and pinacolborane <b>IV-8</b> .....	119
4.8.4.3 Catalysis.....	119
4.9 References.....	121
5 Functionalization of CO <sub>2</sub> with aluminium derivatives.....	127
5.1 Stoichiometric synthesis of propanoic acid derivatives.....	127
5.1.1 Blank reactions.....	127
5.1.2 Reactivity of triethylaluminium <b>V-3</b> and tri( <i>n</i> -butyl)aluminium <b>V-5</b> .....	128
5.1.3 Preliminary DFT calculations.....	131
5.1.4 Reactivity of tri( <i>tert</i> -butyl)aluminium <b>V-8</b> .....	132
5.2 Preliminary catalytic investigations.....	137
5.3 Conclusion and perspectives.....	138
5.4 Experimental part.....	139
5.4.1 General Remarks.....	139
5.4.2 Synthesis of trialkylaluminium derivatives.....	139
5.4.2.1 Synthesis of Al( <i>n</i> Bu) <sub>3</sub> .Et <sub>2</sub> O <b>V-5</b> .....	139
5.4.2.2 Synthesis of Al( <i>t</i> Bu) <sub>3</sub> .Et <sub>2</sub> O <b>V-8</b> .....	140
5.4.3 Synthesis of diethylaluminium propanoate <b>V-4</b> .....	140
5.4.4 Blank tests.....	141
5.4.4.1 Reacting AlEt <sub>3</sub> <b>V-3</b> with CO <sub>2</sub> in [d <sub>8</sub> ]-THF.....	141
5.4.4.2 Reacting AlEt <sub>3</sub> <b>V-3</b> with [(dcpp)Ni(C <sub>2</sub> H <sub>4</sub> )] <b>V-2</b> in [d <sub>8</sub> ]-THF.....	141
5.4.4 Stoichiometric Reactions.....	141
5.4.4.1 Reacting [(dcpp)nickelalactone] <b>V-1</b> with AlEt <sub>3</sub> <b>V-3</b> in [d <sub>8</sub> ]-THF.....	141
5.4.4.2 Reacting <sup>13</sup> C[(dcpp)nickelalactone] <b>V-1</b> ( <sup>13</sup> C) in neat AlEt <sub>3</sub> <b>V-3</b> ..	141
5.4.4.3 Reacting <sup>13</sup> C[(dcpp)nickelalactone] <b>V-1</b> ( <sup>13</sup> C) with Al( <i>n</i> Bu) <sub>3</sub> .Et <sub>2</sub> O <b>V-5</b> in [d <sub>8</sub> ]-THF.....	142
5.4.4.4 Reacting <sup>13</sup> C[(dcpp)nickelalactone] <b>V-1</b> ( <sup>13</sup> C) with Al( <i>t</i> Bu) <sub>3</sub> .Et <sub>2</sub> O <b>V-8</b> in [d <sub>8</sub> ]-THF.....	142
5.4.4.5 Reacting [(dcpp)nickelalactone] <b>V-1</b> in neat Al( <i>t</i> Bu) <sub>3</sub> .Et <sub>2</sub> O <b>V-8</b> ...	143
5.5 References.....	144

**Activation of CO<sub>2</sub> with chelating bis-carbene nickel complexes**

6 Synthesis and reactivity of (bis-NHC)nickel complexes.....	147
6.1 State of the art.....	147
6.1.1 <i>N</i> -heterocyclic carbenes.....	147
6.1.2 Chelating (bis-NHC)nickel complexes.....	148
6.1.2.1 Chelating [(bis-NHC)nickel(II)] complexes.....	148
6.1.2.2 Chelating [(bis-NHC)Ni(0)] complexes.....	150
6.1.3 Research objectives.....	151
6.2 Synthesis of [(bis-NHC)Ni(alkene)] and [(bis-NHC)Ni (alkyne)] complexes..	152
6.2.1 Synthesis of bis-NHC precursors.....	153
6.2.2 Synthesis of [(bis-NHC)Ni(alkene)] complexes.....	154
6.2.3 Synthesis of [(bis-NHC)Ni(alkyne)] complexes.....	156
6.3 Ligand substitution reactions.....	158
6.3.1 Relative stability of unsaturated [(bis-NHC)Ni]-complexes.....	158
6.3.2 Synthesis of [(bis-NHC)Ni(CO) <sub>2</sub> ] complexes.....	159
6.4 Synthesis and reactivity of [(bis-NHC)nickelalactones].....	160
6.4.1 Synthesis of [(bis-NHC)nickelalactones] through ligand substitution.....	160
6.4.2 Synthesis of [(bis-NHC)nickelalactones] through oxidative coupling....	165
6.4.3 Reactivity of [(bis-NHC)nickelalactones].....	167
6.5 Conclusion and perspectives.....	169
6.6 Experimental part.....	170
6.6.1 General remarks.....	170
6.6.2 Synthesis of imidazoles and corresponding imidazolium salts.....	170
6.6.2.1 <i>N</i> - <i>tert</i> -butylimidazole <b>VI-1</b> .....	170
6.6.2.2 ( <i>Lt</i> Bu)H <sub>2</sub> Br <sub>2</sub> <b>VI-5</b> .....	171
6.6.2.3 (LDipp)H <sub>2</sub> Br <sub>2</sub> <b>VI-6</b> .....	171
6.6.2.4 ( <i>Lt</i> Bu) <sup>prop</sup> H <sub>2</sub> Br <sub>2</sub> <b>VI-7</b> .....	172
6.6.3 Synthesis of [(bis-NHC)Ni(0)-alkene] and [-alkyne] complexes.....	172
6.6.3.1 [( <i>Lt</i> Bu)Ni(C <sub>2</sub> H <sub>4</sub> )] <b>VI-9</b> .....	172
6.6.3.2 [(LDipp)Ni(C <sub>2</sub> H <sub>4</sub> )] <b>VI-10</b> .....	173
6.6.3.3 [( <i>Lt</i> Bu)Ni(Ph-C≡C-Ph)] <b>VI-13</b> .....	174
6.6.3.4 [( <i>Lt</i> Bu)Ni(Ph-C≡C-H)] <b>VI-14</b> .....	174
6.6.4 Synthesis of [(bis-NHC)Ni(0)-carbonyl] complexes.....	175
6.6.4.1 [( <i>Lt</i> Bu)Ni(CO) <sub>2</sub> ] <b>VI-15</b> .....	175



6.6.4.2 [(LDipp)Ni(CO) <sub>2</sub> ] <b>VI-16</b> .....	176
6.6.5 Synthesis of [(bis-NHC)nickelalactones].....	176
6.6.5.1 [( <i>Lt</i> Bu)Ni(CH <sub>2</sub> CH <sub>2</sub> COO-κC,κO)] <b>VI-18</b> .....	176
6.6.5.2 <sup>13</sup> C[( <i>Lt</i> Bu)Ni(CH <sub>2</sub> CH <sub>2</sub> COO-κC,κO)] <b>VI-18(<sup>13</sup>C)</b> .....	177
6.6.5.3 [(LDipp)Ni(CH <sub>2</sub> CH <sub>2</sub> COO-κC,κO)] <b>VI-19</b> .....	178
6.6.5.4 [( <i>Lt</i> Bu) <sup>prop</sup> Ni(CH <sub>2</sub> CH <sub>2</sub> COO-κC,κO)] <b>VI-20</b> .....	179
6.6.5.5 [(tmeda)Ni(C(Ph)=C(Ph)COO-κC,κO)] <b>VI-21</b> .....	180
6.6.5.6 [( <i>Lt</i> Bu)Ni(C(Ph)=C(Ph)COO-κC,κO)] <b>VI-22</b> .....	180
6.7 References.....	182
<b>Appendices</b>	
7 Appendices.....	187
7.1 Crystallographic data.....	187
7.1.1 [(dcpp)NiCl <sub>2</sub> ] <b>II-3</b> .....	188
7.1.2 [(dcpp)Ni(toluene)] <b>II-4</b> .....	189
7.1.3 [(dcpp)Ni(Ph)(Cl)] <b>II-14</b> .....	190
7.1.4 [(dcpp)NiCl <sub>2</sub> ] <b>II-16</b> .....	191
7.1.5 [(dcpp)Ni(C <sub>2</sub> H <sub>4</sub> )] <b>IV-3</b> .....	192
7.1.6 [(dcpp)nickelalactone] <b>IV-4</b> .....	193
7.1.7 [(dcpp)Ni(CO) <sub>2</sub> ] <b>IV-23</b> .....	194
7.1.8 [(dcpp)Ni(1-butene)] <b>V-6</b> .....	195
7.1.9 [(dcpp)nickelalactone-Al( <i>t</i> Bu) <sub>3</sub> ] <b>V-9</b> .....	196
7.1.10 [( <i>Lt</i> Bu)Ni(C <sub>2</sub> H <sub>4</sub> )] <b>VI-9</b> .....	197
7.1.11 [( <i>Lt</i> Bu)Ni(PhC≡CPh)] <b>VI-13</b> .....	198
7.1.12 [( <i>Lt</i> Bu)Ni(PhC≡CH)] <b>VI-14</b> .....	199
7.1.13 [( <i>Lt</i> Bu)Ni(CO) <sub>2</sub> ] <b>VI-15</b> .....	200
7.1.14 [( <i>Lt</i> Bu)nickelalactone] <b>VI-18</b> .....	201
7.1.15 [( <i>Lt</i> Bu) <sup>prop</sup> nickelalactone] <b>VI-20</b> .....	202
7.1.16 [( <i>Lt</i> Bu)Ni(C(Ph)=C(Ph)C(O)O)- κC,κO] <b>VI-22</b> .....	203
7.1.17 [( <i>Lt</i> Bu)Ni(CO <sub>3</sub> )] <b>VI-28</b> .....	204
7.2 NMR simulations.....	205
7.3 Résumé de la thèse.....	207

---

## List of Abbreviations

9-BBN	9-Borabicyclo(3.3.1)nonane
Ar	Generic aryl group
BDE	Bond dissociation energy
bipy	Bipyridine
BTTP	<i>tert</i> -Butylimino-tri(pyrrolidino)phosphorane
cat	Catecholborane
cdt	1,5,9-Cyclododecatriene
COD	1,5-Cyclooctadiene
Cy	Cyclohexyl group
d.	Day
dcpe	1,2-Bis(dicyclohexylphosphino)ethane
dcpm	1,1-Bis(dicyclohexylphosphino)methane
dcpp	1,3-Bis(dicyclohexylphosphino)propane
DBU	1,8-Diazabicyclo(5.4.0)undec-7-ene
DFT	Density functional theory
Dipp	(2,6-Diisopropyl)phenyl group
DMAC	Dimethylacetamide
DME	1,2-Dimethoxyethane
dppb	1,4-Bis(diphenylphosphino)butane
dppe	1,2-Bis(diphenylphosphino)ethane
dppf	1,1'-Bis(diphenylphosphino)ferrocene
dppm	1,1-Bis(diphenylphosphino)methane
dppp	1,3-Bis(diphenylphosphino)propane
dtbpe	1,2-Bis(di- <i>tert</i> -butylphosphino)ethane

## List of Abbreviations

---

EPR	Electron paramagnetic resonance
Et	Ethyl group
Et <sub>3</sub> N	Triethylamine
EWG	Electron-withdrawing group
eq.	Equivalent
FT	Fourier transformed
h	Planck constant
h.	Hour
<i>i</i> Pr	Isopropyl
IR	Infrared
k <sub>B</sub>	Boltzmann constant
k <sub>obs</sub>	Rate constant
KO <i>t</i> Bu	Potassium <i>tert</i> -butoxide
Me	Methyl group
min.	Minute
<i>n</i> Bu	<i>n</i> -butyl group
NHC	N-heterocyclic carbene
NMR	Nuclear magnetic resonance
OTf	Triflate
Ph	Phenyl
pin	Pinacolborane
PPh <sub>3</sub>	Triphenylphosphine
py	Pyridine
R	Gas constant
RT	Room temperature

## List of Abbreviations

---

<i>s</i> Bu	<i>sec</i> -butyl
SET	Single electron transfer
<i>t</i> Bu	<i>tert</i> -butyl group
tmeda	N,N,N',N'-tetramethylethane-1,2-diamine
TOF	Turn over frequency
TS	Transition state
X	I, Br, Cl, F
XRD	X-ray diffraction



## General Remarks

The work presented in this dissertation was carried out in the Laboratoire Hétérochimie Fondamentale et Appliquée at the Université de Toulouse III - Paul Sabatier under the guidance of Dr. Nicolas Mézailles and Dr. Noël Nebra-Muñiz from January 2014 to February 2017.

The research presented in this thesis entitled “Nickel Mediated Negishi and Oxidative Couplings” aims at the formation of new C-C bonds by using chelated nickel complexes. This work is divided in two parts and consists overall of six chapters. The first part (Chapter 1 and 2) is dedicated to nickel(bis-phosphine) catalyzed Negishi cross couplings whereas the second part investigates the activation and functionalization of CO<sub>2</sub> with (bis-phosphine) and (bis-NHC)-nickel complexes (Chapter 3 - 6).

## Experimental conditions and theoretical studies

### 1. General procedures

All reactions were carried out under an atmosphere of dry argon using standard Schlenk techniques or in a nitrogen-filled MBraun LabStar glovebox. Acetonitrile, diethyl ether, THF, pentane and toluene were taken from a MBraun SPS-800 solvent purification system. Acetonitrile, methanol and water were degassed by bubbling argon and all the other solvents were degassed by using the freeze-pump-thaw procedure. [d8]-THF, C<sub>6</sub>D<sub>6</sub>, CD<sub>3</sub>CN and MeOD were degassed and stored over 4 Å molecular sieves.

The chemicals were purchased in reagent grade purity from Acros, Alfa-Aesar, Cy-tech and Sigma-Aldrich and were used without further purification. CO, CO<sub>2</sub> and ethylene were purchased from Air Liquide.

### 2. NMR spectroscopy

Solution <sup>1</sup>H, <sup>13</sup>C, <sup>11</sup>B, <sup>19</sup>F and <sup>31</sup>P NMR spectra were recorded at RT on Bruker Avance 300, 400 and 500 MHz spectrometers at the indicated frequencies. Chemical shifts (δ) are expressed in parts per million. <sup>1</sup>H and <sup>13</sup>C chemical shifts are referenced to residual solvent signals. <sup>11</sup>B, <sup>19</sup>F and <sup>31</sup>P chemical shifts are relative respectively to BF<sub>3</sub>.OEt<sub>2</sub>, CFCl<sub>3</sub> and 85 % H<sub>3</sub>PO<sub>4</sub> (aq.) external references. The following abbreviations are used: br, broad; s, singlet; d, doublet; t, triplet; quint, quintuplet; sext, sextet; sept, septuplet; m, multiplet. <sup>1</sup>H and <sup>13</sup>C resonance signals were attributed by means of 2D HSQC and HMBC experiments.

### 3. IR spectroscopy

IR spectra were recorded on a Varian 640 Fourier Transform Infrared Spectrometer.

### 4. X-ray crystallography

Crystallographic data were collected at 193(2) K on a Bruker-AXS Kappa APEX II Quazar diffractometer or on a Bruker D8-Venture Photon 100 diffractometer, with Mo K $\alpha$  radiation ( $\lambda$  = 0,71073 Å) using an oil-coated shock-cooled crystal. The crystals were selected under the

microscope using Stalke's X-Temp 2 device. <sup>[1]</sup> Phi- and omega-scans were used. Space groups were determined on the basis of systematic absences and intensity statistics. Semi-empirical absorption correction was employed. <sup>[2,3]</sup> The structures were solved by direct methods (SHELXS-97), <sup>[4]</sup> and refined using the least-squares method on F<sup>2</sup>. All non-H atoms were refined with anisotropic displacement parameters. Hydrogen atoms were refined isotropically at calculated positions using a riding model with their isotropic displacement parameters constrained to be equal to 1.5 times the equivalent isotropic displacement parameters of their pivot atoms for terminal sp<sup>3</sup> carbon and 1.2 times for all other carbon atoms.

The thermal ellipsoids determined by single crystal X-ray diffraction in this thesis are at the 50 % probability level. The following color code indicating the respective atom type in the depicted molecular structures is used throughout the manuscript: hydrogen: white, carbon: grey, nitrogen: blue, oxygen: red, phosphorus: orange, nickel: dark green, aluminium: light pink.

## 5. Theoretical calculations

Theoretical calculations were performed by Dr. Nicolas Mézailles (Toulouse) at the DFT level theory using the Gaussian 09 program package. <sup>[5]</sup> Basis sets and functionals are detailed in the respective context.

## 6. References

[1] T. Kottke, D. Stalke, *J. Appl. Crystallogr.*, **1993**, *26*, 615 - 619.

[2] Bruker, *SADABS*, Bruker AXS Inc., Madison, Wisconsin, USA, **2006**.

[3] Bruker, *SADABS*, Bruker AXS Inc., Madison, Wisconsin, USA, **2008**.

[4] G. M. Sheldrick, *Acta Crystallogr. A*, **2007**, *64*, 112 - 122.

[5] ] M. J. Frisch, G. W. Trucks, H. B. Schlegel, G. E. Scuseria, M. A. Robb, J. R. Cheeseman, G. Scalmani, V. Barone, B. Mennucci, G. A. Petersson, H. Nakatsuji, M. Caricato, X. Li, H. P. Hratchian, A. F. Izmaylov, J. Bloino, G. Zheng, J. L. Sonnenberg, M. Hada, M. Ehara, K. Toyota, R. Fukuda, J. Hasegawa, M. Ishida, T. Nakajima, Y. Honda, O. Kitao, H. Nakai, T. Vreven, J. A. Montgomery, Jr., J. E. Pearlta, F. Ogliaro, M. Bearpark, J. J. Heyd, E. Brothers, K. N. Kudin, V. N. Staroverov, R. Kobayashi, J. Normand, K. Raghavachari, A. Rendell, J. C.



## General Remarks

---

Burant, S. S. Iyengar, J. Tomasi, M. Cossi, N. Rega, N. J. Millam, M. Klene, J. E. Knox, J. B. Cross, V. Bakken, C. Adamo, J. Jaramillo, R. Gomperts, R. E. Stratmann, O. Yazyev, A. J. Austin, R. Cammi, C. Pomelli, J. W. Ochterski, R. L. Martin, K. Morokuma, V. G. Zakrzewski, G. A. Voth, P. Salvador, J. J. Dannenberg, S. Dapprich, A. D. Daniels, Ö. Farkas, J. B. Foresman, J. V. Ortiz, J. Cioslowski, D. J. Fox, Gaussian 09, Revision D.01, **2009**.

Nickel catalyzed Negishi cross-coupling reactions



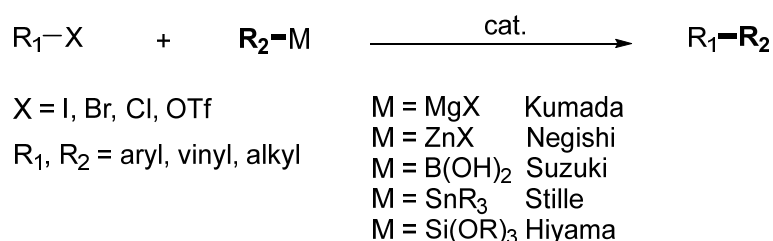
# 1 State of the art

## 1.1 Palladium catalyzed C<sub>sp2</sub>-C<sub>sp2</sub> Negishi cross couplings

### 1.1.1 Advantages of Negishi cross coupling reactions

Cross couplings reactions have advanced to a major tool in synthetic organic chemistry and offer a very efficient method for C-C or C-heteroatom bond formation.<sup>[1]</sup> Cross coupling reactions find important applications among others in the pharmaceutical<sup>[1,2]</sup> and agrochemical industries as well as in material science for the preparation of polymers<sup>[3]</sup>, liquid crystals<sup>[4]</sup> and advanced materials. Richard Heck, Ei-ichi Negishi<sup>[5]</sup> and Akira Suzuki<sup>[6]</sup> were rewarded in 2010 with the Nobel Prize for their pioneering work in the field. More than 40 years after their discovery, the research of always more efficient catalytic systems, which couple ever more challenging substrates still remains a very active field.

Metal catalyzed cross coupling reactions consist in the reaction between an electrophile, commonly an aryl halide and an organometallic species that acts as a nucleophile, as shown in **Scheme 1.1**. The most active systems known to date involve palladium catalysts.<sup>[7,8]</sup>

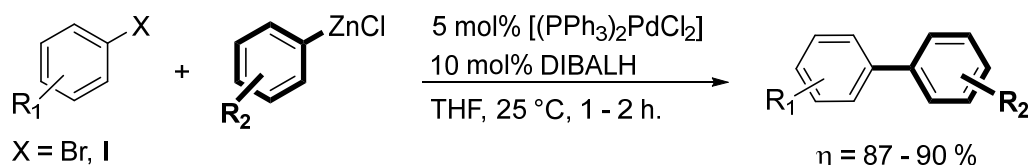


**Scheme 1.1:** General scheme of cross coupling reactions.

Among them, the Negishi reaction employs zinc derivatives as nucleophiles, which present several advantages. First of all, zinc derivatives have a relatively low toxicity and a very large functional group tolerance compared to organolithium and Grignard reagents.<sup>[9,10]</sup> Furthermore, a broad scope of zinc compounds is now available. Knochel especially contributed to the development of synthetic strategies to access a wide variety of derivatives, which are increasingly getting commercialized.<sup>[9]</sup> Additionally, Negishi couplings usually require mild conditions<sup>[9,10]</sup> and can be performed with several transition metals such as palladium and nickel, but also less frequently used iron and cobalt.

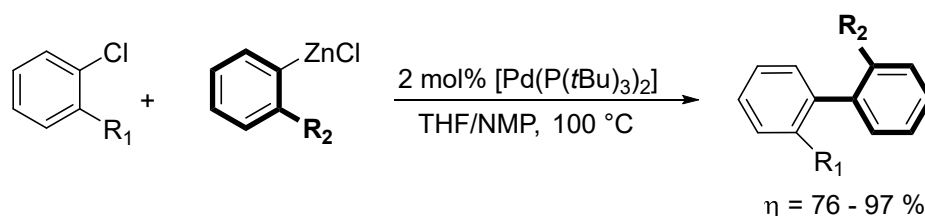
### 1.1.2 Advances in palladium catalyzed C<sub>sp2</sub>-C<sub>sp2</sub> Negishi cross couplings

Since the first report of a palladium catalyzed cross coupling between aryl halides and zinc derivatives by Negishi in 1977,<sup>[11]</sup> the field has attracted a lot of attention.<sup>[9]</sup>



**Scheme 1.2:** First palladium catalyzed Negishi cross coupling.<sup>[11]</sup>

Great progress has been made in the C<sub>sp2</sub>-C<sub>sp2</sub> coupling of aryl chlorides starting from the early 2000s. In 2001, Fu reported the first general procedure for the Negishi cross coupling between aryl chlorides and aryl zinc chlorides.<sup>[12]</sup> The commercially available and air stable palladium catalyst [Pd(P(*t*Bu)<sub>3</sub>)<sub>2</sub>] successfully promotes the coupling of *ortho* substituted, heteroaryl and vinyl substrates at only 2 mol% of catalyst loading in a mixture of THF and NMP at 100 °C, with TON greater than 3000.<sup>[12]</sup>

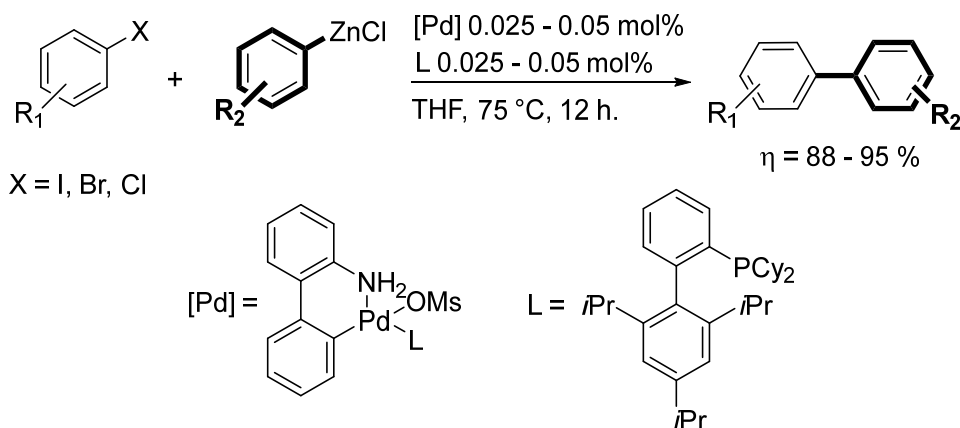


**Scheme 1.3:** First general procedure for the palladium catalyzed Negishi cross coupling of aryl chlorides with zinc derivatives reported by Fu.<sup>[12]</sup>

The following procedures developed by Buchwald<sup>[13, 14]</sup> and Organ<sup>[15, 16]</sup> count to the most efficient and general systems known to date for the palladium catalyzed Negishi coupling of aryl chlorides.

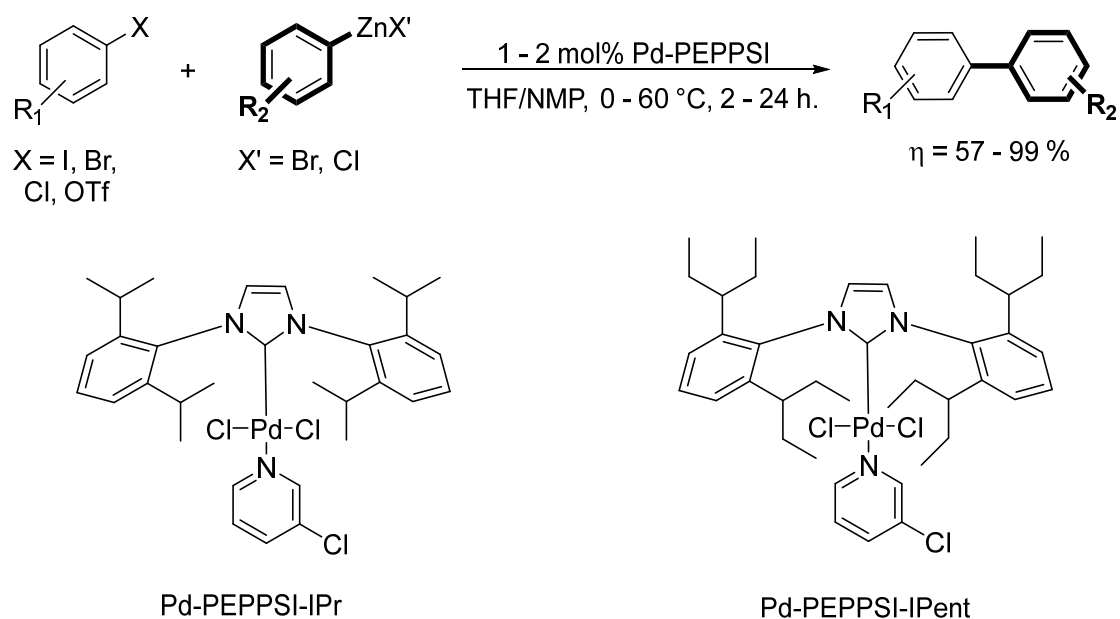
The [Pd<sub>2</sub>(dba)<sub>3</sub>]/RuPhos system<sup>[13]</sup> and the palladacycle precatalyst supported by the dialkylbiaryl monophosphine XPhos<sup>[14]</sup> designed by Buchwald couple a wide range of otherwise challenging heteroaryls and functionalized substrates under mild conditions. [Pd<sub>2</sub>(dba)<sub>3</sub>]/RuPhos allows for efficient production of biaryls at 0.01 mol% catalyst in THF at 70 °C and led for the first time to a tetra *ortho* substituted product.<sup>[13]</sup> The catalyst loading

could even be dropped down to 0.025 - 0.050 mol% at RT with the XPhos ligated palladacycle for the coupling of aryl halides, as shown in **Scheme 1.4**.<sup>[14]</sup>



**Scheme 1.4:** Highly efficient Negishi cross coupling catalyzed by a XPhos palladacycle precatalyst designed by Buchwald.<sup>[14]</sup>

While Buchwald used a phosphine derived catalyst, Organ synthesized in 2006 the easily affordable, air stable and highly active NHC based palladium precatalyst PEPPSI-IPr,<sup>[15]</sup> which enables  $\text{C}_{\text{sp}2}\text{-C}_{\text{sp}2}$ ,  $\text{C}_{\text{sp}2}\text{-C}_{\text{sp}3}$  and  $\text{C}_{\text{sp}3}\text{-C}_{\text{sp}3}$  cross couplings of a very broad scope of iodide, bromide, chloride, triflate, tosylate and mesylate substrates.



**Scheme 1.5:** Highly efficient Pd-PEPPSI-IPr and Pd-PEPPSI-IPent catalyzed Negishi cross coupling between aryl and heteroaryl bromides and chlorides and aryl zinc derivatives.<sup>[15, 16]</sup>

The reaction has a large functional group tolerance and affords the corresponding biaryls in high yields.<sup>[15, 17]</sup> The related PEPPSI-IPent precatalyst disclosed in 2010, can even couple some aryl and heteroaryl bromides and chlorides at 0 °C and tolerates strongly sterically hindered substrates yielding tetra *ortho* substituted biaryls.<sup>[16]</sup>

All the examples presented above support that the palladium catalyzed Negishi cross coupling has advanced to a very powerful tool in the 2000s, that is now widely applied in modern synthetic organic chemistry.

## 1.2 Nickel catalyzed C<sub>sp2</sub>-C<sub>sp2</sub> Negishi cross couplings

### 1.2.1 Advantages and challenges of nickel chemistry

Palladium mediated reactions and especially cross coupling processes have been extensively investigated and are well understood but the corresponding nickel chemistry remains far less explored.

Concern can be raised about the cost and low abundance of palladium. Nickel is therefore often considered as a cheap alternative to noble metal chemistry. Indeed, bulk nickel costs about 2000 times less than palladium<sup>[18]</sup> and most Ni(II) precursors are two orders of magnitude cheaper than their palladium analogues. Nevertheless, some Ni(0) sources such as commonly used [Ni(COD)<sub>2</sub>] can still be quite expensive.

Nickel as a first row transition metal possesses a small atomic radius and usually short metal-ligand bonds. Overall, nickel has a rather hard character compared to its heavier group 10 counterparts.<sup>[18]</sup>

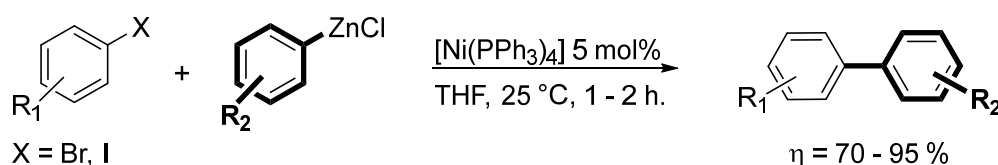
Furthermore, as a late transition metal, nickel is very electron rich and much more electropositive than palladium. This makes oxidative additions more favorable,<sup>[18, 19]</sup> even allowing insertion of nickel in otherwise quite unreactive derivatives such as alkyl halides, esters and ethers.<sup>[18, 20]</sup> Additionally, Ni-C bond dissociation energies (BDE) lie in general lower than Pd-C BDEs, also resulting in low activation barriers for reductive eliminations.<sup>[19]</sup> However, the eliminations are often only slightly exothermic. In contrast reductive eliminations on palladium complexes require higher activation energies but are strongly exothermic, rendering the processes highly favorable and irreversible.<sup>[19]</sup>

Moreover, more oxidation states are readily available to nickel complexes. Whereas most palladium cross coupling mechanisms are polar and involve exclusively Pd(0)/Pd(II) or Pd(II)/Pd(IV) intermediates, stable nickel compounds are commonly found in oxidation states ranging from 0 to +III. [18, 19] Nickel has also a greater propensity to homolytic bond cleavage than palladium, allowing SET and radical processes. [18, 19] A wide variety of mechanisms has thus been disclosed, with Ni(I)/Ni(III) cycles being predominant for the couplings of aryl halides with mono-phosphine substituted nickel complexes. [21, 22] Ni(0)/Ni(II) cycles are observed for cross couplings with phenol derivatives [23, 24] as well as for the amination of aryl chlorides using [(BINAP)Ni( $\eta^2$ -NC-Ph)]. [25] Even Ni(0)/Ni(I)/Ni(II) reaction pathways have been reported for the Negishi cross coupling of alkyl halides [26, 27] and an only Ni(I) based reactivity for the reductive cleavage of aryl ethers with silanes. [28]

Nickel mediated reactions are therefore primarily cost-efficient compared to palladium catalysis but even more importantly they provide an extremely rich and active chemistry, despite the carcinogenic character of numerous nickel complexes. It might be difficult to predict, to control and to understand nickel chemistry but when it is fine-tuned it turns out very efficient and can be able to perform challenging reactions. [19]

### 1.2.2 Advances in nickel catalyzed C<sub>sp2</sub>-C<sub>sp2</sub> Negishi cross couplings

The first nickel catalyzed C<sub>sp2</sub>-C<sub>sp2</sub> Negishi cross coupling was reported as early as 1977. By employing 5 mol% of the Ni(0) precursor [Ni(PPh<sub>3</sub>)<sub>4</sub>] generated from commercially available [Ni(acac)<sub>2</sub>], PPh<sub>3</sub> and DIBALH, Negishi managed to couple aryl halides with aryl zinc derivatives in good to excellent yields within 1 - 2 h. at RT. [11] Since then the field has been ever growing [10] and this paragraph will focus only on the coupling of aryl halides.



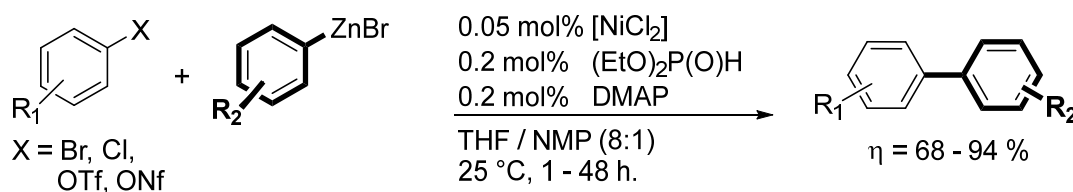
**Scheme 1.6:** First nickel catalyzed Negishi cross-coupling reported in 1977. [11]

Research aimed at using cheap and largely available electrophilic coupling partners as well as lowering the catalyst loadings.



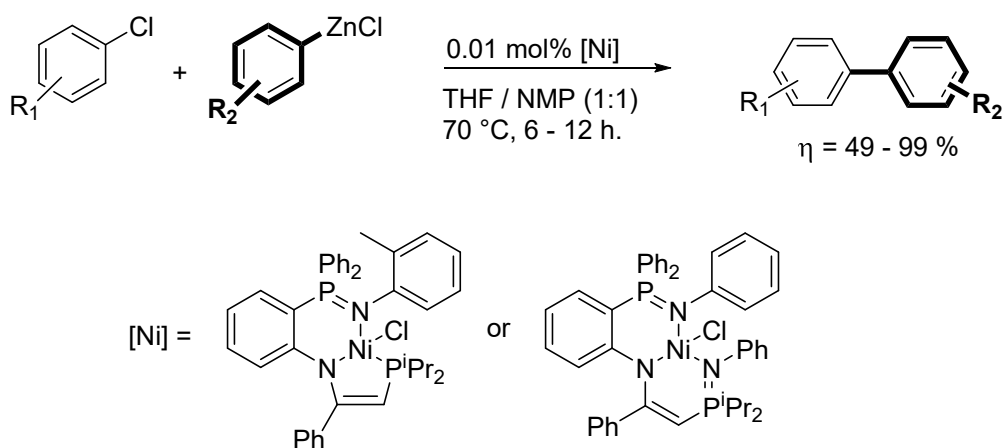
On one side, lots of efforts were especially oriented towards the coupling of cheaper and readily available aryl chlorides in replacement for aryl bromides and iodides. Aryl chlorides are known to be more difficult to couple because of the poorer reactivity of C-Cl bonds compared to C-Br and C-I bonds. Miller reported in 1998 the first Negishi coupling of aryl chlorides catalyzed by 2 mol% of  $[\text{Ni}(\text{acac})_2]/\text{dppf}$ .<sup>[29]</sup> Contributions by de Vries<sup>[30]</sup> and Kappe<sup>[31]</sup> followed in 2002 and 2004.

On the other side, nickel catalyzed Negishi reactions have become increasingly efficient in the last ten years, now being able to compete with their palladium counterparts.<sup>[10]</sup> Thorough ligand optimization initiated by Knochel in 2005 - 2006 allowed for the drastic lowering of the catalytic charge.<sup>[32, 33]</sup> The combination of 0.05 mol% of  $[\text{NiCl}_2]$ , 0.2 mol% of diethylphosphite  $(\text{EtO})_2\text{P}(\text{O})\text{H}$  and 0.2 mol% of DMAP efficiently catalyzes a broad scope of aryl, heteroaryl and alkenyl bromides, sulfonates and activated chlorides in a mixture of THF and N-ethylpyrrolidinone (NEP) at RT. The products are obtained in good yields with only small amounts of homocoupled side product within 1 - 48 h.<sup>[29, 30]</sup>



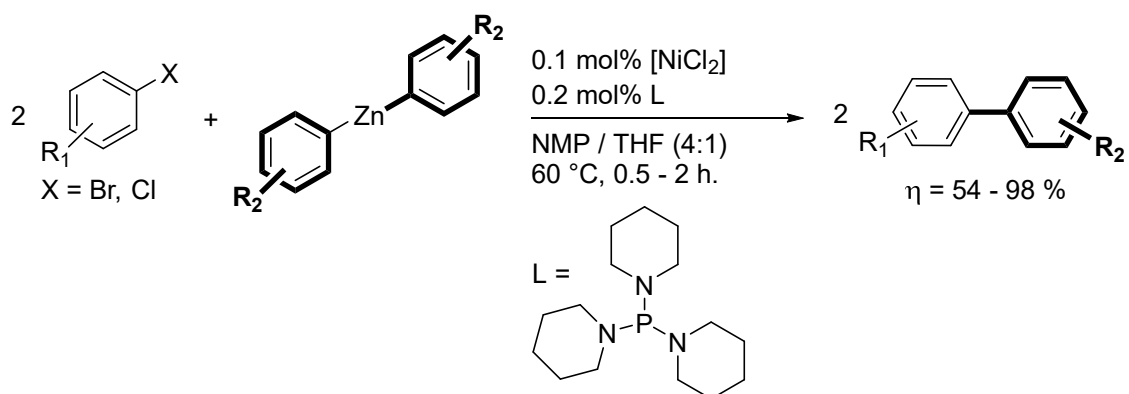
**Scheme 1.7:** Negishi cross coupling procedure developed by Knochel using a combination of  $[\text{NiCl}_2]$ ,  $(\text{EtO})_2\text{P}(\text{O})\text{H}$  and DMAP.<sup>[32, 33]</sup>

Extensive investigations led by Wang between 2007 and 2012 further disclosed the ability of pincer complexes to catalyze Negishi cross couplings involving chloro arenes and chloro pyridines.<sup>[34]</sup> The first efficient and systematic coupling of aryl chlorides, presented in **Scheme 1.8**, was reported in 2007. 0.01 mol% of nickel amido pincer complexes in a 1:1 mixture of THF and NMP were sufficient to synthesize the corresponding biaryls in good to excellent yields at 70 °C. The reaction tolerates a large variety of functional groups except nitro and aldehyde substituents. Higher catalytic charges as well as higher temperatures were required to couple sterically hindered *ortho* derivatives with zinc reagents in good yields.<sup>[35]</sup> Subsequently, Wang reported Negishi couplings between aryl chlorides and aryl zinc chlorides under similar conditions using various nickel pincer complexes<sup>[36 - 39]</sup>, while Chen disclosed the first nickel NHC catalyzed Negishi cross coupling.<sup>[40]</sup>



**Scheme 1.8:** Nickel amido pincer complexes for the Negishi cross coupling between aryl chlorides and phenyl zinc chloride derivatives. <sup>[35]</sup>

In 2011 Frech also described a very general and efficient procedure for the nickel catalyzed Negishi cross-coupling using diarylzinc reagents, in which both aryl moieties are involved in the reaction. <sup>[41]</sup> The highly active aminophosphine based nickel catalyst is generated by mixing NMP solutions of  $[\text{NiCl}_2]$  and 1,1',1''-(phosphanetriyl)tripiperidine in air at RT. A very broad scope of activated, non-activated and sterically hindered *ortho* substituted aryl bromides and chlorides and even heterocyclic substrates were all coupled within 2 h. at 60 °C using 0.1 mol% catalyst. The catalytic loading could even be lowered down to 0.01 - 0.05 mol% and/or RT conditions for several substrates. High conversions and high yields were almost commonly obtained. Compared to other systems no inert atmosphere is required as well as no excess of ligand or other additives making it the most efficient system nowadays. <sup>[41]</sup>



**Scheme 1.9:** General and efficient Negishi cross coupling methodology developed by Frech relying on an aminophosphine nickel catalyst. <sup>[41]</sup>

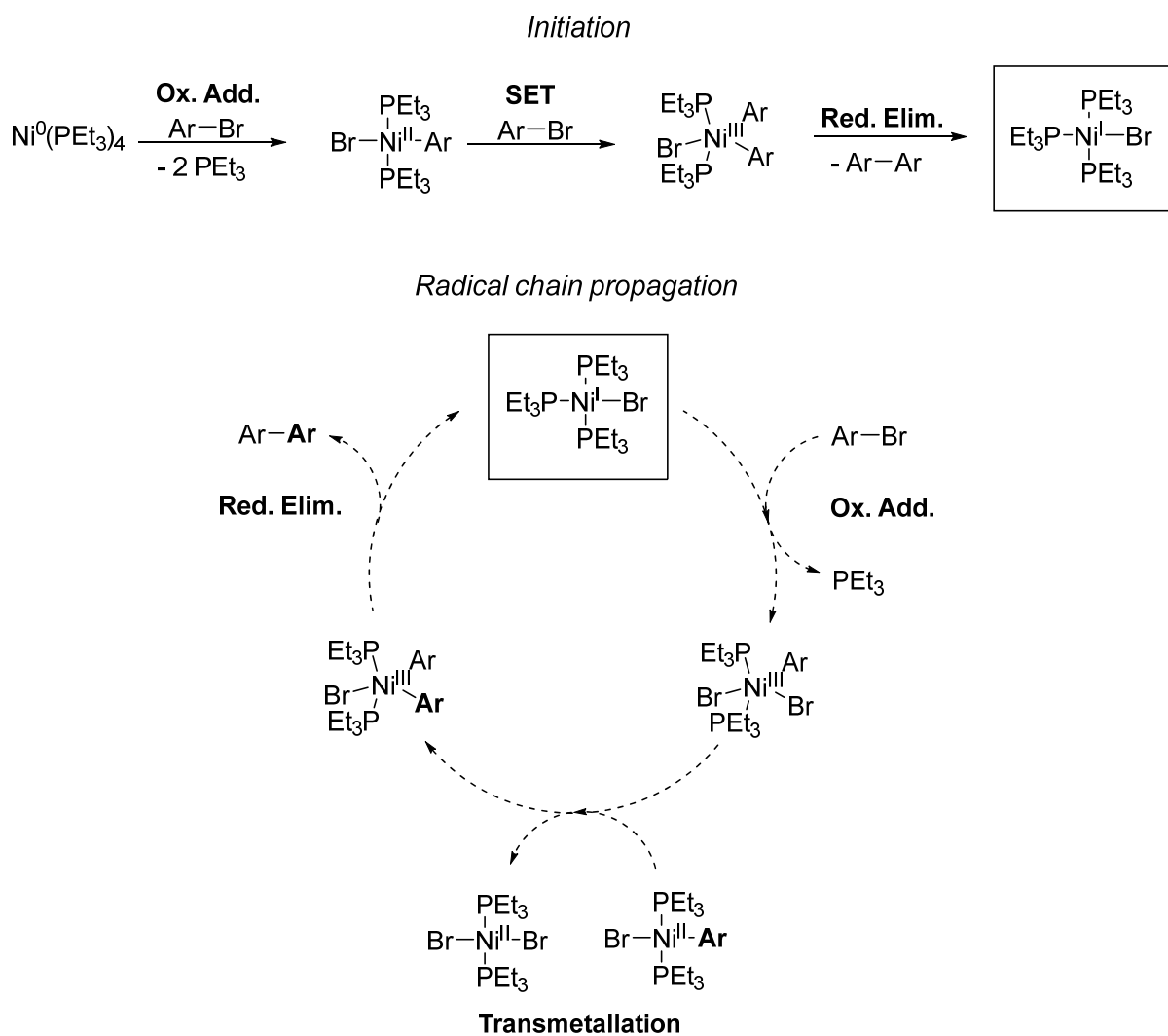
More recently, the Negishi cross coupling between aryl fluorides and zinc reagents has also been achieved by Nakamura by combining  $[\text{Ni}(\text{acac})_2]$  with a diphosphine bearing an alkoxide moiety (POP) <sup>[42]</sup> as well as by Love <sup>[43]</sup> and Wang <sup>[44]</sup> using respectively  $[\text{Ni}(\text{PEt}_3)_2\text{Cl}_2]$  and  $[\text{Ni}(\text{PCy}_3)_2\text{Cl}_2]$ .

The systems presented above count to date to the most general and efficient ones for the nickel catalyzed Negishi cross-couplings. Yet, the reaction mechanisms underlying these processes remain largely unknown.

### 1.2.3 Mechanisms of nickel catalyzed Negishi cross-couplings

Several mechanistic studies on nickel catalyzed Negishi cross couplings have been undertaken. However, they still remain scarce partially due to the tendency of nickel to undergo SET and to generate paramagnetic species, which complicates the investigations. As previously described (1.2.2) a large variety of ligands, nickel precursors and complexes are able to promote efficiently Negishi couplings and provide a great multiplicity of possible mechanisms to achieve the transformation. Nevertheless, the general mechanism for nickel catalyzed Negishi processes should always involve as for palladium at least three elementary steps, which are oxidative addition, transmetalation and reductive elimination.

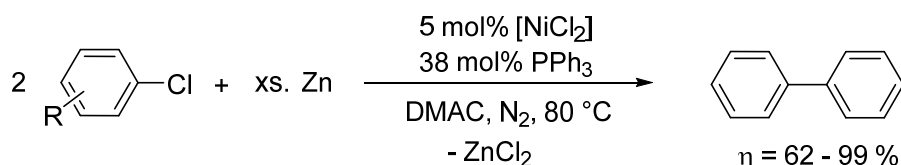
The mechanism of the nickel catalyzed  $\text{C}_{\text{sp}2}\text{-C}_{\text{sp}2}$  coupling between the mono-phosphine substituted oxidative addition product  $[(\text{PEt}_3)_2\text{Ni}(\text{Ar})(\text{Br})]$  and aryl bromides was examined as early as 1979 by Kochi. <sup>[21]</sup> The reaction is initiated by a SET from the trans-arylnickel(II) halide complex to a free aryl bromide and proceeds then through Ni(I) and Ni(III) intermediates as shown in **Scheme 1.10**. <sup>[21]</sup>



**Scheme 1.10:** Radical chain mechanism for the coupling of aryl halides in the presence of mono-phosphines. <sup>[21]</sup>

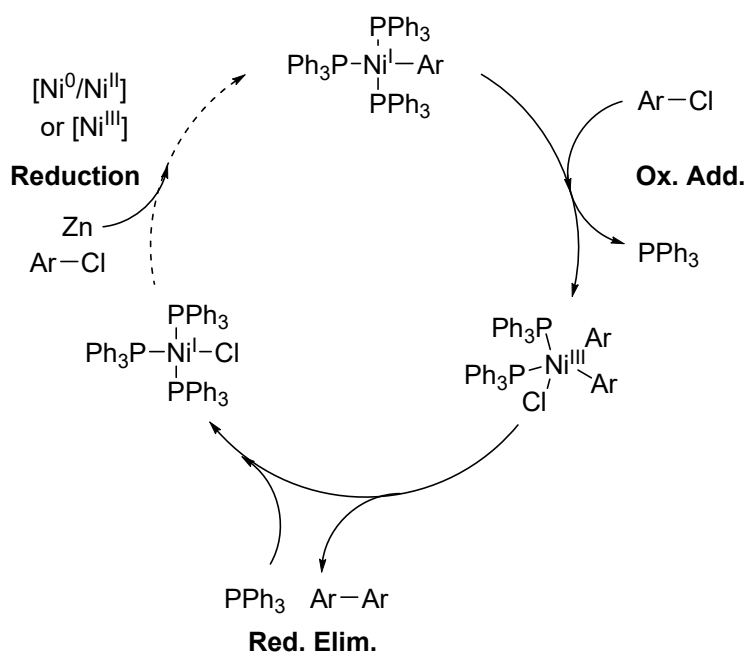
During the first step of the mechanism, the active catalyst  $[(\text{PEt}_3)_3\text{Ni}^{\text{I}}\text{Br}]$  undergoes oxidative addition of an aryl bromide, producing the Ni(III) intermediate  $[(\text{PEt}_3)_2\text{Ni}^{\text{III}}(\text{Ar})(\text{Br})_2]$ . Subsequently, a ligand transmetallation between the arylnickel(III) complex and  $[(\text{PEt}_3)_2\text{Ni}^{\text{II}}(\text{Ar})(\text{Br})]$  leads to a new bis-aryl Ni(III) intermediate  $[(\text{PEt}_3)_2\text{Ni}^{\text{III}}(\text{Ar})_2(\text{Br})]$ . Finally, reductive elimination releases the biaryl and regenerates the catalyst  $[(\text{PEt}_3)_3\text{Ni}^{\text{I}}\text{Br}]$ . <sup>[21]</sup>

Additionally, Colon and Kelsey investigated in 1986 the nickel catalyzed coupling of aryl chlorides to symmetric biaryls in the presence of a reducing metal such as zinc. <sup>[22]</sup> Monodentate triarylphosphines and especially  $\text{PPh}_3$  turned out to be the best ligands for this reaction, where zinc plays a major role as quantitative coupling cannot proceed in its absence. <sup>[22]</sup>



**Scheme 1.11:** Nickel catalyzed coupling of aryl chlorides in the presence of zinc. <sup>[22]</sup>

The mechanism of the reaction slightly differs from the previous one but still predominantly involves Ni(I) and Ni(III) intermediates. The key step of this reaction is the reduction of an arylnickel(II)halide by zinc to prepare the catalytically active arylnickel(I) species  $[(\text{PPh}_3)_3\text{Ni}^{\text{I}}(\text{Ar})]$ . The reaction does not seem to involve any transmetallation between nickel complexes but instead zinc mediated reduction processes. <sup>[22]</sup> A simplified catalytic cycle is depicted in **Scheme 1.12**.

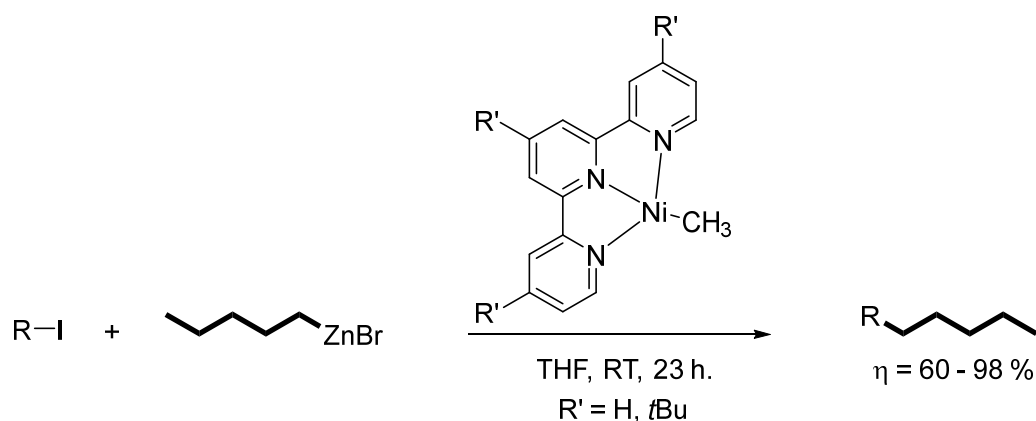


**Scheme 1.12:** Ni(I)/Ni(III) based mechanism for the coupling of aryl chlorides to biaryls in the presence of zinc. <sup>[22]</sup>

Furthermore, Wang <sup>[35]</sup> and Frech <sup>[41]</sup> also postulated radical chain processes and Ni(I)/Ni(III) based mechanisms for Negishi cross couplings relying respectively on nickel amido pincer <sup>[35]</sup> and  $[\text{NiCl}_2]/1,1',1''\text{-}(\text{phosphanetriyl})\text{tripiperidine}$  <sup>[41]</sup> catalysts.

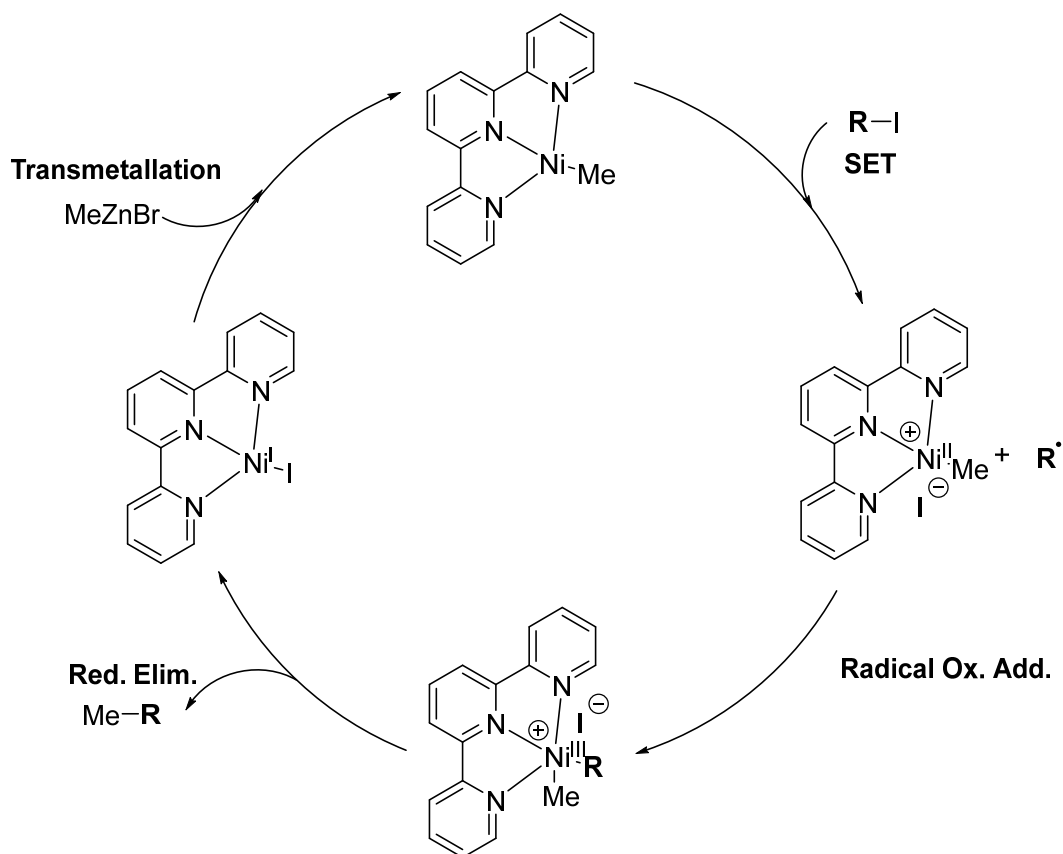
As mechanistic investigations on nickel catalyzed Negishi cross coupling processes are still relatively rare,<sup>[10, 45]</sup> the studies on closely related  $C_{sp^3}$ - $C_{sp^3}$  couplings are also presented here. Two systems involving different types of pyridine containing ligands have been thoroughly investigated.

First of all, Vicic promoted alkyl-alkyl Negishi couplings between alkyl iodides and alkyl zinc bromides *via* the terpyridine nickel complex  $[(\text{terpy})\text{Ni}(\text{Me})]$ .<sup>[46]</sup>



**Scheme 1.13:** Vicic conditions for the  $C_{sp^3}$ - $C_{sp^3}$  Negishi cross coupling catalyzed by  $[(\text{terpy})\text{Ni}(\text{Me})]$ .<sup>[46, 47]</sup>

The analysis of the side products of the reaction evidences a dimerization process of the employed alkyl halides. Radical clock experiments converting iodomethylcyclopropane into olefinic products, additionally point towards a radical based mechanism.<sup>[46]</sup> The isolation and characterization of several  $[(\text{terpy})\text{Ni}]$  complexes lead to the proposed catalytic cycle in **Scheme 1.14**.<sup>[26, 46, 47]</sup>



**Scheme 1.14:** Catalytic cycle proposed on the basis of experimental investigations for the coupling of alkyl iodides with alkyl zinc bromides using  $[(\text{terpy})\text{Ni}(\text{Me})]$  as catalyst. <sup>[26, 46, 47]</sup>

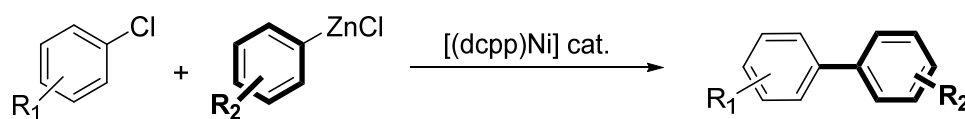
EPR measurements and DFT calculations evidence that catalytically active paramagnetic  $[(\text{terpy})\text{Ni}(\text{Me})]$  is a ligand based radical best described as a Ni(II)-methyl cation with a reduced anionic ligand rather than a Ni(I) complex. <sup>[26]</sup> In the presence of an alkyl halide, SET generates  $[(\text{terpy})\text{Ni}^{\text{II}}(\text{Me})]^+ \text{X}^-$  together with a free alkyl radical. The transmetalation of  $[(\text{terpy})\text{Ni}^{\text{II}}(\text{Me})]^+ \text{I}^-$  with alkyl zinc reagents leading to dialkyl Ni(II)  $[(\text{terpy})\text{Ni}^{\text{II}}(\text{Me})(\text{R})]$  intermediates could be ruled out. <sup>[26, 47]</sup> Recombination of the radical with the nickel complex leads to Ni(III) intermediate  $[(\text{terpy})\text{Ni}^{\text{III}}(\text{Me})(\text{R})]$ , from which the cross coupled product can be reductively eliminated.  $[(\text{terpy})\text{Ni}^{\text{I}}(\text{X})]$  <sup>[46]</sup> which is generated alongside in the process reacts then with the transmetallating alkyl zinc derivative to regenerate  $[(\text{terpy})\text{Ni}(\text{Me})]$ . <sup>[26]</sup> Overall, the oxidative addition occurs after the transmetalation. Ni(I), Ni(II) and Ni(III) intermediates are all involved in this catalysis. DFT calculations performed by Phillips support the feasibility of this catalytic cycle with relatively low activation barriers. <sup>[48]</sup>

Besides, Fu developed a powerful procedure for the coupling of alkyl electrophiles with zinc derivatives relying on a nickel/pybox catalyst.<sup>[27, 49, 50, 51]</sup> Based on these results, Cárdenas studied in 2007 the  $[\text{Ni}(\text{Py})_4\text{Cl}_2]/(\text{S})\text{-}(\text{sBu})\text{-pybox}$  catalyzed cascade cyclization-cross coupling of secondary iodoalkanes with alkyl zinc halides and provided strong experimental and computational evidence for a radical based mechanism.<sup>[52]</sup> Proofs include among others stereoselectivity studies, radical scavenging and radical clock experiments.<sup>[52]</sup> In addition, the mechanism of the  $[\text{Ni}]/\text{pybox}$  catalyzed stereoconvergent Negishi arylation of racemic propargylic bromides, experimentally investigated by Fu in 2014,<sup>[27]</sup> displays strong similarities with the mechanism earlier reported by Vicic.<sup>[26]</sup>

Overall this literature survey shows that most nickel catalyzed  $\text{C}_{\text{sp}2}\text{-C}_{\text{sp}2}$  and  $\text{C}_{\text{sp}3}\text{-C}_{\text{sp}3}$  Negishi cross couplings tend to favor SET and radical processes which mainly generate Ni(I) and Ni(III) intermediates over polar Ni(0)/Ni(II) mechanisms.

### 1.3 Research objectives

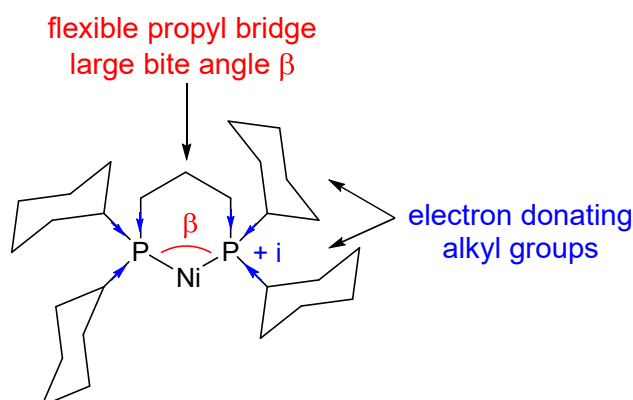
The following chapter will be dedicated to the investigation of the Negishi cross coupling between aryl chlorides and phenyl zinc chloride derivatives catalyzed by  $[(\text{dcpp})\text{Ni}]$  based complexes (dcpp = 1,3-bis(dicyclohexylphosphino)propane).



**Scheme 1.15:**  $[(\text{dcpp})\text{Ni}]$  based Negishi catalysis between aryl halides and phenyl zinc chloride derivatives.

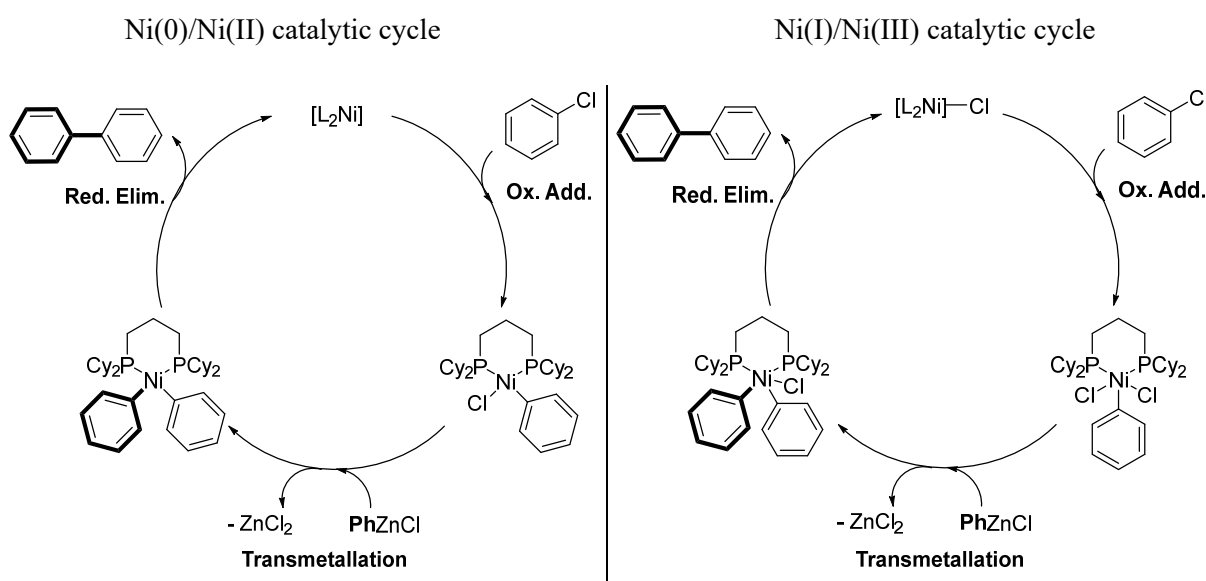
The chelating bis-phosphine dcpp is the ligand of choice for this study. Indeed, strongly donating bis-dialkylphosphines are well known to stabilize unsaturated Ni(0) complexes unlike bis-diarylphosphines like dppe (dppe = 1,2-bis(diphenylphosphino)ethane) and dppp (dppp = 1,3-bis(diphenylphosphino)propane). Moreover, the propyl bridge enforces a large bite angle and provides an enhanced flexibility of the ligand around the nickel center, which further helps stabilizing Ni(0) complexes and intermediates.





**Scheme 1.16:** Properties of the [(dcpP)Ni] system.

The major motivation behind this study is to develop a new, mild and efficient nickel catalysis for the synthesis of asymmetric biaryls and to understand the underlying mechanism. It is of great interest to determine whether the use of a bidentate ligand favors a Ni(0)/Ni(II) mechanism analogous to palladium systems or a Ni(I)/Ni(III) mechanism as previously reported for mono-phosphine based cross couplings with aryl halides. <sup>[21, 22]</sup> **Scheme 1.17** represents both possible catalytic cycles. This mechanistic investigation would help to shed light into complex and unpredictable nickel chemistry and to improve the design of potentially new catalysts for even more efficient processes. This is achieved by performing stoichiometric reactions and catalytic tests with nickel precursors in different oxidation states. The experimental results are supported by DFT calculations carried out by Dr. Nicolas Mézailles at the LHFA (Toulouse).



**Scheme 1.17:** General Ni(0)/Ni(II) and Ni(I)/Ni(III) cross-coupling mechanisms.

## 1.4 References

- [1] C. C. C. Johansson Seechurn, M. O. Kitching, T. J. Colacot, V. Snieckus, *Angew. Chem. Int. Ed.*, **2012**, *51*, 5062 - 5085.
- [2] R. Magano, J. R. Dunetz, *Chem. Rev.*, **2011**, *111*, 2177 - 2250.
- [3] L. Verheyen, P. Leysen, M.-P. Van Den Eede, N. Ceunen, T. Hardeman, G. Koeckelberghs, *Polymer*, **2017**, *108*, 521 - 546.
- [4] N.-H. Chang, M. Kinoshita, Y. Nishihara, *Lecture Notes in Chemistry*, **2013**, *80*, 111 - 135.
- [5] E. Negishi, *Angew. Chem. Int. Ed.*, **2011**, *50*, 6738 - 6764.
- [6] A. Suzuki, *Angew. Chem. Int. Ed.*, **2011**, *50*, 6722 - 6737.
- [7] A. F. Littke, G. C. Fu, *Angew. Chem. Int. Ed.*, **2002**, *41*, 4176 - 4211.
- [8] G. C. Fortman, S. P. Nolan, *Chem. Soc. Rev.*, **2011**, *40*, 5151 - 5169.
- [9] D. Haas, J. M. Hammann, R. Greiner, P. Knochel, *ACS Catal.*, **2016**, *6*, 1540 - 1552.
- [10] V. B. Phapale, D. J. Cárdenas, *Chem. Soc. Rev.*, **2009**, *38*, 1598 - 1607.
- [11] E. Negishi, A. O. King, N. Okukado, *J. Org. Chem.*, **1977**, *42*, 1821 - 1823.
- [12] C. Dai, G. C. Fu, *J. Am. Chem. Soc.*, **2001**, *123*, 2719 - 2724.
- [13] J. E. Milne, S. L. Buchwald, *J. Am. Chem. Soc.*, **2004**, *126*, 13028 - 13032.
- [14] Y. Yang, N. J. Oldenhuis, S. L. Buchwald, *Angew. Chem. Int. Ed.*, **2013**, *52*, 615 - 619.
- [15] M. G. Organ, S. Avola, I. Dubovyk, N. Hadei, E. A. B. Kantchev, C. J. O'Brien, C. Valente, *Chem. Eur. J.*, **2006**, *12*, 4749 - 4755.
- [16] S. Çalimsiz, M. Sayah, D. Mallik, M. G. Organ, *Angew. Chem. Int. Ed.*, **2010**, *49*, 2014 - 2017.
- [17] S. Sase, M. Jaric, A. Metzger, V. Malakhov, P. Knochel, *J. Org. Chem.*, **2008**, *73*, 7380 - 7382.
- [18] S. Z. Tasker, E. A. Standley, T. F. Jamison, *Nature*, **2014**, *509*, 299 - 309.
- [19] V. P. Ananikov, *ACS Catal.*, **2015**, *5*, 1964 - 1971.
- [20] J. Yamaguchi, K. Muto, K. Itami, *Eur. J. Org. Chem.*, **2013**, 19 - 31.

- [21] T. T. Tsou, J. K. Kochi, *J. Am. Chem. Soc.*, **1979**, *101*, 7547 - 7560.
- [22] I. Colon, D. R. Kelsey, *J. Org. Chem.*, **1986**, *51*, 2627 - 2637.
- [23] K. Muto, J. Yamaguchi, K. Itami, *J. Am. Chem. Soc.*, **2013**, *135*, 16384 - 16387.
- [24] Z. Li, S.-L. Zhang, Y. Fu, Q.-X. Guo, L. Liu, *J. Am. Chem. Soc.*, **2009**, *131*, 8815 - 8823.
- [25] S. Ge, R. A. Green, J. F. Hartwig, *J. Am. Chem. Soc.*, **2014**, *136*, 1617 - 1627.
- [26] G. D. Jones, J. L. Martin, C. McFarland, O. R. Allen, R. E. Hall, A. D. Haley, R. J. Brandon, T. Konovalova, P. J. Desrochers, P. Pulay, D. A. Vicic, *J. Am. Chem. Soc.*, **2006**, *128*, 13175 - 13183.
- [27] N. D. Schley, G. C. Fu, *J. Am. Chem. Soc.*, **2014**, *136*, 16588 - 16593.
- [28] J. Cornella, E. Gómez-Bengoa, R. Martin, *J. Am. Chem. Soc.*, **2013**, *135*, 1997 - 2009.
- [29] J. A. Miller, R. P. Farrell, *Tetrahedron Lett.*, **1998**, *39*, 6441 - 6444.
- [30] C. E. Tucker, J. G. De Vries, *Top. Catal.*, **2002**, *19*, 111 - 118.
- [31] P. Walla, C. O. Kappe, *Chem. Commun.*, **2004**, 564 - 565.
- [32] A. Gavryushin, C. Kofink, G. Manolikakes, P. Knochel, *Org. Lett.*, **2005**, *7*, 4871 - 4874.
- [33] A. Gavryushin, C. Kofink, G. Manolikakes, P. Knochel, *Tetrahedron*, **2006**, *62*, 7521 - 7533.
- [34] Z.-X. Wang, N. Liu, *Eur. J. Inorg. Chem.*, **2012**, 901 - 911.
- [35] L. Wang, Z.-X. Wang, *Org. Lett.*, **2007**, *9*, 4335 - 4338.
- [36] C. Zhang, Z.-X. Wang, *Organomet.*, **2009**, *28*, 6507 - 6514.
- [37] N. Liu, L. Wang, Z.-X. Wang, *Chem. Commun.*, **2011**, *47*, 1598 - 1600.
- [38] Q. Zhang, X.-Q. Zhang, Z.-X. Wang, *Dalton Trans.*, **2012**, *41*, 10453 - 10464.
- [39] D. Wu, Z.-X. Wang, *Org. Biomol. Chem.*, **2014**, *12*, 6414 - 6424.
- [40] Z. Xi, Y. Zhou, W. Chen, *J. Org. Chem.*, **2008**, *73*, 8497 - 8501.
- [41] R. Gerber, C. M. Frech, *Chem. Eur. J.*, **2011**, *17*, 11893 - 11904.
- [42] Y. Nakamura, N. Yoshikai, L. Ilies, E. Nakamura, *Org. Lett.*, **2012**, *14*, 3316 - 3319.

- [43] A. D. Sun, K. Leung, A. D. Restivo, N. A. LaBerge, H. Takasaki, J. A. Love, *Chem. Eur. J.*, **2014**, *20*, 3162 - 3168.
- [44] F. Zhu, Z.-X. Wang, *J. Org. Chem.*, **2014**, *79*, 4285 - 4292.
- [45] X. Hu, *Chem. Sci.*, **2012**, *2*, 1867 - 1886.
- [46] T. J. Anderson, G. D. Jones, D. A. Vicic, *J. Am. Chem. Soc.*, **2004**, *126*, 8100 - 8101.
- [47] G. D. Jones, C. McFarland, T. J. Anderson, D. A. Vicic, *Chem. Commun.*, **2005**, 4211 - 4213.
- [48] X. Lin, L. Phillips, *J. Org. Chem.*, **2008**, *73*, 3680 - 3688.
- [49] J. Zhou, G. C. Fu, *J. Am. Chem. Soc.*, **2003**, *125*, 14726 - 14727.
- [50] C. Fischer, G. C. Fu, *J. Am. Chem. Soc.*, **2005**, *127*, 4594 - 4595.
- [51] S. W. Smith, G. C. Fu, *J. Am. Chem. Soc.*, **2008**, *130*, 12645 - 12647.
- [52] V. B. Phapale, E. Buñuel, M. García-Iglesias, D. J. Cárdenas, *Angew. Chem. Int. Ed.*, **2007**, *46*, 8790 - 8795.

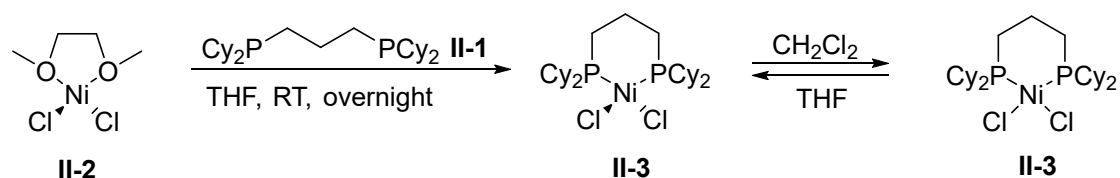


## 2. (Bis-phosphine)nickel-catalyzed Negishi cross coupling

### 2.1 Synthesis of precatalyst [(dcp)nickel(toluene)] **II-4**

#### 2.1.1 Synthesis of Ni(II) precursor [(dcp)NiCl<sub>2</sub>] **II-3**

The [(dcp)NiCl<sub>2</sub>] complex **II-3** is readily synthesized at RT by the stoichiometric reaction between [(DME)NiCl<sub>2</sub>] **II-2** and the bis(dicyclohexylphosphino)propane ligand **II-1** (dcp), following the procedure developed by Matthieu Demange in his thesis. [<sup>1</sup> 31P {<sup>1</sup>H} NMR shows the fast disappearance of the free dcp ligand **II-1** at  $\delta = -6,7$  ppm. The product is gathered as an orange powder in 94 % yield.



**Scheme 2.1:** Synthesis of [(dcp)NiCl<sub>2</sub>] **II-3**.

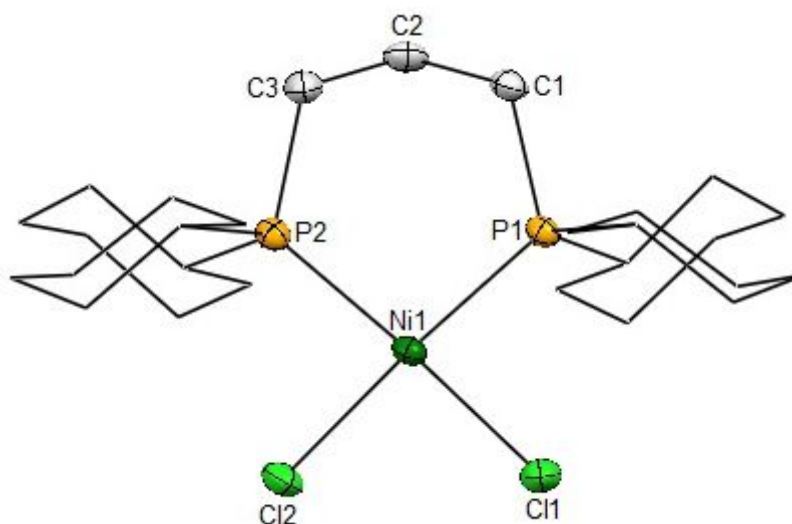
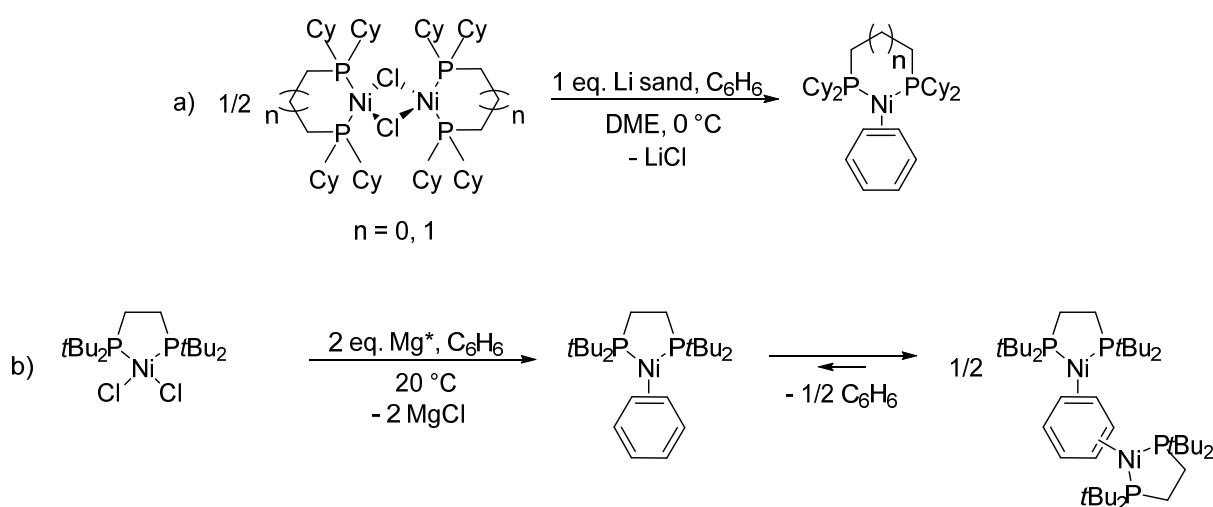


**Figure 2.1:** Molecular structure of [(dcp)NiCl<sub>2</sub>] **II-3** determined by single crystal X-ray diffraction. Hydrogen atoms are omitted for clarity. Selected bond length [Å] and angles [°]: Ni<sub>1</sub>-P<sub>1</sub> 2.196(3), Ni<sub>1</sub>-P<sub>2</sub> 2.187(3), Ni<sub>1</sub>-Cl<sub>1</sub> 2.240(4), Ni<sub>1</sub>-Cl<sub>2</sub> 2.239(3), P<sub>1</sub>-Ni<sub>1</sub>-P<sub>2</sub> 99.40(11), Cl<sub>1</sub>-Ni<sub>1</sub>-Cl<sub>2</sub> 88.55(13), P<sub>1</sub>-Ni<sub>1</sub>-Cl<sub>1</sub> 85.97(12), P<sub>2</sub>-Ni<sub>1</sub>-Cl<sub>2</sub> 86.29(13).

As Matthieu Demange reported, no NMR signal is observed in THF for the poorly soluble  $[(\text{dcpp})\text{NiCl}_2]$  complex **II-3**, suggesting that it has a predominant tetrahedral geometry.<sup>[1]</sup> However, NMR data could be recorded in  $\text{CH}_2\text{Cl}_2$ , in which the complex is fully soluble, showing that in this solvent the nickel center is in a square planar environment. The two geometries thus possess quite similar energies and the equilibrium between both can be shifted by changing the solvent. Single crystals for X-ray diffraction analysis were grown by diffusing petroleum ether in a  $\text{CH}_2\text{Cl}_2$  solution of  $[(\text{dcpp})\text{NiCl}_2]$  **II-3**. The square planar geometry is favored in the solid state, as evidenced by the sum of the angles around the nickel center being equal to  $360.21^\circ$ . The resolved structure presented above in **Figure 2.1** is comparable to Matthieu Demanges one.<sup>[1]</sup>

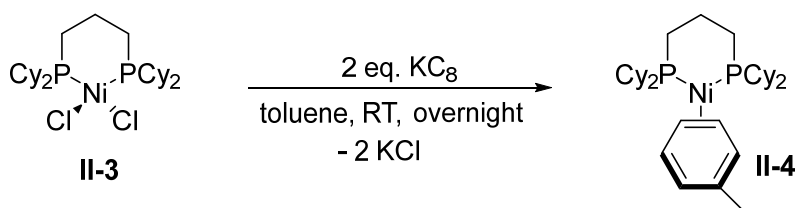
### 2.1.2 Synthesis of Ni(0) complex $[(\text{dcpp})\text{Ni}(\text{toluene})]$ **II-4**

Chelating  $[(\text{bis-phosphine})\text{Ni}(\text{arene})]$  complexes are known since Jonas<sup>[2]</sup> and Pörschke<sup>[3]</sup> reported their synthesis. The Ni(0) complexes are obtained either from Ni(II) or Ni(I) precursors which are reduced by alkali or alkali earth metals in the presence of aromatic compounds, as shown in **Scheme 2.2**. By following this procedure, Jonas managed to prepare among others monometallic  $[(\text{dcpe})\text{Ni}(\text{C}_6\text{H}_6)]$  and  $[(\text{dcpp})\text{Ni}(\text{C}_6\text{H}_6)]$ ,<sup>[2]</sup> which are characterized only by elemental analysis and Pörschke obtained bimetallic trigonal planar  $[[(\text{dtbpe})\text{Ni}]_2(\text{C}_6\text{H}_6)]$ <sup>[3]</sup> with the more sterically hindered *tert*-butyl substituted phosphines.



**Scheme 2.2:** a) Jonas' synthesis of  $[(\text{dcpe})\text{Ni}(\text{C}_6\text{H}_6)]$  and  $[(\text{dcpp})\text{Ni}(\text{C}_6\text{H}_6)]$ ,<sup>[2]</sup> b) Pörschke's synthesis of  $[[(\text{dtbpe})\text{Ni}]_2(\text{C}_6\text{H}_6)]$ .<sup>[3]</sup>

In a similar way, the two electron reduction of [(dcpP)NiCl<sub>2</sub>] **II-3** by KC<sub>8</sub> in toluene, reported by Matthieu Demange, affords the targeted Ni(0) complex [(dcpP)Ni(toluene)] **II-4** together with small amounts of [(dcpP)NiH]<sub>2</sub> **II-5**. The yield of the 16 electron complex [(dcpP)Ni(toluene)] **II-4** could be optimized up to 70 % by working with concentrated solutions, which favor the precipitation of the product.<sup>[1]</sup> As [(dcpP)NiH]<sub>2</sub> **II-5** is much more soluble than [(dcpP)Ni(toluene)] **II-4**, it can be easily filtered away. [(dcpP)Ni(toluene)] **II-4** is then extracted several times in toluene from precipitated KCl and graphite.



**Scheme 2.3:** Synthesis of precatalyst [(dcpP)Ni(toluene)] **II-4**.<sup>[1]</sup>

Interestingly, Nobile already reported the reduction of [(dcpP)NiCl<sub>2</sub>] **II-3** by stoichiometric amounts of sodium sand in toluene in 1992 and suggested the formation of the divalent 14 electron complex [(dcpP)Ni] on the basis of elemental analysis.<sup>[4]</sup> However, the experimental data and especially the <sup>31</sup>P{<sup>1</sup>H} NMR rather indicate the formation of [(dcpP)NiH]<sub>2</sub> **II-5** as the main compound. Indeed, [(dcpP)NiH]<sub>2</sub> **II-5** is characterized by a singlet at  $\delta = 25.0$  ppm in <sup>31</sup>P{<sup>1</sup>H} NMR and a quintet at  $\delta = -10.8$  ppm in <sup>1</sup>H NMR.<sup>[5]</sup> The small amounts of nickel dihydride **II-5** most likely originate from C<sub>sp2</sub> or C<sub>sp3</sub> activation of toluene in [(dcpP)Ni(toluene)] **II-4**. GC-MS analysis of the reaction mixture shows a peak at  $m/z = 182.26$  corresponding to a C<sub>14</sub>H<sub>14</sub> compound, which can be either 4,4'-dimethyl-biphenyl or 1,2-diphenylethane. Upon formation of one of these organic compounds, H<sub>2</sub> is released and trapped by the [(dcpP)Ni]-fragment.

[(dcpP)Ni(toluene)] **II-4** is characterized in <sup>31</sup>P{<sup>1</sup>H} NMR by a singlet at  $\delta = 15.4$  ppm. Despite the coordination of the asymmetric toluene molecule, the two phosphorus atoms are in an apparent equivalent chemical environment. Low temperature NMR experiments were carried out down to -80 °C but the fast equilibration process could not be slowed down. In addition, the integrations in <sup>1</sup>H NMR suggests the coordination of only one toluene ligand per [(dcpP)Ni]-fragment, ruling out a bridged structure, as the one observed by Pörschke for [(dtbpe)Ni]<sub>2</sub>(C<sub>6</sub>H<sub>6</sub>).<sup>[3]</sup>



Single crystals for X-ray diffraction analysis were grown from a concentrated [(dcpp)Ni(toluene)] **II-4** solution at -25 °C. The structure confirms the monomeric nature of the complex as well as the  $\eta^2$  coordination of the toluene ligand. The methyl group of toluene is found to occupy preferentially a *meta* position. The C<sub>1</sub>-C<sub>2</sub> coordinating bond of toluene measures 1.442(2) Å and is only slightly elongated compared to free toluene (1.39 Å). This indicates a weak donation of the [(dcpp)Ni]-fragment in the C-C bond and a poor coordination of the ligand in good agreement with its high sensitivity and reactivity. The bite angle P<sub>1</sub>-Ni<sub>1</sub>-P<sub>2</sub> measures 104.10(4) ° and is larger by 4.7 ° compared to the bite angle of Ni(II) complex [(dcpp)NiCl<sub>2</sub>] **II-3**, proving the flexibility of the dcpp ligand.

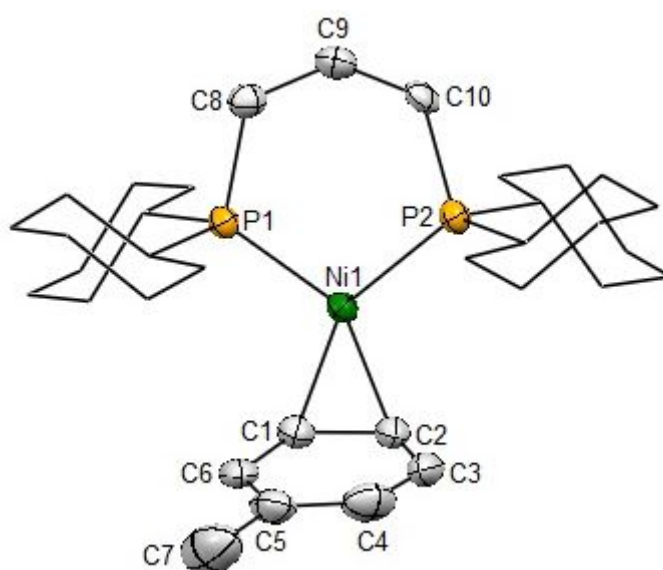
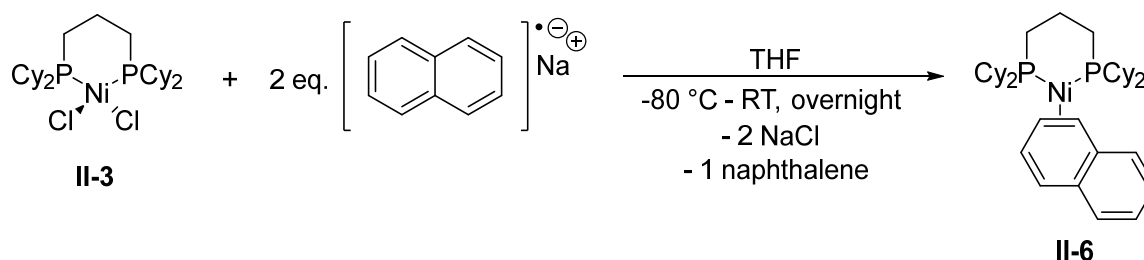


**Figure 2.2:** Molecular structure of [(dcpp)Ni(toluene)] **II-4** determined by single crystal X-ray diffraction. Hydrogen atoms are omitted for clarity. Selected bond length [Å] and angles [°]: Ni<sub>1</sub>-P<sub>1</sub> 2.1465(11), Ni<sub>1</sub>-P<sub>2</sub> 2.1558(12), Ni<sub>1</sub>-C<sub>1</sub> 2.001(4), Ni<sub>1</sub>-C<sub>2</sub> 1.993(4), C<sub>1</sub>-C<sub>2</sub> 1.425(6), C<sub>2</sub>-C<sub>3</sub> 1.413(6), C<sub>3</sub>-C<sub>4</sub> 1.347(6), C<sub>4</sub>-C<sub>5</sub> 1.422(6), C<sub>5</sub>-C<sub>6</sub> 1.353(6), C<sub>5</sub>-C<sub>7</sub> 1.519(6), P<sub>1</sub>-Ni<sub>1</sub>-P<sub>2</sub> 104.10(4), C<sub>1</sub>-Ni<sub>1</sub>-C<sub>2</sub> 41.80(16).

[(dcpp)Ni(toluene)] **II-4** is particularly suitable for catalysis and mechanistic investigations due to its good solubility and high reactivity. Applications in Negishi cross coupling reactions will therefore be discussed in the rest of the chapter. Nevertheless, the difficulties encountered during its synthesis and its high temperature and air sensitivity, prompted the research group to develop alternative complexes. [(dcpp)Ni(naphthalene)] **II-6**, synthesized by Florian D'Accriscio during his PhD thesis, results from the two electron reduction of [(dcpp)NiCl<sub>2</sub>] **II-3** by 2 eq. of sodium naphthalenide, as shown in **Scheme 2.4**.<sup>[2]</sup> [(dcpp)Ni(naphthalene)] **II-6**

is easier to handle than [(dcp)Ni(toluene)] **II-4** and can be kept as a solid at RT over long period of time. <sup>[6]</sup>



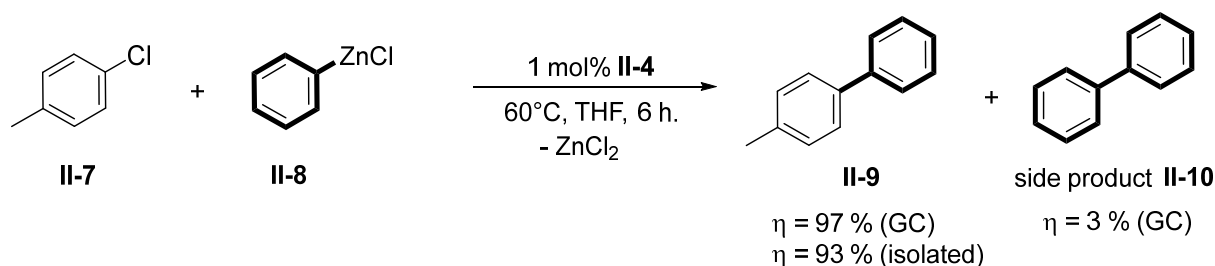
**Scheme 2.4:** Synthesis of [(dcp)Ni(naphthalene)] **II-6**. <sup>[6]</sup>

## 2.2. Negishi cross coupling

### 2.2.1 Testing [(dcp)Ni(toluene)] **II-4** in Negishi cross coupling

The catalytic activity of the highly reactive [(dcp)Ni(toluene)] complex **II-4** was tested in Negishi cross coupling reactions. Cheap and commercially available aryl chlorides were chosen as electrophiles. The coupling of aryl chlorides still remains challenging because of the larger bond dissociation energy (BDE) of C-Cl bonds ( $95 \text{ kcal}\cdot\text{mol}^{-1}$ ) <sup>[7]</sup> compared to C-Br ( $79 \text{ kcal}\cdot\text{mol}^{-1}$ ) <sup>[7]</sup> or C-I bonds ( $64 \text{ kcal}\cdot\text{mol}^{-1}$ ), <sup>[7]</sup> which makes the oxidative addition to a metal(0) complex more difficult.

In a first test 4-chlorotoluene **II-7** is reacted with phenylzinc chloride **II-8** in the presence of 1 mol% of [(dcp)Ni(toluene)] **II-4**, as shown in **Scheme 2.5**. Most satisfyingly the expected biphenyl **II-9** is obtained in 97 % GC-yield together with 3 % of homocoupled product **II-10** after 6 h. at 60 °C. After work-up, 4-methylbiphenyl **II-9** could be isolated in 93 % yield.



**Scheme 2.5:** [(dcp)Ni(toluene)] **II-4** catalyzed Negishi cross coupling between 4-chlorotoluene **II-7** and phenylzinc chloride **II-8**.

When the amount of nickel complex is reduced to 0.2 mol%, this model reaction performs slower: 19 h. are required to complete the reaction. At 0.01 % catalyst loading, the yield reaches 21 % after 58 h. and 47 % after 138 h., while the turnover frequency (TOF) keeps constant at 35 h<sup>-1</sup>. This proves that the catalyst remains active over long periods of time and does not undergo any decomposition. The results are summarized in **Table 2.1**.

**Table 2.1:** Optimization of the reaction conditions: varying the catalyst loading.

Entry	Catalyst loading (mol%)	Reaction time (h)	Conversion (%)	TOF (h <sup>-1</sup> )
1	1	6	97	17
2	0.2	19	98	26
3	0.01	58	21	36
4	0.01	138	47	34

## 2.2.2 Reaction scope

With these efficient conditions in hand, the scope of the reaction was explored. The following experiments were performed using 0.2 mol% of [(dcp)Ni(toluene)] **II-4**.

First of all, the electronic nature of the *para* substituent of the aryl chloride is modulated. As expected, electron donating groups on the electrophile, such as methyl or methoxy moieties, slow down the reaction. At 0.2 mol% of [(dcp)Ni(toluene)] **II-4**, the reaction is complete within 16 h. for chlorobenzene **II-11**, 19 h. for 4-chlorotoluene **II-7** and 32 h. for 4-chloroanisole (**Entry 3 - 5**). On the other hand, electron withdrawing groups like, a methyl ester or a CF<sub>3</sub> unit, considerably increase the reaction rate. Full conversion is reached within only 1 h. for 4-chlorotrifluorotoluene **II-12** and 6 h. for methyl 4-chlorobenzoate (**Entry 1 - 2**). All the results are collected in **Table 2.2**.

**Table 2.2:** Influence of the *para* substituent of the aryl chloride on the reaction time.

Entry	<i>para</i> substituent	Reaction time (h)	Isolated yield (%)
1	CF <sub>3</sub>	1	94
2	CO <sub>2</sub> Me	6	92
3	H	16	98
4	CH <sub>3</sub>	19	93
5	OMe	32	90

Afterwards, the electronic properties of the zinc derivative are varied. As commonly observed, adding an electron rich methoxy substituent on the *para* position of the nucleophilic reagent results in faster coupling. **Table 2.3** compares the reaction times between cross couplings carried out with PhZnCl **II-8** and 4-OMePhZnCl **II-13**. For example, 4-chlorotoluene **II-7** is coupled within 19 h. with PhZnCl **II-8** whereas only 8 h. are required with 4-OMePhZnCl **II-13** (**Entry 4**). Similarly, the reaction time decreases from 6 h. to 1 h. 30 min. for methyl 4-chlorobenzoate by switching from the electron neutral to the electron rich phenyl chloride (**Entry 2**).

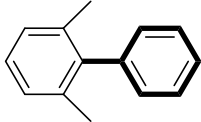
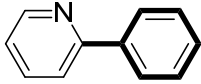
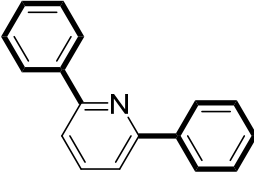
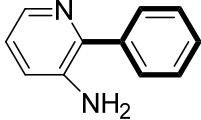
**Table 2.3:** Comparison between the reaction times of [(dcpp)Ni(toluene)] **II-4** catalyzed Negishi cross coupling using either PhZnCl **II-8** or OMe-PhZnCl **II-13**.

Entry	<i>para</i> substituent	Reaction time (h)		Yield (%)	
		PhZnCl	4-OMe-PhZnCl	PhZnCl	4-OMe-PhZnCl
1	CF <sub>3</sub>	1	0.5	94	91
2	CO <sub>2</sub> Me	6	1.5	92	89
3	H	16	4	98	90
4	CH <sub>3</sub>	19	8	93	88

By increasing the catalyst loading to 1 mol% more challenging substrates could also be efficiently coupled within short reaction times. The reaction between the *ortho* disubstituted 2,6-dimethylphenyl chloride and PhZnCl **II-8** affords the corresponding biphenyl in 75 % yield after 7 h.

Moreover, several chloropyridines also proved to be good coupling partners. For example, 2-chloropyridine is coupled with PhZnCl **II-8** in 96 % isolated yield in only 2 h. The reaction does even tolerate functional amino groups. When 2-chloro-3-amino-pyridine undergoes Negishi cross coupling, 90 % of 2-phenyl-3-aminopyridine are isolated after 4 h. The results are summarized in **Table 2.4**.

**Table 2.4:** [(dcpp)Ni(toluene)] **4** catalyzed Negishi cross coupling of challenging substrates.

Entry	R-PhCl	Product	Reaction time (h)	Isolated yield (%)
1	2,6-(Me) <sub>2</sub> PhCl		7	75
2	2-ClPy		2	96
3	2,6-Cl <sub>2</sub> Py		6	58
4	2-Cl-3-NH <sub>2</sub> Py		4	90

In summary, the [(dcpp)Ni(toluene)] **II-4** catalyzed Negishi cross couplings between aryl chlorides and phenyl zinc chloride derivatives allow the formation of biaryl compounds in good yields, under mild conditions and with low catalyst loading. While [(dcpp)Ni(toluene)] **II-4** cannot compete with Wang's nickel amido pincer complexes,<sup>[8]</sup> it still gets close to the performance of Frech's [NiCl<sub>2</sub>]/1,1',1''-(phosphanetriyl)tripiperidine system<sup>[9]</sup> and figures among highly efficient catalysts for the Negishi cross coupling of aryl chlorides.

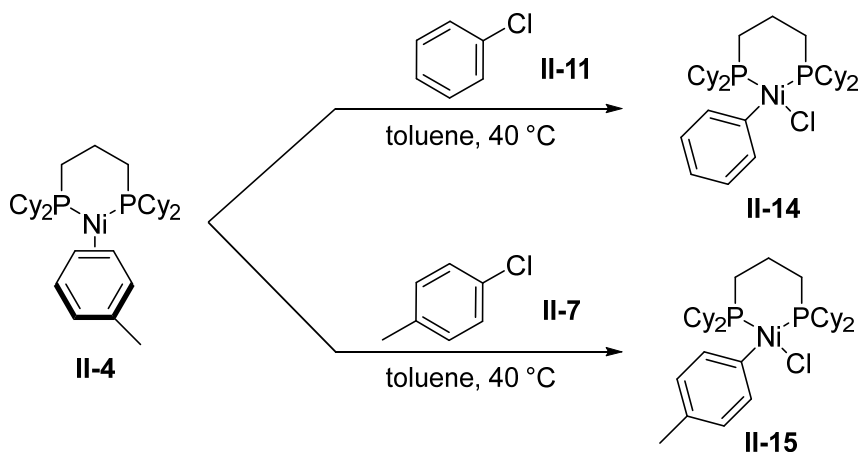
## 2.3 Mechanistic investigations

### 2.3.1 Stoichiometric reactions

Mechanistic investigations are undertaken in order to determine whether the reaction with the strongly donating bidentate dcpp ligand is going through a Ni(0)/Ni(II) or a Ni(I)/Ni(III) catalytic cycle. Stoichiometric reactions are carried out to study the feasibility and the outcome of each elementary step of the reaction, namely oxidative addition, transmetallation and reductive elimination.

## 2.3.1.1 Oxidative addition

The oxidative addition was examined first.  $[(\text{dcpp})\text{Ni}(\text{toluene})]$  **II-4** has been reacted with chlorobenzene **II-11** at 40 °C, resulting in the oxidative addition of the C-Cl bond to the nickel center and quantitative formation of the Ni(II) complex  $[(\text{dcpp})\text{Ni}(\text{Ph})(\text{Cl})]$  **II-14**, as represented in **Scheme 2.6**.



**Scheme 2.6:** Oxidative addition of aryl chlorides to  $[(\text{dcpp})\text{Ni}(\text{toluene})]$  **II-4**.

$[(\text{dcpp})\text{Ni}(\text{Ph})(\text{Cl})]$  **II-14** is characterized by two sets of doublets in  $^{31}\text{P}\{^1\text{H}\}$  NMR at  $\delta = 5.8$  ppm and  $\delta = 19.0$  ppm with a coupling constant of  $^2J_{\text{P},\text{P}} = 48.4$  Hz. Single crystals for X-ray diffraction analysis have been grown from a THF solution layered with pentane at -25 °C.  $[(\text{dcpp})\text{Ni}(\text{Ph})(\text{Cl})]$  **II-14** crystallizes in the P-1 centrosymmetric space group and has a square planar geometry in agreement with its diamagnetism as shown in **Figure 2.3**. The analogous  $[(\text{dcpp})\text{Ni}(\text{tolyl})(\text{Cl})]$  **II-15** complex can be similarly obtained from the oxidative addition of 4-CH<sub>3</sub>PhCl **II-7** to the  $[(\text{dcpp})\text{Ni}(0)]$ -fragment. These two experiments prove that the oxidative addition of aryl chlorides to  $[(\text{dcpp})\text{Ni}(\text{toluene})]$  **II-4** is a low energy process.

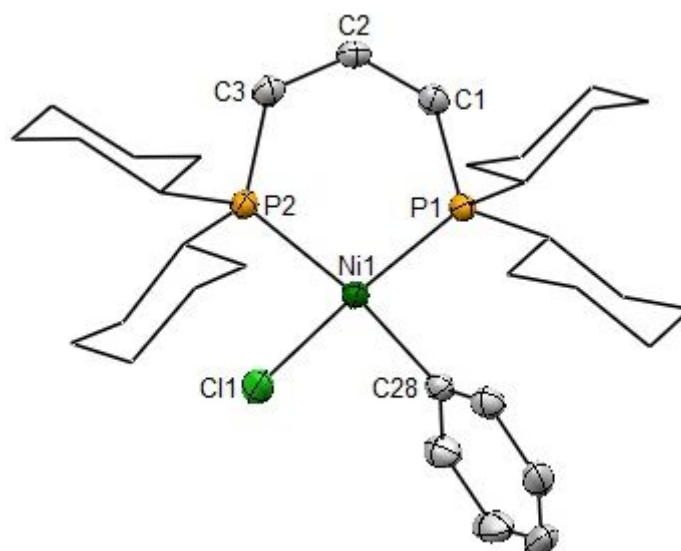
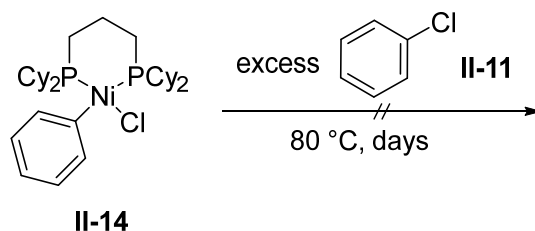


**Figure 2.3:** Molecular structure of [(dcpp)Ni(Ph)(Cl)] **II-14** determined by single crystal X-ray diffraction. Hydrogen atoms are omitted for clarity. Selected bond length [Å] and angles [°]: Ni<sub>1</sub>-P<sub>1</sub> 2.1565(4), Ni<sub>1</sub>-P<sub>2</sub> 2.2528(4), Ni<sub>1</sub>-C<sub>28</sub> 1.9292(15), Ni<sub>1</sub>-Cl<sub>1</sub> 2.2170(4), P<sub>1</sub>-Ni<sub>1</sub>-P<sub>2</sub> 98.086(16), C<sub>28</sub>-Ni<sub>1</sub>-Cl<sub>1</sub> 86.42(4).

At this point it is important to verify that the oxidative addition product [(dcpp)Ni(Ph)(Cl)] **II-14** is not involved in side reactions leading to homocoupling. Furthermore, it is essential to determine whether a transmetalation or a single electron transfer (SET) is more favorable at this stage of the reaction.

Kochi reported in the late 1970s the biaryl formation from the coupling between the monophosphine substituted oxidative addition product [(PEt<sub>3</sub>)<sub>2</sub>Ni(Ar)(Br)] and aryl bromides. The reaction is initiated by a single electron transfer (SET) from the trans-arylnickel(II) halide complex to the aryl bromide and proceeds then through Ni(I) and Ni(III) intermediates. This SET process is kinetically more favorable than the transmetalation/reductive elimination sequence.<sup>[10, 11]</sup> Colon and Kelsey analogously showed in 1986 that the nickel catalyzed coupling between two arylchlorides in the presence of a reducing metal such as zinc involves the reduction of the arylnickel(II) halide by the metal into an arylnickel(I) active species.<sup>[12]</sup>

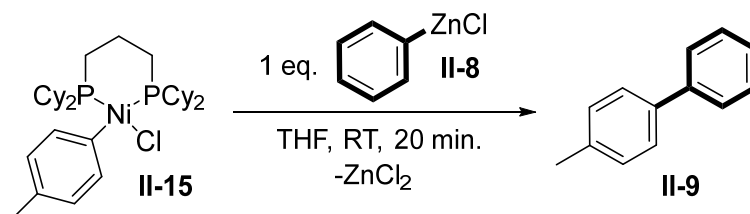
Therefore, the possibility of a redox reaction between the Ni(II) complex [(dcpp)Ni(Ph)(Cl)] **II-14** and an aryl chloride was investigated. However, when [(dcpp)Ni(Ph)(Cl)] **II-14** is heated for days at 80 °C with an excess of chlorobenzene **II-11**, no reaction is observed. The strong coordination of the bidentate phosphine prevents the reduction to a Ni(I) species and subsequent formation of homocoupled product **II-10** and shuts down a Ni(I)/Ni(III) catalytic cycle.



**Scheme 2.7:** Absence of redox reaction between the oxidative addition product [(dcpP)Ni(Ph)(Cl)] **II-14** and chlorobenzene **II-11**.

### 2.3.1.2 Transmetallation and reductive elimination

The focus is then laid on transmetallation and reductive elimination. The addition of 1 eq. of transmetallating reagent PhZnCl **II-8** to [(dcpP)Ni(tolyl)(Cl)] **II-15** leads to quantitative formation of the expected cross coupled product, 4-methylbiphenyl **II-9**, at RT within 20 min. During the reaction no homocoupled product (biphenyl **II-10**) is produced, confirming the lack of Ni(I) intermediates. This reaction therefore demonstrates that both the transmetallation and the reductive elimination are easily achievable and have low activation barriers.

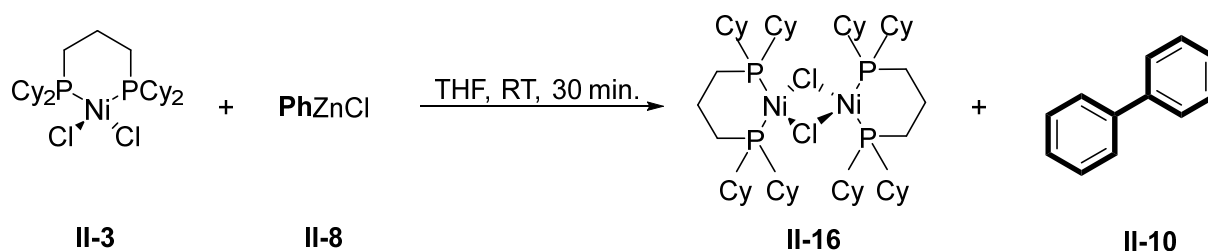


**Scheme 2.8:** Reaction between [(dcpP)Ni(tolyl)(Cl)] **II-15** and PhZnCl **II-8** at RT.

### 2.3.1.3 Synthesis and reactivity of Ni(I) complex [(dcpP)NiCl]<sub>2</sub> **II-16**

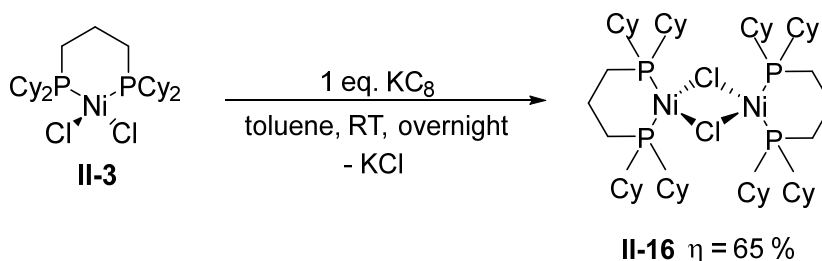
When [(dcpP)NiCl<sub>2</sub>] **II-3** is reacted with stoichiometric amounts of PhZnCl **II-8**, the Ni(I) dimer [(dcpP)NiCl]<sub>2</sub> **II-16** is formed together with biphenyl **II-10** and crystallizes out of the solution at RT. This Ni(I) complex (**II-16**) is the product of the comproportionation between Ni(0) and Ni(II) species, that occurs faster than the transmetallation with PhZnCl **II-8**. Similar Ni(I) dimers are already known and have also been previously synthesized through the comproportionation of various Ni(0) and [(bis-phosphine)NiCl<sub>2</sub>] complexes. <sup>[2, 13]</sup>





**Scheme 2.9:** Reactivity between [(dcppe)NiCl<sub>2</sub>] **II-3** and a stoichiometric amount of PhZnCl **II-8**: generation of the Ni(I) dimer [(dcppe)NiCl]<sub>2</sub> **II-16**.

Alternatively to the comproportionation, Ni(I) complexes can be obtained from the reaction between Ni(II) precursors and reducing agents such as sodium and potassium naphthalenide<sup>[13]</sup> or K<sub>C<sub>8</sub></sub>.<sup>[14]</sup> The one electron reduction of [(dcppe)NiCl<sub>2</sub>] **II-3** by 1 eq. of K<sub>C<sub>8</sub></sub>, reported by Matthieu Demange, produces the desired [(dcppe)NiCl]<sub>2</sub> dimer **II-14** in 65 % yield.<sup>[1]</sup>



**Scheme 2.10:** Synthesis of [(dcppe)NiCl]<sub>2</sub> **II-16**.<sup>[1]</sup>

The X-band EPR spectrum of paramagnetic [(dcppe)NiCl]<sub>2</sub> **II-16** was recorded at RT. A *g*-factor of 2.154 and a hyperfine coupling constant  $A_{\text{iso}}(^{31}\text{P}, n = 2) = 72.2 \text{ G}$  were determined. These parameters are in good agreement with the data previously measured by Hillhouse for the related [(dtbpe)NiCl]<sub>2</sub> complex.<sup>[15]</sup>

In addition, the crystal structure of the dimer **II-16** could be resolved by X-ray diffraction analysis.<sup>[1]</sup> Two [(dcppe)nickel]-fragments are linked together by two bridging chlorides. Both Ni(I) centers are in a tetrahedral environment and no interaction is observed between both metallic atoms. The distance between both nickel centers (3.3134 Å) is greater than the sum of their van der Waals radii (3.26 Å).

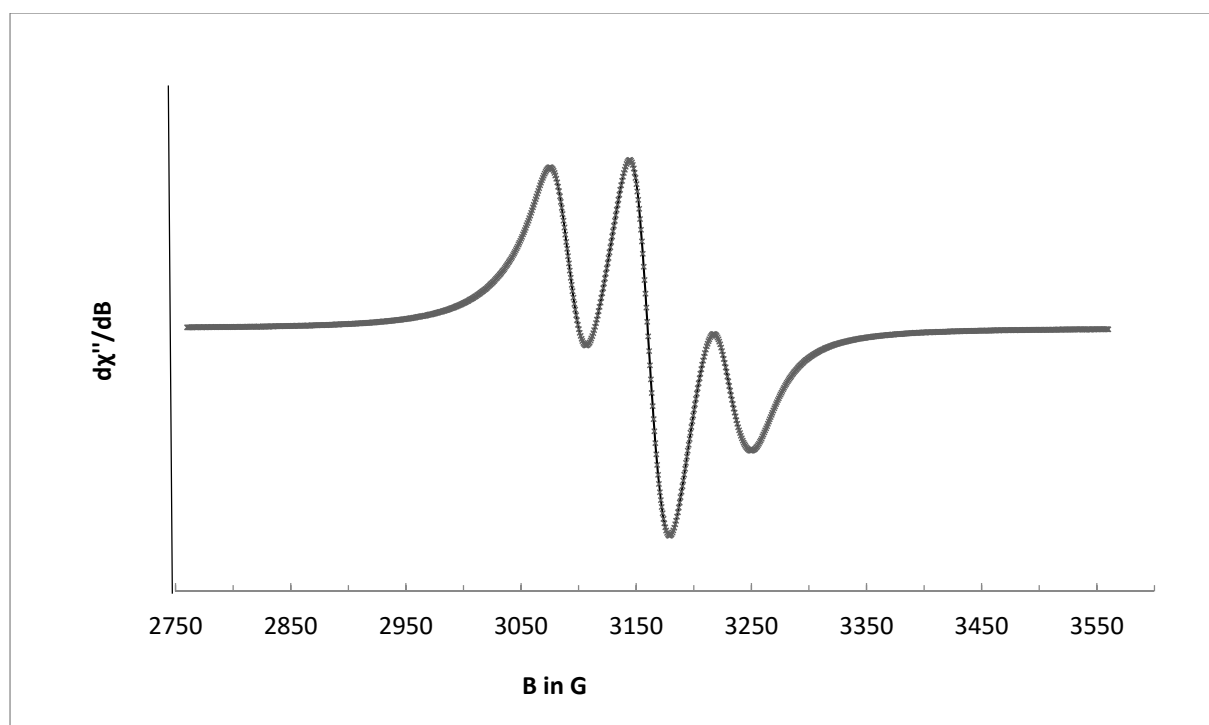


**Figure 2.4:** Room Temperature X-Band EPR Spectrum of Ni(I) complex  $[(\text{dcpp})\text{NiCl}]_2$  **II-16**.

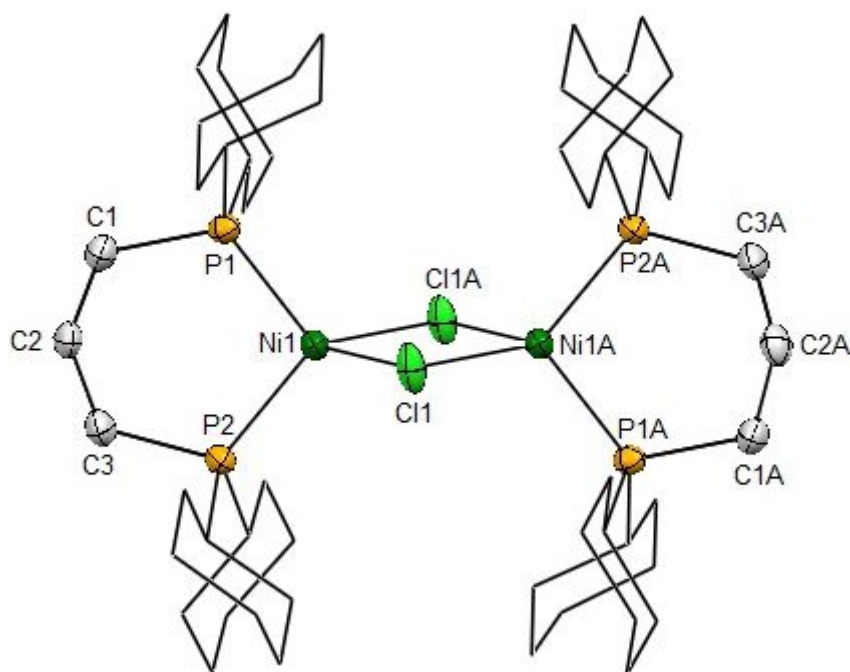
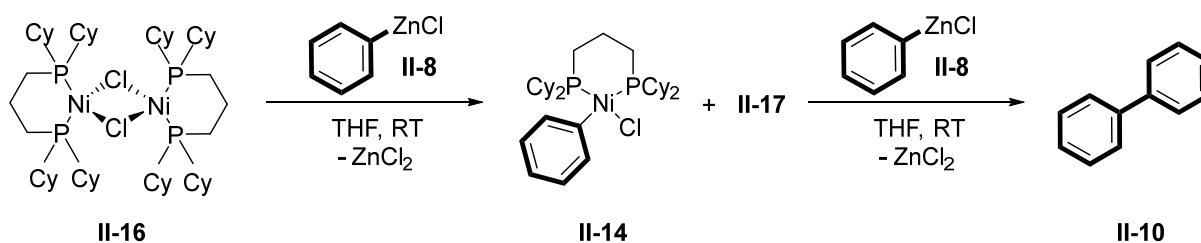


**Figure 2.5:** Molecular structure of  $[(\text{dcpp})\text{NiCl}]_2$  **II-16** determined by single crystal X-ray diffraction. Hydrogen atoms are omitted for clarity. Selected bond length [ $\text{\AA}$ ] and angles [ $^\circ$ ]:  $\text{Ni}_1\text{-P}_1$  2.1856(4),  $\text{Ni}_1\text{-P}_2$  2.1918(4),  $\text{Ni}_1\text{-Cl}_1$  2.3779(4),  $\text{Ni}_1\text{-Cl}_{1A}$  2.3361(4),  $\text{Ni}_{1A}\text{-Cl}_1$  2.3361(4),  $\text{P}_1\text{-Ni}_1\text{-P}_2$  101.721(17),  $\text{Cl}_1\text{-Ni}_1\text{-Cl}_{1A}$  90.688(15).

The reactivity of the dimeric Ni(I) complex  $[(\text{dcpp})\text{NiCl}]_2$  **II-16** has been investigated to further rule out the involvement of a Ni(I)/Ni(III) catalytic cycle.

$[(\text{dcpp})\text{NiCl}]_2$  **II-16** does not react with an excess of chlorobenzene **II-11** in toluene even after days at RT. However, when  $[(\text{dcpp})\text{NiCl}]_2$  **II-16** is reacted with a stoichiometric amount of  $\text{PhZnCl}$  **II-8**,  $[(\text{dcpp})\text{Ni}(\text{Ph})(\text{Cl})]$  **II-14** and a new compound characterized by a singlet at  $\delta = 56.0$  ppm in  $^{31}\text{P}\{^1\text{H}\}$  NMR (**II-17**) are formed at RT within minutes. This mixture rapidly evolves as  $[(\text{dcpp})\text{Ni}(\text{Ph})(\text{Cl})]$  **II-14** further reacts with  $\text{PhZnCl}$  **II-8** to give the homocoupled product  $\text{Ph-Ph}$  **II-10**, which is identified by GC-MS spectrometry. Unfortunately, the second compound at  $\delta = 56.0$  ppm **II-17** could not be separated from the other products or crystallized and remains therefore unidentified.



**Scheme 2.11:** Reaction between Ni(I) complex  $[(\text{dcpp})\text{NiCl}]_2$  **II-16** and  $\text{PhZnCl}$  **II-8**.

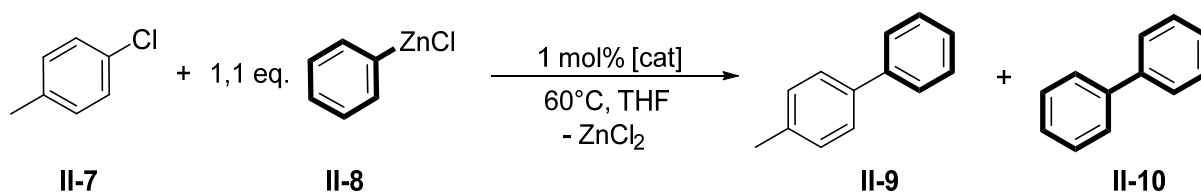
This experiment shows that the  $[(\text{dcpp})\text{nickel}]$ -system, readily evolves from Ni(I) compounds to mixtures of diamagnetic Ni(II) and/or Ni(0) complexes in the presence of  $\text{PhZnCl}$  **II-8**. It also provides an explanation for the formation of minor amounts of homocoupled product **II-10** during the catalysis, which thus involves the intermediacy of Ni(I) complexes.

Hence, these stoichiometric reactions show that all elementary steps of the catalytic cycle: oxidative addition, transmetalation and reductive elimination are facile at RT and in agreement with the mild catalysis conditions. Ni(0) and Ni(II) intermediates could be observed and/or isolated from the independent reaction steps and are favored over Ni(I) complexes.

### 2.3.2 Catalytic activity of Ni(0), Ni(I) and Ni(II) precursors

All catalytic reactions presented above in **2.2** are carried out using the highly sensitive Ni(0) precatalyst  $[(\text{dcpp})\text{Ni}(\text{toluene})]$  **II-4**. The catalytic activity of various nickel complexes in

different oxidation states is then tested to confirm the involvement of a Ni(0)/Ni(II) catalytic cycle. The Negishi coupling between 4-chlorotoluene **II-7** and PhZnCl **II-8** at 1 mol% of catalyst in THF at 60 °C is chosen as standard reaction for the comparison of the catalysts. The results can be found in **Table 2.5**.



**Scheme 2.12:** Standard reaction conditions chosen for the nickel catalyzed Negishi cross coupling to compare various catalysts.

It is first verified that more easily manipulated Ni(II) complexes give similar results to [(dcpp)Ni(toluene)] **II-4**. The precatalyst [(dcpp)NiCl<sub>2</sub>] **II-3** and the isolated oxidative addition intermediate [(dcpp)Ni(Ph)(Cl)] **II-14** produce respectively 97 % and 95 % GC yield of cross coupled product **II-9** together with 3 % and 5 % homocoupled product **II-10** within 6 h., supporting a Ni(0)/Ni(II) active catalytic cycle.

However, when the isolated Ni(I) complex [(dcpp)NiCl]<sub>2</sub> **II-16** is used instead, the reaction performs sluggishly, reaching 40 % conversion after 72 h. The coupling is also less selective affording only 7 % of the desired 4-methylbiphenyl **II-9** and 33 % of biphenyl **II-10**, the homocoupled product. This specific Ni(I) complex **II-16** is not an active species of the catalysis and demonstrates that a Ni(I)/Ni(III) cycle is much less efficient for this transformation.

**Table 2.5:** Comparison of the conversion of the Negishi cross coupling reactions performed with nickel precursors at different oxidation states.

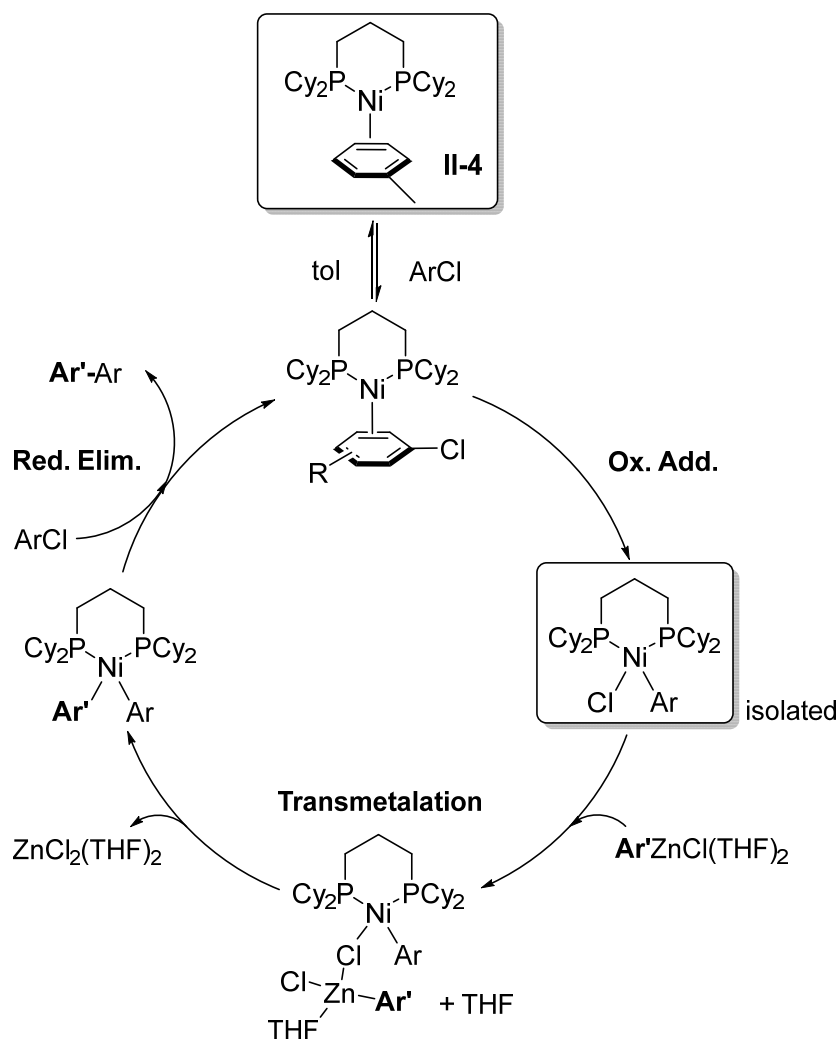
Entry	Oxidation state	Catalyst	Time (h.)	% Conv.	
				4-CH <sub>3</sub> Ph-Ph	Ph-Ph
1	Ni(0)	[(dcpp)Ni(toluene)] <b>II-4</b>	6	97	3
2	Ni(II)	[(dcpp)NiCl <sub>2</sub> ] <b>II-3</b>	5	97	3
3	Ni(II)	[(dcpp)Ni(Ph)(Cl)] <b>II-14</b>	6	95	5
4	Ni(I)	[(dcppNiCl) <sub>2</sub> ] <b>II-16</b>	72	7	33

These results are in contrast to previously reported nickel catalyzed Negishi cross couplings, which are shown to involve Ni(I)/Ni(III) cycles with different ligand systems.<sup>[11, 16 - 18]</sup> Nevertheless, in parallel to these investigations, Hartwig demonstrated in 2014 that the use of [(BINAP)Ni( $\eta^2$ -NC-Ph)] (BINAP = 2,2'-bis(diphenylphosphino)-1,1'-binaphthyl) in the catalytic coupling of aryl chlorides with amines and ammonia also enforces a Ni(0)/Ni(II) reaction pathway.<sup>[19, 20]</sup>

### 2.3.3 Proposed catalytic cycle

In light of the performed stoichiometric and catalytic reactions, a catalytic cycle is proposed in **Scheme 2.13** for the [(dcpp)Ni(toluene)] **II-4** catalyzed Negishi cross coupling between aryl halides and phenyl zinc chloride derivatives. The reaction consists of three elementary steps: oxidative addition of the aryl chloride to [(dcpp)Ni(0)], transmetallation at [(dcpp)Ni(Ar)(Cl)] with Ar'ZnCl and reductive elimination from [(dcpp)Ni(Ar)(Ar')]. All these elementary steps are achievable under mild conditions and involve either Ni(0) or Ni(II) intermediates.

In order to identify the resting state of the catalyst, the reaction of 4-chlorotrifluorotoluene **II-12** with PhZnCl **II-8** catalyzed by 1 mol% of [(dcpp)Ni(toluene)] **II-4** is monitored at 60 °C by <sup>31</sup>P{<sup>1</sup>H} NMR spectroscopy. The only species observed throughout the reaction, at 30 %, 70 % and at *ca.* full conversion, is characterized by two doublets at  $\delta = 5.9$  ppm and  $\delta = 19.7$  ppm, with  $^2J_{P,P} = 56.0$  Hz. This complex displays almost identical spectroscopic features to [(dcpp)Ni(4-CF<sub>3</sub>Ph)(Cl)] **II-18**, that is, two doublets at  $\delta = 5.9$  ppm and  $\delta = 19.3$  ppm, with  $^2J_{P,P} = 53.0$  Hz in C<sub>6</sub>D<sub>6</sub>. It might either correspond to the oxidative addition product [(dcpp)Ni(4-CF<sub>3</sub>Ph)(Cl)] **II-18** or to the heterobimetallic adduct with PhZnCl **II-8** [(dcpp)Ni(4-CF<sub>3</sub>Ph)( $\mu$ -Cl)Zn(Cl)(Ph)(THF)], making the transmetallation the rate determining step of the reaction. In contrast to Hartwig's [(BINAP)Ni( $\eta^2$ -NC-Ph)] complex that evolves to [(BINAP)<sub>2</sub>Ni] during the course of the catalysis,<sup>[19]</sup> the dcpp ligand prevents the decomposition of the catalyst.



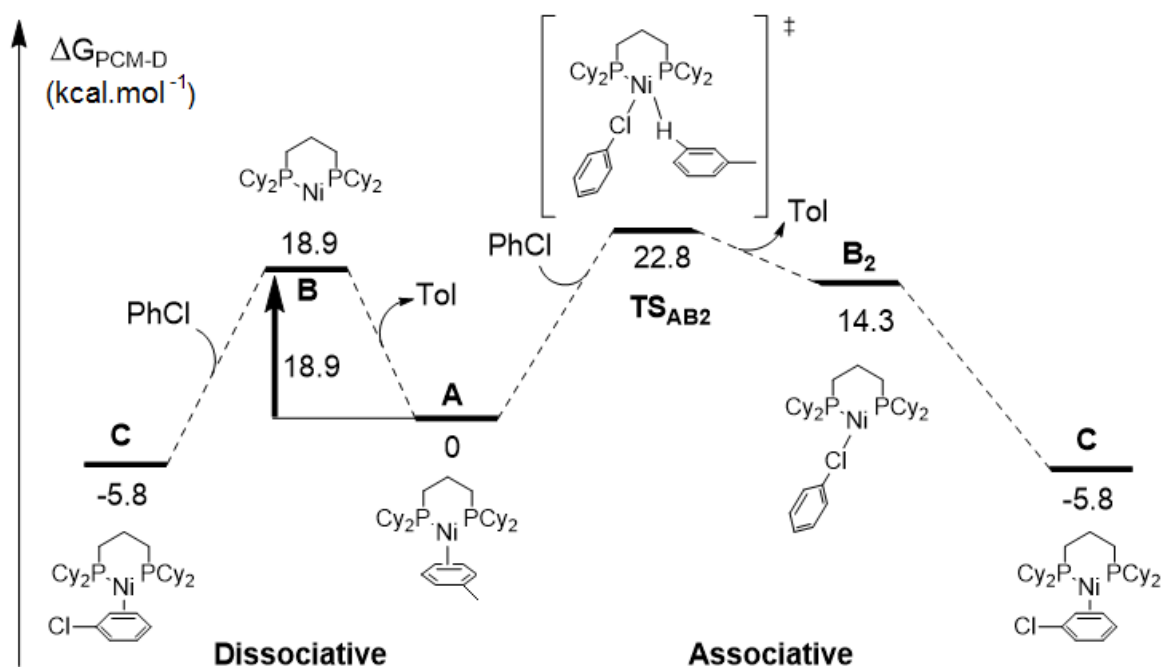
**Scheme 2.13:** Proposed mechanism for the  $[(\text{dcpp})\text{Ni}(\text{toluene})]$  II-4 catalyzed Negishi cross coupling, suggested by the stoichiometric and catalytic investigations.

## 2.4 DFT calculations

The mechanism of the reaction was additionally investigated by DFT calculations. This study further supports the feasibility of the Ni(0)/Ni(II) catalytic cycle presented above in 2.3.3. The calculations were performed with the Gaussian09 suite of software,<sup>[21]</sup> using the B3PW91 functional,<sup>[22, 23]</sup> the 6-31G\* basis set for all non-metallic atoms<sup>[24]</sup> and the all-electron Def2-TZVP basis set for nickel and zinc.<sup>[25]</sup> Single point calculations allowed to take into account the solvent's effects and the dispersion interactions. In this paragraph the numbering of the molecules will be replaced by the letters **A - H** used for the calculations.

### 2.4.1 Coordination of chlorobenzene

The entry into the catalytic cycle was computed first as shown in **Scheme 2.14**. During this step the toluene ligand of the Ni(0) precatalyst  $[(\text{dcpp})\text{Ni}(\text{toluene})]$  **A** is displaced by the aryl chloride. Two possible mechanisms have been considered: a dissociative and an associative one, which lie close in energy.



**Scheme 2.14:** Reaction pathways for the coordination of chlorobenzene **II-11**.

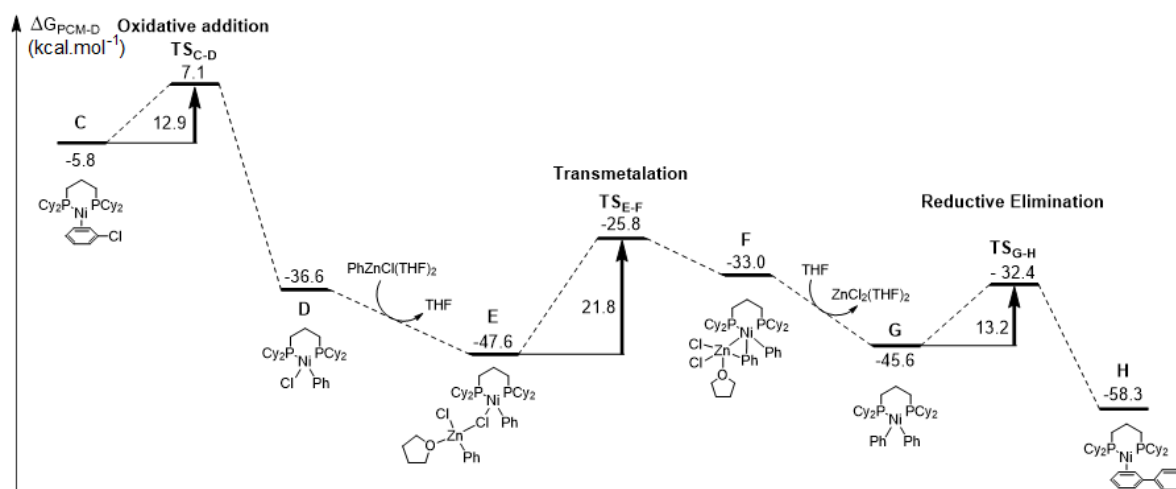
The dissociation of the labile  $\eta^2$  coordinated toluene from the 16 electron complex  $[(\text{dcpp})\text{Ni}(\text{toluene})]$  **A** generates a highly reactive 14 electron nickel fragment **B**. The activation barrier for this process reaches  $18.9 \text{ kcal.mol}^{-1}$ , which means that the energy required to enter the catalytic cycle is low. Upon addition of an aryl chloride,  $\eta^2$  coordinated 16 electron complex  $[(\text{dcpp})\text{Ni}(\text{PhCl})]$  **C** is obtained. The Ni(0) complex **C** lies  $5.8 \text{ kcal.mol}^{-1}$  lower in energy compared to **A**.

The associative mechanism involves an 18 electron transition state  $\text{TS}_{\text{AB2}}$ , which features both the departing toluene and the incoming aryl chloride as  $\eta^1$  ligands. Evolution to complex **C**  $[(\text{dcpp})\text{Ni}(\text{PhCl})]$  occurs through the  $\eta^1$  coordinated intermediate **B<sub>2</sub>**. The overall activation barrier for this pathway reaches  $22.8 \text{ kcal.mol}^{-1}$  and makes it therefore less favorable by  $3.9 \text{ kcal.mol}^{-1}$  than the previously described dissociative mechanism.

However, the entropy is inaccurately taken into account by DFT calculations. As the entropy increases in the dissociative mechanism but decreases in the associative mechanism through the transition state  $\text{TS}_{\text{AB2}}$ , it is overall difficult to draw any conclusion on the most favorable pathway.

## 2.4.2 Catalytic process

In the next step, the catalytic process itself was computed as depicted in **Scheme 2.15**. The  $\eta^2$  coordinated  $[(\text{dcpp})\text{Ni}(\text{PhCl})]$  complex **C** undergoes oxidative addition in the C-Cl bond, leading to Ni(II) complex  $[(\text{dcpp})\text{Ni}(\text{Ph})(\text{Cl})]$  **D**, which has been experimentally isolated. The transition state  $\text{TS}_{\text{C-D}}$  has been calculated to be  $12.9 \text{ kcal.mol}^{-1}$  higher in energy than **C**, which is very low considering the difficulty usually encountered to perform the oxidative addition in C-Cl bonds. This demonstrates the electron rich nature of the  $[(\text{dcpp})\text{Ni}]$ -fragment. The reaction is extremely exergonic, liberating  $30.8 \text{ kcal.mol}^{-1}$ .



**Scheme 2.15:** Reaction pathway for one catalytic cycle starting from the aryl chloride complex **C**.

Afterwards, the organozinc reagent  $\text{PhZnCl}(\text{THF})_2$  coordinates to **D** and forms the heterobimetallic complex **E**, which lies  $9.0 \text{ kcal.mol}^{-1}$  lower in energy. Explicit THF molecules have been taken into account in order to maintain the zinc atom in a tetrahedral geometry. In complex **E**, the zinc is surrounded by a phenyl, a chloride, a THF molecule and a bridging chlorine atom from **D**. It is the strength of this bridging Zn-Cl bond that renders the coordination process exergonic.



The transition state  $\text{TS}_{\text{EF}}$  for the transmetallation itself could then be found 21.8 kcal.mol<sup>-1</sup> above **E**. In  $\text{TS}_{\text{EF}}$  the Ni-Cl and Zn-Cl bonds are respectively 0.10 Å longer and 0.16 Å shorter than in **E**, showing the chloride transfer from the nickel to the zinc atom. Though the Zn-Ph bond is only slightly elongated by 0.07 Å and the Ni-Ph bond is still rather long measuring 2.58 Å. Furthermore, a very short Ni-Zn intermetallic distance of 2.59 Å is calculated. The distance is clearly shorter than the sum of the van der Waals radii (3.02 Å) and just a bit longer than the sum of the covalent radii (2.52 Å), suggesting a metallophilic interaction. Transition states with analogous short interactions have already been calculated for Pd-Zn<sup>[26, 27, 28]</sup> and Pd-Au/Sn-Au<sup>[29]</sup> species and were linked to lower activation energies. They are however absent in Pd-Sn transition states.<sup>[29]</sup>

The transition state leads to **F** which lies 14.6 kcal.mol<sup>-1</sup> higher than **E**. **F** is another heterobimetallic complex with a phenyl ring bridging the nickel and the zinc atoms. The Ni-C (2.04 Å) and the Zn-C (2.20 Å) bond lengths indicate that the phenyl is almost fully transferred to the nickel. The elimination of ZnCl<sub>2</sub>(THF)<sub>2</sub> from **F** releases **G**, which lies 12.6 kcal.mol<sup>-1</sup> lower in energy. The whole transmetallation process is exergonic with an energy gain from **D** to **G** of 9.0 kcal.mol<sup>-1</sup>.

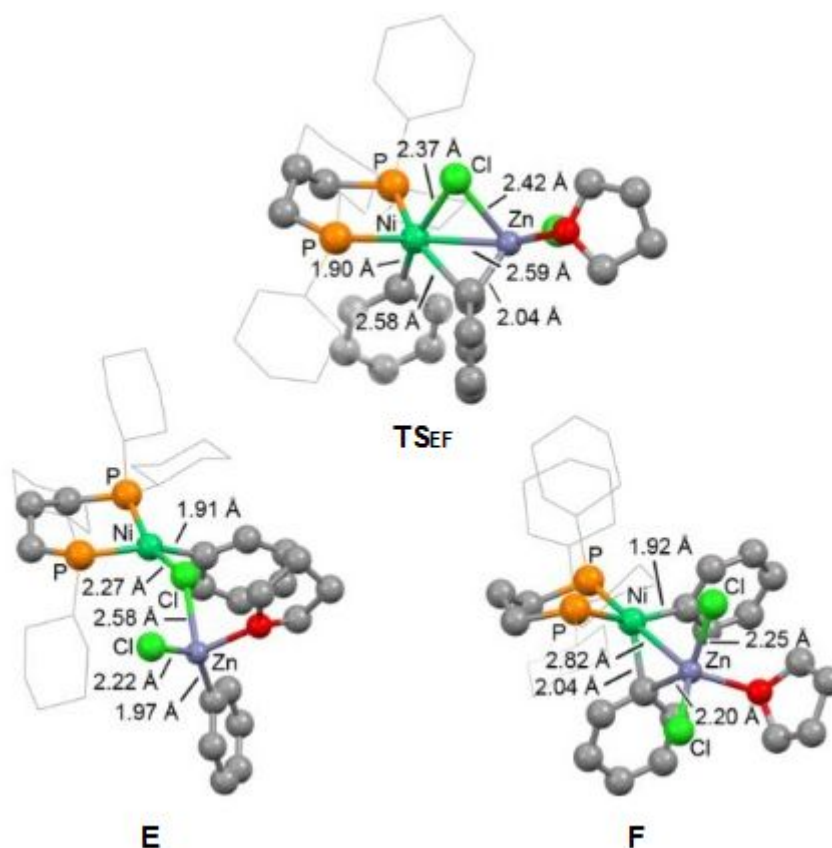


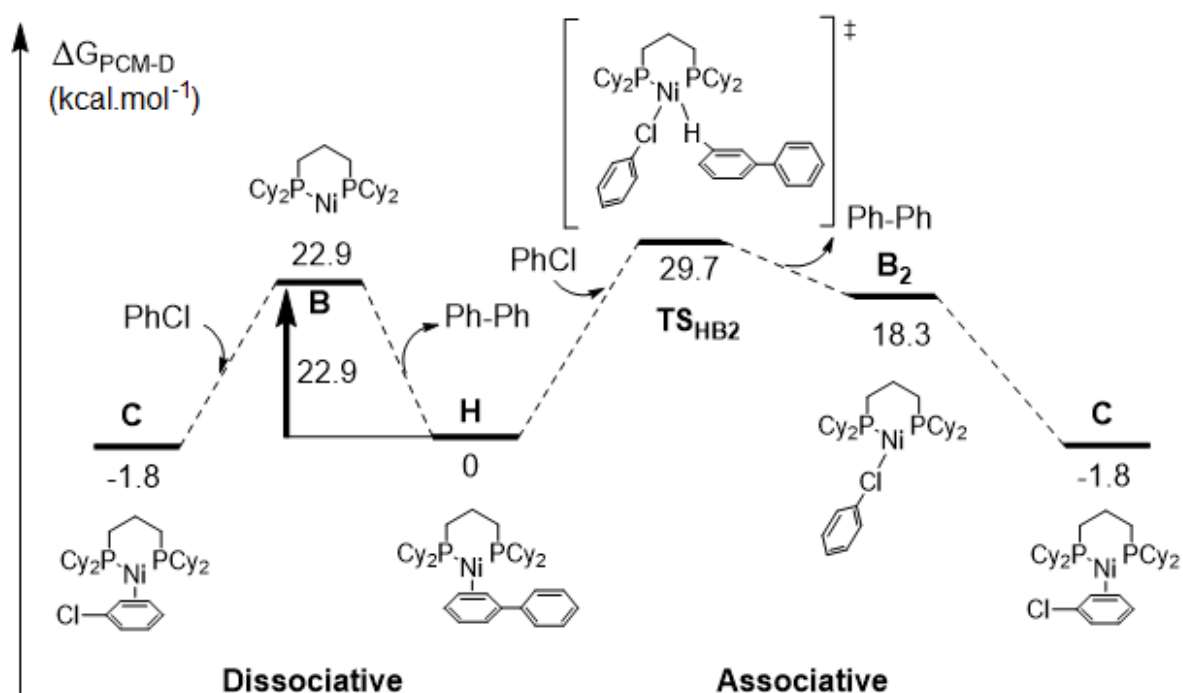
**Figure 2.6:** Computed structures of **E** (left),  $\text{TS}_{\text{EF}}$  (top) and **F** (right).

The reductive elimination of biphenyl from **G** is facile as the transition state  $\text{TS}_{\text{GH}}$  lies only 13.2 kcal.mol<sup>-1</sup> higher than **G**. In the Ni(0) complex **H**, the biphenyl remains coordinated to the nickel center in a  $\eta^2$  fashion similar to the coordination observed for toluene in complex **A**.

Overall, each catalytic cycle is exergonic by 52.5 kcal.mol<sup>-1</sup>. The rate determining step is the transmetalation with a moderate activation barrier of 21.8 kcal.mol<sup>-1</sup> in good agreement with the mild reaction conditions.

### 2.4.3 Product to reagent exchange

Finally, the product to reagent exchange that closes the catalytic cycle and regenerates [(dcpp)Ni(PhCl)] **C** from the biphenyl complex **H** was investigated. The dissociative and the associative mechanisms were here again both computed. For clarity the energy of **H** is set to 0 in **Scheme 2.16**.



**Scheme 2.16:** Reaction pathways for the product to reagent exchange: regeneration of  $\eta^2$  aryl chloride complex **C**.

The dissociation of the  $\eta^2$  coordinated biphenyl from **H** requires 22.9 kcal.mol<sup>-1</sup>. Similarly to the ligand to substrate exchange, the reaction proceeds through the highly electron deficient intermediate **B**, that takes in an aryl chloride moiety to produce  $\eta^2$  coordinated [(dcpp)Ni(PhCl)] **C**. The product to substrate exchange is exergonic by 1.8 kcal.mol<sup>-1</sup>.

The associative mechanism proceeds through an 18 electron transition state **TS<sub>HB2</sub>** that bears two  $\eta^1$  coordinated ligands. Dissociation of the biphenyl leads to intermediate **B<sub>2</sub>**, which features an  $\eta^1$  coordinated PhCl, that rearranges itself into  $\eta^2$  coordinated [(dcpp)Ni(PhCl)] **C**. The transition state **TS<sub>HB2</sub>** is located 29.7 kcal.mol<sup>-1</sup> above **H**, which makes it 6.8 kcal.mol<sup>-1</sup> higher in energy than the 14 electron intermediate **B** found for the dissociative pathway. Therefore, an associative ligand exchange seems out of reach.

Overall, the low activation barrier (22.9 kcal.mol<sup>-1</sup>) evidences that the liberation of the biphenyl product and the regeneration of [(dcpp)Ni(PhCl)] **C** is a favorable and facile process in agreement with the mild reaction conditions, that allows to engage into further catalytic cycles.

Hence, the DFT calculations support the experimental observations and corroborate the presence of an active Ni(0)/Ni(II) catalytic cycle. The activation energies for all elementary steps are reasonably low, in excellent agreement with the mild catalytic conditions. The highest barriers that need to be overcome reach respectively 21.8 kcal.mol<sup>-1</sup> and 22.9 kcal.mol<sup>-1</sup> for the transmetallation and the product to reagent exchange, which makes them the rate determining steps.

## 2.5 Conclusion and perspectives

The synthesis of the Ni(0) arene complex [(dcpp)Ni(toluene)] **II-4**, achieved by the two electron reduction of the Ni(II) precursor [(dcpp)NiCl<sub>2</sub>] **II-3** with KC<sub>8</sub> in toluene, provides a highly reactive catalyst for the Negishi cross coupling. [(dcpp)Ni(toluene)] **II-4** catalyzes efficiently the reaction between aryl chlorides and an equimolar amount of phenyl zinc chloride derivatives at low catalyst loadings down to 0.2 mol%, under mild conditions. The catalyst remains active over long periods of time and does not show any sign of deactivation. Electron poor and electron rich substrates could be coupled in excellent yields and even challenging *ortho* disubstituted aryl chlorides or chloropyridines afforded the cross coupled products in good yields. Remarkably, the reaction also tolerates the amino functional group. This is the first time that a strongly electron donating bis-phosphine supported catalyst proves to be excellent for this type of nickel catalyzed process.

Stoichiometric experiments supported by DFT calculations demonstrate the involvement of a Ni(0)/Ni(II) catalytic cycle upon use of chelating bis-phosphine ligands. All three elementary steps, *i.e.* oxidative addition, transmetallation and reductive elimination, are facile processes at RT and generate exclusively Ni(0) and Ni(II) intermediates among which [(dcpp)Ni(Ph)(Cl)] **II-14** could be isolated and characterized. The DFT calculations further confirm that the oxidative addition and reductive elimination have particularly low activation barriers whereas the transmetallation and product to reagent exchange constitutes the rate determining steps. The catalyst's resting state is found to be either the oxidative addition product [(dcpp)Ni(Ph)(Cl)] **II-14** or its adduct with PhZnCl **II-8** [(dcpp)Ni(Ph)[ $\mu$ -Cl]Zn(Cl)(Ph)(THF)].

No redox processes leading to Ni(I) intermediates could be identified in the reaction and isolated Ni(I) complex [(dcpp)NiCl]<sub>2</sub> **II-16** preferentially generates diamagnetic Ni(II) and/or Ni(0) species in the presence of PhZnCl **II-8**. When Ni(I) compounds are involved in the Negishi cross coupling, they lead to poor conversions and selectivities, favoring the homocoupled product over the cross coupled product. The use of a strongly donating bidentate bis-phosphine ligand is therefore key to shut down a Ni(I)/Ni(III) catalytic cycle.

It would be interesting to study the impact of the strongly donating bis-phosphine ligand dcpp on other nickel catalyzed reactions such as the Suzuki-Miyaura cross coupling. Efforts will be especially directed towards the investigation of the mechanism in order to determine whether the reaction performs similarly to the Ni(0)/Ni(II) Negishi cross coupling. Florian D'Accriscio

extensively studied the Suzuki-Miyaura cross coupling during his PhD and showed that the Ni(0)/Ni(II) mechanism is highly substrate dependent. [6]

Furthermore, the [(dcpp)Ni]-platform could be tested towards other challenging coupling reactions such as borylations or cyanations.

## 2.6 Experimental part

### 2.6.1 General remarks

All reactions were carried out under an atmosphere of dry argon using standard Schlenk techniques or in a nitrogen-filled MBraun LabStar glovebox. Dichloromethane, Et<sub>2</sub>O, pentane, THF and toluene were taken from an MBraun SPS-800 solvent purification system, freeze-pump-thaw degassed and stored over 4 Å molecular sieves. C<sub>6</sub>D<sub>6</sub> and CD<sub>2</sub>Cl<sub>2</sub> were degassed and stored over 4 Å molecular sieves.

All the chemicals were purchased in reagent grade purity from Acros, Cytech and Sigma-Aldrich and were used without further purification.

### 2.6.2 Synthesis of the dcpp ligand **II-1** <sup>[1]</sup>

The synthesis of the dcpp ligand **II-1** was upscaled following a procedure described in Mathieu Demange's thesis. <sup>[1]</sup> *n*-BuLi (1.6 M in hexanes, 37.9 mL, 6.05×10<sup>-2</sup> mol, 1 eq.) is added at -78 °C to a 90 mL THF solution of dicyclohexylphosphine (12.0 g, 6.05×10<sup>-2</sup> mol, 1 eq.). The reaction mixture is allowed to come back to RT over 2 h. The solution turns yellow and a white precipitate falls out. <sup>31</sup>P{<sup>1</sup>H} NMR spectroscopy shows a single resonance at δ = -13.0 ppm which corresponds to the lithiated phosphine. At -78 °C, 1,3-dichloropropane (2.59 mL, 2.72×10<sup>-2</sup> mol, 0.45 eq.) is added to LiPCy<sub>2</sub>. The solution is kept for 15 min at -78 °C before it is stirred overnight at RT. The solvent is removed under reduced pressure and the residue is taken up in pentane in order to precipitate all the salt. The solution is filtered off and the product is dried under vacuum. The dcpp ligand **II-1** is isolated as a pale yellow gel in 97 % yield (11.52 g).

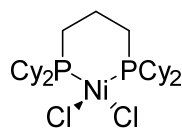
<sup>1</sup>H NMR (300 MHz, C<sub>6</sub>D<sub>6</sub>): δ 0.65 - 2.38 (m, 50H, Cy + CH<sub>2</sub>) ppm.

<sup>13</sup>C{<sup>1</sup>H} NMR (75 MHz, C<sub>6</sub>D<sub>6</sub>): δ 25.6 – 30.1 (Cy + CH<sub>2</sub>) ppm.

<sup>31</sup>P{<sup>1</sup>H} NMR (121,5 MHz, C<sub>6</sub>D<sub>6</sub>): δ - 6.7 (s) ppm.

### 2.6.3 Synthesis of (dcpp)nickel complexes

#### 2.6.3.1. Synthesis of [(dcpp)NiCl<sub>2</sub>] **II-3** <sup>[1]</sup>



The dcpp ligand **II-1** (1.09 g,  $2.50 \times 10^{-3}$  mol, 1 eq.) is added at RT to a THF suspension (30 mL) of [(DME)NiCl<sub>2</sub>] **II-2** (0.78 g,  $2.50 \times 10^{-3}$  mol, 1 eq.). The reaction mixture is stirred overnight at RT and an orange solid fall out of the solution. The supernatant is filtered away, the product is washed 2 × with Et<sub>2</sub>O, 2 × with pentane and dried under vacuum. [(dcpp)NiCl<sub>2</sub>] **II-3** is gathered as an orange powder in 94 % yield (1.33 g). Single crystals for X-ray diffraction analysis are obtained by diffusion of petroleum ether in a dichloromethane solution of the complex.

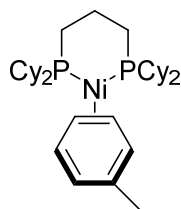
<sup>1</sup>H NMR (500 MHz, CD<sub>2</sub>Cl<sub>2</sub>): δ 1.21 - 1.31 (m, 8H, CH<sub>2</sub> Cy), 1.36 (sextt,  $J_{H,H} = 12.5$  Hz,  $J_{H,H} = 3.5$  Hz, 8H, CH<sub>2</sub> Cy), 1.54 (sextd,  $J_{H,H} = 12.5$  Hz,  $J_{H,H} = 3.5$  Hz, 8H, CH<sub>2</sub> Cy), 1.70 - 1.91 (m, 16H, CH<sub>2</sub> + CH<sub>2</sub> Cy), 2.34 (d,  $J_{H,H} = 12.5$  Hz, 4H, CH or CH<sub>2</sub> αP), 3.00 (t,  $J_{H,H} = 12.5$  Hz, 4H, CH or CH<sub>2</sub> αP) ppm.

<sup>13</sup>C{<sup>1</sup>H}{<sup>31</sup>P} NMR (125 MHz, CD<sub>2</sub>Cl<sub>2</sub>): δ 16.8, 21.0, 26.5, 27.4, 28.0, 29.7, 32.0 (CH<sub>2</sub> Cy + CH<sub>2</sub>), 38.0 (CH Cy αP) ppm.

<sup>31</sup>P{<sup>1</sup>H} NMR (208 K, 202.4 MHz, CD<sub>2</sub>Cl<sub>2</sub>): δ 19.6 (s) ppm.

**Elt. Anal.** Calcd for C<sub>27</sub>H<sub>50</sub>Cl<sub>2</sub>NiP<sub>2</sub> (564.21): C, 57.27; H, 8.90. Found: C, 57.31; H, 8.79.

#### 2.6.3.2 Synthesis of [(dcpp)Ni(toluene)] **II-4**



[(dcpp)NiCl<sub>2</sub>] **II-3** (200 mg,  $3.53 \times 10^{-4}$  mol, 1 eq.) and KC<sub>8</sub> (100 mg,  $7.42 \times 10^{-4}$  mol, 2.1 eq.) are suspended in 10 mL of toluene and the reaction mixture is stirred overnight at RT. [(dcpp)Ni(η<sup>2</sup>- toluene)] **II-4** and [(dcpp)NiH]<sub>2</sub> **II-5** are extracted from precipitated KCl and graphite through successive centrifugations. The first fraction contains most of the [(dcpp)NiH]<sub>2</sub> **II-5** and is therefore put aside. At best only 7 % of [(dcpp)NiH]<sub>2</sub> **II-5** were produced. Yellow fractions 2 - 5 containing [(dcpp)Ni(toluene)] **II-4** are collected and titrated

by  $^{31}\text{P}\{^1\text{H}\}$  NMR with  $\text{PPh}_3$  as internal standard. The complex is kept as a toluene solution at  $-25\text{ }^\circ\text{C}$ . Single crystals for X-ray diffraction analysis could be grown from this solution.

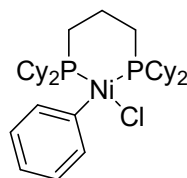
Matthieu Demange reported a different workup:  $\text{KCl}$  and graphite are eliminated by filtration. The solution is taken to dryness affording exclusively  $[(\text{dcpp})\text{Ni}(\text{toluene})]$  **II-4** as a yellow powder in 83 % yield (170 mg).<sup>[1]</sup>

$^1\text{H}$  NMR (300 MHz,  $\text{C}_6\text{D}_6$ ): 0.86 - 2.21 (m, 53H, Cy +  $\text{CH}_2$  +  $\text{CH}_3$ ), 7.01 - 7.57 (m, 5H, Ph) ppm.

$^{13}\text{C}\{^1\text{H}\}$  NMR (75 MHz,  $\text{C}_6\text{D}_6$ ):  $\delta$  20.9 - 39.2 (Cy +  $\text{CH}_2$  +  $\text{CH}_3$ ), 128.5 - 136.2 (Ph) ppm.

$^{31}\text{P}\{^1\text{H}\}$  NMR (121.5 MHz,  $\text{C}_6\text{D}_6$ ):  $\delta$  15.4 (s) ppm.

### 2.6.3.3 Synthesis of $[(\text{dcpp})\text{Ni}(\text{Ph})(\text{Cl})]$ **II-14**



Chlorobenzene **II-11** ( $10.2\text{ }\mu\text{L}$ ,  $1.0\times 10^{-4}$  mol, 1 eq.) is added at RT to a 5 mL toluene solution of  $[(\text{dcpp})\text{Ni}(\text{toluene})]$  **II-4** (58.7 mg,  $1.0\times 10^{-4}$  mol, 1 eq.). After 4 min. at  $40\text{ }^\circ\text{C}$  the solution becomes light yellow. All volatiles are removed under reduced pressure and the remaining solid is washed with  $2 \times 5\text{ mL}$  of pentane. The oxidative addition product  $[(\text{dcpp})\text{Ni}(\text{Ph})(\text{Cl})]$  **II-14** is finally gathered as a yellow solid in 89 % yield (54.1 mg). Single crystals for X-ray diffraction analysis were grown from a THF solution layered with pentane at  $-25\text{ }^\circ\text{C}$ .

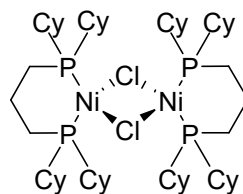
$^1\text{H}$  NMR (300 MHz,  $\text{C}_6\text{D}_6$ ): 0.95 - 2.81 (m, 50 H, Cy +  $\text{CH}_2$ ), 7.08 - 7.94 (m, 5H, Ph) ppm.

$^{13}\text{C}\{^1\text{H}\}$  NMR (75 MHz,  $\text{C}_6\text{D}_6$ ):  $\delta$  18.1 - 35.4 (Cy +  $\text{CH}_2$ ), 122.0 - 136.9 (Ph) ppm.

$^{31}\text{P}\{^1\text{H}\}$  NMR (121.5 MHz,  $\text{C}_6\text{D}_6$ ):  $\delta$  5.8 (d,  $^2J_{\text{P,P}} = 48.4\text{ Hz}$ , 1P), 19.0 (d,  $^2J_{\text{P,P}} = 48.4\text{ Hz}$ , 1P) ppm.

**Elt. Anal.** Calcd for  $\text{C}_{33}\text{H}_{55}\text{ClNiP}_2$  (606.28): C, 65.20; H, 9.12. Found: C, 65.23; H, 9.17.



2.6.3.4 Synthesis of [(dcpp)NiCl]<sub>2</sub> **II-16** <sup>[1]</sup>

[(dcpp)NiCl]<sub>2</sub> **II-3** (283 mg, 5.00×10<sup>-4</sup> mol, 1 eq.) and KC<sub>8</sub> (78 mg, 5.00×10<sup>-4</sup> mol, 1 eq.) are suspended in 5 mL of toluene. The reaction mixture is stirred overnight at RT, KCl and graphite fall out of the solution. The toluene is filtered away, [(dcpp)NiCl]<sub>2</sub> **II-16** is further extracted with THF and taken to dryness. The paramagnetic Ni(I) complex **II-16** is gathered as a light red product in 65 % yield (172.5 mg).

**X-Band EPR** at RT:  $g = 2.154$ ,  $A_{\text{iso}}(^3\text{P}, n = 2) = 72.2 \text{ G}$ .

**Elt. Anal.** Calcd for C<sub>54</sub>H<sub>100</sub>Cl<sub>2</sub>Ni<sub>2</sub>P<sub>4</sub> (1058.49): C, 61.10; H, 9.49. Found: C, 61.01; H, 9.64.

## 2.6.4 Negishi cross coupling

2.6.4.1 Synthesis of PhZnCl.LiCl **II-8**

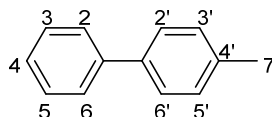
Small pieces of lithium previously crushed with a hammer (307 mg, 4.42×10<sup>-2</sup> mol, 3 eq.) are added to a 15 mL THF solution of chlorobenzene **II-11** (1.632 g, 1.45×10<sup>-2</sup> mol, 1 eq.) at -20 °C. The reaction mixture is stirred for 5 h. between 0 °C and -20 °C. The solution turns yellow to brown and a green precipitate is formed. In a second Schlenk ZnCl<sub>2</sub> (1.98 g, 1.45×10<sup>-2</sup> mol, 1 eq.) is solubilized in 8 mL of THF and cooled down to -20 °C. The phenyllithium is then cannulated to the ZnCl<sub>2</sub> solution while staying at -20 °C. The reaction is further stirred overnight at RT and the solution turns light yellow. The volatiles are removed under reduced pressure and PhZnCl.LiCl **II-8** is redissolved in 10 mL of THF. The concentration of the PhZnCl.LiCl solution **II-8** is determined by titration with iodine, following the procedure developed by Knochel. <sup>[30]</sup>

## 2.6.4.2 General procedure for Negishi cross coupling

In a typical experiment, the precatalyst [(dcpp)Ni(toluene)] **II-4** is weighted in the glovebox and introduced in a Schlenk. THF is then added, followed by the appropriate amounts of aryl chloride and organozinc reagent. The reaction mixture is heated to 60 °C and its progression followed by GC-MS spectrometry. The volatiles are evaporated upon completion of the reaction

and the product is extracted with dichloromethane. The organic phase is washed twice with water. The collected organic phases are dried over magnesium sulfate, filtered and concentrated on the rotary evaporator to afford the crude product. In the last step the product is purified by column chromatography.

A representative example is given below:



**4-methylbiphenyl II-9** - Following the general protocol 1 mol% of [(dcp)Ni(toluene)] **II-4** (5.88 mg,  $1.0 \times 10^{-5}$  mol) is dissolved in 2 mL of THF. 4-chlorotoluene **II-7** (119  $\mu$ L,  $1.00 \times 10^{-3}$  mol, 1 eq.) and PhZnCl **II-8** ( $1.1 \times 10^{-3}$  mol, 1,1 eq.) are added to the solution, which is reacted at 60 °C. After work up 4-methylbiphenyl **II-9** is collected as a white solid in 93 % yield (156.5 mg). (eluent: ethylacetate/pentane = 10/90).

**$^1\text{H}$  NMR** (300 MHz,  $\text{CDCl}_3$ ): 2.50 (s, 3H,  $\text{CH}_3$ ), 7.35 (d,  $^3J_{\text{H,H}} = 7.8$  Hz, 2H, CH 2'/6' (ortho)), 7.43 (t,  $^3J_{\text{H,H}} = 7.8$  Hz, 1H, CH 4 (para)), 7.53 (t,  $^3J_{\text{H,H}} = 7.8$  Hz, 2H, CH 3/5 (meta)), 7.61 (d,  $^3J_{\text{H,H}} = 8.4$  Hz, 2H, CH 3'/5' (meta)), 7.70 (d,  $^3J_{\text{H,H}} = 7.8$  Hz, 2H, CH 2/6 (ortho)) ppm.

**$^{13}\text{C}\{^1\text{H}\}$  NMR** (75 MHz,  $\text{CDCl}_3$ ):  $\delta$  21.2 ( $\text{CH}_3$ ), 127.1, 127.2, 128.8, 129.6, 130.9, 137.1, 138.5, 141.3 ppm.

## 2.7 References

- [1] Matthieu Demange, Thèse de doct., Ecole polytechnique, Paris, **2013**.
- [2] K. Jonas, *J. Organomet. Chem.*, **1974**, *78*, 273 - 279.
- [3] I. Bach, K.-R. Pörschke, R. Goddard, C. Kopsike, C. Krüger, A. Ruffinska, K. Seevogel, *Organomet.*, **1996**, *15*, 4959 - 4966.
- [4] P. Mastrorilli, G. Moro, C. F. Nobile, M. Latronico, *Inorg. Chim. Acta*, **1992**, *192*, 183 - 187.
- [5] K. Jonas, G. Wilke, *Angew. Chem. Int. Ed.*, **1970**, *9*, 312 - 313.
- [6] Florian D'Accriscio, Thèse de doct., Université Paul Sabatier, Toulouse, **2017**.
- [7] Y.-R. Luo, *Handbook of Bond Dissociation Energies in Organic Compounds*, CRC Press, Boca Raton, FL, **2003**.
- [8] L. Wang, Z.-X. Wang, *Org. Lett.*, **2007**, *9*, 4335 - 4338.
- [9] R. Gerber, C. M. Frech, *Chem. Eur. J.*, **2011**, *17*, 11893 - 11904.
- [10] D. G. Morrell, J. K. Kochi, *J. Am. Chem. Soc.*, **1975**, *97*, 7262 - 7270.
- [11] T. T. Tsou, J. K. Kochi, *J. Am. Chem. Soc.*, **1979**, *101*, 7547 - 7560.
- [12] I. Colon, D. R. Kelsey, *J. Org. Chem.*, **1986**, *51*, 2627 - 2637.
- [13] F. Scott, C. Krüger, P. Betz, *J. Organomet. Chem.*, **1990**, *387*, 113 - 121.
- [14] D. J. Mindiola, G. L. Hillhouse, *J. Am. Chem. Soc.*, **2001**, *123*, 4623 - 4624.
- [15] D. J. Mindiola, R. Waterman, D. M. Jenkins, G. L. Hillhouse, *Inorg. Chim. Acta*, **2002**, *345*, 299 - 308.
- [16] G. D. Jones, J. L. Martin, C. McFarland, O. R. Allen, R. E. Hall, A. D. Haley, R. J. Brandon, T. Konovalova, P. J. Desrochers, P. Pulay, D. A. Vicic, *J. Am. Chem. Soc.*, **2006**, *128*, 13175 - 13183.
- [17] V. B. Phapale, E. Buñuel, M. García-Iglesias, D. J. Cárdenas, *Angew. Chem. Int. Ed.*, **2007**, *46*, 8790 - 8795.
- [18] N. D. Schley, G. C. Fu, *J. Am. Chem. Soc.*, **2014**, *136*, 16588 - 16593.

- [19] S. Ge, R. A. Green, J. F. Hartwig, *J. Am. Chem. Soc.*, **2014**, *136*, 1617 - 1627.
- [20] R. A. Green, J. F. Hartwig, *Angew. Chem. Int. Ed.*, **2015**, *54*, 3768 - 3772.
- [21] M. J. Frisch, G. W. Trucks, H. B. Schlegel, G. E. Scuseria, M. A. Robb, J. R. Cheeseman, G. Scalmani, V. Barone, B. Mennucci, G. A. Petersson, H. Nakatsuji, M. Caricato, X. Li, H. P. Hratchian, A. F. Izmaylov, J. Bloino, G. Zheng, J. L. Sonnenberg, M. Hada, M. Ehara, K. Toyota, R. Fukuda, J. Hasegawa, M. Ishida, T. Nakajima, Y. Honda, O. Kitao, H. Nakai, T. Vreven, J. A. Montgomery, Jr., J. E. Peralta, F. Ogliaro, M. Bearpark, J. J. Heyd, E. Brothers, K. N. Kudin, V. N. Staroverov, R. Kobayashi, J. Normand, K. Raghavachari, A. Rendell, J. C. Burant, S. S. Iyengar, J. Tomasi, M. Cossi, N. Rega, N. J. Millam, M. Klene, J. E. Knox, J. B. Cross, V. Bakken, C. Adamo, J. Jaramillo, R. Gomperts, R. E. Stratmann, O. Yazyev, A. J. Austin, R. Cammi, C. Pomelli, J. W. Ochterski, R. L. Martin, K. Morokuma, V. G. Zakrzewski, G. A. Voth, P. Salvador, J. J. Dannenberg, S. Dapprich, A. D. Daniels, Ö. Farkas, J. B. Foresman, J. V. Ortiz, J. Cioslowski, D. J. Fox, Gaussian 09, Revision D.01, **2009**.
- [22] A. D. Becke, *J. Chem. Phys.*, **1993**, *98*, 5648 - 5652.
- [23] J. P. Perdew, Y. Wang, *Phys. Rev. B*, **1992**, *45*, 13244 - 13249.
- [24] P. C. Hariharan, J. A. Pople, *Theor. Chim. Acta*, **1973**, *28*, 213 - 222.
- [25] F. Weigend, R. Ahlrichs, *Phys. Chem. Chem. Phys.*, **2005**, *7*, 3297 - 3305.
- [26] B. Fuentes, M. García-Melchor, A. Lledós, F. Maseras, J. A. Casares, G. Ujaque, P. Espinet, *Chem. Eur. J.*, **2010**, *16*, 8596 - 8599.
- [27] M. García-Melchor, B. Fuentes, A. Lledós, J. A. Casares, G. Ujaque, P. Espinet, *J. Am. Chem. Soc.*, **2011**, *133*, 13519 - 13526.
- [28] A. B. González-Pérez, R. Álvarez, O. Nieto Faza, Á. R. de Lera, J. M. Aurrecoechea, *Organomet.*, **2012**, *31*, 2053 - 2058.
- [29] J. DelPozo, D. Carrasco, M. Pérez-Temprano, M. García-Melchor, R. Álvarez, J. A. Casares, P. Espinet, *Angew. Chem. Int. Ed.*, **2013**, *52*, 2189 - 2193.
- [30] A. Krasovskiy, P. Knochel, *Synthesis*, **2006**, 890 - 891.



Activation of CO<sub>2</sub> with chelating bis-phosphine  
nickel complexes



## 3 Functionalization of CO<sub>2</sub> towards acrylates

### 3.1 The economic challenges of CO<sub>2</sub>

#### 3.1.1 CO<sub>2</sub> from waste to resource

The concentration of CO<sub>2</sub> in the atmosphere has been growing exponentially since the beginning of the industrial area in middle of the 19<sup>th</sup> century and has recently reached 400 ppm, which represents 2750 billion tons. <sup>[1, 2]</sup> In percentage, CO<sub>2</sub> is the fourth gas in the atmosphere after dinitrogen, dioxygen and argon and is especially known as the main greenhouse gas, which is responsible for global warming and climate changes.

Nowadays, the global industry is still primarily based on fossil fuels such as petroleum, coal and natural gas and releases 30 Gton.year<sup>-1</sup> of CO<sub>2</sub>. Most organic products are also still synthesized through successive oxidations of hydrocarbons. <sup>[1, 2]</sup> The conversion of CO<sub>2</sub> into valuable chemicals could help reducing greenhouse gas emissions and developing sustainable alternatives to the fossil fuel based energy and chemical productions. First efforts were made in the late 1970s to functionalize CO<sub>2</sub> into value added chemicals, but this research field especially attracted a lot of attention in the last 15 years.

#### 3.1.2 Thermodynamic and kinetic stability of CO<sub>2</sub>

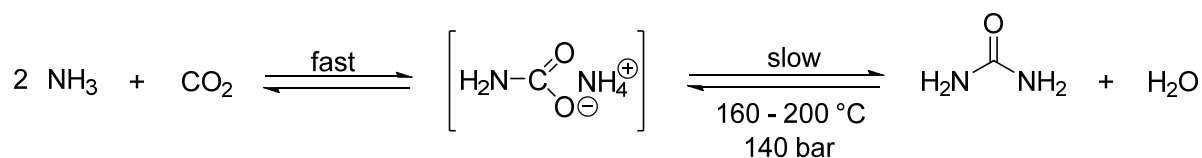
CO<sub>2</sub> is an abundant, cheap and non-toxic renewable resource, which costs only 15 - 20 €/ton. <sup>[1]</sup> It has a linear structure with double bonds between the carbon and the oxygen atoms. Though the thermodynamic and kinetic stability of CO<sub>2</sub> limits its reactivity. Indeed, most targeted chemicals lie higher in energy than CO<sub>2</sub>, which makes the reactions endergonic and activation barriers are commonly very high. <sup>[3]</sup> Therefore, catalytic processes, which generate highly energetic intermediates, are developed in order to overcome these difficulties. A lot of efforts are currently directed towards the reduction of CO<sub>2</sub> into formic acid, <sup>[4, 5]</sup> methanol <sup>[4, 5, 6]</sup> or methane <sup>[4, 7]</sup> and the reductive functionalization of CO<sub>2</sub> into value added chemicals such as amides or amins. <sup>[8, 9]</sup> Numerous homogeneous transition metal and organocatalyzed reactions have been described in the literature. <sup>[10, 11]</sup>



### 3.1.3 Industrial production of chemicals from CO<sub>2</sub>

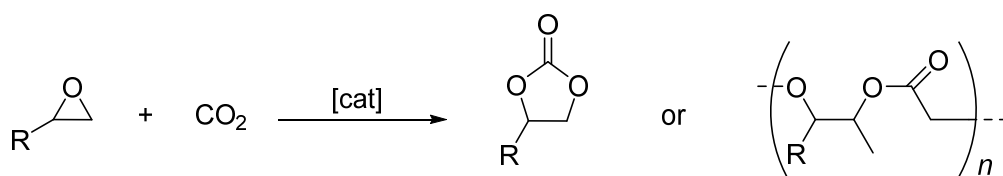
CO<sub>2</sub> already finds three main applications in large scale industrial processes for the synthesis of urea, carbonates and salicylic acid. [1, 2]

First of all, the Bosch-Meiser reaction provides 120 Mton.year<sup>-1</sup> of urea, [12] which is used for the synthesis of fertilizers and polymers. During this process, ammonia and CO<sub>2</sub> are first quickly converted to an intermediate carbamate, which slowly generates urea and water at high temperatures and high pressures, as shown in **Scheme 3.1**. [13]



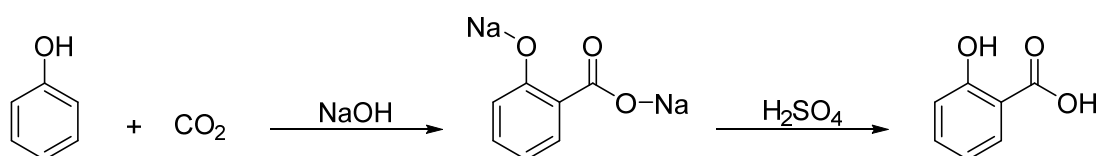
**Scheme 3.1:** Production of urea by the Bosch-Meiser process. [13]

Furthermore, carbonates can be generated by the reaction between epoxides and CO<sub>2</sub> (**Scheme 3.2**). Polycarbonates are essential in the polymer industry, whereas cyclic carbonates make good solvents for lithium-ion batteries. [14, 15]



**Scheme 3.2:** Production of linear and cyclic carbonates from the reaction between epoxides and CO<sub>2</sub>. [14, 15]

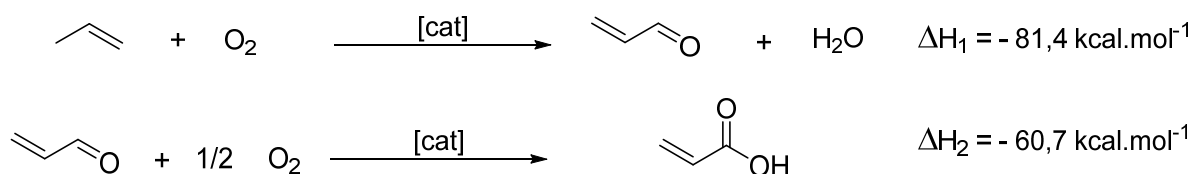
Finally, salicylic acid is synthesized from phenol and CO<sub>2</sub> in the Kolbe-Schmitt reaction by successive basic and acid treatments. The esterification of salicylic acid by acetic anhydride further affords aspirin®. [16]



**Scheme 3.3:** Synthesis of salicylic acid from phenol and CO<sub>2</sub>. [16]

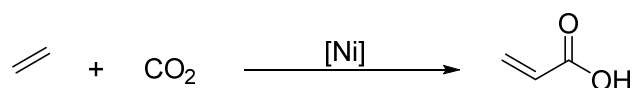
### 3.1.4 Design of new reactions involving CO<sub>2</sub>

Nowadays, 180 Mton.year<sup>-1</sup> of CO<sub>2</sub> are used for the production of chemicals, which represents only 0.6 % of the total amount of CO<sub>2</sub> released in a year. From an academic and industrial point of view, an equally interesting challenge is the catalytic production of  $\alpha,\beta$ -unsaturated acrylic acid from ethylene and CO<sub>2</sub>. Acrylic acid is currently produced in a two stage process by the catalytic oxidation of propylene over a mixture of metal oxides, as presented in **Scheme 3.4**. Propylene is first reacted with molecular oxygen to acrolein, which is further oxidized to acrylic acid. [17, 18, 19] The global market for acrylic acid reaches 5.4 Mton.year<sup>-1</sup> and is particularly relevant for the polymer industry. Sodium acrylate can be functionalized into water absorbent polymers commonly used in diapers. Yet, most acrylic acid is converted into related esters, which after polymerization with various monomers affords textiles, adhesives and coating materials. [19]



**Scheme 3.4:** Two step synthesis of acrylic acid through the oxidation of propylene by dioxygen. [19]

Nevertheless, it would be desirable to develop an economically attractive and more sustainable synthesis of acrylates. This chapter describes the advances on the synthesis of acrylate derivatives from ethylene and CO<sub>2</sub>. Several transition metals have been considered to perform this reaction, [20] however only nickel based chemistry [21] will be discussed here.



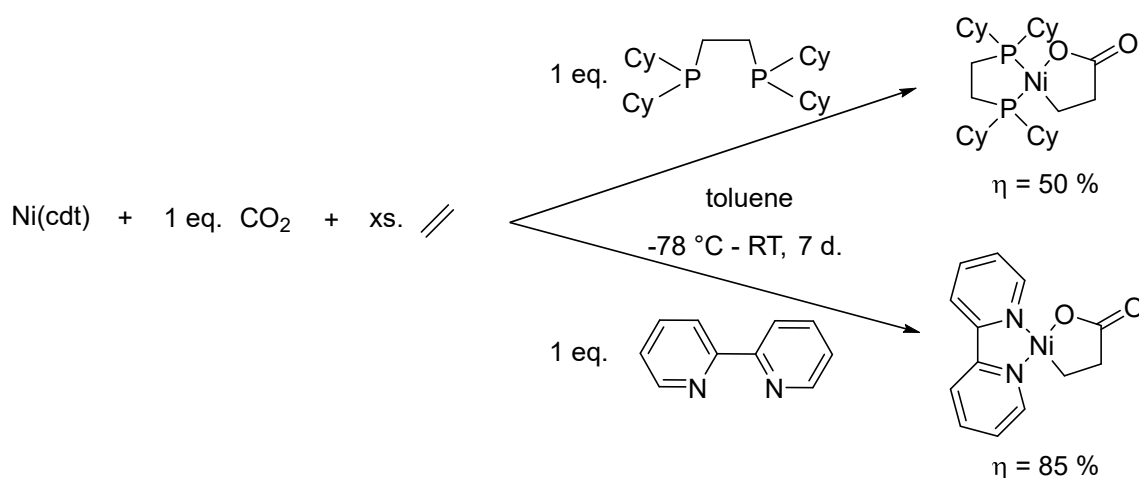
**Scheme 3.5:** Dream reaction: metal catalyzed synthesis of acrylic acid from ethylene and CO<sub>2</sub>.

## 3.2. Towards the formation of acrylates from ethylene and CO<sub>2</sub>

### 3.2.1 Synthesis of nickelalactones

#### 3.2.1.1 Oxidative coupling between ethylene and CO<sub>2</sub>

A sustainable production of acrylates can be initiated by the oxidative coupling of ethylene and CO<sub>2</sub> at a transition metal. Hoberg was the first to achieve this reaction in 1983 on a Ni(0) complex. [22] Under a pressure of ethylene and CO<sub>2</sub>, and in the presence of a bidentate ligand, either dcpe or bipyridine, [Ni(cdt)] is converted to oxanickelacyclopentanes, as shown in **Scheme 3.6**. [(dcpe)nickelalactone] and [(bipy)nickelalactone] are obtained in 50 % and 85 % yield and display a characteristic carboxylic absorption band in IR spectroscopy at 1620 cm<sup>-1</sup> and 1635 cm<sup>-1</sup> respectively. [22] Addition of different alkenes to the nickelalactones produces a mixture of metallacycles and demonstrates that the oxidative coupling is reversible. Furthermore, hydrolysis of the nickelalactones provides propanoic acid and addition of CO generates succinic anhydride. [22]



**Scheme 3.6:** First oxidative couplings between ethylene and CO<sub>2</sub> at Ni(0) complexes. [22]

Following this methodology, several nickelalactones with different amine, phosphine [23] or mixed P,N ligands [24] and various alkenes [24, 25, 26] and dienes [27–30] were synthesized by Hoberg and Walther. [31–35] Noticeably, in 1987 the square planar, 16 electron amine substituted nickelalactone [(DBU)<sub>2</sub>Ni(κO,κC-OC(O)CH<sub>2</sub>CH<sub>2</sub>)] could be crystallized. [36]

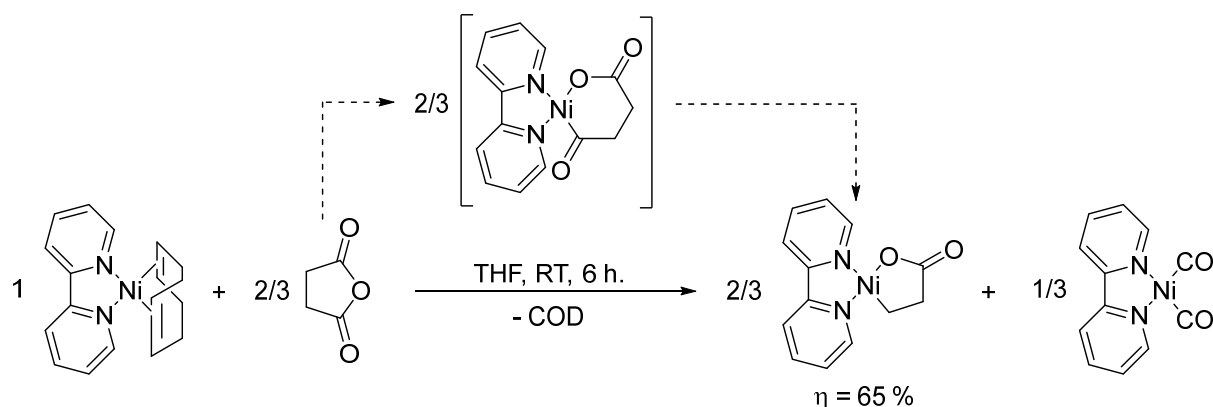
A DFT study from 2004 by Papai using the B3LYP/SDDP methodology shows that the oxidative coupling between ethylene and CO<sub>2</sub> at bipyridine and bis-phosphine Ni(0) complexes

proceeds through a single step C-C bond formation from  $[(L_2)Ni(C_2H_4)]$  and CO<sub>2</sub>.<sup>[37]</sup> In the case of [(bipy)nickelalactone] the oxidative coupling has a low activation barrier and is an exergonic process by 16.6 kcal.mol<sup>-1</sup>.<sup>[37]</sup> Yet, a later DFT study at the M06L level of theory on a broad set of bis-phosphine nickelalactones reveals that the stability of the nickelalactones is correlated to the ligand's bite angle.<sup>[38]</sup> If the bite angle of the chelating ligand is smaller than 92°, the nickelalactone is stable. However, when the bite angle becomes larger, the nickelalactones are increasingly difficult to synthesize through oxidative coupling and are more prone to decomposition.<sup>[38]</sup>

### 3.2.1.1 Alternative synthesis of nickelalactones

More convenient strategies have been developed to synthesize hardly accessible nickelalactones by oxidative coupling in order to investigate their reactivity.

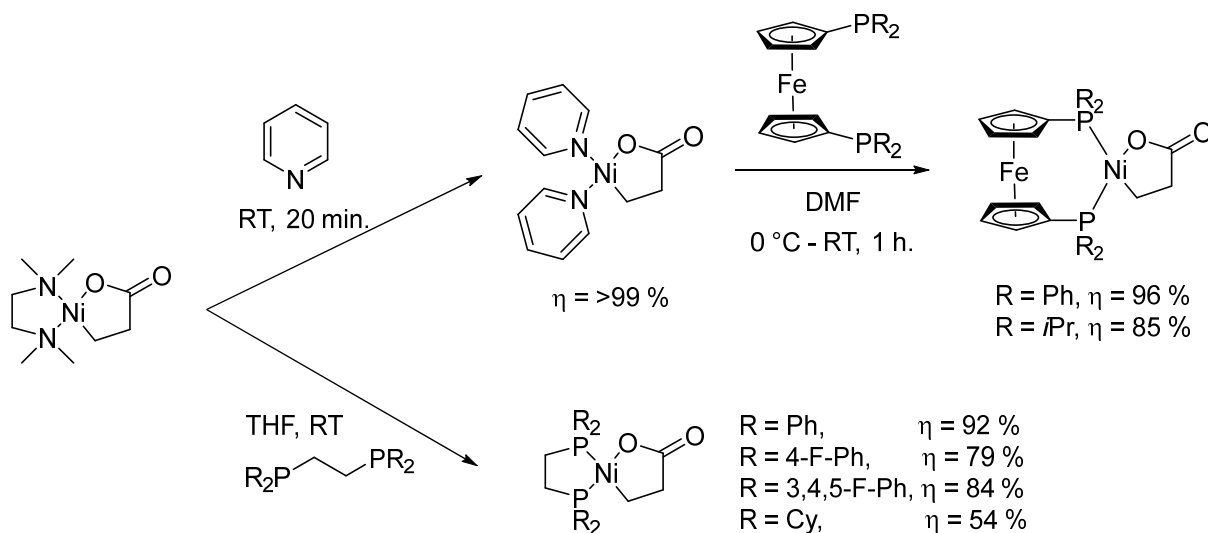
The first nickelalactones were obtained by Uhlig in good yields through the decarbonylation of nickel anhydride complexes, as shown in **Scheme 3.7**.<sup>[39]</sup> Cyclic anhydrides can easily undergo oxidative addition on Ni(0) complexes affording oxanickelacycles, which decompose upon heating and loss of CO to more stable nickelalactones. Addition of phthalic,<sup>[39]</sup> succinic<sup>[39]</sup> and glutaric anhydrides<sup>[40]</sup> to [(bipy)Ni(COD)] or [(bipy)Ni(Et)<sub>2</sub>]<sup>[41]</sup> has successfully generated the corresponding [(bipy)nickelalactones]. Widely used [(tmeda)nickelalactone] is also commonly synthesized through this reaction.<sup>[42]</sup>



**Scheme 3.7:** Synthesis of [(bipy)nickelalactone] from [(bipy)Ni(COD)] and succinic anhydride.<sup>[39]</sup>

Numerous nickelalactones have further been synthesized by simple ligand substitution, especially from [(tmeda)nickelalactone] and [(py)<sub>2</sub>nickelalactone].<sup>[43, 44, 45]</sup> Stronger σ donating

chelating bis-phosphines easily displace the diamine and the labile pyridines under mild conditions. By using this strategy, Walther largely contributed to broaden the scope of available nickelalactones. <sup>[43, 44, 45]</sup> A few substitution reactions can be found in **Scheme 3.8**.



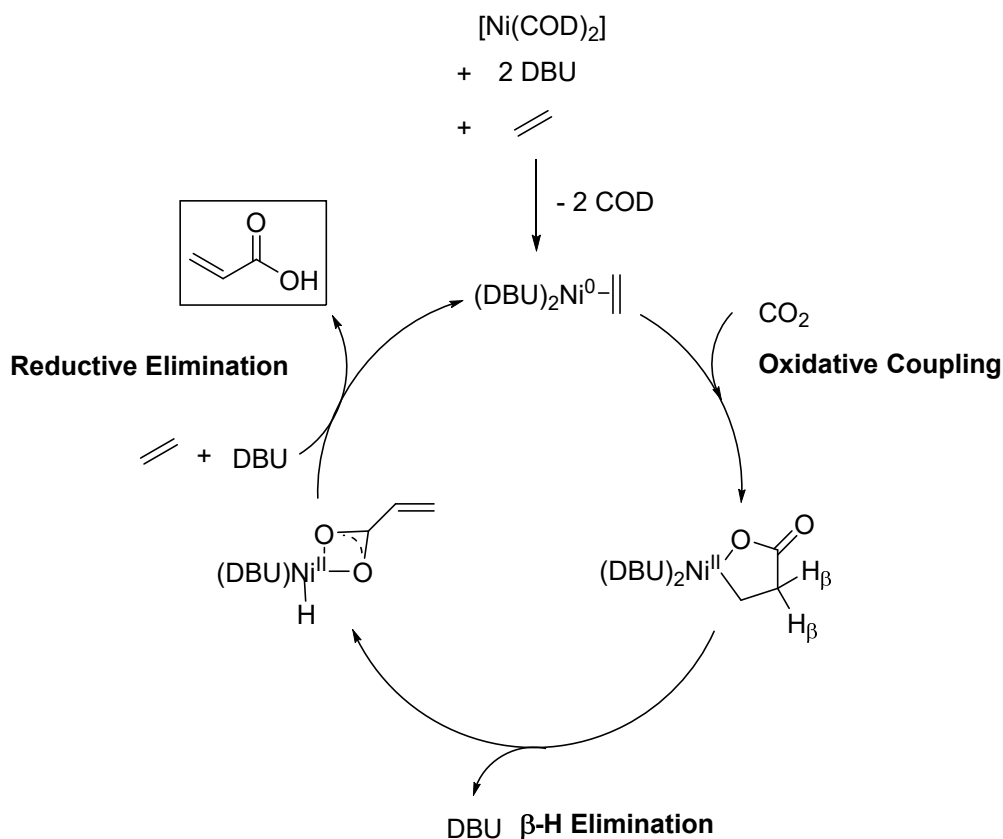
**Scheme 3.8:** Synthesis of [(bis-phosphine)nickelalactones] through ligand substitutions. <sup>[43, 44, 45]</sup>

### 3.2.2 Stoichiometric production of acrylates

The procedure to synthesize nickelalactones is well established. However, the conversion of nickelalactones to acrylate derivatives still remains difficult. The most straight forward pathway consists in  $\beta$  hydride elimination, followed by reductive elimination liberating the acrylate. Yet, large Ni-H $\beta$  distances and strong Ni-O bonds make the process inefficient.

#### 3.2.2.1 Theoretical investigations and first reports of $\beta$ hydride eliminations

A DFT study at the B3LYP/LANL2DZ level of theory, realized by Buntine in 2007 on [(DBU)<sub>2</sub>Ni] complexes, explores the feasibility of such a reaction process. <sup>[46]</sup> The oxidative coupling of ethylene and CO<sub>2</sub> to acrylates is divided in three elementary steps, namely oxidative coupling,  $\beta$  hydride elimination and reductive elimination (see **Scheme 3.9**).

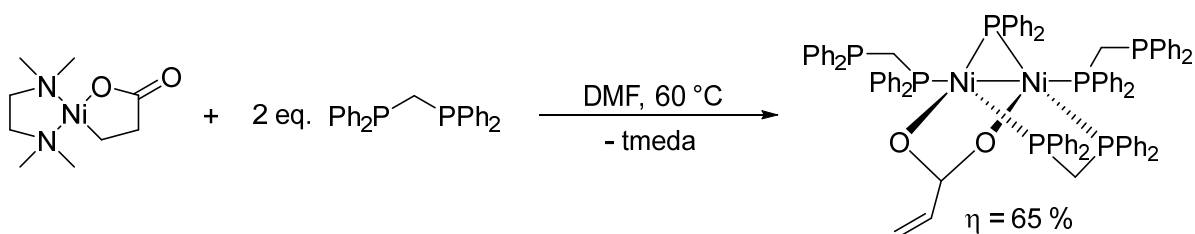


**Scheme 3.9:** Catalytic cycle computed by Buntine for the production of acrylic acid from ethylene and CO<sub>2</sub> at [(DBU)<sub>2</sub>Ni] complexes. <sup>[46]</sup>

First of all, the formation of the nickelalactone is exergonic by 4.1 kcal.mol<sup>-1</sup> with respect to the starting materials. The thermodynamic stability of the nickelalactone drives the reaction despite a high activation barrier reaching  $\Delta G^\ddagger = 29.0$  kcal.mol<sup>-1</sup>, as similarly reported by Papai. <sup>[37]</sup> Afterwards, the direct  $\beta$  hydride elimination from the five membered cycle proves to be impossible. <sup>[37, 46]</sup> Geometry constrains keep the  $\beta$  hydrogen atoms away from the nickel center. However, partial elongation of the Ni-O bond releases sufficient ring tension to allow  $\beta$  agostic interactions and the formation of a [(hydrido)(acrylate)Ni]-complex, which lies 9.2 kcal.mol<sup>-1</sup> above the nickelalactone. The kinetic barrier of  $\Delta G^\ddagger = 35.2$  kcal.mol<sup>-1</sup> is the highest to overcome during the cycle, <sup>[46]</sup> which was also later confirmed by calculations at the M06L level of theory carried out on bis-phosphine nickel complexes. <sup>[38]</sup> Finally, the liberation of acrylic acid through reductive elimination and the regeneration of the catalyst [(DBU)<sub>2</sub>Ni(C<sub>2</sub>H<sub>4</sub>)] can proceed through several pathways but is always endergonic by at least 12.9 kcal.mol<sup>-1</sup> with a minimal activation barrier of  $\Delta G^\ddagger = 24.9$  kcal.mol<sup>-1</sup>. Therefore, all three calculated kinetic barriers for each elementary step are high but not unbridgeable. <sup>[38, 46]</sup> The

main hurdle to the production of acrylic acid is the overall unfavorable thermodynamics of the system with a positive  $\Delta G = 10.2 \text{ kcal}\cdot\text{mol}^{-1}$ .<sup>[46]</sup>

Despite all the reported obstacles,  $\beta$  hydride eliminations on nickelalactones were already observed by Hoberg in the late 1980s while heating DBU complexes and recovering unsaturated carboxylic acids upon hydrolysis.<sup>[26, 36]</sup> Furthermore, in 2006 Walther *et al.* managed to convert for the first time a nickelalactone into a nickel acrylate complex, as depicted in **Scheme 3.10**.<sup>[44]</sup> The dppm ligand induces  $\beta$  hydride elimination under mild conditions and affords after rearrangement a dimeric Ni(I) complex, displaying a Ni-Ni single bond and bearing a bridging acrylate in 65 % yield.<sup>[44]</sup>

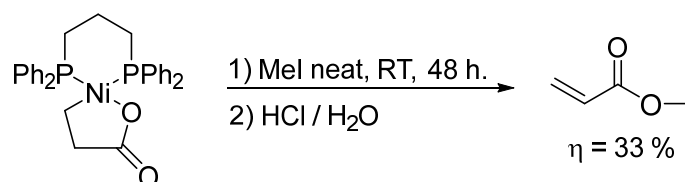


**Scheme 3.10:** First conversion of a nickelalactone into a nickel acrylate complex by means of a dppm ligand.<sup>[44]</sup>

Even though isolated cases of  $\beta$  hydride elimination from nickelalactones had been described,<sup>[26, 36, 44]</sup> there were no general procedures to generate free acrylates before 2010. Strategies were especially directed towards weakening the Ni-O bond to cause  $\beta$  hydride elimination.

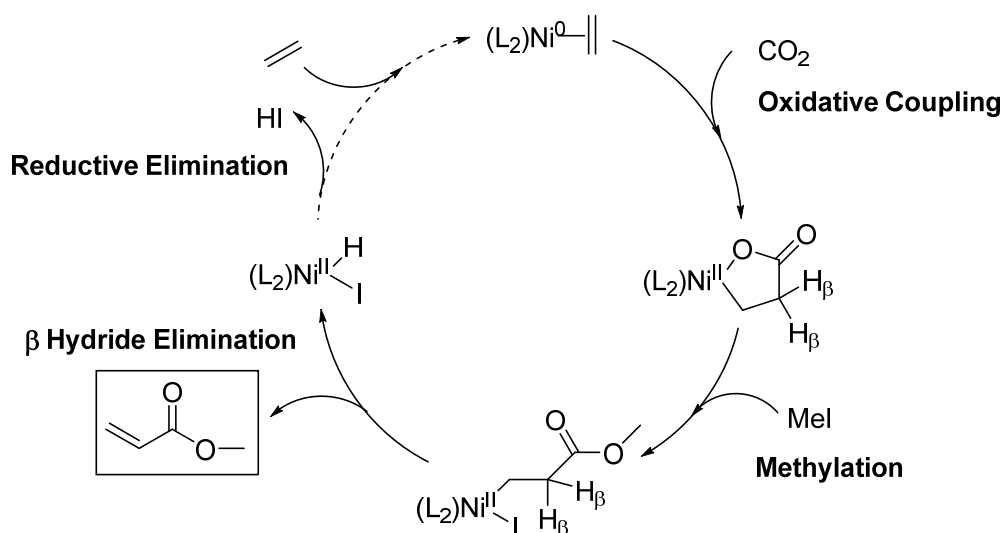
### 3.2.2.2 Cleavage of nickelalactones by strong electrophiles

The first approach relies on the cleavage of nickelalactones by electrophiles. In 2010, Rieger showed that the reaction between [(dppp)nickelalactone] and electrophilic methyl iodide (MeI) in CH<sub>2</sub>Cl<sub>2</sub> at RT leads to the formation of methyl acrylate, which was observed after hydrolysis by NMR spectroscopy and ESI mass spectrometry.<sup>[47]</sup> The yield of the reaction could be improved up to 33 % in neat MeI, although the solubility of [(dppp)nickelalactone] is limited in this solvent. *In situ* IR measurements confirm the disappearance of the C=O absorption bands of the nickelalactone at 1627 cm<sup>-1</sup> and 1322 cm<sup>-1</sup> and the formation of a C=O absorption band at 1732 cm<sup>-1</sup>, originating from the new acrylate.<sup>[47]</sup>



**Scheme 3.11:** Reaction between [(dppp)nickelalactone] and methyl iodide in CH<sub>2</sub>Cl<sub>2</sub> at RT leading to the formation of methyl acrylate. <sup>[47]</sup>

The reaction consists in the methylation of the nickelalactone, which opens the cycle and potentially generates a flexible methyl propanoate nickel complex. The  $\beta$  hydrogens become available for agostic interactions. Subsequent  $\beta$  hydride elimination releases methyl acrylate and forms a Ni(II) hydrido iodo complex. <sup>[47]</sup> A simplified hypothetical catalytic cycle is presented in **Scheme 3.12**.



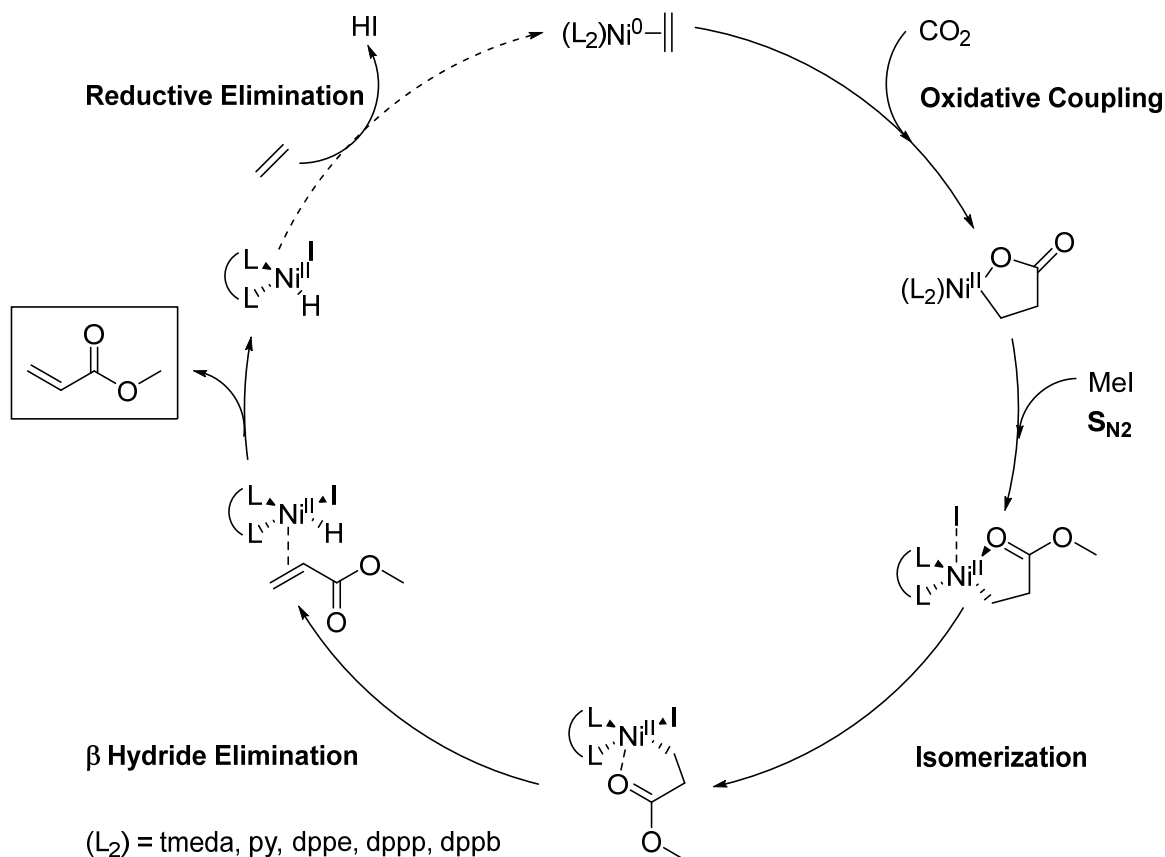
**Scheme 3.12:** Simplified hypothetic catalytic cycle for the production of methyl acrylate from ethylene, CO<sub>2</sub> and methyl iodide. <sup>[47]</sup>

In the following years, the reaction conditions have been optimized by varying either the ligand on the nickelalactone and the related palladalactone <sup>[48, 49]</sup> (chelating P- and N-donor ligands) or the methylating reagent (MeOTf, CH<sub>3</sub>CH<sub>2</sub>I, CF<sub>3</sub>CH<sub>2</sub>I). <sup>[49, 50]</sup> In addition, reaction intermediates have been identified. Methyl propanoate nickel complexes  $[(L)Ni(CH_2CH_2C(O)OMe)(X)]$  (X = I, OTf) could be detected by IR spectroscopy <sup>[48]</sup> and were further isolated. <sup>[49]</sup> The presence of nickel hydride complexes  $[(L)Ni(H)(X)]$  has also been confirmed by <sup>1</sup>H NMR spectroscopy. <sup>[49]</sup>



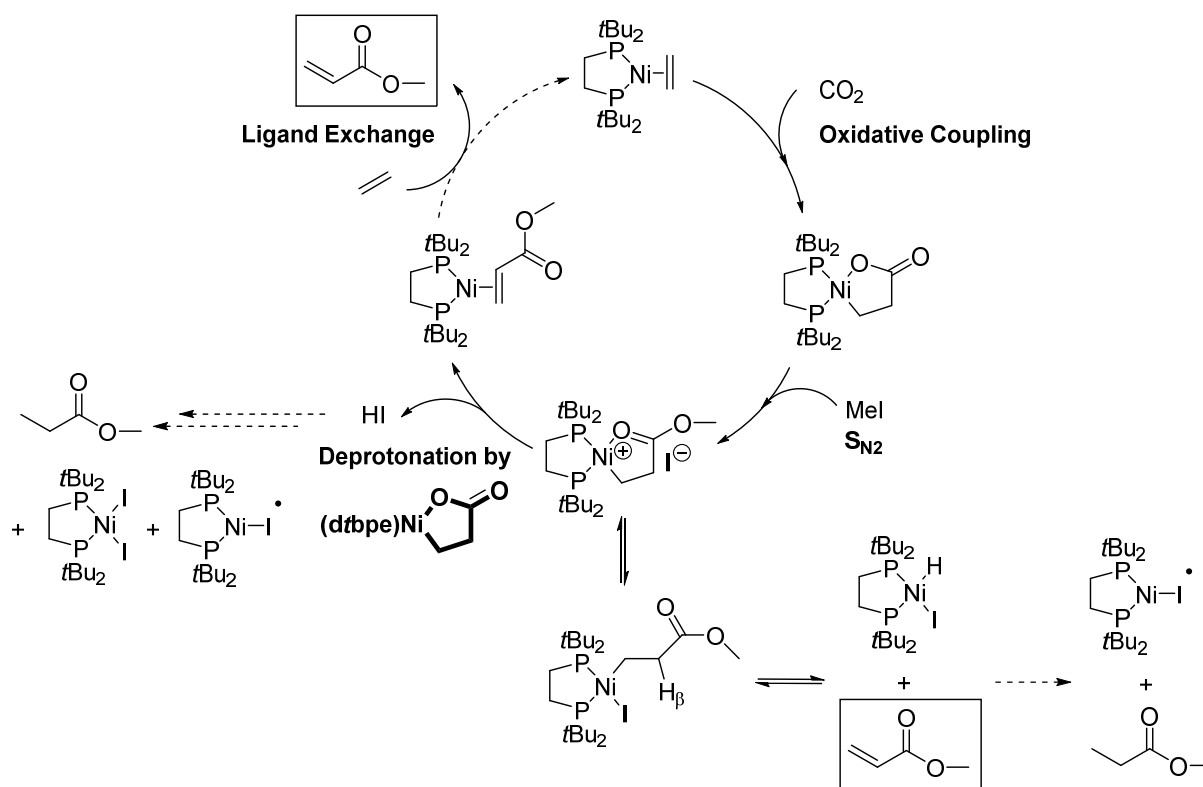
However, the reaction still faces several problems such as the competition between reductive and  $\beta$  hydride elimination producing iodopropanoates,<sup>[48]</sup> the formation of acidic side products (HI), that can degrade reaction intermediates and the use of methyl iodide that easily undergoes oxidative addition on Ni(0) complexes like [(dppp)Ni(C<sub>2</sub>H<sub>4</sub>)].<sup>[47]</sup>

In 2014, Xu and Sautet proposed a more detailed mechanism for this reaction on the basis of DFT calculations using a XYG3/XO3 approach.<sup>[51]</sup> The cleavage of the nickelalactone through methyl iodide proceeds through a S<sub>N</sub>2 reaction, which requires less than  $\Delta G^\ddagger = 20.3 \text{ kcal.mol}^{-1}$  for various bidentate N- and P- type donor ligands. The oxygen atom of the carbonyl moiety attacks MeI, prior the insertion of iodide to the nickel center. The generated five coordinated nickel complex bear the weakly coordinated iodide in an apical position and can easily undergo isomerization at energy barriers lower than  $\Delta G^\ddagger = 14.3 \text{ kcal.mol}^{-1}$ . Iodide-oxygen interconversion facilitates  $\beta$  hydride elimination and the formation of a [(hydrido)(acrylate)Ni]-complex [(L)<sub>2</sub>Ni( $\eta^2$ -CH<sub>2</sub>=CHC(O)OMe)(H)(I)]. After further isomerization, methyl acrylate is decoordinated and [(L)<sub>2</sub>Ni(H)(I)] formed alongside. However, the regeneration of the catalyst and the overall Gibb's free energy of the reaction  $\Delta G = 19.1 \text{ kcal.mol}^{-1}$  are unfavorable, preventing catalytic applications.<sup>[51]</sup> This DFT study clearly shows that the activation barriers for the production of acrylates in the presence of methyl iodide are lower and within experimental reach compared to the one previously calculated in the absence of any kind of additives.<sup>[46]</sup> Ligands have minimal influence on the energetic situation of the main reaction pathway. Nevertheless, by tuning the ligand side reactions such as ligand decoordination, dissociation or lactone rearrangements can be inhibited. Interestingly, the polarity of the solvent also plays a key role in destabilizing side reaction intermediates.<sup>[51]</sup> The potential catalytic cycle can be found in **Scheme 3.13**.



**Scheme 3.13:** Hypothetic catalytic cycle for the production of methyl acrylate through the cleavage of nickelalactones by methyl iodide computed by Xu and Sautet. <sup>[51]</sup>

In 2013, Limbach and Hofmann also investigated the nickel mediated formation of acrylates from ethylene, CO<sub>2</sub> and methyl iodide by DFT calculations at the BP86/def2-SV(P) level of theory and supported their work by experimental results. <sup>[52]</sup> The study is carried out on the *dtbpe* chelating bis-phosphine and the discovered mechanism differs from the one previously suggested by the experimental investigations <sup>[47, 48, 49]</sup> and Xu and Sautet's calculations. <sup>[51]</sup> The formation of acrylates would be rather promoted by the assistance of an external base instead of the electrophilic methyl iodide. <sup>[52]</sup> The classically assumed pathway would merely be a side reaction leading to the same product. <sup>[52]</sup> The full catalytic cycle with possible side processes is depicted in **Scheme 3.14**. <sup>[52]</sup>



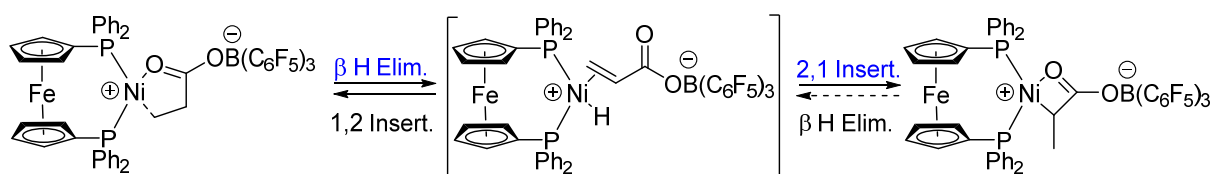
**Scheme 3.14:** Hypothetic catalytic cycle for the base assisted production of methyl acrylate computed by Limbach and Hofmann. <sup>[52]</sup>

The reaction between (dtbpe)nickelalactone and MeI most likely proceeds through an S<sub>N</sub>2 reaction pathway, with a low activation barrier of  $\Delta G^\ddagger = 17.4 \text{ kcal.mol}^{-1}$  in agreement with the mild reaction conditions reported earlier. <sup>[47, 48, 49]</sup> The methylation occurs at the carbonyl oxygen of the nickelalactone, providing the cationic nickel compound [(dtbpe)Ni(CH<sub>2</sub>CH<sub>2</sub>C(OMe)=O)]<sup>+</sup>I<sup>-</sup>. This reaction intermediate could be independently synthesized by adding acidic H(Et<sub>2</sub>O)<sub>2</sub>BAR<sub>F</sub> to the methyl acrylate complex [(dtbpe)Ni(CH<sub>2</sub>=CHC(O)OMe)]. The nickel complex is in equilibrium with the analogous four membered cationic nickelalactone. The isomerization occurs through  $\beta$  agostic intermediates with an overall barrier of  $\Delta G^\ddagger = 22.0 \text{ kcal.mol}^{-1}$ , which is comparable to the experimentally measured  $\Delta G^\ddagger = 21.5 \text{ kcal.mol}^{-1}$  during kinetic investigations. In order to generate the  $\pi$  methyl acrylate nickel complex [(dtbpe)Ni(CH<sub>2</sub>=CHC(O)OMe)], the  $\beta$  agostic intermediate must be deprotonated, releasing HI. <sup>[53]</sup> Even a neutral nickelalactone is basic enough to carry out the deprotonation with an activation barrier of  $\Delta G^\ddagger = 15.8 \text{ kcal.mol}^{-1}$ , which was also verified empirically. The problematic step is still the release of the acrylate and the regeneration of the catalyst, which would require  $\Delta G^\ddagger = 24.0 \text{ kcal.mol}^{-1}$ , but has not been achieved so far. <sup>[52]</sup>

In an energetically less favorable side process, the cationic nickelalactone might be converted to the open chain nickel propanoate complex  $[(dtbpe)Ni(CH_2CH_2C(O)OMe)]^+$ , which further undergoes  $\beta$  hydride elimination. Methyl acrylate is then released along the formation of  $[(dtbpe)Ni(H)(I)]$ . This decomposition mechanism as well as the loss of hydroiodic acid, lead to side products such as propanoates, Ni(I) and Ni(II) iodo complexes, which have been observed experimentally. <sup>[52]</sup>

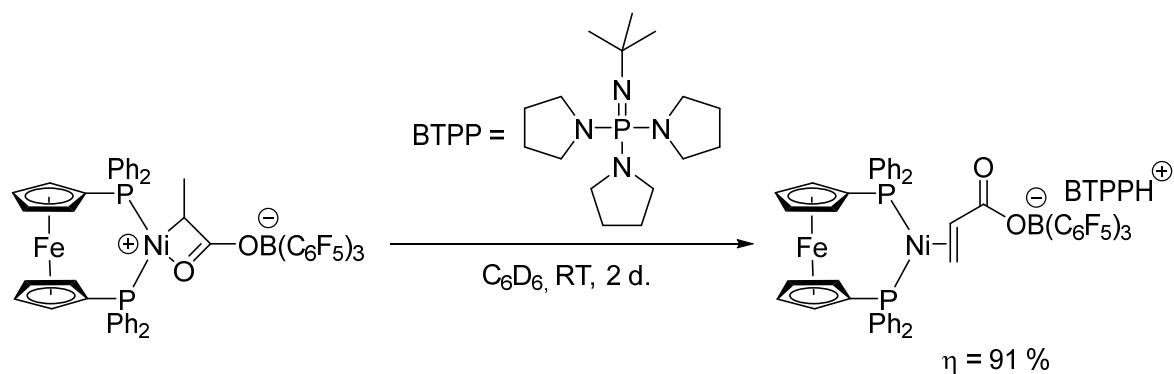
### 3.2.2.3 Cleavage of nickelalactones by bases

The second approach for the production of acrylates is based on the activation of nickelalactones by Lewis acids, followed by base induced  $\beta$  hydride elimination, as suggested by Limbach and Hofmann's <sup>[52]</sup> and Pidko's <sup>[38]</sup> DFT calculations. This concept was experimentally established by Bernskoetter in 2013, through the use of strongly Lewis acidic  $B(C_6F_5)_3$  in combination with a mild neutral base to promote the formation of acrylate derivatives. <sup>[54]</sup> When  $[(dppf)nickelalactone]$  is reacted with  $B(C_6F_5)_3$  at RT, the formation of a 5 membered Lewis activated  $\gamma$  nickelalactone is observed, which is converted over time to the thermodynamically more stable 4 membered Lewis activated  $\beta$  nickelalactone, as shown in **Scheme 3.15**. Additionally, the reaction between  $[(dppf)Ni(\eta^2\text{-acrylic acid})]$  and  $B(C_6F_5)_3$  also leads spontaneously to a mixture of both activated lactones. The generation of the four membered  $\beta$  nickelalactone most likely originates from  $\beta$  hydride elimination on the  $\gamma$ -nickelalactone- $B(C_6F_5)_3$  adduct, that forms a non-detected nickel hydride acrylate complex, and is followed by a 2,1 insertion of the acryl borate moiety. <sup>[54]</sup>



**Scheme 3.15:** Isomerization of the  $[(dppf)\text{-}\gamma\text{-nickelalactone}]\text{-}B(C_6F_5)_3$  adduct into the  $[(dppf)\text{-}\beta\text{-nickelalactone}]\text{-}B(C_6F_5)_3$  adduct through a transient nickel hydride acrylate intermediate. <sup>[54]</sup>

Afterwards, the nickel acrylate complex could be afforded in the presence of neutral organic bases like the phosphazene BTPP or DBU. Deprotonation might occur in the  $\alpha$  position of the four membered  $\beta$  nickelalactone through the transient nickel hydride acrylate complex. <sup>[54]</sup>



**Scheme 3.16:** Generation of the [(dppf)Ni(η<sup>2</sup>-acrylate)] complex through deprotonation of the [(dppf)-β-nickelalactone] by phosphazene BTTP. <sup>[54]</sup>

The η<sup>2</sup> coordinated acrylate is further expelled upon addition of ethylene. However, subsequent exposure to CO<sub>2</sub> did not provide the corresponding [(dppf)nickelalactone] and close the cycle. <sup>[54]</sup>

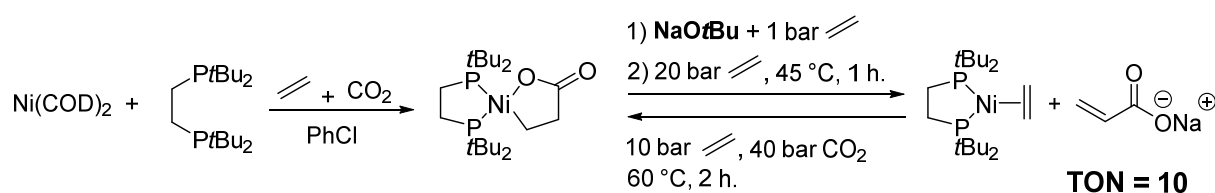
In a later contribution from 2014, Bernskoetter similarly evidenced the role of the weaker Lewis acidic sodium cation, that assists the isomerization of 5 membered activated γ-nickelalactone into 4 membered β-nickelalactone and might help β hydride elimination processes. <sup>[55]</sup> The sodium cation acts thermodynamically by stabilizing and releasing ring strain on the β-lactone and kinetically by lowering the activation barrier of the isomerization compared to a system without any Lewis acid. <sup>[55]</sup>

Hence, two strategies have been successfully established to convert nickelalactones into acrylate derivatives in stoichiometric reactions using either strong electrophiles <sup>[47 – 50]</sup> or a combination of a Lewis acid and a base. <sup>[54, 55]</sup>

### 3.2.3 Catalytic production of acrylates

The first catalytic formation of acrylates starting from ethylene and CO<sub>2</sub> was achieved only in 2012 by Limbach *et al.* <sup>[56]</sup> The endergonic carboxylation of ethylene ( $\Delta G_R^0 = 10.2 \text{ kcal.mol}^{-1}$ ) <sup>[46]</sup> can be made exergonic by the addition of a base ( $\Delta G_R^0 = -13.4 \text{ kcal.mol}^{-1}$  for NaOH), generating an acrylate salt instead of acrylic acid. <sup>[57]</sup> Indeed, the use of strong bases such as alkoxides (NaOtBu) or amides (NaHMDS) enabled for the first time efficient conversion from

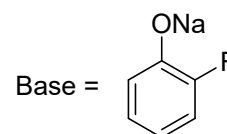
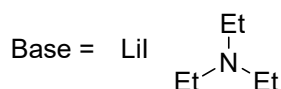
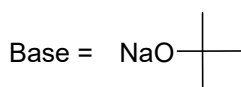
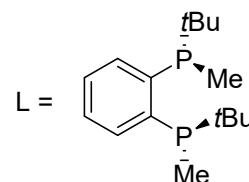
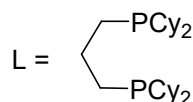
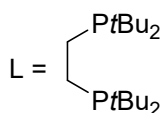
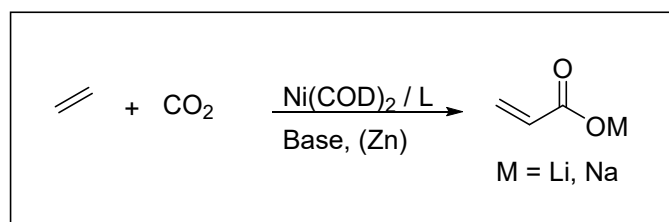
[(*dtbpe*)nickelalactone] to sodium [(*dtbpe*)Ni(acrylate)]. It turns out that instead of having directly a  $\beta$ -hydride elimination on the nickelalactone, the base abstracts an acidic proton in  $\alpha$  of the carbonyl group and the ligand rearranges itself to an acrylate. The sodium cation is of major importance as in its absence no reaction takes place and the regeneration of [(*dtbpe*)Ni(C<sub>2</sub>H<sub>4</sub>)] performs sluggishly. The setup of the catalytic process was intricate as it required for each cycle a CO<sub>2</sub> rich regime to generate the nickelalactone followed by a CO<sub>2</sub> poor regime to release the sodium acrylate and avoid side reactions between alkoxides and CO<sub>2</sub>.<sup>[58]</sup> Nevertheless, TON of 10 could be achieved.<sup>[56]</sup>



**Scheme 3.17:** First stepwise catalytic production of sodium acrylate from ethylene and CO<sub>2</sub>.<sup>[56]</sup>

In 2014 Vogt improved the TON of this reaction up to 21 in a one pot catalysis using a combination of LiI, Et<sub>3</sub>N and Zn dust.<sup>[59]</sup> The mechanism is slightly different as LiI promotes the  $\beta$ -hydride elimination under release of HI. Here again the use of an alkali metal cation proved to be of primary importance as it activates the nickelalactone and significantly lowers the activation barrier for  $\beta$ -hydride elimination. Et<sub>3</sub>N is used to trap the liberated acid and prevent the formation of lithium propanoate. The zinc powder reduces Ni(II) complexes back to catalytically active Ni(0) intermediates.<sup>[59]</sup>

Finally, in 2014 Limbach<sup>[60]</sup> managed to reach TON of 107, the highest reported to date, by tuning the base and replacing sodium *tert*-butoxide by sodium 2-fluorophenolate. Phenolates are basic enough to carry out the deprotonation but poorly nucleophilic as not to react with CO<sub>2</sub>. The methodology was also successfully tested on ten membered macrocyclic diphosphine nickelalactones<sup>[61]</sup> and could be expanded to various alkenes and dienes.<sup>[60]</sup>



**TON = 10**  
(2012)

**TON = 21**  
(2014)

**TON = 107**  
(2014)

**Scheme 3.18:** Reaction systems and TON recently described for the nickel catalyzed formation of acrylates from ethylene and CO<sub>2</sub>.<sup>[56, 59, 60]</sup>

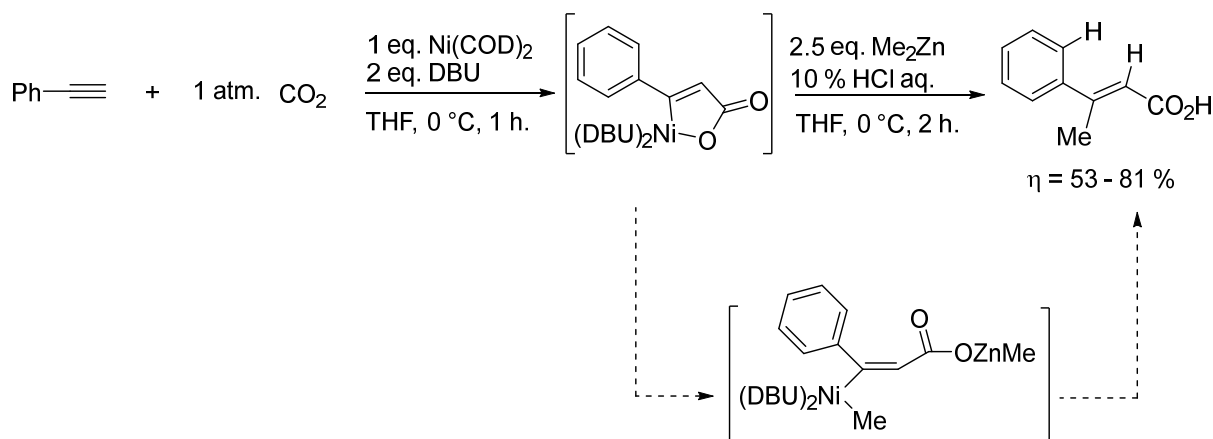
Related palladium catalysis was also achieved in 2015 by Limbach following a similar methodology. However, maximum TON only reached 29<sup>[62]</sup> and was further optimized by Schaub to 106 by the end of 2015.<sup>[57]</sup>

### 3.3 Research objectives

The stoichiometric and especially catalytic synthesis of acrylates from nickelalactones still necessitates major improvements to render the process viable for industrial application. The aim of this research project is therefore to synthesize new nickelalactones and to explore innovative pathways for the generation of acrylate derivatives. Transmetalation can be a promising alternative for the synthesis of valuable chemicals under mild conditions from ethylene and CO<sub>2</sub>.

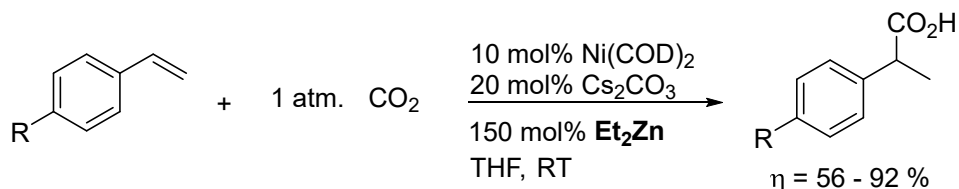
In the early 2000s, Mori already treated nickelalactones, synthesized from the oxidative coupling between alkynes<sup>[63, 64]</sup> or 1,3-dienes<sup>[65, 66, 67]</sup> and CO<sub>2</sub>, with zinc derivatives such as Me<sub>2</sub>Zn, Et<sub>2</sub>Zn or PhZnCl, as illustrated in **Scheme 3.19**. In a first step the nickelalactone is

opened to an acrylate or propanoate complex and in a second step the product is reductively eliminated from the nickel. When the zinc reagent possesses  $\beta$  hydrogens,  $\beta$  hydride elimination on the transferred alkyl moiety can precede reductive elimination.<sup>[63, 66]</sup> In all cases carboxylic acids were obtained in high yields and good regio and stereoselectivities. Some reactions could even be performed catalytically.<sup>[64, 66, 67]</sup>



**Scheme 3.19:** Alkylative carboxylation of alkynes using CO<sub>2</sub> and Me<sub>2</sub>Zn.<sup>[63]</sup>

Rovis also investigated in two contributions<sup>[68, 69]</sup> the reactivity of nickelalactones towards zinc derivatives and achieved decarbonylative cross coupling of cyclic anhydrides<sup>[68]</sup> and reductive carboxylation of styrenes<sup>[69]</sup> (**Scheme 3.20**) producing in both cases carboxylic acid derivatives. Though preliminary mechanistic investigations suggest that the later reaction, presented in **Scheme 3.20**, does actually not proceed through nickelalactones but rather through nickel hydride intermediates.<sup>[69]</sup>

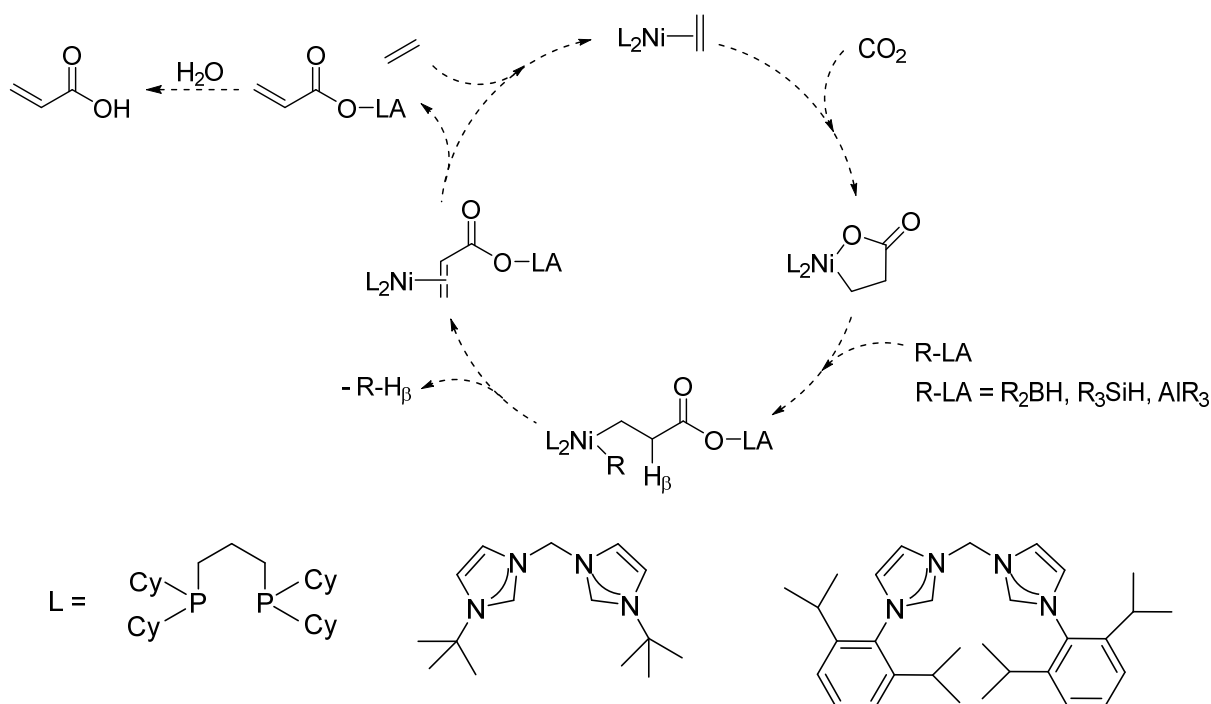


**Scheme 3.20:** Reductive carboxylation of styrene using CO<sub>2</sub> and Et<sub>2</sub>Zn.<sup>[69]</sup>

These reports all demonstrate that CO<sub>2</sub> can be successfully reduced and integrated into valuable chemicals through the use of a transmetallating reagent. However, acrylates have never been generated through this synthetic approach.



Hence, in this work, nickelalactones obtained from the oxidative coupling between ethylene and CO<sub>2</sub>, will be directly subjected to various oxophilic transmetallating reagents, to attempt the synthesis of acrylates. Zinc derivatives do not seem suitable as they favor reductive elimination over  $\beta$  hydride elimination after cleaving the nickelalactones.<sup>[63 - 69]</sup> Nevertheless, by changing the nature and the properties of the transmetallating reagents, it might be possible to tune the reactivity in favor of  $\beta$  hydride elimination and trigger the formation of acrylates, as shown in **Scheme 3.21**.



**Scheme 3.21:** Potential reactivity of nickelalactones with transmetallating reagents.

The main part of this work is committed to large bite angle chelating bis-phosphine nickelalactones. After successful synthesis of the nickelalactones, these will be subjected to various oxophilic transmetallating reagents such as boranes, silanes or aluminium derivatives to induce ring cleavage at the nickel center.

Moreover, the chemistry of related chelating bis-NHC complexes has been targeted. New procedures will be described for the synthesis of yet unknown [(bis-NHC)nickelalactones]. Changing the electronic and steric properties of the ligands might help to bypass the high CO<sub>2</sub> pressures sometimes required for the generation of nickelalactones through oxidative coupling and ease  $\beta$  hydride elimination processes. The reactivity of the new [(bis-NHC)nickelalactones]

can then be tested either under reported catalytic conditions <sup>[59, 60]</sup> or towards transmetallating reagents to generate acrylates.

### 3.4 References

- [1] M. Aresta, *Carbon Dioxide as Chemical Feedstock*, Wiley-VCH, Weinheim, **2010**.
- [2] C. Song, *Catal. Today*, **2006**, *115*, 2 - 32.
- [3] M. Peters, B. Köhler, W. Kuckshinrichs, W. Leitner, P. Markewitz, T. E. Müller, *ChemSusChem*, **2011**, *4*, 1216 - 1240.
- [4] W. Wang, S. P. Wang, X. B. Ma, J. L. Gong, *Chem. Soc. Rev.*, **2011**, *40*, 3703 - 3727.
- [5] W. H. Wang, Y. Himeda, J. T. Muckerman, G. F. Manbeck, E. Fujita, *Chem. Rev.*, **2015**, *115*, 12936 - 12973.
- [6] A. Goepfert, M. Czaun, J.-P. Jones, G. K. S. Prakash, G. A. Olah, *Chem. Soc. Rev.*, **2014**, *43*, 7995 - 8048.
- [7] M. A. A. Aziz, A. A. Jalil, S. Triwahyono, A. Ahmad, *Green Chem.*, **2016**, *17*, 2647 - 2663.
- [8] C. Das Neves Gomes, O. Jacquet, C. Villiers, P. Thuéry, M. Ephritikhine, T. Cantat, *Angew. Chem. Int. Ed.*, **2012**, *51*, 187 - 190.
- [9] G. Jin, C. G. Werncke, Y. Escudié, S. Sabo-Etienne, S. Bontemps, *J. Am. Chem. Soc.*, **2015**, *137*, 9563 - 9566.
- [10] M. Cokoja, B. Rieger, W. A. Herrmann, F. E. Kühn, *Angew. Chem. Int. Ed.*, **2011**, *50*, 8510 - 8537.
- [11] K. Huang, C.-L. Sun, Z.-J. Shi, *Chem. Soc. Rev.*, **2011**, *40*, 2435 - 2452.
- [12] *Market Study: Urea*, Ceresana Research, **2012**.
- [13] J. H. Meessen, H. Petersen, in *Ullmann's Encyclopedia of Industrial Chemistry, Urea*, 6 ed., Wiley-VCH, Berlin, **2002**.
- [14] T. Sakakura, J.-C. Choi, H. Yasuda, *Chem. Rev.*, **2007**, *107*, 2365 - 2387.
- [15] D. J. Darensbourg, *Chem. Rev.*, **2007**, *107*, 2388 - 2410.
- [16] A. S. Lindsey, H. Jeskey, *Chem. Rev.*, **1957**, *57*, 583 - 620.
- [17] N. Nojiri, Y. Sakai, Y. Watanabe, *Catal. Rev.*, **1995**, *37*, 145 - 178.

- [18] M. M. Bettahar, G. Costentin, L. Savary, J. C. Lavalley, *Appl. Catal. A: Gen.*, **1996**, *145*, 1 - 48.
- [19] M. M. Lin, *Appl. Catal. A: Gen.*, **2001**, *207*, 1 - 16.
- [20] M. Hollering, B. Dutta, F. Z. Kühn, *Coord. Chem. Rev.*, **2016**, *309*, 51 - 67.
- [21] S. Kraus, B. Rieger, *Top. Organomet. Chem.*, **2016**, *53*, 199 - 224.
- [22] H. Hoberg, D. Schaefer, *J. Organomet. Chem.*, **1983**, *251*, C51 - C53.
- [23] H. Hoberg, D. Schaefer, G. Burkhart, C. Krüger, M. J. Romão, *J. Organomet. Chem.*, **1984**, *266*, 203 - 224.
- [24] H. Hoberg, A. Ballesteros, A. Sigan, *J. Organomet. Chem.*, **1991**, *403*, C19 - C22.
- [25] H. Hoberg, D. Schaefer, *J. Organomet. Chem.*, **1982**, *236*, C28 - C30.
- [26] H. Hoberg, Y. Peres, A. Milchereit, *J. Organomet. Chem.*, **1986**, *307*, C38 - C40.
- [27] H. Hoberg, B. Apotecher, *J. Organomet. Chem.*, **1984**, *270*, C15 - C17.
- [28] H. Hoberg, S. Groß, A. Milchereit, *Angew. Chem.*, **1987**, *99*, 567 - 569.
- [29] H. Hoberg, Y. Peres, A. Milchereit, S. Gross, *J. Organomet. Chem.*, **1988**, *345*, C17 - C19.
- [30] H. Hoberg, D. Bärhausen, *J. Organomet. Chem.*, **1989**, *379*, C7 - C11.
- [31] D. Walther, E. Dinjus, J. Sieler, L. Andersen, O. Lindqvist, *J. Organomet. Chem.*, **1984**, *276*, 99 - 107.
- [32] D. Walther, E. Dinjus, *Z. Chem.*, **1982**, *22*, 228 - 229.
- [33] E. Dinjus, D. Walther, H. Schuetz, W. Schade, *Z. Chem.*, **1983**, *23*, 303 - 304.
- [34] D. Walther, E. Dinjus, *Z. Chem.*, **1984**, *24*, 63.
- [35] D. Walther, E. Dinjus, H. Görls, J. Sieler, O. Lindqvist, L. Andersen, *J. Organomet. Chem.*, **1985**, *286*, 103 - 114.
- [36] H. Hoberg, Y. Peres, C. Krüger, Y.-H. Tsay, *Angew. Chem.*, **1987**, *99*, 799 - 800.
- [37] I. Pápai, G. Schubert, I. Mayer, G. Besenyei, M. Aresta, *Organomet.*, **2004**, *23*, 5252 - 5259.

- [38] G. Yang, B. Schäffner, M. Blug, E. J. M. Hensen, E. A. Pidko, *ChemCatChem*, **2014**, *6*, 800 - 807.
- [39] E. Uhlig, G. Fehske, B. Nestler, *Z. Anorg. Allg. Chem.*, **1980**, *465*, 141 - 146.
- [40] K. Sano, T. Yamamoto, A. Yamamoto, *Chem. Lett.*, **1983**, 115 - 118.
- [41] R. Fischer, D. Walther, G. Bräunlich, B. Undeutsch, W. Ludwig, H. Bandmann, *J. Organomet. Chem.*, **1992**, *427*, 395 - 407.
- [42] R. Fischer, B. Nestler, H. Schütz, *Z. Anorg. Allg. Chem.*, **1989**, *577*, 111 - 114.
- [43] J. Langer, R. Fischer, H. Görls, D. Walther, *J. Organomet. Chem.*, **2004**, *689*, 2952 - 2962.
- [44] R. Fischer, J. Langer, A. Malassa, D. Walther, H. Görls, G. Vaughan, *Chem. Commun.*, **2006**, 2510 - 2512.
- [45] J. Langer, R. Fischer, H. Görls, D. Walther, *Eur. J. Inorg. Chem.*, **2007**, 2257 - 2254.
- [46] D. C. Graham, C. Mitchell, M. I. Bruce, G. F. Metha, J. H. Bowie, M. A. Buntine, *Organomet.*, **2007**, *26*, 6784 - 6792.
- [47] C. Bruckmeier, M. W. Lehenmeier, R. Reichardt, S. Vagin, B. Rieger, *Organomet.*, **2010**, *29*, 2199 - 2202.
- [48] S. Y. T. Lee, M. Cokoja, M. Drees, Y. Li, J. Mink, W. A. Herrmann, F. E. Kühn, *ChemSusChem*, **2011**, *4*, 1275 - 1279.
- [49] S. Y. T. Lee, A. Abdul Ghani, V. D'Elia, M. Cokoja, W. A. Herrmann, J.-M. Basset, F. E. Kühn, *New. J. Chem.*, **2013**, *37*, 3512 - 3517.
- [50] Z. Zhang, F. Guo, F. E. Kühn, J. Sun, M. Zhou, X. Fang, *Appl. Organometal. Chem.*, **2017**, *31*, e3567.
- [51] W. Guo, C. Michel R. Schwiedernoch, R. Wischert, X. Xu, P. Sautet, *Organomet.*, **2014**, *33*, 6369 - 6380.
- [52] P. N. Plessow, L. Weigel, R. Lindner, A. Schäfer, F. Rominger, M. Limbach, P. Hofmann, *Organomet.*, **2013**, *32*, 3327 - 3338.
- [53] M. Limbach, J. Miller, S. Schunk, WO 2011/107559A2, **2011**.
- [54] D. Jin, T. J. Schmeier, P. G. Williard, N. Hazari, W. H. Bernskoetter, *Organomet.*, **2013**, *32*, 2152 - 2159.

- [55] D. Jin, P. G. Williard, N. Hazari, W. H. Bernskoetter, *Chem. Eur. J.*, **2014**, *20*, 3205 - 3211.
- [56] M. L. Lejkowski, R. Lindner, T. Kageyama, G. É. Bódizs, P. N. Plessow, I. B. Müller, A. Schäfer, F. Rominger, P. Hofmann, C. Futter, S. A. Schunk, M. Limbach, *Chem. Eur. J.*, **2012**, *18*, 14017 - 14025.
- [57] S. Manzini, N. Huguet, O. Trapp, T. Schaub, *Eur. J. Org. Chem.*, **2015**, *32*, 7122 - 7130.
- [58] W. Behrendt, G. Gattow, M. Dräger, *Z. Anorg. Allg. Chem.*, **1973**, *397*, 237 - 246.
- [59] C. Hendriksen, E. A. Pidko, G. Yang, B. Schöffner, D. Vogt, *Chem. Eur. J.*, **2014**, *20*, 12037 - 12040.
- [60] N. Huguet, I. Jevtovikj, A. Gordillo, M. L. Lejkowski, R. Lindner, M. Bru, A. Y. Khalimon, F. Rominger, S. A. Svhunk, P. Hofmann, M. Limbach, *Chem. Eur. J.*, **2014**, *20*, 16858 - 16862.
- [61] I. Knopf, D. Tofan, D. Beetstra, A. Al-Nezari, K. Al-Bahily, C. C. Cummins, *Chem. Sci.*, **2016**, DOI:10.1039/C6SC03614G.
- [62] S. C. E. Stieber, N. Huguet, T. Kageyama, I. Jevtovikj, P. Ariyananda, A. Gordillo, S. A. Schunk, F. Rominger, P. Hofmann, M. Limbach, *Chem. Commun.*, **2015**, 10907 - 10909.
- [63] M. Takimoto, K. Shimizu, M. Mori, *Org. Lett.*, **2001**, *3*, 3345 - 3347.
- [64] K. Shimizu, M. Takimoto, Y. Sato, M. Mori, *Org. Lett.*, **2005**, *7*, 195 - 197.
- [65] M. Takimoto, M. Mori, *J. Am Chem. Soc.*, **2001**, *123*, 2895 - 2896.
- [66] M. Takimoto, M. Mori, *J. Am. Chem. Soc.*, **2002**, *124*, 10008 - 10009.
- [67] M. Takimoto, Y. Nakamura, K. Kimura, M. Mori, *J. Am. Chem. Soc.*, **2004**, *126*, 5956 - 5957.
- [68] E. M. O'Brien, E. A. Bercot, T. Rovis, *J. Am. Chem. Soc.*, **2003**, *125*, 10498 - 10499.
- [69] C. M. Williams, J. B. Johnson, T. Rovis, *J. Am. Chem. Soc.*, **2008**, *130*, 14936 - 14937.



## 4 Functionalization of CO<sub>2</sub> with boranes

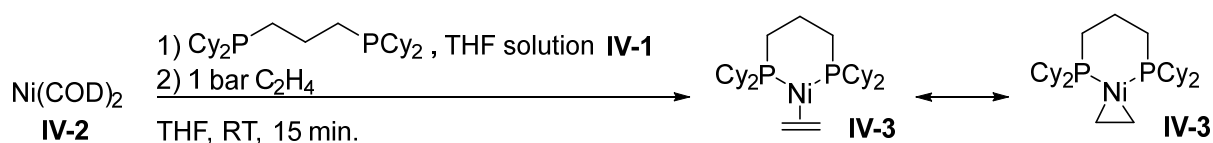
The oxidative coupling between ethylene and CO<sub>2</sub> at chelating bis-phosphine nickel complexes and subsequent reactivity with boranes will be discussed in this chapter. Chelating bis-phosphines with large bite angles, already selected for this type of chemistry and previously investigated in our group (**Chapter 2**)<sup>[1]</sup>, constitute the ligands of choice for this study.

### 4.1 Synthesis of [(dcpp)Ni(C<sub>2</sub>H<sub>4</sub>)] **IV-3** and [(dcpp)nickelalactone] **IV-4**

In order to investigate the reductive functionalization of CO<sub>2</sub> at [(dcpp)nickel]-complexes, the metal-organic intermediates [(dcpp)Ni(C<sub>2</sub>H<sub>4</sub>)] **IV-3** and [(dcpp)nickelalactone] **IV-4** have been independently synthesized.

#### 4.1.1 Synthesis of [(dcpp)Ni(C<sub>2</sub>H<sub>4</sub>)] **IV-3**

Starting from commercially available [Ni(COD)<sub>2</sub>] **IV-2**, [(dcpp)Ni(C<sub>2</sub>H<sub>4</sub>)] **IV-3** is obtained through successive ligand substitutions, as shown in **Scheme 4.1**. The first 1,5-cyclooctadiene moiety is displaced by one equivalent of dcpp ligand **IV-1**, while the second is displaced by applying a pressure of ethylene. The complex is gathered as a yellow powder in 64 % yield. <sup>31</sup>P{<sup>1</sup>H} NMR shows a single resonance at δ = 25.5 ppm. The ethylenic protons are found at δ = 1.52 ppm in <sup>1</sup>H NMR and the corresponding carbon atoms appear at δ = 31.87 ppm in <sup>13</sup>C NMR. The peaks are strongly shifted upfield, due to the electron richness of the [(dcpp)Ni]-fragment and the strong π back donation from the nickel center to the coordinated olefin. This symmetric complex could therefore also be described as a metallacyclopropane. Single crystals were grown by heating a THF solution to reflux and allowing it to slowly cool down back to RT.



**Scheme 4.1:** Synthesis of [(dcpp)Ni(C<sub>2</sub>H<sub>4</sub>)] **IV-3** from [Ni(COD)<sub>2</sub>] **IV-2** through successive ligand substitutions.



X-ray diffraction analysis shows that [(dcpp)Ni(C<sub>2</sub>H<sub>4</sub>)] **IV-3** crystallizes in the P2<sub>1/n</sub> space group in an approximately square planar environment. The bite angle P<sub>1</sub>-Ni<sub>1</sub>-P<sub>2</sub> measures 104.50(10)° which is comparable to the already reported [(dtbpp)Ni(C<sub>2</sub>H<sub>4</sub>)]<sup>[2]</sup> (P-Ni-P = 104.700(15)°). The C<sub>4</sub>-C<sub>5</sub> ethylene bond length of 1.407(15) Å ([[(dtbpp)Ni(C<sub>2</sub>H<sub>4</sub>)] C-C = 1.392(39) Å<sup>[2]</sup>) lies between a carbon-carbon single (1.54 Å) and double bond (1.34 Å), further evidencing the strong π-back donation from the nickel center to the ethylene.

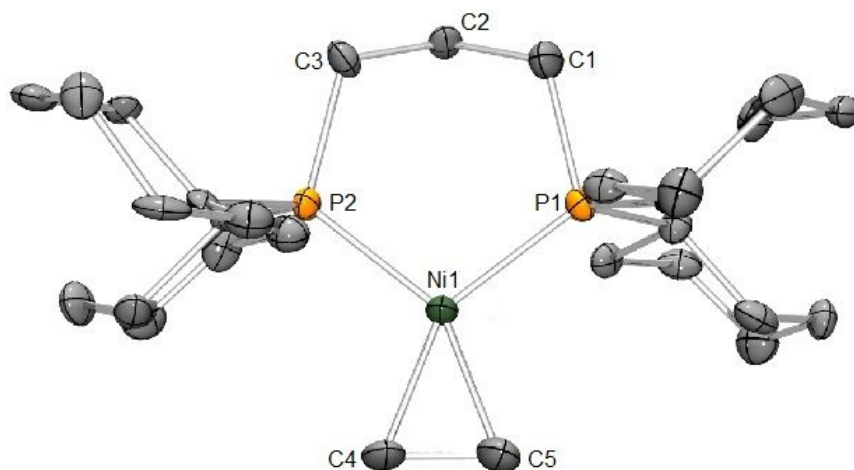


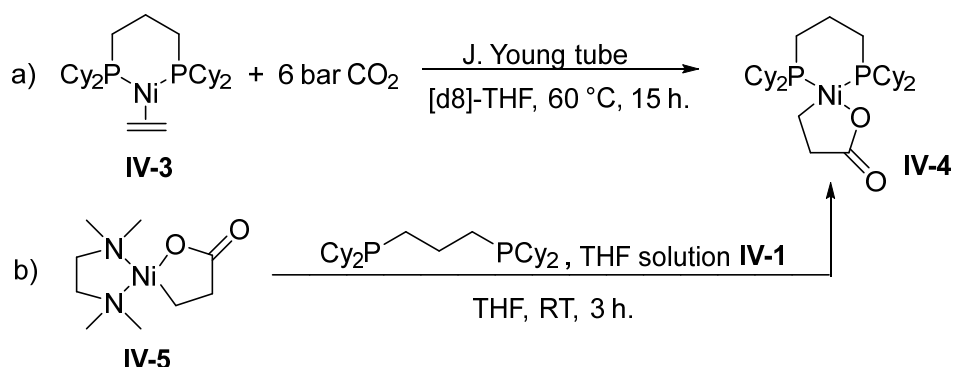
**Figure 4.1:** Molecular structure of [(dcpp)Ni(C<sub>2</sub>H<sub>4</sub>)] **IV-3** determined by single crystal X-ray diffraction. Hydrogen atoms are omitted for clarity. Selected bond length [Å] and angles [°]: C<sub>4</sub>-C<sub>5</sub> 1.407(15), P<sub>1</sub>-Ni<sub>1</sub>-P<sub>2</sub> 104.50(10).

#### 4.1.2 Synthesis of [(dcpp)nickelalactone] **IV-4**

[(dcpp)nickelalactone] **IV-4** is expected to be formed through the oxidative coupling between [(dcpp)Ni(C<sub>2</sub>H<sub>4</sub>)] **IV-3** and CO<sub>2</sub>. No reaction is observed after applying 1 bar of CO<sub>2</sub> to a J. Young tube containing a [(dcpp)Ni(C<sub>2</sub>H<sub>4</sub>)] **IV-3** solution. However, at 6 bar of CO<sub>2</sub>, small amounts of a new product are observed by <sup>31</sup>P{<sup>1</sup>H} NMR. The two sets of doublets at δ = 10.4 ppm (<sup>2</sup>J<sub>P,P</sub> = 32.8 Hz) and δ = 32.1 ppm (<sup>2</sup>J<sub>P,P</sub> = 32.8 Hz) are attributed to [(dcpp)nickelalactone] **IV-4**. Better conversions are expected by reaching higher pressures. An equilibrium between [(dcpp)Ni(C<sub>2</sub>H<sub>4</sub>)] **IV-3** and [(dcpp)nickelalactone] **IV-4** is thus apparent.

Therefore, an alternative, reaction pathway starting from [(tmeda)nickelalactone]<sup>[3]</sup> **IV-5** has been designed to generate [(dcpp)nickelalactone] **IV-4**. The diamine is easily displaced at RT by the chelating bis-phosphine **IV-1**, affording [(dcpp)nickelalactone] **IV-4** as a yellow to light orange powder in 68 % yield. <sup>31</sup>P{<sup>1</sup>H} NMR confirms that the complex obtained through ligand

substitution and the one observed after applying a CO<sub>2</sub> pressure to [(dcpp)Ni(C<sub>2</sub>H<sub>4</sub>)] **IV-3** are identical.



**Scheme 4.2:** Synthesis of [(dcpp)nickelalactone] **IV-4** through a) oxidative coupling at 6 bar of CO<sub>2</sub> and b) ligand substitution from [(tmeda)nickelalactone] **IV-5**.

Single crystals of [(dcpp)nickelalactone] **IV-4** were grown at RT from a THF solution layered with pentane. The first structure of a propyl bridged nickelalactone is shown in **Figure 4.2**. The geometry around the Ni(II) center is square planar. The bite angle P<sub>1</sub>-Ni<sub>1</sub>-P<sub>2</sub> measuring 99.66(2) ° is smaller as expected than the [(dcpp)Ni(C<sub>2</sub>H<sub>4</sub>)] **IV-3** bite angle (104.50(10) °). The Ni<sub>1</sub>-O<sub>1</sub> bond length (1.9074(18) Å) is about 0.05 Å longer than in [(diamine)nickelalactones] (1.8655(13) Å for [(dipyridine)nickelalactone],<sup>[4]</sup> 1.868(3) Å for [(DBU)<sub>2</sub>nickelalactone],<sup>[5]</sup> 1.854(2) Å for [(tmeda)nickelalactone] **IV-5**,<sup>[6]</sup> 1.8448(1) Å for [(2,2'-bipyridine)nickelalactone]<sup>[7]</sup>) and in the range of the other crystalized [(bis-phosphine)nickelalactones]<sup>[2, 8, 9]</sup> (1.890(2) Å for [(dcpe)nickelalactone],<sup>[8]</sup> 1.889(2) Å for [(dtbpe)nickelalactone]<sup>[2]</sup>). The elongation of the Ni-O bond is expected to facilitate β-hydride elimination processes.

[(dcpp)nickelalactone] **IV-4** is stable in air for 2 h. and can be kept in the glovebox over months at RT. In comparison bulkier [(dtbpp)nickelalactone] **IV-6** (<sup>31</sup>P {<sup>1</sup>H} NMR: δ = 22.9 ppm (d, <sup>2</sup>J<sub>P, P</sub> = 15.8 Hz); δ = 42.8 ppm (d, <sup>2</sup>J<sub>P, P</sub> = 15.8 Hz)) synthesized from [(tmeda)nickelalactone] **IV-5**, readily decomposes within 1 d. to [(dtbpp)Ni(C<sub>2</sub>H<sub>4</sub>)] **IV-7** and CO<sub>2</sub> in THF at RT. [(dtbpf)nickelalactone], which also has a large bite angle (104.33 °) and bulky substituents shows similar instability at RT.<sup>[10]</sup>

However, at 60 °C [(dcpp)nickelalactone] **IV-4** gives quantitative formation of [(dcpp)Ni(C<sub>2</sub>H<sub>4</sub>)] **IV-3** within 3 d. At higher temperatures the equilibrium between both complexes is largely shifted towards [(dcpp)Ni(C<sub>2</sub>H<sub>4</sub>)] **IV-3** [(dippf)nickelalactone]<sup>[10]</sup> also

undergoes reductive decoupling upon heating. However, no formation of [(dcpp)<sub>2</sub>Ni] is observed unlike for aryl substituted [(dppe)],<sup>[2]</sup> [(dppp)]<sup>[2, 9]</sup> and [(dppf)nickelalactones].<sup>[10]</sup>

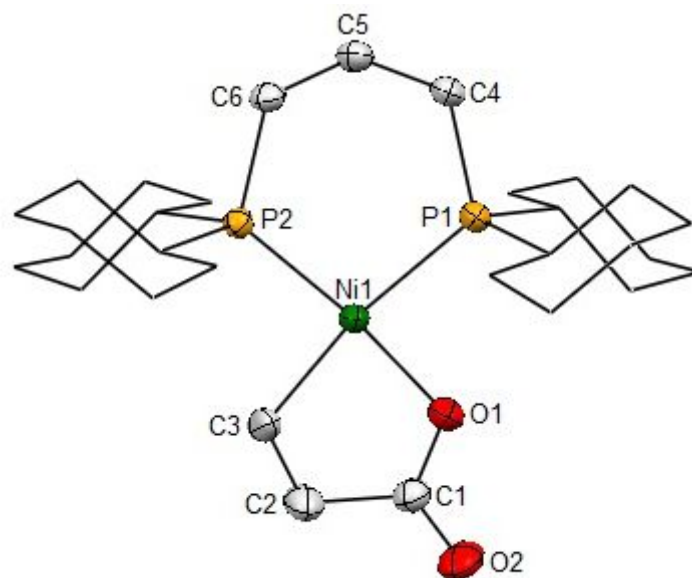
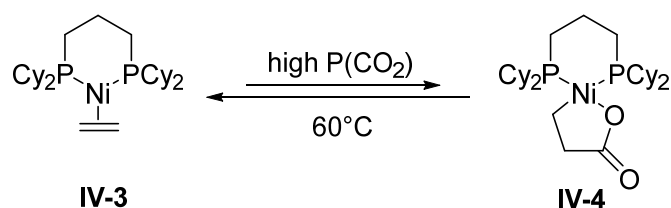


**Figure 4.2:** Molecular structure of [(dcpp)nickelalactone] **IV-4** determined by single crystal X-ray diffraction. Hydrogen atoms are omitted for clarity. Selected bond length [Å] and angles [°]: Ni<sub>1</sub>-O<sub>1</sub> 1.9074(18), Ni<sub>1</sub>-C<sub>3</sub> 1.968(3), C<sub>1</sub>-O<sub>2</sub> 1.214(3), P<sub>1</sub>-Ni<sub>1</sub>-P<sub>2</sub> 99.66(2).

## 4.2 Kinetic Study

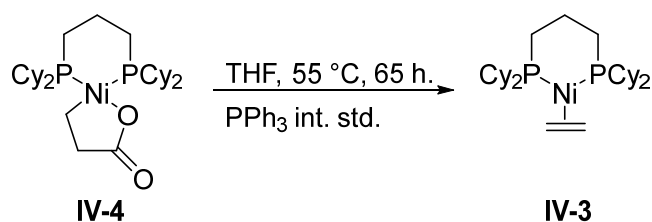
The equilibrium between [(dcpp)Ni(C<sub>2</sub>H<sub>4</sub>)] **IV-3** and [(dcpp)nickelalactone] **IV-4** has been investigated through kinetic studies. On one hand, high CO<sub>2</sub> pressures enable the oxidative coupling on [(dcpp)Ni(C<sub>2</sub>H<sub>4</sub>)] **IV-3** and generate [(dcpp)nickelalactone] **IV-4**. On the other hand, moderate temperatures draw the reaction backwards and reductively decouple [(dcpp)nickelalactone] **IV-4** to [(dcpp)Ni(C<sub>2</sub>H<sub>4</sub>)] **IV-3** and CO<sub>2</sub> as depicted in **Scheme 4.3**.



**Scheme 4.3:** Equilibrium between [(dcpp)Ni(C<sub>2</sub>H<sub>4</sub>)] **IV-3** and [(dcpp)nickelalactone] **IV-4**.

As the solubility of [(dcpnp)Ni(C<sub>2</sub>H<sub>4</sub>)] **IV-3** is limited in all common organic solvents, the concentration of [(dcpnp)nickelalactone] **IV-4** is monitored instead in all kinetic experiments.

First of all, a known amount of [(dcpnp)nickelalactone] **IV-4** is heated at 55 °C in THF with PPh<sub>3</sub> as internal standard. The decay of [(dcpnp)nickelalactone] **IV-4** is followed by <sup>31</sup>P{<sup>1</sup>H} NMR spectroscopy. (see Experimental part 4.8.4.1 for more details)



**Scheme 4.4:** Reductive decoupling of [(dcpnp)nickelalactone] **IV-4** in THF at 55 °C, followed by <sup>31</sup>P{<sup>1</sup>H} NMR over 65 h. PPh<sub>3</sub> is used as internal standard.

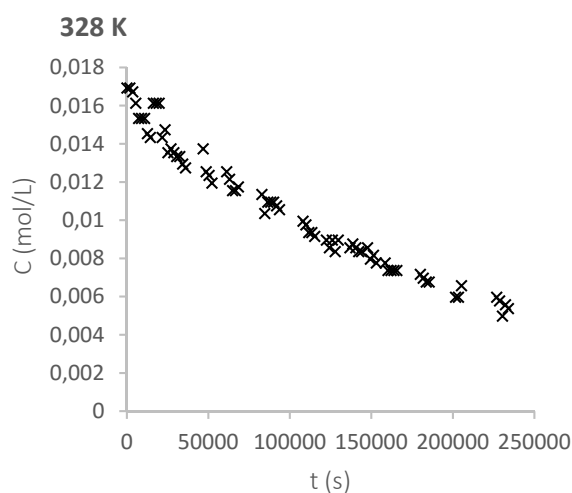


**Figure 4.3:** Kinetic profile of the reaction in THF at 55 °C.

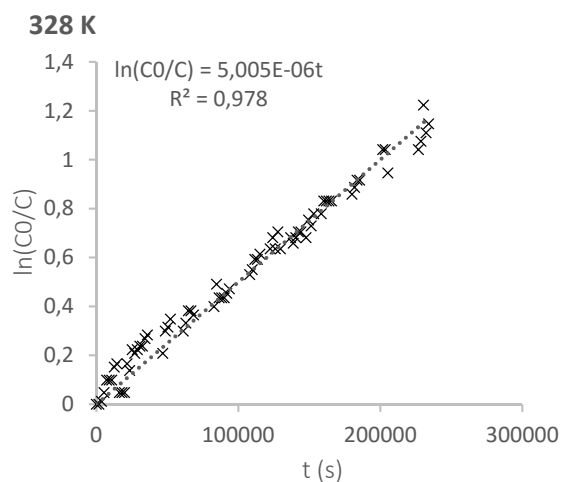


**Figure 4.4:** ln([Nilactone]<sub>0</sub>/[Nilactone]) as a function of time for the reaction in THF at 55 °C.

A zero-order reaction is excluded since plotting the concentration of [(dcpnp)nickelalactone] **IV-4** ([Nilactone]) as a function of time does not result in a linear slope. However, plotting ln([Nilactone]<sub>0</sub>/[Nilactone]) as a function of time does result in a linear slope. The reaction hence follows a first order kinetics. Interestingly, Limbach *et. al.* reported partial first order

kinetics with respect to [(dtbpe)Ni(C<sub>2</sub>H<sub>4</sub>)] for the generation of [(dtbpe)nickelalactone] from [(dtbpe)Ni(C<sub>2</sub>H<sub>4</sub>)] under 40 bar of CO<sub>2</sub> in chlorobenzene at 60 °C. [2]

The  $\Delta G^\ddagger$  of the transition state can be obtained by inserting the determined rate constant  $k_{obs}$  in the Eyring equation (**Equation 4.1**).

**Equation 4.1**

$$\Delta G^\ddagger = RT \left( \ln \left( \frac{k_B T}{h} \right) - \ln(k_{obs}) \right)$$

At 55 °C in THF  $\Delta G^\ddagger = 27.21 \text{ kcal.mol}^{-1}$ . This value seems coherent, since harsher conditions are required to push the reaction forward on either side.

Afterwards, the experiment has been repeated at different temperatures ranging from 60 °C to 90 °C. The solvent has been switched from THF to toluene. The plots  $\ln([\text{Nilactone}]_0/[\text{Nilactone}]) = f(t)$  are represented in **Figure 4.5** to **4.8**. The calculated rate constants  $k_{obs}$  and the corresponding  $\Delta G^\ddagger$  values can be found in **Table 4.1**. The average  $\Delta G^\ddagger$  value is of  $27.39 \text{ kcal.mol}^{-1}$ .

**Table 4.1:** Rate constants and calculated  $\Delta G^\ddagger$  values for different temperatures.

Temperature (°C)	Solvent	$k_{obs} \text{ (s}^{-1}\text{)}$	$\Delta G^\ddagger \text{ (kcal.mol}^{-1}\text{)}$
55	THF	$5.005 \times 10^{-6}$	27.21
60	toluene	$7.365 \times 10^{-6}$	27.38
70	toluene	$2.691 \times 10^{-5}$	27.34
80	toluene	$7.735 \times 10^{-5}$	27.42
90	toluene	$1.861 \times 10^{-4}$	27.58
mean value	-	-	27.39

This temperature variation allows to further get access to the activation parameters  $\Delta H^\ddagger$  and  $\Delta S^\ddagger$  of the reaction. These can be directly read from an Eyring plot (**Equation 4.2**).

**Equation 4.2**

$$\ln \left( \frac{k_{obs}}{T} \right) = - \frac{\Delta H^\ddagger}{R} \times \frac{1}{T} + \ln \left( \frac{k_B}{h} \right) + \frac{\Delta S^\ddagger}{R}$$

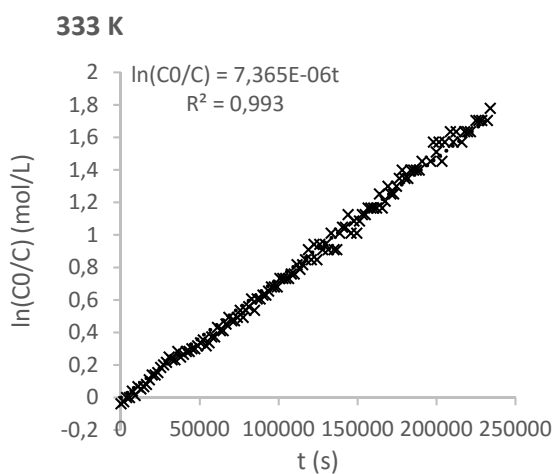


**Figure 4.5:**  $\ln([\text{Nilactone}]_0/[\text{Nilactone}])$  over time for the reaction in toluene at 60° C.

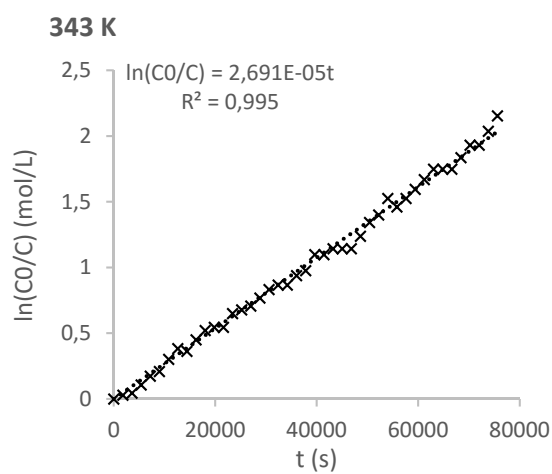


**Figure 4.6:**  $\ln([\text{Nilactone}]_0/[\text{Nilactone}])$  over time for the reaction in toluene at 70 °C.

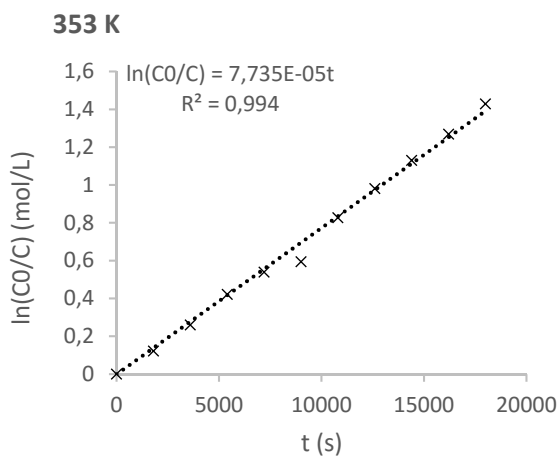


**Figure 4.7:**  $\ln([\text{Nilactone}]_0/[\text{Nilactone}])$  over time for the reaction in toluene at 80° C.

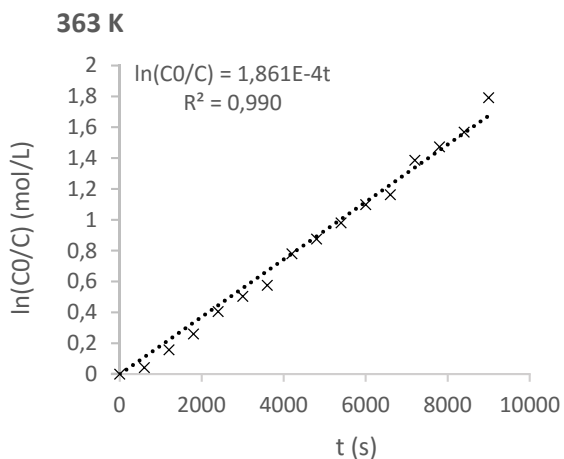


**Figure 4.8:**  $\ln([\text{Nilactone}]_0/[\text{Nilactone}])$  over time for the reaction in toluene at 90 °C.

**Table 4.2** gives the activation parameters determined by the Eyring plot. The reaction is mainly enthalpy driven. The entropy contribution  $\Delta S^\ddagger$  is small.

**Table 4.2:** Activation parameters for the conversion of [(dcpn)nickelalactone] **IV-4** into [(dcpn)Ni(C<sub>2</sub>H<sub>4</sub>)] **IV-3** and CO<sub>2</sub> obtained by the Eyring plot.

$\Delta H^\ddagger$ [kcal.mol <sup>-1</sup> ]	25.17
$\Delta S^\ddagger$ [cal.mol <sup>-1</sup> .K <sup>-1</sup> ]	-6.50
$\Delta G^\ddagger$ [kcal.mol <sup>-1</sup> ]	27.33 (for 333 K) 27.46 (for 353 K)

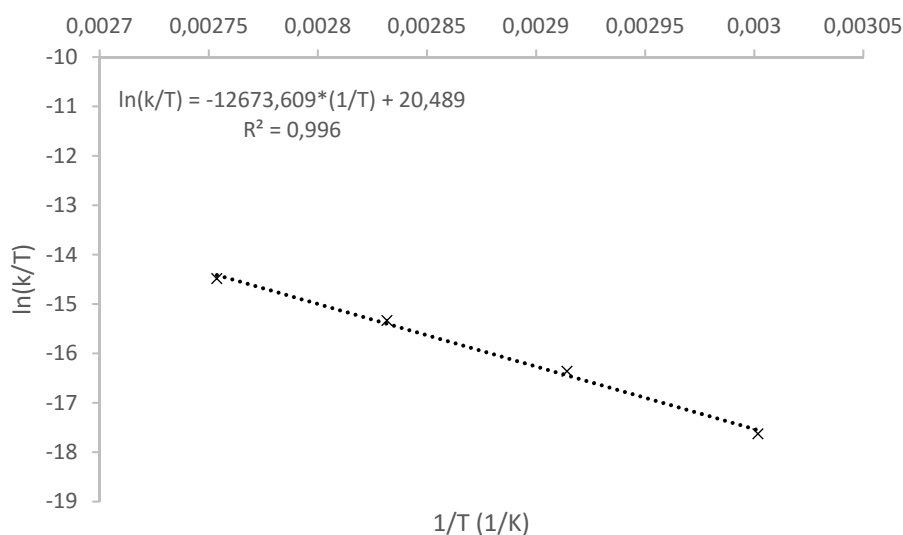


**Figure 4.9:** Eyring plot for the conversion of [(dcpn)nickelalactone] **IV-4** into [(dcpn)Ni(C<sub>2</sub>H<sub>4</sub>)] **IV-3** and CO<sub>2</sub> between 60 °C and 90 °C. Slope: -12673.609 K; intercept: 20.489.

Overall, [(dcpn)nickelalactone] **IV-4** can be synthesized by oxidative coupling with ethylene under harsher pressure conditions. However, [(dcpn)nickelalactone] **IV-4** stands in equilibrium with [(dcpn)Ni(C<sub>2</sub>H<sub>4</sub>)] **IV-3**. The reactivity of [(dcpn)nickelalactone] **IV-4** towards boranes will be discussed in the rest of the chapter.

### 4.3 Reactivity between [(dcp)nickel]-complexes and boranes

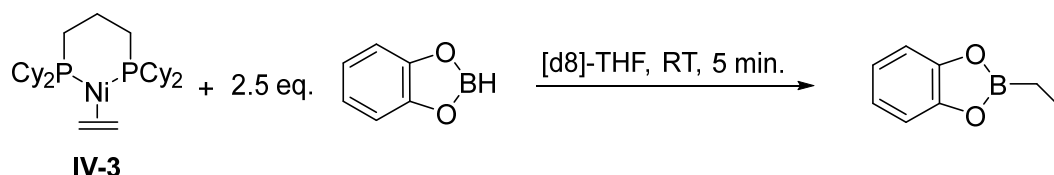
As an alternative to strong electrophiles<sup>[6, 11-14]</sup> and bases,<sup>[2, 15-17]</sup> the use of boranes as transmetallating reagents will be tested in order to cleave [(dcp)nickelalactone] **IV-4** and to generate acrylate derivatives.

#### 4.3.1 Choosing an appropriate borane

The oxidative coupling between ethylene and CO<sub>2</sub> at the [(dcp)Ni]-fragment should not be hindered by the presence of a borane, required to further convert [(dcp)nickelalactone] **IV-4** into value added chemicals. Hydroboration can be considered as a competitive side reaction during the oxidative coupling. In order to smoothly fulfill the oxidative coupling and the following transmetallation with a borane, the overall reaction pathway always needs to lie lower in energy than the activation barriers required for hydroboration processes. Therefore, it was first of all made sure that boranes did not directly hydroborate ethylene or [(dcp)Ni(C<sub>2</sub>H<sub>4</sub>)] **IV-3**. Three boranes were tested: 9-BBN, catecholborane and pinacolborane.

9-BBN easily hydroborates ethylene in THF at RT without the assistance of any metal. <sup>11</sup>B{<sup>1</sup>H} NMR in [d<sub>8</sub>]-THF displays a sharp peak at δ = 71.7 ppm, which is shifted to δ = 88.3 ppm when the product is taken back to CDCl<sub>3</sub>. This matches the value given for ethyl-9-BBN in the literature.<sup>[18]</sup>

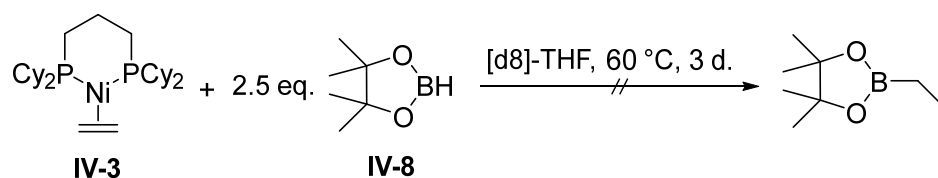
Catecholborane on the other hand does not hydroborate ethylene efficiently without any additives. Nevertheless, catecholborane reacts immediately with [(dcp)Ni(C<sub>2</sub>H<sub>4</sub>)] **IV-3** in THF at RT. Ethylcatecholborane is detected quantitatively by <sup>1</sup>H and <sup>11</sup>B{<sup>1</sup>H} NMR as well as GC-MS spectrometry. These stoichiometric investigations suggest that 9-BBN and catecholborane are not suited for the reductive functionalization of ethylene and CO<sub>2</sub>.



**Scheme 4.5:** Reaction between [(dcp)Ni(C<sub>2</sub>H<sub>4</sub>)] **IV-3** and catecholborane in [d<sub>8</sub>]-THF at RT.



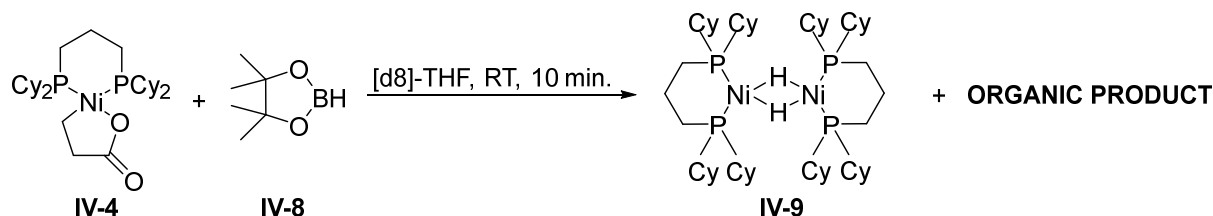
However, pinacolborane **IV-8** does not react with ethylene nor with [(dcppe)Ni(C<sub>2</sub>H<sub>4</sub>)] **IV-3** in THF. When [(dcppe)Ni(C<sub>2</sub>H<sub>4</sub>)] **IV-3** is mixed with 2.5 eq. of pinacolborane **IV-8** in [d<sub>8</sub>]-THF, no hydroboration is observed even after 3 d. at 60 °C. Therefore, pinacolborane **IV-8** will be the reagent of choice for the transmetalation of [(dcppe)nickelalactone] **IV-4**.



**Scheme 4.6:** Absence of reaction between [(dcppe)Ni(C<sub>2</sub>H<sub>4</sub>)] **IV-3** and pinacolborane **IV-8** in [d<sub>8</sub>]-THF at 60 °C.

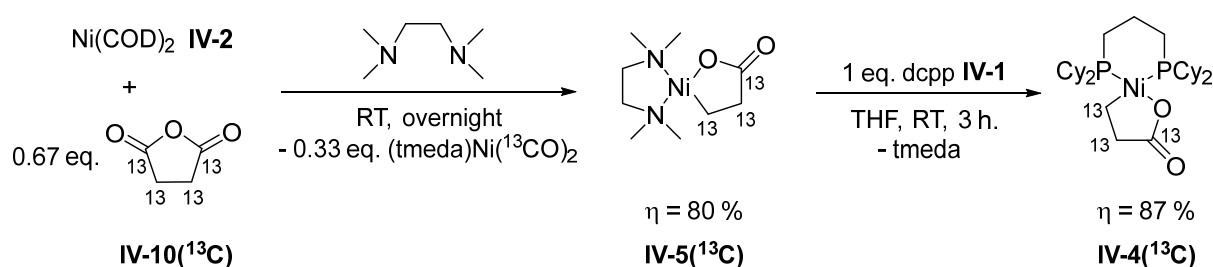
### 4.3.2 Reactivity between [(dcppe)nickelalactone] **IV-4** and pinacolborane **IV-8**

The reactivity between [(dcppe)nickelalactone] **IV-4** and pinacolborane **IV-8** has been investigated. Therefore, [(dcppe)nickelalactone] **IV-4** has been reacted with pinacolborane **IV-8** in THF at RT. Within 10 min. the solution turns deep red and <sup>31</sup>P {<sup>1</sup>H} NMR shows a singlet at δ = 25.0 ppm, corresponding to the known nickel dihydride complex [(dcppe)NiH]<sub>2</sub> **IV-9**. A quintet at δ = -10.1 ppm in <sup>1</sup>H NMR <sup>[19]</sup> and single crystal analysis <sup>[20]</sup> give additional proof. An organic product must be simultaneously released in the course of the reaction but could not be properly identified at this point. This is also supported by <sup>1</sup>H DOSY NMR separating a complex with a diffusion coefficient of D = 7.6 × 10<sup>-10</sup> m<sup>2</sup>.s<sup>-1</sup> from lighter organic products with a D = 1.6 × 10<sup>-9</sup> m<sup>2</sup>.s<sup>-1</sup>.



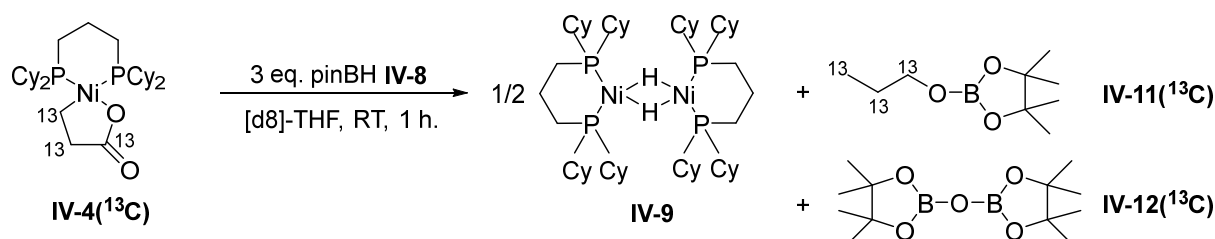
**Scheme 4.7:** Reaction between [(dcppe)nickelalactone] **IV-4** and pinacolborane **IV-8** in [d<sub>8</sub>]-THF at RT. After 10 min. formation of [(dcppe)NiH]<sub>2</sub> **IV-9** is observed.

In order to follow the formation of the organic product and to gain mechanistic insights on the reaction, <sup>13</sup>C labelled [(dcpp)nickelalactone] **IV-4**(<sup>13</sup>C) has been synthesized. **Scheme 4.8** describes the two step synthesis of the labelled complex. <sup>13</sup>C labelled succinic anhydride **IV-10**(<sup>13</sup>C) is reacted with [Ni(COD)<sub>2</sub>] **IV-2** in tmeda according to Fischer's procedure.<sup>[3]</sup> Ligand substitution and decarbonylation afford <sup>13</sup>C[(tmeda)nickelalactone] **IV-5**(<sup>13</sup>C) in 80 % yield. Afterwards, by following the procedure developed in 4.1.2, <sup>13</sup>C[(dcpp)nickelalactone] **IV-4**(<sup>13</sup>C) is isolated in 87 % yield.



**Scheme 4.8:** Two step synthesis of <sup>13</sup>C[(dcpp)nickelalactone] **IV-4**(<sup>13</sup>C).

The reaction has then been repeated with <sup>13</sup>C[(dcpp)nickelalactone] **IV-4**(<sup>13</sup>C). The reaction conditions could be optimized. It turns out that 3 eq. of pinacolborane **IV-8** are required to complete the reaction. In addition, three set of signals are observed by <sup>13</sup>C NMR at the end of the reaction. The spectrum is depicted in **Figure 4.10**. A doublet at  $\delta = 10.3$  ppm ( $^1J_{C,C} = 137.7$  Hz), a doublet of doublet at  $\delta = 25.2$  ppm ( $^1J_{C,C} = 137.7$  Hz,  $^1J_{C,C} = 151.5$  Hz) and a doublet at  $\delta = 66.7$  ppm ( $^1J_{C,C} = 151.5$  Hz), each integrating for one carbon atom are assigned to the propyl chain of the organic product. Surprisingly, no signals are observed between 180 and 220 ppm indicating that the carbonyl function has been reduced. A small doublet at  $\delta = 24.7$  ppm could arise from <sup>13</sup>C natural abundance in the methyl groups of pinacolborane **IV-8**.



**Scheme 4.9:** Reaction between <sup>13</sup>C[(dcpp)nickelalactone] **IV-4**(<sup>13</sup>C) and 3 eq. of pinacolborane **IV-8**.

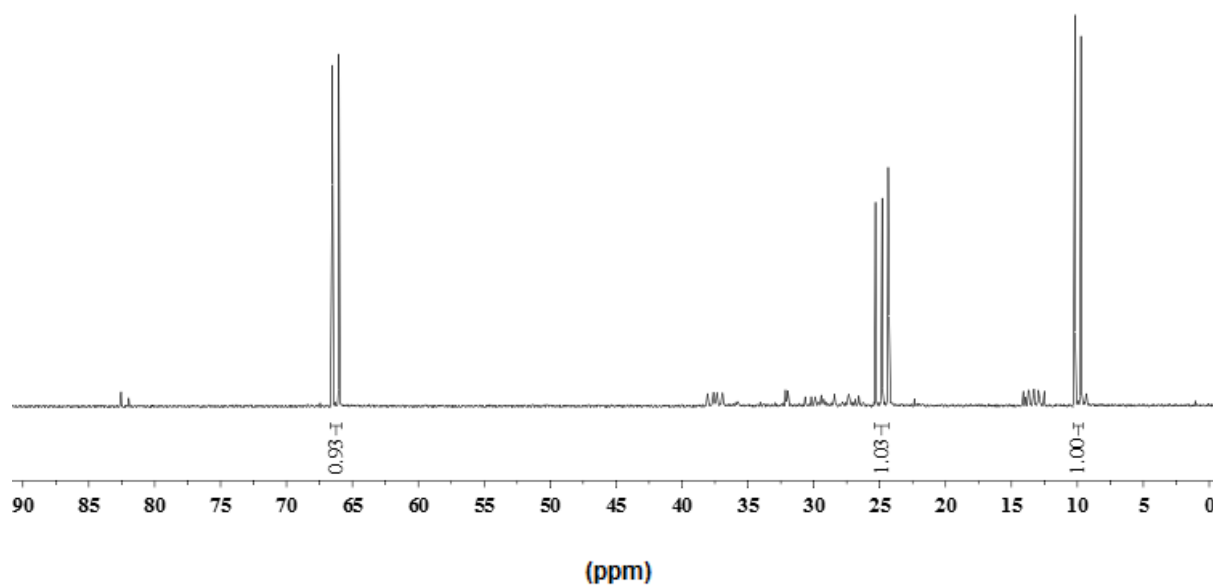


**Figure 4.10:** <sup>13</sup>C{<sup>1</sup>H} NMR spectrum at 75 MHz of the reaction between <sup>13</sup>C[(dcpp)nickelalactone] **IV-4**(<sup>13</sup>C) and 3 eq. of pinacolborane **IV-8** at RT. For more clarity solvent has been switched from [d<sub>8</sub>]-THF to C<sub>6</sub>D<sub>6</sub>.

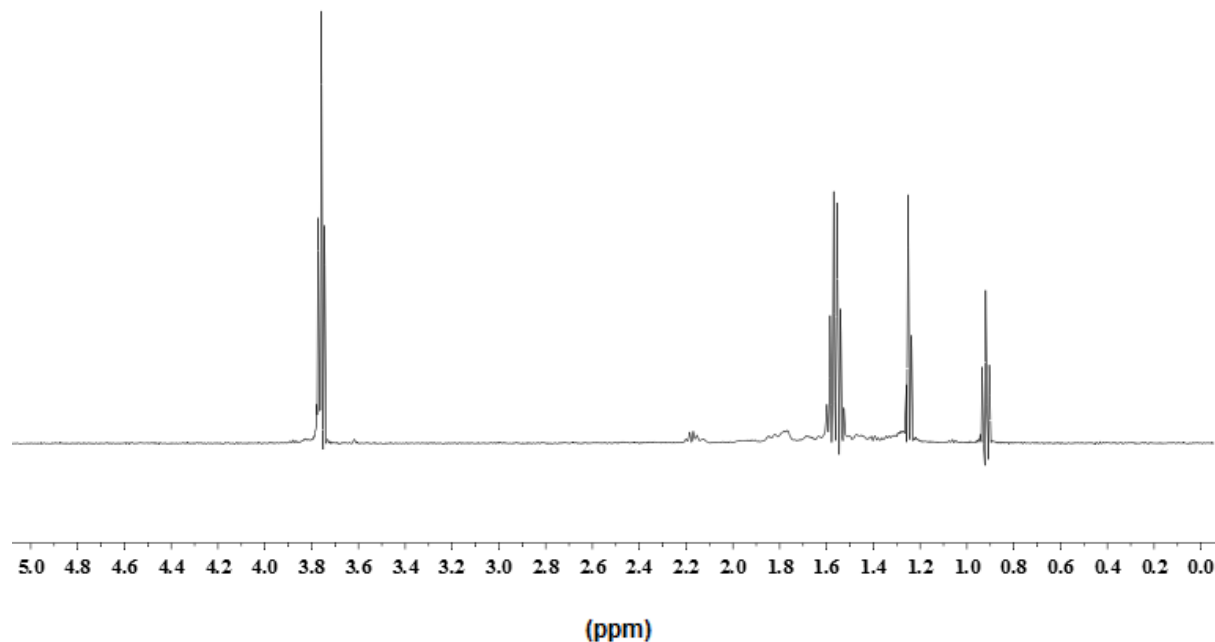
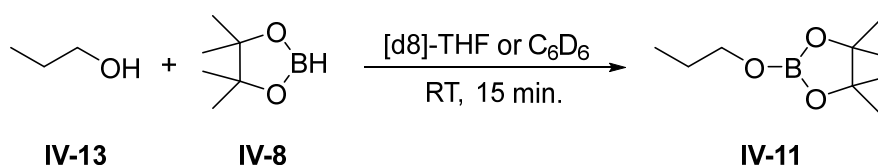


**Figure 4.11:** <sup>1</sup>H{<sup>13</sup>C} 1D HSQC NMR spectrum at 500 MHz of the reaction between <sup>13</sup>C[(dcpp)nickelalactone] **IV-4**(<sup>13</sup>C) and 3 eq. of pinacolborane **IV-8** at RT in [d<sub>8</sub>]-THF.

<sup>1</sup>H 1D-HSQC experiments give access to the protons directly bound to <sup>13</sup>C carbons. Together with classical 2D-HSQC analysis, the protons of the organic product could be unambiguously identified. Terminal <sup>13</sup>CH<sub>3</sub> appears as a triplet at δ = 0.92 ppm (<sup>3</sup>J<sub>H,H</sub> = 7.5 Hz); <sup>13</sup>CH<sub>2</sub> as a pseudo sextet at δ = 1.56 ppm (<sup>3</sup>J<sub>H,H</sub> = 7.5 Hz, <sup>3</sup>J<sub>H,H</sub> = 7.0 Hz) and <sup>13</sup>CH<sub>2</sub>O as a triplet at δ = 3.76 ppm (<sup>3</sup>J<sub>H,H</sub> = 7.0 Hz). An additional signal at δ = 1.25 ppm belongs to the methyl groups of the pinacolborane **IV-8** moieties, the <sup>13</sup>C natural abundance not being negligible anymore over all the identical carbon atoms. <sup>11</sup>B{<sup>1</sup>H} and <sup>11</sup>B NMR highlight the presence of two borate moieties with two peaks at 21.6 and 22.5 ppm.

The NMR experiments hence suggest the formation of <sup>13</sup>C-propoxypinacolborane **IV-11**(<sup>13</sup>C) as well as diboroxane pinBOBpin **IV-12**.

A spiking experiment has been conducted in order to provide further structure confirmation of the organic product. Propoxypinacolborane **IV-11** can be independently synthesized from propanol **IV-13** and pinacolborane **IV-8** either in C<sub>6</sub>D<sub>6</sub> or in [d<sub>8</sub>]-THF.



**Scheme 4.10:** Alternative synthesis of propoxypinacolborane **IV-11**.

Thus, in an independent experiment, the reaction between [(dcpp)nickelalactone] **IV-4** and pinacolborane **IV-8** is followed by <sup>1</sup>H NMR using mesitylene as internal standard. The reaction is quantitative and the conversion reaches 98 % after 1 h. at RT. Upon addition of 5 eq. of propoxypinacolborane **IV-11** the corresponding peaks and integrations increase consequently, proving that the organic product of the reaction is indeed propoxypinacolborane **IV-11**. The <sup>1</sup>H NMR spectra of the spiking experiment can be found in **Figure 4.12**.

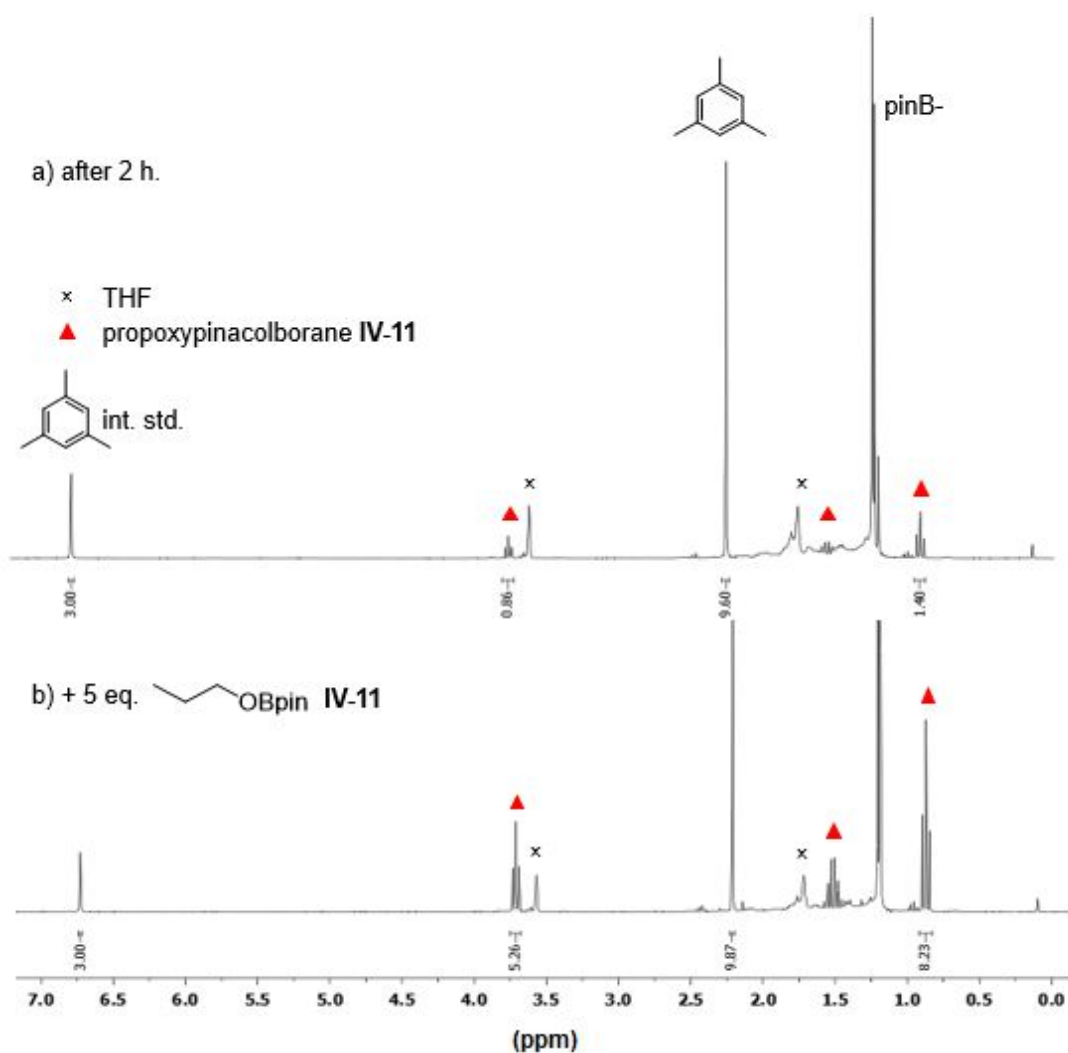


**Figure 4.12:** <sup>1</sup>H NMR spectra of the spiking experiment. a) Reaction between [(dcpp)nickelalactone] **IV-4** and 3 eq. of pinacolborane **IV-8** after 2 h. at RT. b) After addition of 5 eq. of propoxypinacolborane **IV-11**.

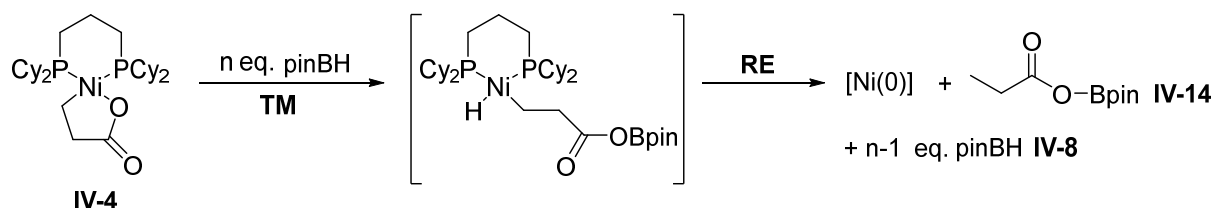
These experiments show that pinacolborane **IV-8** readily reacts with [(dcpp)nickelalactone] **IV-4** at RT. The reaction disfavors β hydride elimination processes and does not afford the expected acrylate derivative. Nevertheless, [(dcpp)nickelalactone] **IV-4** is cleaved by transmetallation and remarkably the resulting ester is also reduced during the course of the reaction. In this way a propanol derivative **IV-11** is formed along with diboroxane **IV-12**. Despite earlier reports by Mori <sup>[21 - 24]</sup> and Rovis <sup>[25]</sup> on the cleavage of nickelalactones by zinc reagents leading to carboxylic acid derivatives, there are no precedents in the literature for this reaction. This is the first homogeneous nickel mediated synthesis of propanol derivatives from ethylene and CO<sub>2</sub>.

## 4.4 Mechanistic investigations

It is of great interest to elucidate the mechanism of this reaction. The reduction of [(dcpp)nickelalactone] **IV-4** to propoxypinacolborane **IV-11** requires overall 3 eq. of pinacolborane **IV-8**. The driving force of the reaction is the formation of strong B-O bonds evidenced by the release of diboroxane pinBOBpin **IV-12**. The borane plays both the role of the reductant and of an oxygen scavenger.

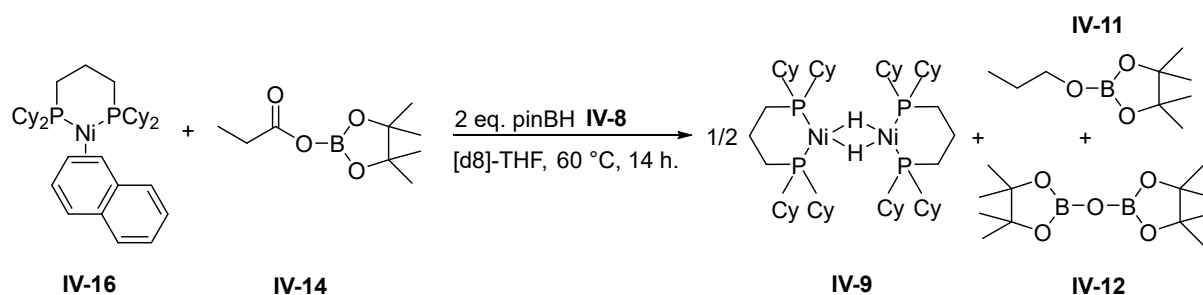
### 4.4.1 Cleavage of [(dcpp)nickelalactone] **IV-4** through pinacolborane **IV-8**

The first equivalent of pinacolborane **IV-8** is used for the transmetalation and cleavage of the Ni-O bond, leading to a transient open chain propanoate nickel complex. Facile reductive elimination generates Ni(0) together with propanoic acid pinacolborane ester **IV-14**, as shown in **Scheme 4.11**.



**Scheme 4.11:** First step of the mechanism of the reaction between [(dcpp)nickelalactone] **IV-4** and pinacolborane **IV-8**.

Propanoic acid pinacolborane ester **IV-14** can be independently synthesized from propanoic acid **IV-15** and an excess of pinacolborane **IV-8** in C<sub>6</sub>D<sub>6</sub>. It is to be noted, that propanoic acid pinacolborane ester **IV-11** is not reduced by pinacolborane **IV-8** under the reaction conditions. However, the reaction between [(dcpp)Ni(naphthalene)] **IV-16** and propanoic acid pinacolborane ester **IV-14** in the presence of pinacolborane **IV-8** leads after 14 h at 60 °C to propoxypinacolborane **IV-11** and diboroxane **IV-12**. The reaction is slower compared to the direct reduction of [(dcpp)nickelalactone] **IV-4** with pinacolborane **IV-8** due to the stabilization of the Ni(0) by the naphthalene moiety. This reaction proves that propanoic acid pinacolborane ester **IV-14** is a reaction intermediate.

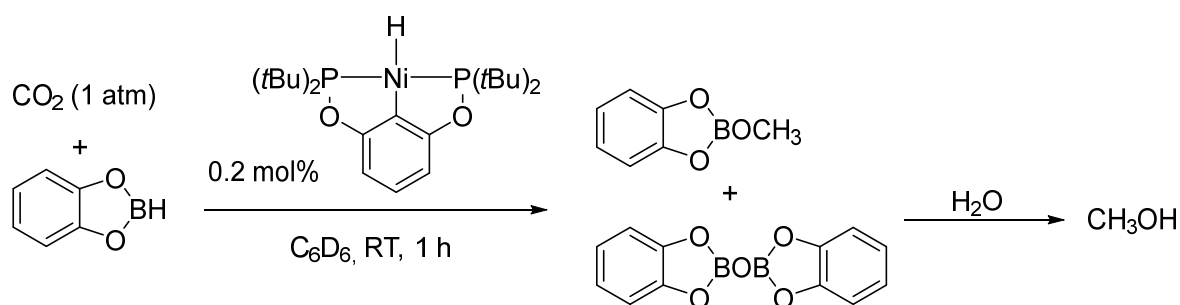


**Scheme 4.12:** Reaction between  $[(\text{dcpp})\text{Ni}(\text{naphthalene})]$  **IV-16** and propanoic acid pinacolborane ester **IV-14** in the presence of pinacolborane **IV-8**.

Until here, the reaction fits nicely with the expected results. The further reduction to propanol derivatives remains unknown. Three different mechanisms could be considered for the reduction of propanoic acid pinacolborane ester **IV-14** to propoxypinacolborane **IV-11**.

#### 4.4.2 Reduction of propanoic acid pinacolborane ester **IV-14** through a metal hydride

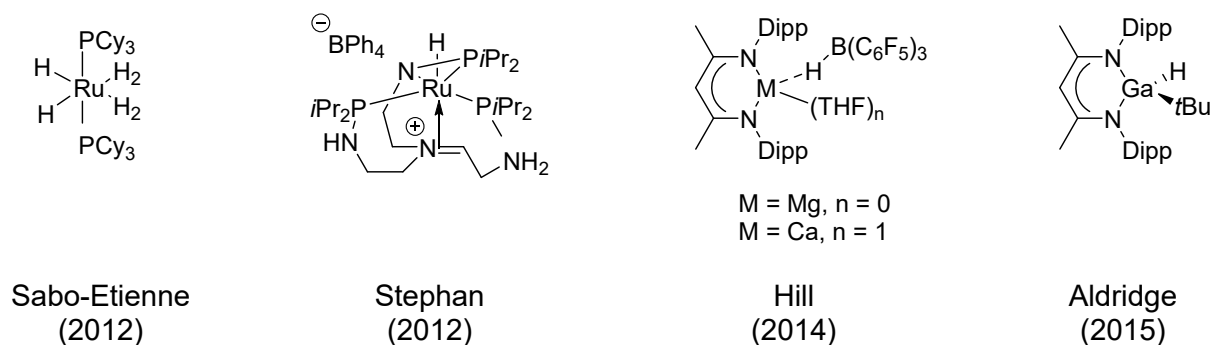
The first pathway is inspired by the reduction of CO<sub>2</sub> and carbonyls with boranes using metal hydride complexes. <sup>[26, 27]</sup> Guan first reported in 2010 the catalytic hydroboration of CO<sub>2</sub> to methoxide derivatives using a PCP pincer nickel hydride complex and catecholborane. With a 500:1 borane to nickel-hydride ratio, TOF of  $495\text{ h}^{-1}$  could be achieved. <sup>[28]</sup>



**Scheme 4.13:** Guan's catalytic reduction of CO<sub>2</sub> with catecholborane using a PCP pincer nickel hydride complex. <sup>[28]</sup>

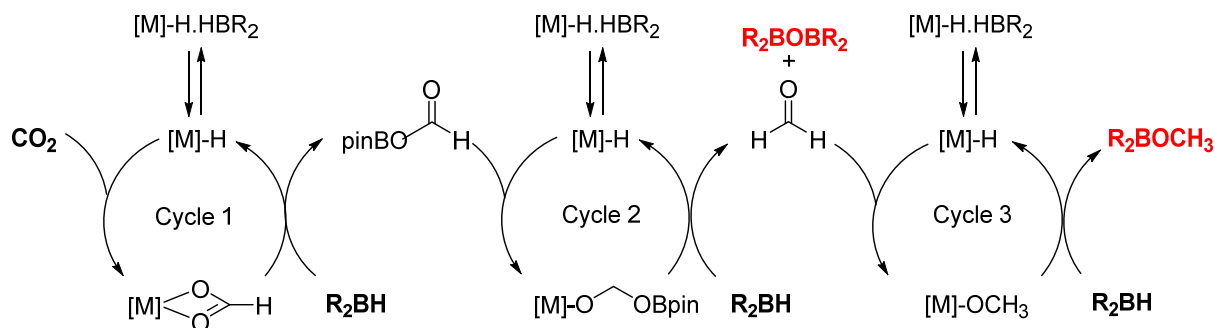
Later other research groups discovered similar reactivity driven by different metal hydride complexes. In 2012 Sabo-Etienne <sup>[29]</sup> and Stephan <sup>[30]</sup> describe the catalytic reduction of CO<sub>2</sub> into methoxy-pinacolborane by ruthenium hydrides. Alkaline earth hydride complexes as the

β-diketiminato magnesium and calcium hydrido-tris(pentafluorophenyl)borates<sup>[31]</sup> and an ambiphilic β-diketiminato gallium hydride<sup>[32]</sup> also exhibit analogous reactivity even though they perform less efficiently compared to the transition metals (TOF for Mg = 0.07 h<sup>-1</sup>, Ca = 0.1 h<sup>-1</sup> and Ga = 2.5 h<sup>-1</sup>).



**Scheme 4.14:** Metal hydride catalysts used for the reduction of CO<sub>2</sub> by pinacolborane to methanol derivatives.

Guan thoroughly investigated the mechanism of these reductions both experimentally<sup>[28, 33, 34]</sup> and by DFT calculations.<sup>[35]</sup> The reaction consists of three interlinked catalytic cycles to reach the methanol derivatives. Each cycle requires one equivalent of borane and reduces CO<sub>2</sub> by one step. In this way formatoborane, formaldehyde and methoxyborane are successively generated. Formates and methoxyboranes have been observed by NMR spectroscopy and could be crystallized<sup>[28, 29, 33]</sup>, whereas formaldehyde remained an elusive compound for a long time. Sabo-Etienne and Bontemps finally managed to trap formaldehyde with methanol<sup>[36]</sup> and 2,6-bis(diisopropyl)aniline.<sup>[37]</sup>



**Scheme 4.15:** Mechanism of CO<sub>2</sub> reduction by boranes catalyzed by metal hydride complexes. The cycle is drawn relying on Guan's experimental and computational investigations.<sup>[34, 35]</sup>



The reaction proceeds through successive C=O insertions in the metal-hydride bond, followed by borane mediated B-H / O-M  $\sigma$ -bond metathesis. Altogether a first hydride is transferred from the metal center to the C=O bond and then a second hydride is transferred from the borane to the metal center to regenerate the catalyst and release the product. [28, 35]

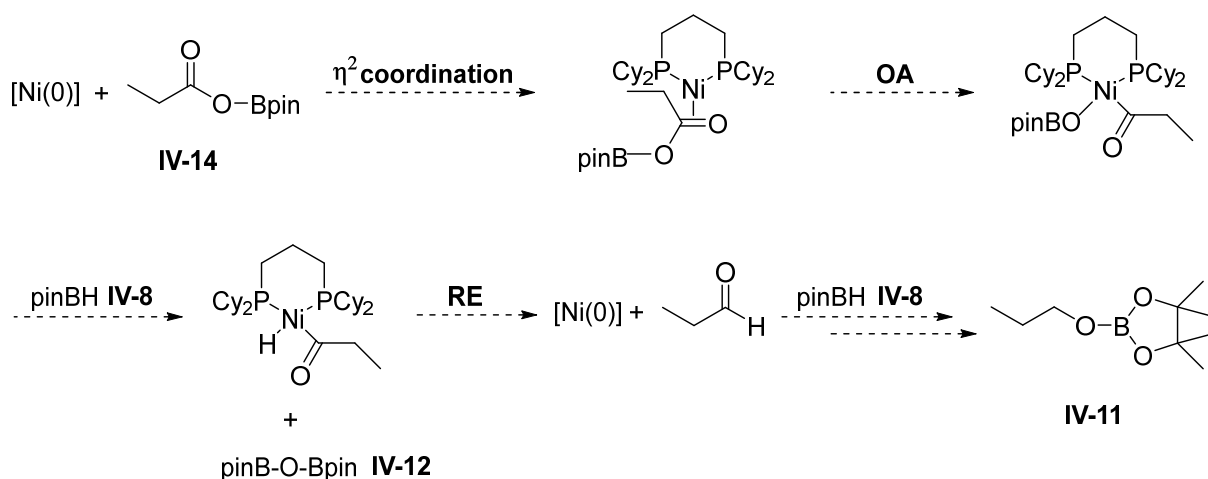
The metal- or main group-hydride catalyzed reductions of CO<sub>2</sub> into formate derivatives [38, 39] and of carbonyls into alcohol derivatives [40 - 47] corresponds either to the first or the last step of the previously proposed catalytic cycle. The various literature reports support the same C=O insertion,  $\sigma$ -bond metathesis mechanism described above.

The only requirement for such a mechanism is the presence of a nickel hydride complex. Isolated [(dcp)NiH]<sub>2</sub> **IV-9** has been tested as a potential catalyst. However, the dihydride does not reduce propanoic acid pinacolborane ester **IV-14** in the presence of pinacolborane **IV-8** even after extensive heating at 60 °C. Therefore, [(dcp)NiH]<sub>2</sub> **IV-9** is considered as a resting state. However, that doesn't rule out the presence of other catalytically active nickel hydride species.

Additional experiments will be undertaken in order to quantify [(dcp)NiH]<sub>2</sub> **IV-9** at the end of the reaction with an internal standard. The amount of [(dcp)NiH]<sub>2</sub> **IV-9** should help discriminating between the proposed mechanisms. The reduction of propanoic acid pinacolborane ester **IV-14** through a metal hydride would appear plausible if the yield of [(dcp)NiH]<sub>2</sub> **IV-9** almost reaches 100 %. [(dcp)NiH]<sub>2</sub> **IV-9** could arise from the recombination of less stable hydridic intermediates. Though, if the yield does not exceed 50 %, other mechanisms, especially involving Ni(I) intermediates (**4.4.4**), would seem more likely.

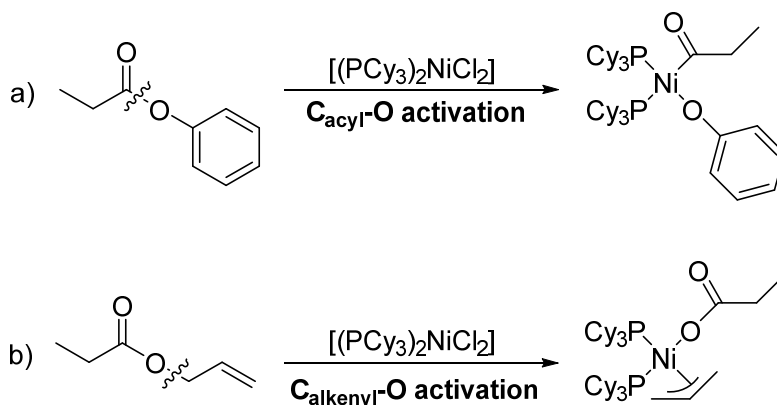
#### 4.4.3 Reduction of propanoic acid pinacolborane ester through oxidative addition

An alternative pathway for the reduction of propanoic acid pinacol ester **IV-14** could be initiated by  $\eta^2$  coordination of the C=O double bond to the naked Ni(0) fragment, followed by oxidative addition of nickel into the C=O bond. Reaction of the nickel-acyl complex with pinacolborane **IV-8** would generate diboroxane pinBOBpin **IV-12** and formaldehyde. The possible reaction scheme is depicted below.



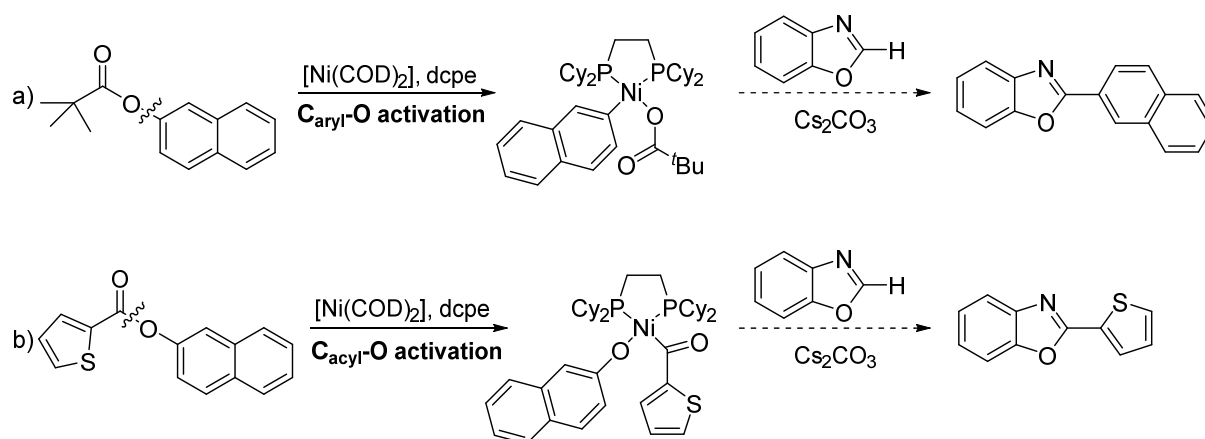
**Scheme 4.16:** Reduction of the carbonyl through an oxidative addition mechanism.

In the 1970s, Yamamoto already described the oxidative addition of esters<sup>[48, 49]</sup> and ethers<sup>[50]</sup> to Ni(0) complexes. There are two possible ways to cleave an ester as represented in **Scheme 4.17**. The cleavage depends on the nature of the ester and of the ligands and was determined by analyzing the outcome of the reaction. The oxidative addition in the acyl group is observed when  $[\text{Ni}(\text{COD})_2]$  is reacted with aryl carboxylates in the presence of phosphine ligands such as  $\text{PPh}_3$  or  $\text{PCy}_3$ . The aromatic substituent is essential to achieve the cleavage in this position.<sup>[48, 49]</sup> On the other hand, allyl or vinyl carboxylates preferentially undergo oxidative addition in the C(O)O-R bond.<sup>[48]</sup> This topic is still actively investigated as Love systematically studied in 2016 the behavior of esters and thioesters towards stoichiometric amounts of  $[(\text{dtbpe})_2\text{Ni}(\text{C}_6\text{H}_6)]$ .<sup>[51]</sup>



**Scheme 4.17:** Oxidative addition of a) phenyl propanoate and b) allyl acetate to  $[\text{Ni}(\text{COD})_2]$  in the presence of  $\text{PPh}_3$ .<sup>[48, 49]</sup>

In the last ten years, several research groups have taken advantage of this reactivity to perform nickel catalyzed cross coupling reactions using phenol derivatives as electrophiles. Aryl esters are relatively cheap, stable and in part readily available and therefore good candidates to complement or replace aryl halides. In 2008, Garg<sup>[52]</sup> and Shi<sup>[53]</sup> reported the first [(PCy<sub>3</sub>)<sub>2</sub>NiCl<sub>2</sub>] catalyzed Suzuki-Miyaura cross couplings between aryl carboxylates and boronic acids or aryl boroxins, involving a C<sub>aryl</sub>-O bond activation. Subsequently, Itami developed the coupling between 1,3-azoles and aryl pivalates<sup>[54]</sup> depicted in **Scheme 4.18** and could isolate in 2013 the first oxidative addition product of naphthalene-2-yl pivalate to a [(dcpe)Ni(0)]-complex closely related to our [(dcpp)Ni]-system.<sup>[55]</sup> Martin extended the concept of C<sub>aryl</sub>-O bond activation to enantioselective processes<sup>[56]</sup> and silylations.<sup>[57]</sup> Similarly to aryl halides, a mechanism involving successive oxidative addition, transmetallation and reductive elimination is proposed for most systems. Stoichiometric<sup>[55]</sup> and computational investigations<sup>[58]</sup> support the feasibility of the oxidative addition of a C<sub>aryl</sub>-O bond to a nickel complex.

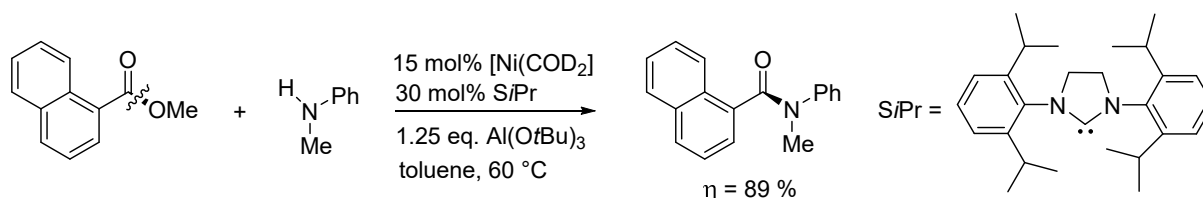


**Scheme 4.18:** Itami's nickel catalyzed coupling between benzoaxoles and a) naphthyl pivalate<sup>[54, 55]</sup> or b) naphthalene-2-yl thiophene-2-carboxylate.<sup>[59]</sup>

Interestingly, Itami managed to switch the reactivity in favor of the C<sub>acyl</sub>-O bond activation by replacing the *tert*-butyl group of the aryl carboxylates by thienyl<sup>[59]</sup> or pyridine<sup>[60]</sup> substituents, leading to decarbonylative cross coupling reactions. Houk<sup>[61]</sup> and Fu<sup>[62]</sup> investigated Itami's results in depth by DFT calculations, trying to disclose the different mechanisms and to understand the origin of the various reactivities. It turns out that in any case the presence of an aromatic system is of utmost importance to achieve the oxidative addition of the C<sub>aryl</sub>-O and

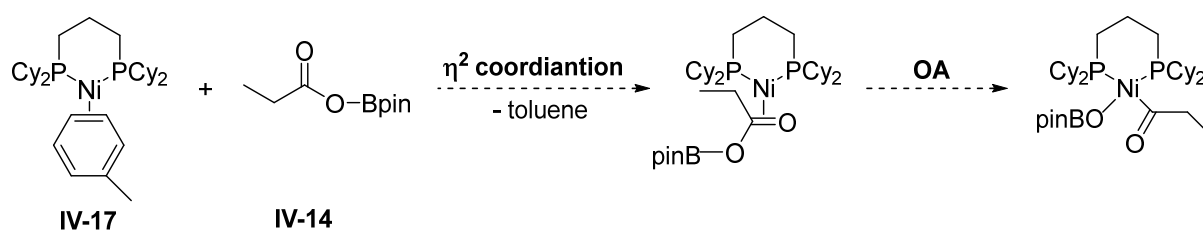
C<sub>acyl</sub>-O bonds of an ester to the nickel center. The  $\pi$  electrons of the naphthyl moiety systematically assist the cleavage of C-O bonds.

More recently, Houk and Garg finally disclosed the nickel catalyzed activation of C<sub>acyl</sub>-O bonds of methyl esters in the presence of Al(O*t*Bu)<sub>3</sub>. An extensive aromatic system must still be present in all the methyl esters to achieve the coupling with anilines in good yields. [63]



**Scheme 4.19:** Houk and Garg's nickel catalyzed activation of C<sub>acyl</sub>-O bonds of methyl esters. [63]

Therefore, in order to test the reaction pathway suggested above, the highly reactive Ni(0) complex [(dcpP)Ni(toluene)] **IV-17** will be reacted with propanoic acid pinacolborane ester **IV-14**. The ester is expected to form a new  $\eta^2$  coordinated [(dcpP)Ni]-complex, as shown in **Scheme 4.20**. Then, considering the strong B-O bond, oxidative addition can be performed only in the C<sub>acyl</sub>-O bond CH<sub>3</sub>CH<sub>2</sub>C(O)-OBpin of the ester. However, the lack of  $\pi$  electrons in the molecule, which proved to be essential in all the processes presented above, probably disfavors the reaction.

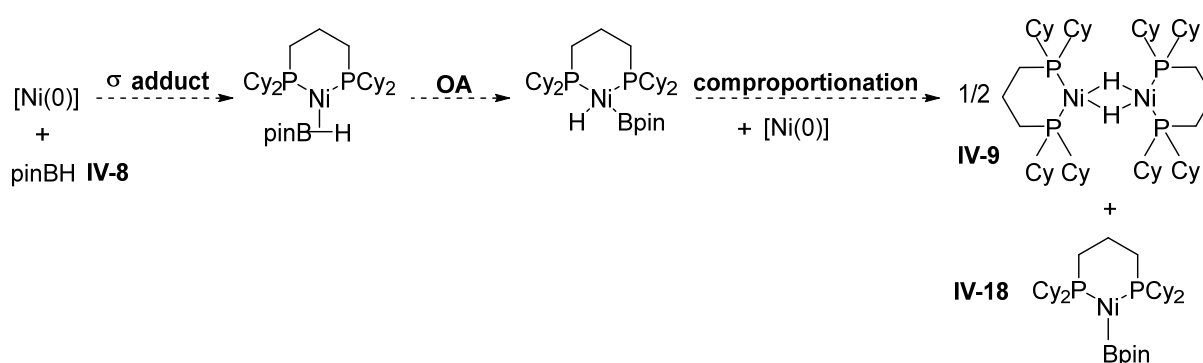


**Scheme 4.20:** Additional planned experiment: reaction between the Ni(0) complex [(dcpP)Ni(toluene)] **IV-17** and propanoic acid pinacolborane ester **IV-14**.

#### 4.4.4 Reduction of propanoic acid pinacolborane ester **IV-14** through Ni(I) intermediates

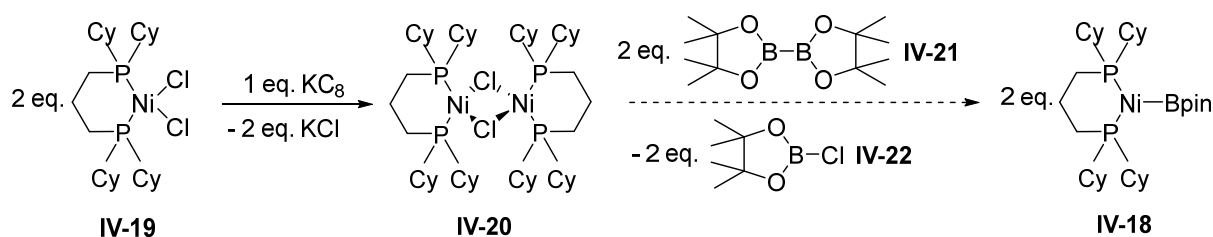
The last pathway is based on the reactivity of Ni(I) boryl intermediates. The oxidative addition of nickel in the C-O bond of propanoic acid pinacolborane ester **IV-14** can be in competition with the oxidative addition of nickel in the B-H bond of pinacolborane **IV-8**. The reaction would be initiated by the formation of a  $\sigma$ -borane adduct between pinacolborane **IV-8** and the [(dcp)Ni(0)]-fragment, eventually ending in the oxidative addition of nickel in the B-H bond. Sigma-alkylborane nickel complexes have already been isolated, starting from nickel dihydride complexes [(R<sub>2</sub>P-(CH<sub>2</sub>)<sub>2</sub>-PR<sub>2</sub>)NiH]<sub>2</sub> (R = Cy, *i*Pr, *t*Bu).<sup>[64]</sup> Moreover, the analogous oxidative addition of hydrosilanes to {[*(dtbpe)*Ni]<sub>2</sub>(C<sub>6</sub>H<sub>6</sub>)} is also known.<sup>[65]</sup> In addition, a recent study on the hydroboration of ketones mediated by [(*bipy*)Ni(COD)] also discusses the possibility of an alternative to the nickel hydride based mechanism relying on the oxidative addition of pinacolborane **IV-8**.<sup>[66]</sup>

The Ni(II) complex [(dcp)Ni(H)(Bpin)], resulting from the oxidative addition of pinacolborane **IV-8** to the [(dcp)Ni(0)]-fragment, can then disproportionate in the presence of remaining Ni(0), leading to Ni(I) intermediates. This would explain the formation of [(dcp)NiH]<sub>2</sub> **IV-9** and rationalize the presence of a Ni(I) boryl active catalyst [(dcp)Ni(Bpin)], as shown in **Scheme 4.21**. A related mechanism supported by stoichiometric, kinetic and computational investigations has been suggested for the first time by Martin *et. al.* for the nickel catalyzed reductive cleavage of aryl ethers with silanes.<sup>[67]</sup> A paramagnetic three coordinate Ni(I) silyl complex {(*dtbpe*)Ni[Si(Mes)<sub>2</sub>H]}}, which is related to Martin's proposed active Ni(I) silyl catalyst [(PCy<sub>3</sub>)<sub>2</sub>NiSiEt<sub>3</sub>], could be independently isolated by Hillhouse.<sup>[68]</sup>



**Scheme 4.21:** Generation of a Ni(I) boryl complex for the reduction of propanoic acid pinacol ester **IV-14**.

In order to elucidate this mechanism, a preliminary experiment has been performed. The reaction between [(dcpP)Ni(naphthalene)] **IV-16** and pinacolborane **IV-8** indeed leads to the formation of [(dcpP)NiH]<sub>2</sub> **IV-9**, which is observed by <sup>31</sup>P{<sup>1</sup>H} NMR spectroscopy. Further experiments involving EPR spectroscopy as well as the independent synthesis of the to date unknown [(dcpP)Ni(I)boryl] complex are now needed to prove this approach. **Scheme 4.21** proposes a reaction pathway to the targeted compound. Dimeric Ni(I) complex [(dcpP)NiCl]<sub>2</sub> **IV-20** is obtained after one electron reduction of [(dcpP)NiCl<sub>2</sub>] **IV-19** through KC<sub>8</sub>. In the next step, the dimer is broken down through the addition of bis(pinacolato)diborane B<sub>2</sub>pin<sub>2</sub> **IV-21**, affording the Ni(I) boryl complex [(dcpP)Ni(Bpin)] **IV-18** and *B*-chloropinacolborane pinBCl **IV-22**. The reaction will be driven by the formation of the strong B-Cl bond.



**Scheme 4.22:** Proposed reaction pathway for the synthesis of Ni(I) boryl complex [(dcpP)Ni(Bpin)] **IV-18**.

However, it remains unclear how [(dcpP)Ni(Bpin)] **IV-18** promotes the reduction of propanoic acid pinacolborane ester **IV-14** into propoxypinacolborane **IV-11**.

Hence, the stoichiometric mechanistic investigations confirm that [(dcpP)nickelalactone] **IV-4** is cleaved by 1 eq. of pinacolborane **IV-8** and subsequent reductive elimination generates propanoic acid pinacolborane ester **IV-14** as a reaction intermediate. Theoretical considerations supported by preliminary experimental results could not fully disclose the mechanism of the reduction of propanoic acid pinacolborane **IV-14** into propoxypinacolborane **IV-11**. Even though the reduction of propanoic acid pinacolborane ester **IV-14** through oxidative addition of the C=O bond into intermediate Ni(0) species seems less likely than nickel hydride or Ni(I) boryl assisted mechanisms, there is to date not enough evidence to rule out one of these reaction pathways. The additional experiments mentioned before will hopefully provide deeper mechanistic insights.

Nevertheless, considering the promising stoichiometric results on the nickel mediated synthesis of propanol derivatives from ethylene and CO<sub>2</sub>, the research was then oriented towards the development of a catalytic application.

## 4.5 Stepwise catalytic cycle

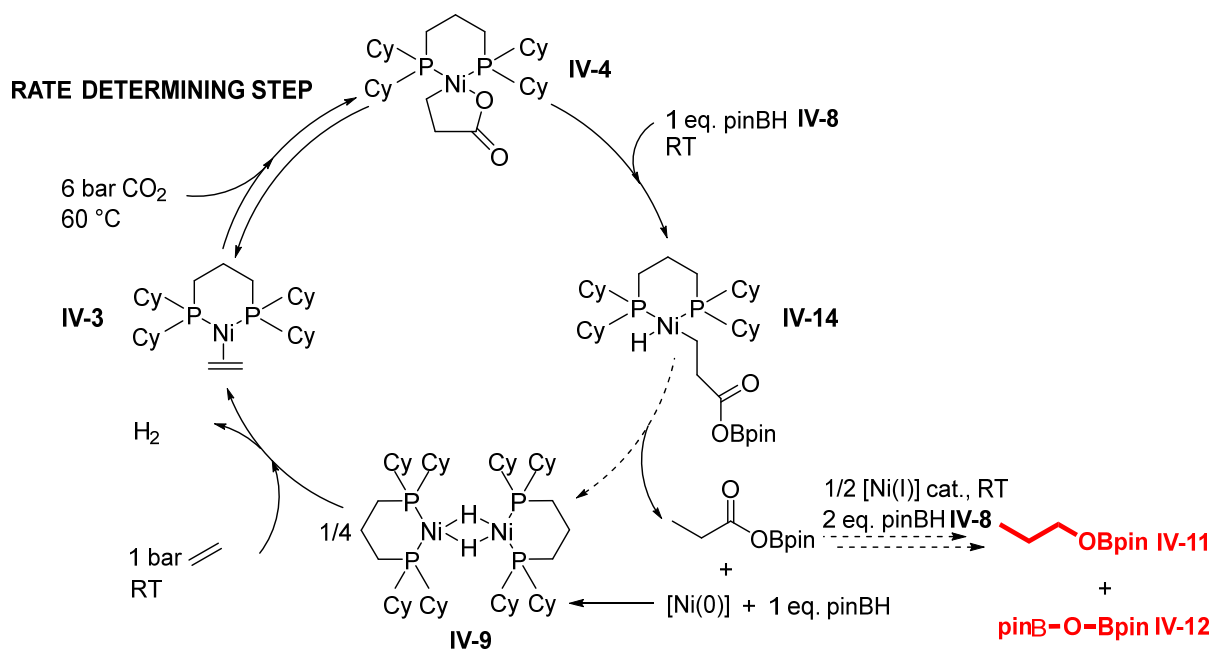
Next, the feasibility of a catalytic cycle has been investigated step by step.

At 6 bar of CO<sub>2</sub> and 60 °C, [(dcp)Ni(C<sub>2</sub>H<sub>4</sub>)] **IV-3** can be oxidatively coupled in small amounts to [(dcp)nickelalactone] **IV-4**, as discussed in paragraph 4.1.2. Catalysis would require higher CO<sub>2</sub> pressures and moderate heating in an autoclave to achieve this reaction efficiently.

During the next step [(dcp)nickelalactone] **IV-4** reacts quickly at RT with 3 eq. of pinacolborane **IV-8** to generate the nickel dihydride complex [(dcp)NiH]<sub>2</sub> **IV-9** together with propoxy pinacolborane **IV-11** and pinBOBpin **IV-12**. One equivalent of borane does the transmetallation and opens the nickelalactone, the other ones participate in the reduction of the ester to an alcohol derivative.

Finally, the catalyst [(dcp)Ni(C<sub>2</sub>H<sub>4</sub>)] **IV-3** must be regenerated during the last step through ligand exchange. Diamagnetic [(dcp)NiH]<sub>2</sub> **IV-9** is formally made of two paramagnetic Ni(I) units. X ray diffraction analysis reveals that the nickel centers are bridged by two hydrogen atoms, forming 3 center 2 electron bonds. <sup>[20]</sup> [(dcp)NiH]<sub>2</sub> **IV-9** presents overall the reactivity of Ni(0) complexes and is rather considered as a non-classical hydride, with a hydrogen molecule interacting with two Ni(0) units. <sup>[19, 69]</sup> Indeed, Jonas and Wilke previously reported, that [(dcp)NiH]<sub>2</sub> **IV-9** can be converted to [(dcp)Ni(C<sub>2</sub>H<sub>4</sub>)] **IV-3** within 20 min. at RT under 1 bar of ethylene, thereby providing a pathway to close the catalytic cycle. <sup>[19]</sup>

Therefore, all elementary steps required for the reaction: oxidative coupling, transmetallation with subsequent reduction of the carbonyl and ligand exchange appear to be achievable under relatively mild conditions. Oxidative coupling needing harsher pressure conditions is presumably the rate determining step. The proposed catalytic cycle is represented in **Scheme 4.23**.

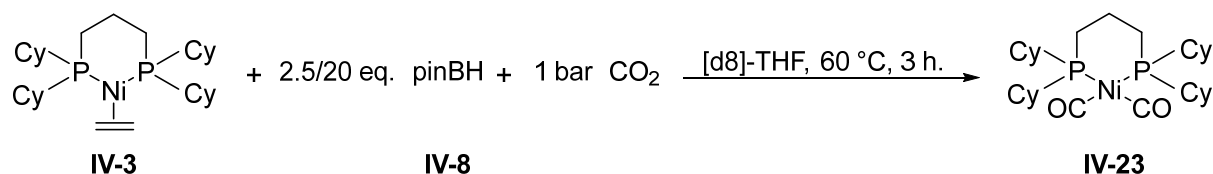


**Scheme 4.23:** Proposed catalytic cycle for the reaction between ethylene, CO<sub>2</sub> and pinacolborane **IV-8** at the [(dcpp)Ni]-center.

## 4.6 Catalysis

The first catalytic attempt was run using 5 bar of ethylene, 30 bar of CO<sub>2</sub> and 10 mol% of [(dcpp)nickelalactone] **IV-4**. After 22 h. at 60 °C the main product was surprisingly the symmetric nickel biscarbonyl complex [(dcpp)Ni(CO)<sub>2</sub>] **IV-23**. Under these catalytic conditions, the reduction of CO<sub>2</sub> into CO is favored over the conversion of ethylene and CO<sub>2</sub> into propoxypinacolborane **IV-11**. The thermodynamic stability of [(dcpp)Ni(CO)<sub>2</sub>] **IV-23** poisons the whole reaction. Stoichiometric reactions were carried out in order to understand the origin of carbon monoxide and to get better control of the catalysis.

First of all, the reactions between [(dcpp)Ni(C<sub>2</sub>H<sub>4</sub>)] **IV-3** and various amounts of pinacolborane **IV-8** (2.5 and 20 eq.) under 1 bar of CO<sub>2</sub> give selectively [(dcpp)Ni(CO)<sub>2</sub>] **IV-23** at 60 °C.



**Scheme 4.24:** Reaction between [(dcpp)Ni(C<sub>2</sub>H<sub>4</sub>)] **IV-3** and pinacolborane **IV-8** under 1 bar of CO<sub>2</sub>.



The complex is characterized by a singlet at  $\delta = 27.0$  ppm in  $^{31}\text{P}\{^1\text{H}\}$  NMR as well as two stretching bands at  $1918\text{ cm}^{-1}$  and  $1980\text{ cm}^{-1}$  in FTIR spectroscopy. The decreased frequencies of the CO bands compared to free carbon monoxide ( $2143\text{ cm}^{-1}$ ) evidence the  $\pi$ -back donation from the nickel center to the CO ligands. Single crystals for X-ray diffraction analysis were grown directly from the THF solution at  $-25\text{ }^\circ\text{C}$ . The structure is depicted below in **Figure 4.13**. The nickel center is in a distorted tetrahedral environment. The  $\text{C}_1\text{O}_1$  ( $1.151(5)\text{ \AA}$ ) and  $\text{C}_2\text{O}_2$  ( $1.144(4)\text{ \AA}$ ) bonds are slightly elongated through the  $\pi$ -back donation and therefore weakened compared to free carbon monoxide ( $1.128\text{ \AA}$ ). Similar chelating bis-phosphine nickel biscarbonyls have also been crystallized. <sup>[59, 70 - 74]</sup> Among them diphenylphosphino-2-hydroxypropane nickel bis-carbonyl <sup>[71]</sup> presents very close structural parameters whereas phenylphosphinopropane nickel bis-carbonyl <sup>[70]</sup> has shorter Ni-C and C-O bonds due to weaker donation. Among the 1,2-(dialkylphosphino)ethane series, except for the smaller bite angles,  $[(\text{dcpe})\text{Ni}(\text{CO})_2]$  <sup>[59]</sup> and  $[(\text{dippe})\text{Ni}(\text{CO})_2]$  <sup>[72]</sup> also display comparable bond lengths and angles.

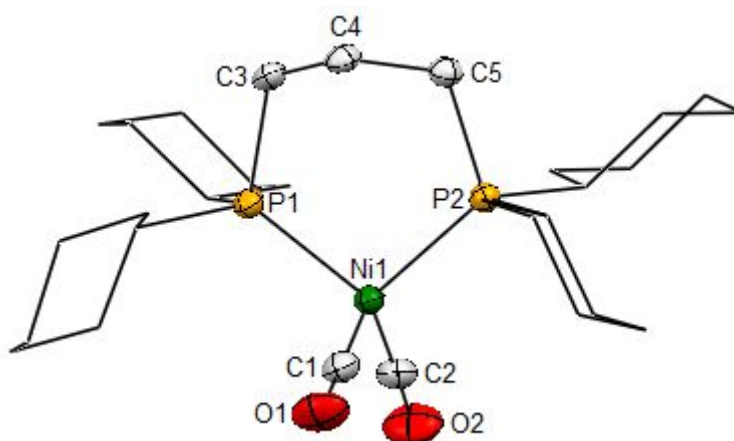
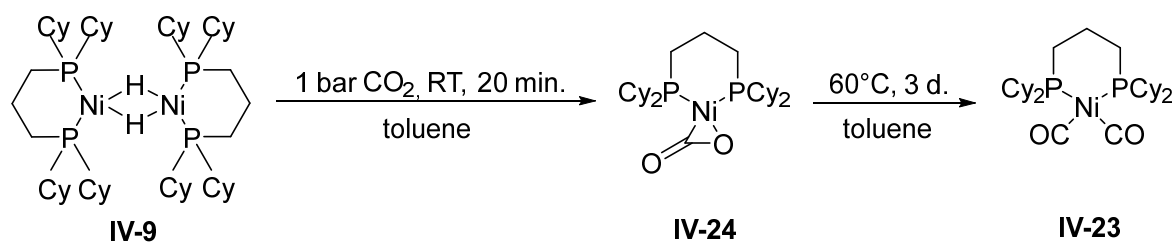


**Figure 4.13:** Molecular structure of  $[(\text{dcppe})\text{Ni}(\text{CO})_2]$  **IV-23** determined by single crystal X-ray diffraction. Hydrogen atoms are omitted for clarity. Selected bond length [ $\text{\AA}$ ] and angles [ $^\circ$ ]:  $\text{Ni}_1\text{-P}_1$   $2.2189(10)$ ,  $\text{Ni}_1\text{-P}_2$   $2.2202(10)$ ,  $\text{Ni}_1\text{-C}_1$   $1.768(4)$ ,  $\text{Ni}_1\text{-C}_2$   $1.768(4)$ ,  $\text{C}_1\text{-O}_1$   $1.151(5)$ ,  $\text{C}_2\text{-O}_2$   $1.144(4)$ ,  $\text{P}_1\text{-Ni}_1\text{-P}_2$   $101.83(4)$ ,  $\text{C}_1\text{-Ni}_1\text{-C}_2$   $111.62(17)$ .

The reaction between  $[(\text{dcppe})\text{Ni}(\text{C}_2\text{H}_4)]$  **IV-3** and pinacolborane **IV-8** under a  $\text{CO}_2$  atmosphere clearly shows that the reduction of  $\text{CO}_2$  into CO occurs under mild conditions and is favored over the formation of propoxypinacolborane **IV-11**. This was unexpected regarding all the previously performed stoichiometric reactions.

Furthermore, the production of [(dcpP)Ni(CO)<sub>2</sub>] **IV-23** from other catalytic steps has then been considered. The nickel bis-carbonyl complex **IV-23** could be generated during the reduction of propanoic acid pinacolborane ester **IV-14** into propoxypinacolborane **IV-11**. Decarbonylation pathways may prevail under catalytic conditions that require heating and elevated ethylene and CO<sub>2</sub> pressures. Sabo-Etienne reported that the catalytic reduction of CO<sub>2</sub> with pinacolborane **IV-8** by a ruthenium hydride complex generates among others a ruthenium bis-carbonyl species that drops the catalytic activity. The decarbonylation, that likely originates from transient formaldehyde, highly depends on the catalytic loading and the reaction time. [29]

Moreover, [(dcpP)Ni(CO)<sub>2</sub>] **IV-23** could arise from the reaction between [(dcpP)NiH]<sub>2</sub> **IV-9** and CO<sub>2</sub> during the regeneration of [(dcpP)Ni(C<sub>2</sub>H<sub>4</sub>)] **IV-3**. Therefore, [(dcpP)NiH]<sub>2</sub> **IV-9** has been reacted with 1 bar of CO<sub>2</sub>. The reaction is much cleaner in toluene compared to THF. At RT the main product observed by <sup>31</sup>P{<sup>1</sup>H} NMR is the known [(dcpP)Ni(CO)<sub>2</sub>] **IV-24** complex, characterized by two doublets at δ = 7.55 ppm (<sup>2</sup>J<sub>P,P</sub> = 28.2 Hz) and δ = 43.42 ppm (<sup>2</sup>J<sub>P,P</sub> = 28.2 Hz). [75] Upon heating at 60 °C [(dcpP)Ni(CO)<sub>2</sub>] **IV-24** is slowly transformed into [(dcpP)Ni(CO)<sub>2</sub>] **IV-23**. Similar reactivity under identical conditions had already been previously reported by Garcia [76] and Hillhouse [77] for the [(dtbpe)NiH]<sub>2</sub> complex. [(dippe)NiH]<sub>2</sub>, though, forms in the presence of CO<sub>2</sub> a more complex mixture of various carbonyl complexes, among which [(dippe)Ni(CO)<sub>2</sub>], along with phosphine oxides. [76]

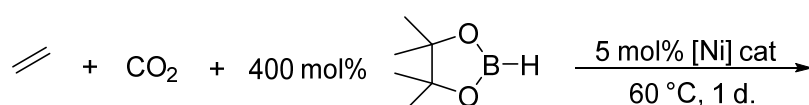


**Scheme 4.25:** Reaction between [(dcpP)NiH]<sub>2</sub> **IV-9** and CO<sub>2</sub> in toluene.

The generation of [(dcpP)Ni(CO)<sub>2</sub>] **IV-23** is unlikely to happen at this stage of the catalysis, as the reaction performs slowly compared to hydrogen-ethylene exchange and requires more time than the experimental catalytic conditions (1 d.).

In light of all these stoichiometric reactions, the formation of [(dcpb)Ni(CO)<sub>2</sub>] **IV-23** is likely to occur during the first step of the catalysis, *i.e.* the oxidative coupling, which is also the most challenging one. Minor amounts of [(dcpb)Ni(CO)<sub>2</sub>] **IV-23** could potentially also be formed from side reactions at later stages of the catalysis. In order to favor the oxidative coupling between ethylene and CO<sub>2</sub> over the reduction of CO<sub>2</sub> into CO, the catalytic conditions have been varied. Unfortunately, the experiments yet remained unsuccessful. The results are summarized in **Table 4.3**.

**Table 4.3:** Various catalytic conditions tested for the synthesis of propoxypinacolborane **IV-11**.



Entry	Catalyst	P(C <sub>2</sub> H <sub>4</sub> ) (bar)	P(CO <sub>2</sub> ) (bar)	Solvent	Products
1	[(dcpb)nickelalactone]	5	30	THF	[(dcpb)Ni(CO) <sub>2</sub> ]
2	[(dcpb)nickelalactone]	9	20	THF	[(dcpb)Ni(CO) <sub>2</sub> ]
3	[Ni(COD) <sub>2</sub> ] + dcpe	9	20	THF	[(dcpe)Ni(CO) <sub>2</sub> ]
4	[Ni(COD) <sub>2</sub> ] + dcpm	9	20	THF	mixture

First of all, the ethylene/CO<sub>2</sub> ratio has been modified. However, by decreasing the CO<sub>2</sub> pressure from 30 bar to 20 bar while increasing the ethylene pressure from 5 bar to 9 bar, no improvement could be observed. It would be interesting to completely switch the pressure ratio and saturate the autoclave with ethylene. Vogt for example observes the best TON for the synthesis of acrylates promoted by LiI/Et<sub>3</sub>N with 5 bar of CO<sub>2</sub> and 25 bar of ethylene. <sup>[14]</sup>

Afterwards, the influence of the catalyst was investigated. It was noticed empirically that nickelalactones with smaller bite angles were easier to generate. <sup>[2]</sup> Therefore, by choosing chelating bis-phosphines with shorter spacers such as dcpe or dcpm, the oxidative coupling between ethylene and CO<sub>2</sub> at the nickel will be facilitated. In the ideal case it would even become more favorable than the reduction of CO<sub>2</sub> into CO. Though, under the chosen conditions, the mixture of [Ni(COD)<sub>2</sub>] **IV-2** and dcpe **IV-25** also affords preferentially [(dcpe)Ni(CO)<sub>2</sub>] **IV-26**, which is characterized by a singlet at δ = 63.4 ppm in <sup>31</sup>P{<sup>1</sup>H} NMR. <sup>[78]</sup> On the other side the catalysis with [Ni(COD)<sub>2</sub>] **IV-2** and dcpm **IV-27** leads to a mixture of unidentified products in <sup>31</sup>P{<sup>1</sup>H} NMR. Propoxypinacolborane **IV-11** could not

be identified in <sup>1</sup>H NMR. The catalytic activity of further complexes such as [(tmeda)nickelalactone] might as well be tested.

A last approach would consist in changing the solvent to dioxane or toluene for example. Especially the use of apolar solvents would dramatically limit the solubility CO<sub>2</sub> in solution and might prevent the reduction of CO<sub>2</sub> into CO.

To date, the nickel mediated synthesis of propanol derivatives from ethylene and CO<sub>2</sub> cannot be performed catalytically. However, several tracks presented above can still be explored to finally achieve the catalysis.

## 4.7 Conclusion

The chemistry of electron rich chelating bis-phosphine [(dcp)nickel]-complexes was explored especially towards ethylene and CO<sub>2</sub>. The [(dcp)Ni(C<sub>2</sub>H<sub>4</sub>)] **IV-3** complex was synthesized from [Ni(COD)<sub>2</sub>] **IV-2** in 64 % yield and [(dcp)nickelalactone] **IV-4** could be obtained from [(tmeda)nickelalactone] **IV-5** in 68 % yield. These two complexes stand in equilibrium: the oxidative coupling between [(dcp)Ni(C<sub>2</sub>H<sub>4</sub>)] **IV-3** and CO<sub>2</sub> is observed above 6 bar of CO<sub>2</sub>, while moderate temperatures reductively decouple [(dcp)nickelalactone] **IV-4**. The activation parameters of the equilibrium were determined through a kinetic study.  $\Delta G^\ddagger$  measures in average 27.4 kcal.mol<sup>-1</sup> and the reaction is mainly enthalpy driven.

In a second step, the cleavage of [(dcp)nickelalactone] **IV-4** by pinacolborane **IV-8** was investigated. In the presence of 3 eq. of pinacolborane **IV-8**, the reaction generates [(dcp)NiH]<sub>2</sub> **IV-9** and forms quantitatively propoxypinacolborane **IV-11** along with diboroxane pinBOBpin **IV-12**. The first equivalent of pinacolborane **IV-11** is involved in the transmetallation and opens [(dcp)nickelalactone] **IV-11** to afford a highly reactive [(dcp)Ni(0)]-fragment and propanoic acid pinacolborane ester **IV-14**. The rest of the mechanism is not clear yet. The reduction of the ester into a propanol derivative could be achieved through three different pathways: through a nickel hydride catalyst, through oxidative addition of nickel in the C=O bond or through nickel(I) boryl intermediates. To date, none of them could be ruled out. Further experiments are planned to test each of these hypotheses and to get better insight into the mechanism.

The catalytic production of propanoate derivatives from ethylene and CO<sub>2</sub> was considered at last. A catalytic cycle consisting in oxidative coupling between [(dcp)Ni(C<sub>2</sub>H<sub>4</sub>)] **IV-3** and CO<sub>2</sub>, transmetallation with pinacolborane **IV-8**, followed by the reduction of the intermediate ester into propoxypinacolborane **IV-11** and ligand substitution from [(dcp)NiH]<sub>2</sub> **IV-9** to regenerate [(dcp)Ni(C<sub>2</sub>H<sub>4</sub>)] **IV-3** could be built up stoichiometrically and run step by step. Oxidative addition requiring high CO<sub>2</sub> pressures is presumably the rate determining step. However, the reaction performs poorly under catalytic conditions favoring the production of [(dcp)Ni(CO)<sub>2</sub>] **IV-23** over propoxypinacolborane **IV-11**. Even by varying the ethylene/CO<sub>2</sub> pressure ratio or changing the catalyst's precursor, the reduction of CO<sub>2</sub> into CO could not be avoided. More reaction conditions such as different solvents, different temperatures, new pressure ratios or new catalysts will be screened in order to try to overcome this problem.

Overall, this is the first report of the reductive functionalization of a nickelalactone into a propanoate derivative with a borane.

## 4.8 Experimental part

### 4.8.1 General Remarks

All reactions were carried out under an atmosphere of dry argon using standard Schlenk techniques or in a nitrogen-filled MBraun LabStar glovebox. Diethyl ether, pentane, THF and toluene were taken from an MBraun SPS-800 solvent purification system, freeze-pump-thaw degassed and stored over 4 Å molecular sieves. C<sub>6</sub>D<sub>6</sub> and [d<sub>8</sub>]-THF were degassed and stored over 4 Å molecular sieves.

[(tmeda)nickelalactone]<sup>[3]</sup> **IV-5** and [(dcpp)NiH]<sub>2</sub><sup>[19]</sup> **IV-9** were synthesized according to published procedures. All the other chemicals were purchased in reagent grade purity from Acros, Cytech and Sigma-Aldrich and were used without further purification. Ethylene, CO and CO<sub>2</sub> were purchased from Air Liquide.

### 4.8.2 Synthesis of organic products

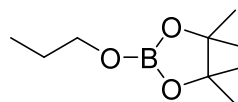
#### 4.8.2.1 Synthesis of the dcpp ligand **IV-1**<sup>[75]</sup>

The synthesis of the dcpp ligand **IV-1** was upscaled following a procedure described in Mathieu Demange's thesis.<sup>[75]</sup> *n*-BuLi (1.6 M in hexanes, 37.9 mL, 6.05×10<sup>-2</sup> mol, 1 eq.) is added at -78 °C to a 90 mL THF solution of dicyclohexylphosphine (12.0 g, 6.05×10<sup>-2</sup> mol, 1 eq.). The reaction mixture is allowed to come back to RT over 2 h. The solution turns yellow and a white precipitate falls out. <sup>31</sup>P{<sup>1</sup>H} NMR spectroscopy shows a single resonance at δ = -13.0 ppm which corresponds to the lithiated phosphine. At -78 °C, 1,3-dichloropropane (2.59 mL, 2.72×10<sup>-2</sup> mol, 0.45 eq.) is added to LiPCy<sub>2</sub>. The solution is kept for 15 min at -78 °C before it is stirred overnight at RT. The solvent is removed under reduced pressure and the residue is taken up in pentane in order to precipitate all the salt. The solution is filtered off and the product is dried under vacuum. The dcpp ligand **IV-1** is isolated as a pale yellow gel in 97 % yield (11.52 mg).

<sup>1</sup>H NMR (300 MHz, C<sub>6</sub>D<sub>6</sub>): δ 0.65 - 2.38 (m, 50H, Cy + CH<sub>2</sub>) ppm.

<sup>13</sup>C{<sup>1</sup>H} NMR (75 MHz, C<sub>6</sub>D<sub>6</sub>): δ 25.62 - 30.14 (Cy + CH<sub>2</sub>) ppm.

<sup>31</sup>P{<sup>1</sup>H} NMR (121,5 MHz, C<sub>6</sub>D<sub>6</sub>): δ - 6.7 (s) ppm.

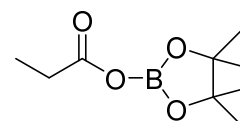
4.8.2.2 Synthesis of propoxypinacolborane **IV-11**

A C<sub>6</sub>D<sub>6</sub> or [d<sub>8</sub>]-THF solution (0.7 mL) of pinacolborane **IV-8** (72.6 μL, 5.00×10<sup>-4</sup> mol, 1 eq.) is prepared in a J. Young tube. Propanol **IV-13** (37.6 μL, 5.00×10<sup>-4</sup> mol, 1 eq.) is added and the reaction mixture is thoroughly shaken. Hydrogen gas evolution is observed and the reaction is finished after 15 min at RT. Propoxypinacolborane **IV-11** is used in situ and has not been isolated.

<sup>1</sup>H NMR (300 MHz, [d<sub>8</sub>]-THF): δ 0.87 (t, <sup>3</sup>J<sub>H,H</sub> = 7.2 Hz, 3H, CH<sub>3</sub>), 1.19 (s, 12H, C(CH<sub>3</sub>)<sub>2</sub> pinB), 1.51 (m, 2H, CH<sub>2</sub>), 3.71 (t, <sup>3</sup>J<sub>H,H</sub> = 6.6 Hz, 2H, OCH<sub>2</sub>) ppm.

<sup>13</sup>C{<sup>1</sup>H} NMR (75 MHz, [d<sub>8</sub>]-THF): δ 10.4 (CH<sub>3</sub>), 24.8 (C(CH<sub>3</sub>)<sub>2</sub> pinB), 25.5 (CH<sub>2</sub>), 66.7 (OCH<sub>2</sub>), 82.7 (C(CH<sub>3</sub>)<sub>2</sub> pinB) ppm.

<sup>11</sup>B NMR (96 MHz, [d<sub>8</sub>]-THF): δ 21.3 (s) ppm.

4.8.2.3 Synthesis of propanoic acid pinacolborane ester **IV-14**

Propanoic acid (37.4 μL, 5.00×10<sup>-4</sup> mol, 1 eq.) is added to an excess of pinacolborane **IV-8** (108.9 μL, 7.50×10<sup>-4</sup> mol, 1.5 eq.) in C<sub>6</sub>D<sub>6</sub> (0.7 mL). The solution in the J. Young tube is thoroughly shaken and hydrogen gas evolution is observed. The reaction is finished after 45 min. at RT. Propanoic acid pinacolborane ester **IV-14** is the main product of the reaction. It has not been isolated as it is degraded under vacuum. <sup>[36]</sup>

<sup>1</sup>H NMR (300 MHz, C<sub>6</sub>D<sub>6</sub>): δ 0.84 (t, <sup>3</sup>J<sub>H,H</sub> = 7.5 Hz, 3H, CH<sub>3</sub>), 1.05 (s, 12H, C(CH<sub>3</sub>)<sub>2</sub> pinB), 2.01 (q, <sup>3</sup>J<sub>H,H</sub> = 7.5 Hz, 2H, CH<sub>2</sub>) ppm.

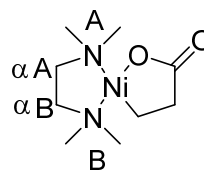
<sup>13</sup>C{<sup>1</sup>H} NMR (75 MHz, C<sub>6</sub>D<sub>6</sub>): δ 8.9 (CH<sub>3</sub>), 24.6 (C(CH<sub>3</sub>)<sub>2</sub> pinB), 28.6 (CH<sub>2</sub>), 83.2 (C(CH<sub>3</sub>)<sub>2</sub> pinB), 171.1 (C=O) ppm.

<sup>11</sup>B-NMR (96 MHz, C<sub>6</sub>D<sub>6</sub>): δ 22.8 (s) ppm.



### 4.8.3 Synthesis of [(dcpp)-nickel]-complexes

#### 4.8.3.1 Synthesis of [(tmeda)nickelalactone] **IV-5** <sup>[3]</sup>



[(tmeda)nickelalactone] **IV-5** is synthesized according to a published procedure. <sup>[3]</sup> [Ni(COD)<sub>2</sub>] **IV-2** (1.653 g, 6.00×10<sup>-3</sup> mol, 1 eq.) is suspended with succinic anhydride **IV-10** (413.2 mg, 4.13×10<sup>-3</sup> mol, 0.69 eq.) in tmeda (8 mL). The reaction mixture is stirred overnight at RT. The solution turns first yellow then brownish and a precipitate is formed. The supernatant is filtered away, the product is washed 3 × with Et<sub>2</sub>O and dried under vacuum. If the product is not green but brown at this stage of the reaction, the Schlenk is opened to air for a few minutes until the product turns green. This process is slightly exothermic. The product is then stored back under inert atmosphere. [(tmeda)nickelalactone] **IV-5** is finally collected as a green powder in 90.5 % yield (923.0 mg).

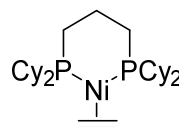
<sup>1</sup>H NMR (300 MHz, CD<sub>2</sub>Cl<sub>2</sub>): δ 0.39 (t, <sup>3</sup>J<sub>H,H</sub> = 7.5 Hz, 2H, Ni-CH<sub>2</sub>), 1.78 (t, <sup>3</sup>J<sub>H,H</sub> = 7.5 Hz, 2H, C(O)-CH<sub>2</sub>), 2.27 (s, 4H, N-CH<sub>2</sub> αA + αB), 2.32 (s, 2H, N(CH<sub>3</sub>)<sub>2</sub> B), 2.54 (s, 2H, N(CH<sub>3</sub>)<sub>2</sub> A) ppm.

<sup>13</sup>C{<sup>1</sup>H} NMR (75 MHz, CD<sub>2</sub>Cl<sub>2</sub>): δ -0.8 (Ni-CH<sub>2</sub>), 37.5 (C(O)-CH<sub>2</sub>), 47.1 (N(CH<sub>3</sub>)<sub>2</sub> A), 49.2 (N(CH<sub>3</sub>)<sub>2</sub> B), 56.6 (CH<sub>2</sub> αA), 61.5 (CH<sub>2</sub> αB), 180.4 (C=O) ppm.

<sup>13</sup>C[(tmeda)nickelalactone] **IV-5**(<sup>13</sup>C) is synthesized by following the same procedure. Starting from [Ni(COD)<sub>2</sub>] **IV-2** (1.00 g, 3.62×10<sup>-3</sup> mol, 1 eq.) and <sup>13</sup>C labelled succinic anhydride **IV-10**(<sup>13</sup>C) (251.4 mg, 2.42×10<sup>-3</sup> mol, 0.67 eq.) in 7 mL of tmeda, <sup>13</sup>C[(tmeda)nickelalactone] **IV-5**(<sup>13</sup>C) is gathered as a green powder in 80 % yield (480.9 mg).

<sup>1</sup>H NMR (300 MHz, CD<sub>2</sub>Cl<sub>2</sub>): δ 0.49 (d, <sup>1</sup>J<sub>C,H</sub> = 130.2 Hz, 2H, Ni-CH<sub>2</sub>), 1.79 (t, <sup>1</sup>J<sub>C,H</sub> = 125.1 Hz, 2H, C(O)-CH<sub>2</sub>), 2.27 (s, 4H, N-CH<sub>2</sub> αA + αB), 2.32 (s, 2H, N(CH<sub>3</sub>)<sub>2</sub> B), 2.54 (s, 2H, N(CH<sub>3</sub>)<sub>2</sub> A) ppm.

<sup>13</sup>C{<sup>1</sup>H} NMR (75 MHz, CD<sub>2</sub>Cl<sub>2</sub>): δ -0.8 (d, <sup>1</sup>J<sub>C,C</sub> = 33.8 Hz, Ni-CH<sub>2</sub>), 38.0 (m, C(O)-CH<sub>2</sub>), 47.0 (N(CH<sub>3</sub>)<sub>2</sub> A), 49.2 (N(CH<sub>3</sub>)<sub>2</sub> B), 56.5 (CH<sub>2</sub> αA), 61.4 (CH<sub>2</sub> αB), 189.5 (dd, <sup>1</sup>J<sub>C,C</sub> = 45.2 Hz, C=O) ppm.

4.8.3.2 Synthesis of [(dcpP)Ni(C<sub>2</sub>H<sub>4</sub>)] **IV-3**

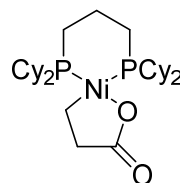
[Ni(COD)<sub>2</sub>] **IV-2** (250 mg, 9.06×10<sup>-4</sup> mol, 1 eq.) is suspended in 10 mL of THF and reacted with the dcpP ligand **IV-1** (*C* = 0.759 mol.L<sup>-1</sup> in THF, 1.19 mL, 9.06×10<sup>-4</sup> mol, 1 eq.). The yellow reaction mixture, containing the [(dcpP)Ni]<sub>2</sub>(COD)] dimer, is freeze-pump-thaw degassed and 1 bar of ethylene is applied to the Schlenk. The solution is stirred for 15 min. at RT and a new slightly brighter yellow complex falls out. The solvent is removed under reduced pressure, the product is taken up with pentane in the glovebox and transferred to a centrifugation vial. [(dcpP)Ni(C<sub>2</sub>H<sub>4</sub>)] **IV-3** is washed 3 × with pentane and then transferred back to a Schlenk to dry the product under vacuum. [(dcpP)Ni(C<sub>2</sub>H<sub>4</sub>)] **IV-3** is collected as a yellow powder in 64 % yield (301.6 mg). The complex has a very poor solubility in all common organic solvents. Single crystals for X-ray diffraction analysis were grown by heating a THF solution of [(dcpP)Ni(C<sub>2</sub>H<sub>4</sub>)] **IV-3** to reflux and letting it slowly cool down to RT.

<sup>1</sup>H NMR (500 MHz, [d<sub>8</sub>]-THF): δ 1.14 - 1.38 (m, Cy + CH<sub>2</sub>), 1.48 (br s, Cy + CH<sub>2</sub>), 1.52 (s, 4H, CH<sub>2</sub> ethylene)\*, 1.60 - 1.86 (m, Cy + CH<sub>2</sub>), 2.14 (s, Cy + CH<sub>2</sub>), 2.30 (s, Cy + CH<sub>2</sub>) ppm.

<sup>13</sup>C{<sup>1</sup>H}{<sup>31</sup>P} NMR (125, [d<sub>8</sub>]-THF): δ 22.5, 27.3, 28.1, 29.6, 30.0 (Cy + CH<sub>2</sub>), 31.7 (CH<sub>2</sub> ethylene)\*, 37.7 ppm.

<sup>31</sup>P{<sup>1</sup>H} NMR (121.5 MHz, [d<sub>8</sub>]-THF): δ 25.2 (s) ppm.

\* The chemical shifts of the ethylenic protons and carbons were determined on <sup>13</sup>C[(dcpP)Ni(C<sub>2</sub>H<sub>4</sub>)] **IV-3**(<sup>13</sup>C). For the protons <sup>1</sup>H 1D-HSQC and 2D-HSQC experiments were performed and for the carbons a <sup>13</sup>C{<sup>1</sup>H}{<sup>31</sup>P} NMR was recorded.

4.8.3.3 Synthesis of (dcpP)nickelalactone **IV-4**

[(tmeda)nickelalactone] **IV-5** (350 mg, 1.42×10<sup>-3</sup> mol, 1eq.) is reacted with the dcpP ligand **IV-1** (*C* = 0.917 mol.L<sup>-1</sup> in THF, 1.70 mL, 1.56×10<sup>-3</sup> mol, 1,1 eq.) in THF (15 mL). The reaction mixture is stirred for 3 h. at RT. Pentane is added (≈ 70 mL) and the solution is stirred to precipitate [(dcpP)nickelalactone] **IV-4**. The supernatant is filtered away. The product is

washed 2 × with Et<sub>2</sub>O and 2 × with pentane and then dried overnight under vacuum. [(dcpp)nickelalactone] **IV-4** is gathered as a yellow to light orange powder in 68 % yield (546,3 mg). Crystals for X-ray diffraction analysis are grown at RT by diffusing pentane in a THF solution of [(dcpp)nickelalactone] **IV-4**.

<sup>1</sup>H NMR (500 MHz, [d8]-THF): δ 0.68 (m, 2H, Ni-CH<sub>2</sub>)<sup>\*</sup>, 1.16 - 2.00 (m, Cy + CH<sub>2</sub>), 2.02 (m, 2H, C(O)-CH<sub>2</sub>)<sup>\*</sup>, 2.26 (m, Cy + CH<sub>2</sub>), 2.50 (m, Cy + CH<sub>2</sub>) ppm.

<sup>13</sup>C{<sup>1</sup>H} NMR (125 MHz, [d8]-THF): δ 13.1 (Ni-CH<sub>2</sub>)<sup>\*</sup>, 18.5, 22.7, 27.0, 27.1, 27.8, 28.1, 28.4, 29.2, 29.9, 30.2, 32.1 (Cy + CH<sub>2</sub>), 34.6 (CH αP), 37.2 (CH αP), 37.4 (C(O)-CH<sub>2</sub>)<sup>\*</sup>, 186.6 (C=O)<sup>\*</sup> ppm.

<sup>31</sup>P{<sup>1</sup>H} NMR (121,5 MHz, [d8]-THF): δ 10.4 (d, <sup>2</sup>J<sub>P,P</sub> = 32.8 Hz), 32.1 (d, <sup>2</sup>J<sub>P,P</sub> = 32.8 Hz) ppm.

IR (ATR, cm<sup>-1</sup>): ν = 1650 (m).

\* The chemical shifts of the protons and carbons from the lactone were determined on <sup>13</sup>C[(dcpp)nickelalactone] **IV-4**(<sup>13</sup>C). For the protons <sup>1</sup>H 1D-HSQC and 2D-HSQC experiments were performed and for the carbons a <sup>13</sup>C{<sup>1</sup>H}{<sup>31</sup>P} NMR was recorded.

<sup>13</sup>C[(dcpp)nickelalactone] **IV-4**(<sup>13</sup>C) is synthesized by following the same procedure. Starting from <sup>13</sup>C[(tmeda)nickelalactone] **IV-5**(<sup>13</sup>C) (250.0 mg, 1.00×10<sup>-3</sup> mol, 1 eq.) and dcpp **IV-1** (C = 0.829 mol.L<sup>-1</sup> in THF, 1.33 mL, 1.10×10<sup>-3</sup> mol, 1.1 eq), <sup>13</sup>C[(dcpp)nickelalactone] **IV-4**(<sup>13</sup>C) is isolated as a yellow powder in 87 % yield (494.1 mg).

<sup>1</sup>H NMR (500 MHz, [d8]-THF): δ 0.68 (d, <sup>1</sup>J<sub>C,H</sub> = 130.5 Hz, 2H, Ni-CH<sub>2</sub>), 1.16 - 2.00 (m, Cy + CH<sub>2</sub>), 2.02 (d, <sup>1</sup>J<sub>C,H</sub> = 125.0 Hz, 2H, C(O)-CH<sub>2</sub>), 2.26 (br s, Cy + CH<sub>2</sub>), 2.50 (br s, Cy + CH<sub>2</sub>) ppm.

<sup>13</sup>C{<sup>1</sup>H}{<sup>31</sup>P} NMR (125 MHz, [d8]-THF): δ 13.1 (d, <sup>1</sup>J<sub>C,C</sub> = 32.88 Hz, Ni-CH<sub>2</sub>), 18.5, 22.7, 27.0, 27.1, 27.8, 28.1, 28.4, 29.2, 29.9, 30.2, 31.7, 32.1 (Cy + CH<sub>2</sub>), 34.6 (CH αP), 37.2 (CH αP), 37.4 (dd, <sup>1</sup>J<sub>C,C</sub> = 32.88 Hz, <sup>1</sup>J<sub>C,C</sub> = 52.13 Hz, C(O)-CH<sub>2</sub>), 186.6 (d, <sup>1</sup>J<sub>C,C</sub> = 52.13 Hz, C=O) ppm.

<sup>31</sup>P{<sup>1</sup>H} NMR (121.5 MHz, [d8]-THF): δ 9.5 - 10.4 (m), 31.4 - 31.9 (m) ppm.

## 4.8.4 Description of typical reaction set-ups

### 4.8.4.1 Kinetic experiments

[(dcpp)nickelalactone] **IV-4** (10.0 mg,  $1.76 \times 10^{-5}$  mol) is dissolved in 0.8 mL of [d<sub>8</sub>]-THF or [d<sub>8</sub>]-toluene in a J. Young tube. PPh<sub>3</sub> (4.5 - 6 mg) is added as an internal standard. The tube is heated to the desired temperature (55 - 90 °C) and the decay of [(dcpp)nickelalactone] **IV-4** is followed by <sup>31</sup>P{<sup>1</sup>H} NMR.

### 4.8.4.2 Reaction between [(dcpp)nickelalactone] **IV-4** and pinacolborane **IV-8**

[(dcpp)nickelalactone] **IV-4** (15.0 mg,  $2.64 \times 10^{-5}$  mol, 1 eq.) is dissolved in 0.8 mL of [d<sub>8</sub>]-THF in a J. Young tube. Pinacolborane **IV-8** (11.5 μL,  $7.93 \times 10^{-5}$  mol, 3 eq.) is added and the reaction is thoroughly shaken. The solution turns red within minutes. The reaction is followed by NMR spectroscopy and is almost finished after 1 h. at RT. Trimethoxybenzene (6.7 mg,  $3.98 \times 10^{-5}$  mol) can be added as internal standard.

For the spiking experiment, propoxypinacolborane **IV-11** ( $C = 0.714 \text{ mol.L}^{-1}$  in [d<sub>8</sub>]-THF, 185.1 μL,  $1.32 \times 10^{-4}$  mol, 5 eq.) has been added to the reaction mixture after 4 h. at RT. The evolution of the peaks and integrations was followed by <sup>1</sup>H NMR.

### 4.8.4.3 Catalysis

The catalytic experiments are performed in 4 mL vials from Supelco, closed by polypropylene hole caps with PTFE/silicone septa. Three of these vials can fit at the same time in the glass holder of the autoclave.

A catalytic amount of [(dcpp)nickelalactone] **IV-4** (28.5 mg,  $5.00 \times 10^{-5}$  mol, 5 mol%) is weighted into a vial equipped with a small magnetic stirring bar and dissolved in 2 mL of THF. Pinacolborane **IV-8** (580.4 μL,  $4.0 \times 10^{-3}$  mol, 400 mol%) is added and the vial is closed. A small piece of cannula is inserted in the septum to equilibrate the pressures in the tube and in the autoclave during the reaction. The autoclave is then pressurized with the gas at the lowest pressure, followed by the gas at the highest pressure. Typically, ethylene is introduced first (5 - 9 bar), followed by CO<sub>2</sub> (20 - 30 bar). The autoclave is heated for 24 h. at 60 °C. At the end

of the reaction, the autoclave is cooled down to RT and depressurized. The reaction mixture is recovered in the glovebox and analyzed by NMR spectroscopy.

---

## 4.9 References

- [1] E. Nicolas, A. Ohleier, F. D'Accriscio, A-F. Pécharman, M. Demange, P. Ribagnac, J. Ballester, C. Gosmini, N. Mézailles, *Chem. Eur. J.*, **2015**, *21*, 7690 - 7694.
- [2] M. L. Lejkowski, R. Lindner, T. Kageyama, G. É. Bódizs, P. N. Plessow, I. B. Müller, A. Schäfer, F. Rominger, P. Hofmann, C. Futter, S. A. Schunk, M. Limbach, *Chem. Eur. J.*, **2012**, *18*, 14017 - 14025.
- [3] R. Fischer, B. Nestler, H. Schütz, *Z. Anorg. All. Chem.*, **1989**, *577*, 111 - 114.
- [4] J. Langer, R. Fischer, H. Görls, D. Walther, *J. Organomet. Chem.*, **2004**, *689*, 2952 - 2962.
- [5] H. Hoberg, Y. Peres, C. Krüger, Y. H. Tsay, *Angew. Chem. Int. Ed.*, **1987**, *26*, 771 - 773.
- [6] S. Y. T. Lee, M. Cokoja, M. Drees, Y. Li, J. Mink, W. A. Herrmann, F. E. Kühn, *ChemSusChem*, **2011**, *4*, 1275 - 1279.
- [7] B. Hipler, M. Döring, C. Dubs, H. Görls, T. Hübler, E. Uhlig, *Z. Anorg. All. Chem.*, **1998**, *624*, 1329 - 1335.
- [8] H. Hoberg, D. Schäfer, *J. Organomet. Chem.*, **1983**, *251*, C51 - C53.
- [9] R. Fischer, J. Langer, A. Malassa, D. Walther, H. Görls, G. Vaughan, *Chem. Commun.*, **2006**, *23*, 2510 - 2512.
- [10] J. Langer, R. Fischer, H. Görls, D. Walther, *Eur. J. Inorg. Chem.*, **2007**, 2257 - 2264.
- [11] C. Bruckmeier, M. W. Lehenmeier, R. Reichardt, S. Vagin, B. Rieger, *Organomet.*, **2010**, *29*, 2199 - 2202.
- [12] S. Y. T. Lee, A. Abdul Ghani, V. D'Elia, M. Cokoja, W. A. Herrmann, J-M. Basset, F. E. Kühn, *New. J. Chem.*, **2013**, *37*, 3512 - 3517.
- [13] Z. Zhang, F. Guo, F. E. Kühn, J. Sun, M. Zhou, X. Fang, *Appl. Organometal. Chem.*, **2017**, *31*, e3567.
- [14] C. Hendriksen, E. A. Pidko, G. Yang, B. Schöffner, D. Vogt, *Chem. Eur. J.*, **2014**, *20*, 12037 - 12040.
- [15] D. Jin, T. J. Schmeier, P. G. Williard, N. Hazari, W. H. Bernskoetter, *Organomet.*, **2013**, *32*, 2152 - 2159.

- [16] N. Huguet, I. Jevtovikj, A. Gordillo, M. L. Lejkowski, R. Lindner, M. Bru, A. Y. Khalimon, F. Rominger, S. A. Svhunk, P. Hofmann, M. Limbach, *Chem. Eur. J.*, **2014**, *20*, 16858 - 16862.
- [17] S. Manzini, N. Huguet, O. Trapp, T. Schaub, *Eur. J. Org. Chem.*, **2015**, *32*, 7122 - 7130.
- [18] B. Wrackmeyer, O. L. Tok, *Z. Naturforschung B*, **2005**, *60*, 259 - 264.
- [19] K. Jonas, G. Wilke, *Angew. Chem. Int. Ed.*, **1970**, *9*, 312 - 313.
- [20] B. L. Barnett, C. Krüger, Y. H. Tsay, R. H. Summerville, R. Hoffmann, *Chem. Ber.*, **1977**, *110*, 3900 - 3909.
- [21] M. Takimoto, K. Shimizu, M. Mori, *Org. Lett.*, **2001**, *3*, 3345 - 3347.
- [22] K. Shimizu, M. Takimoto, Y. Sato, M. Mori, *Org. Lett.*, **2005**, *7*, 195 - 197.
- [23] M. Takimoto, M. Mori, *J. Am. Chem. Soc.*, **2001**, *123*, 2895 - 2896.
- [24] M. Takimoto, M. Mori, *J. Am. Chem. Soc.*, **2002**, *124*, 10008 - 10009.
- [25] E. M. O'Brien, E. A. Bercot, T. Rovis, *J. Am. Chem. Soc.*, **2003**, *125*, 10498 - 10499.
- [26] S. Bontemps, *Coord. Chem. Rev.*, **2016**, *308*, 117 - 130.
- [27] C. C. Chong, R. Kinjo, *ACS Catal.*, **2015**, *5*, 3228 - 3259.
- [28] S. Chakraborty, J. Zhang, J. A. Krause, H. Guan, *J. Am. Chem. Soc.*, **2010**, *132*, 8872 - 8873.
- [29] S. Bontemps, L. Vendier, S. Sabo-Etienne, *Angew. Chem. Int. Ed.*, **2012**, *51*, 1671 - 1674.
- [30] M. J. Sgro, D. W. Stephan, *Angew. Chem. Int. Ed.*, **2012**, *51*, 11343 - 11345.
- [31] M. D. Anker, M. Arrowsmith, P. Bellham, M. S. Hill, G. Kociok-Köhn, D. J. Liptrot, M. F. Mahon, C. Weetman, *Chem. Sci.*, **2014**, *5*, 2826 - 2830.
- [32] J. A. B. Abdalla, I. M. Riddlestone, R. Tirfin, S. Aldridge, *Angew. Chem. Int. Ed.*, **2015**, *54*, 5098 - 5102.
- [33] S. Chakraborty, Y. J. Patel, J. A. Krause, H. Guan, *Polyhedron*, **2012**, *32*, 30 - 34.
- [34] S. Chakraborty, J. Zhang, Y. J. Patel, J. A. Krause, H. Guan, *Inorg. Chem.*, **2013**, *52*, 37 - 47.
- [35] F. Huang, C. Zhang, J. Jiang, Z.-X. Wang, H. Guan, *Inorg. Chem.*, **2011**, *50*, 3816 - 3825.

- [36] S. Bontemps, S. Sabo-Etienne, *Angew. Chem. Int. Ed.*, **2013**, *52*, 10253 - 10255.
- [37] S. Bontemps, L. Vendier, S. Sabo-Etienne, *J. Am. Chem. Soc.*, **2014**, *136*, 4419 - 4425.
- [38] R. Shintani, K. Nozaki, *Organomet.*, **2013**, *32*, 2459 - 2462.
- [39] H.-W. Suh, L. M. Guard, N. Hazari, *Chem. Sci.*, **2014**, *5*, 3859 - 3872.
- [40] A. Y. Khalimon, P. Farha, L. G. Kuzmina, G. I. Nikonov, *Chem. Commun.*, **2012**, *48*, 455 - 457.
- [41] S. Bagherzadeh, N. P. Mankad, *Chem. Commun.*, **2016**, *52*, 3844 - 3846.
- [42] M. Arrowsmith, T. J. Hadlington, M. S. Hill, G. Kociok-Köhn, *Chem. Commun.*, **2012**, *48*, 4567 - 4569.
- [43] P. A. Lummis, M. R. Momeni, M.W. Lui, R. McDonald, M. J. Ferguson, M. Miskolzie, A. Brown, E. Rivard, *Angew. Chem. Int. Ed.*, **2014**, *53*, 9347 - 9351.
- [44] D. Mukherjee, H. Osseili, T. P. Spaniol, J. Okuda, *J. Am. Chem. Soc.*, **2016**, *138*, 10790 - 10793.
- [45] A. J. Blake, A. Cunningham, A. Ford, S. J. Teat, S. Woodward, *Chem. Eur. J.*, **2000**, *6*, 3586 - 3594.
- [46] T. J. Hadlington, M. Hermann, G. Frenking, C. Jones, *J. Am. Chem. Soc.*, **2014**, *136*, 3028 - 3031.
- [47] C. C. Chong, H. Hirao, R. Kinjo, *Angew. Chem. Int. Ed.*, **2015**, *54*, 190 - 194.
- [48] J. Ishizu, T. Yamamoto, A. Yamamoto, *Chem. Lett.*, **1976**, 1091 - 1094.
- [49] T. Yamamoto, J. Ishizu, T. Kohara, S. Komiya, A. Yamamoto, *J. Am. Chem. Soc.*, **1980**, *102*, 3758 - 3764.
- [50] T. Yamamoto, J. Ishizu, A. Yamamoto, *Chem. Lett.*, **1979**, 1385 - 1386.
- [51] A. N. Desnoyer, F. W. Friese, W. Chiu, M. W. Drover, B. O. Patrick, J. A. Love, *Chem. Eur. J.*, **2016**, *22*, 4070 - 4077.
- [52] K. W. Quasdorf, X. Tian, N. K. Garg, *J. Am. Chem. Soc.*, **2008**, *130*, 14422 - 14423.
- [53] B.-T. Guan, Y. Wang, B.-J. Li, D.-G. Yu, Z. J. Shi, *J. Am. Chem. Soc.*, **2008**, *130*, 14468 - 14470.



- [54] K. Muto, J. Yamaguchi, K. Itami, *J. Am. Chem. Soc.*, **2012**, *134*, 169 - 172.
- [55] K. Muto, J. Yamaguchi, K. Itami, *J. Am. Chem. Soc.*, **2013**, *135*, 16384 - 16387.
- [56] J. Cornella, E. P. Jackson, R. Martin, *Angew. Chem. Int. Ed.*, **2015**, *54*, 4075 - 4078.
- [57] C. Zarate, R. Martin, *J. Am. Chem. Soc.*, **2014**, *136*, 2236 - 2239.
- [58] Z. Li, S.-L. Zhang, Y. Fu, Q.-X. Guo, L. Liu, *J. Am. Chem. Soc.*, **2009**, *131*, 8815 - 8823.
- [59] K. Amaike, K. Muto, J. Yamaguchi, K. Itami, *J. Am. Chem. Soc.*, **2012**, *134*, 13573 - 13576.
- [60] K. Muto, J. Yamaguchi, D. G. Musaev, K. Itami, *Nat. Commun.*, **2015**, *6*, 7508.
- [61] X. Hong, Y. Liang, K. N. Houk, *J. Am. Chem. Soc.*, **2014**, *136*, 2017 - 2025.
- [62] Q. Lu, H. Yu, Y. Fu, *J. Am. Chem. Soc.*, **2014**, *136*, 8252 - 8260.
- [63] L. Hie, N. F. Fine Nathel, X. Hong, Y.-F. Yang, K. N. Houk, N. K. Garg, *Angew. Chem. Int. Ed.*, **2016**, *55*, 2810 - 2814.
- [64] M. G. Crestani, M. Muñoz-Hernández, A. Arévalo, A. Acosta-Ramírez, J. J. García, *J. Am. Chem. Soc.*, **2005**, *127*, 18066 - 18073.
- [65] V. M. Iluc, G. L. Hillhouse, *Tetrahedron*, **2006**, *62*, 7577 - 7582.
- [66] A. E. King, S. C. E. Stieber, N. J. Henson, S. A. Kozimor, B. L. Scott, N. C. Smythe, A. D. Sutton, J. C. Gordon, *Eur. J. Inorg. Chem.*, **2016**, 1635 - 1640.
- [67] J. Cornella, E. Gómez-Bengoa, R. Martin, *J. Am. Chem. Soc.*, **2013**, *135*, 1997 - 2009.
- [68] V. M. Iluc, G. L. Hillhouse, *J. Am. Chem. Soc.*, **2010**, *132*, 11890 - 11892.
- [69] C. F. Lovitt, G. Frenking, G. S. Girolami, *Organomet.*, **2012**, *31*, 4122 - 4132.
- [70] M. Baacke, S. Morton, O. Stelzer, W. S. Sheldrick, *Chem. Ber.*, **1980**, *113*, 1343 - 1355.
- [71] S. Reinhard, P. Šoba, F. Rominger, J. Blümel, *Adv. Synth. Catal.*, **2003**, *345*, 589 - 602.
- [72] L. González-Sebastián, M. Flores-Alamo, J. J. García, *Organomet.*, **2013**, *32*, 7186 - 7194.
- [73] L. González-Sebastián, M. Flores-Alamo, J. J. García, *Organomet.*, **2012**, *31*, 8200 - 8207.
- [74] P. W. G. Ariyananda, M. T. Kieber-Emmons, G. P. A. Yap, C. G. Riordan, *Dalton Trans.*, **2009**, 4359 - 4369.

[75] Matthieu Demange, Thèse de doct., Ecole polytechnique, Paris, **2013**.

[76] L. González-Sebastián, M. Flores-Alamo, J. J. García, *Dalton Trans.*, **2011**, *40*, 9116 - 9122.

[77] J. S. Anderson, V. M. Iluc, G. L. Hillhouse, *Inorg. Chem.*, **2010**, *49*, 10203 - 10207.

[78] M. A. Bennett, D. C. R. Hockless, M. G. Humphrey, M. Schultz, E. Wenger, *Organomet.*, **1996**, *15*, 928 - 933.



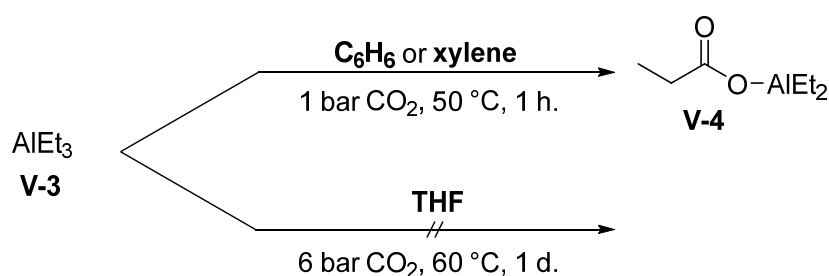
## 5 Functionalization of CO<sub>2</sub> with aluminium derivatives

After the successful synthesis of propanol derivatives from nickelalactones and boranes, the research turned towards softer aluminium compounds. The reactivity between [(dcp)nickel]-complexes and trialkyl aluminium derivatives has been explored. AlR<sub>3</sub> transmetallating reagents are expected, as pinacolborane, to cleave the Ni-O bond of [(dcp)nickelalactone] **V-1** and induce lactone ring opening providing the possibility of a β-hydride elimination.

### 5.1 Stoichiometric synthesis of propanoic acid derivatives

#### 5.1.1 Blank reactions

A good candidate for transmetallation should be inert towards CO<sub>2</sub> and [(dcp)Ni(C<sub>2</sub>H<sub>4</sub>)] **V-2**. Accordingly, the reactivity of AlEt<sub>3</sub> **V-3** has been tested. The literature reports facile reduction of CO<sub>2</sub> into diethylaluminium propanoate **V-4** in aromatic solvents as benzene or xylene. <sup>[1, 2]</sup> Nevertheless, the reaction does not take place in THF even under 6 bar of CO<sub>2</sub> and heating to 60 °C for 1 d. Even though CO<sub>2</sub> has a greater solubility in THF compared to benzene, the coordinating ability of THF hampers the reaction.

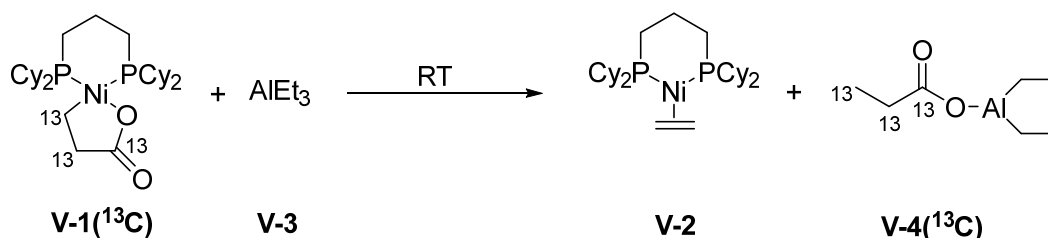


**Scheme 5.1:** Different reactivity between AlEt<sub>3</sub> **V-3** and CO<sub>2</sub> in aromatic solvents compared to THF.

Besides [(dcp)Ni(C<sub>2</sub>H<sub>4</sub>)] **V-2** does not display either any reactivity with AlEt<sub>3</sub> **V-3** even after 1 d. at 60 °C.

### 5.1.2 Reactivity of triethylaluminium **V-3** and tri(*n*-butyl)aluminium **V-5**

First of all, [(dcp)nickelalactone] **V-1** has been reacted with commercially available AlEt<sub>3</sub> **V-3** in THF at RT as shown in **Scheme 5.2**. <sup>31</sup>P{<sup>1</sup>H} NMR shows the formation of [(dcp)Ni(C<sub>2</sub>H<sub>4</sub>)] **V-2**, which is also confirmed by single crystal X ray diffraction. With 1.5 eq. of AlEt<sub>3</sub> **V-3** the reaction performs sluggishly, yielding 6 % of [(dcp)Ni(C<sub>2</sub>H<sub>4</sub>)] **V-2** after 21 h. By using a large excess of AlEt<sub>3</sub> **V-3** (25 wt% in toluene, 56.5 eq.) full conversion is reached within 30 min. Additionally, <sup>1</sup>H, <sup>13</sup>C and 2D HSQC and HMBC NMR reveal the formation of diethylaluminium propanoate **V-4**.

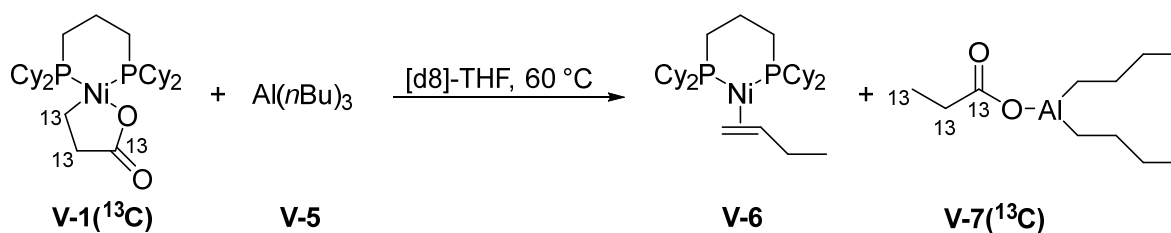


**Scheme 5.2:** Reaction between <sup>13</sup>C[(dcp)nickelalactone] **V-1**(<sup>13</sup>C) and AlEt<sub>3</sub> **V-3** at RT.

However, [(dcp)nickelalactone] **V-1** is easily decomposed into [(dcp)Ni(C<sub>2</sub>H<sub>4</sub>)] **V-2** and CO<sub>2</sub> (see 4.1.2 and 4.2 for detailed information). Therefore, additional experiments were performed in order to prove that [(dcp)Ni(C<sub>2</sub>H<sub>4</sub>)] **V-2** directly arises from the reaction between [(dcp)nickelalactone] **V-1** and AlEt<sub>3</sub> **V-3** and not from reductive decoupling.

When the reaction is repeated with <sup>13</sup>C[(dcp)nickelalactone] **V-1**(<sup>13</sup>C), the <sup>31</sup>P{<sup>1</sup>H} NMR spectrum is identical to the one obtained from the reaction without <sup>13</sup>C labelling. This proves that the ethylene moiety of [(dcp)Ni(C<sub>2</sub>H<sub>4</sub>)] **V-2** comes from the transmetalation with AlEt<sub>3</sub> **V-3** and not from the decomposition of [(dcp)nickelalactone] **V-1** itself.

Further evidence is given by the analogous reaction between [(dcp)nickelalactone] **V-1** and Al(*n*Bu)<sub>3</sub> **V-5**, for which [(dcp)Ni(1-butene)] **V-6** and di(*n*-butyl)aluminium propanoate **V-7** are identified as products.



**Scheme 5.3:** Reaction between <sup>13</sup>C[(dcpp)nickel]lactone **V-1**(<sup>13</sup>C) and Al(*n*Bu)<sub>3</sub> **V-5** in [d<sub>8</sub>]-THF generating [(dcpp)Ni(1-butene)] **V-6** and <sup>13</sup>C labelled di(*n*-butyl)aluminium propanoate **V-7**(<sup>13</sup>C).

The reaction is slower compared to AlEt<sub>3</sub> **V-3**. Nevertheless, by using an excess of Al(*n*Bu)<sub>3</sub> **V-5** (19 eq.) and heating to 60 °C, all starting [(dcpp)nickel]lactone **V-1** can be converted within 1 d. Remarkably no [(dcpp)Ni(C<sub>2</sub>H<sub>4</sub>)] **V-2** is observed under these conditions, while usually [(dcpp)nickel]lactone **V-1** starts to be reductively decoupled at 60 °C in THF. [(dcpp)Ni(1-butene)] **V-6** had been previously isolated during the investigations on Negishi cross couplings and could therefore be easily identified. The complex **V-6** appears as an AB system between  $\delta = 22.7$  ppm and  $\delta = 23.6$  ppm in <sup>31</sup>P{<sup>1</sup>H} NMR (<sup>2</sup>J<sub>P, P</sub> = 31.0 Hz), as shown in **Figure 5.1**.

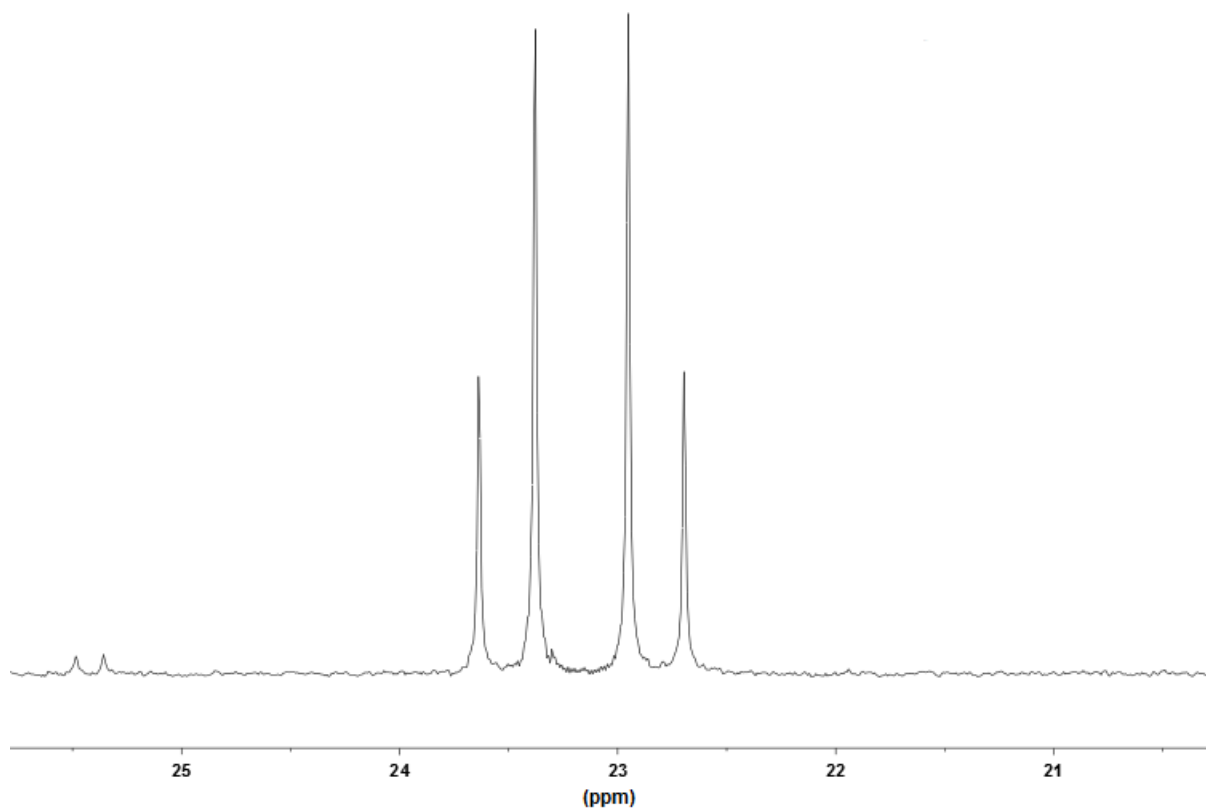


**Figure 5.1:** <sup>31</sup>P{<sup>1</sup>H} NMR spectrum of [(dcpp)Ni(1-butene)] **V-6** in THF at RT.

[(dcpP)Ni(1-butene)] **V-6** crystallizes in the unusual space group P1. The geometry around the nickel center is square planar as evidenced in **Figure 5.2**. The bite angle P<sub>1</sub>Ni<sub>1</sub>P<sub>2</sub> is comparable to the one of [(dcpP)Ni(C<sub>2</sub>H<sub>4</sub>)] **V-2** (104.01(5) ° vs. 104.50(1) °). The C<sub>1</sub>C<sub>2</sub> bond distance is clearly in the range of a double bond (C<sub>1</sub>C<sub>2</sub> = 1.375(8) Å).

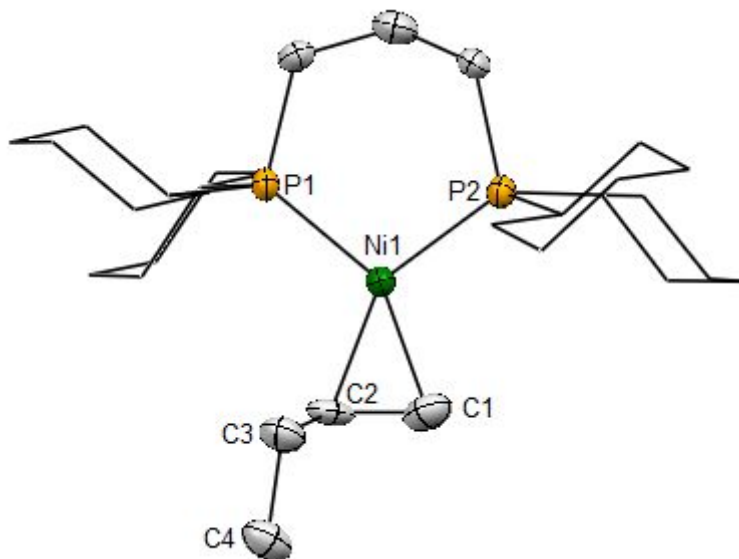
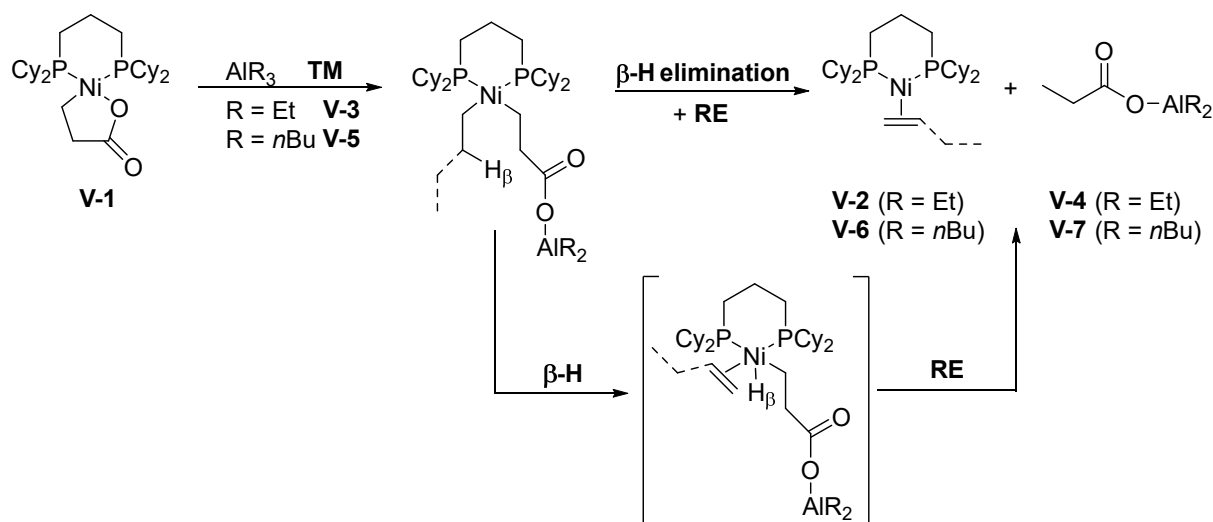


**Figure 5.2:** Molecular structure of [(dcpP)Ni(1-butene)] **V-6** determined by single crystal X-ray diffraction. Hydrogen atoms are omitted for clarity. Selected bond length [Å] and angles [°]: Ni<sub>1</sub>-C<sub>1</sub> 1.956(5), Ni<sub>1</sub>-C<sub>2</sub> 1.975(5), C<sub>1</sub>-C<sub>2</sub> 1.375(8), C<sub>2</sub>-C<sub>3</sub> 1.529(7), C<sub>3</sub>-C<sub>4</sub> 1.524(7), P<sub>1</sub>-Ni<sub>1</sub>-P<sub>2</sub> 104.01(5), C<sub>1</sub>-Ni<sub>1</sub>-C<sub>2</sub> 40.9(2).

**Scheme 5.4** proposes a mechanism for the synthesis of dialkylaluminium propanoates from [(dcpP)nickelalactone] **V-1** and AlR<sub>3</sub> derivatives. The trialkylaluminium derivatives presumably form Lewis adducts with [(dcpP)nickelalactone] **V-1**. The activated metallacycle are then more prone to the cleavage of the Ni-O bond and resulting ring opening. The reaction further proceeds through β-hydride elimination on the transferred alkyl moiety of AlR<sub>3</sub>, followed by reductive elimination leading invariably to dialkylaluminium propanoate together with the corresponding [(dcpP)Ni(alkene)] complex.

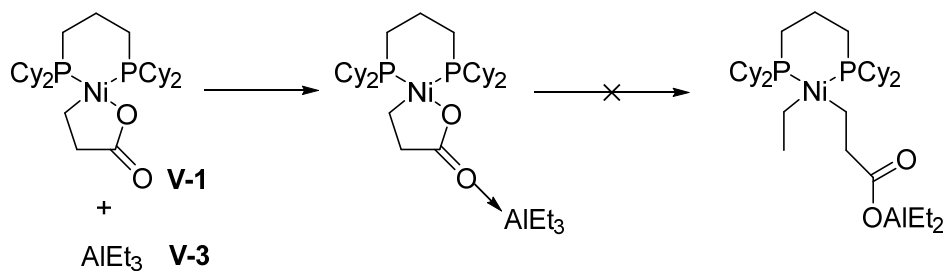


**Scheme 5.4:** Proposed mechanism for the reaction between [(dcpp)nickelalactone] **V-1** and AlR<sub>3</sub> derivatives leading to the formation of dialkylaluminium propanoates.

### 5.1.3 Preliminary DFT calculations

DFT calculations were undertaken in order to gain deeper mechanistic insights on the reaction between [(dcpp)nickelalactone] **V-1** and AlEt<sub>3</sub> **V-3**. The calculations were performed using the B3PW91 functional and the 6-31G\* basis set for C, H, O, P and Al atoms and the RECP Stuttgart basis set for nickel. The cyclohexyl groups of the ligand and the ethyl groups of AlEt<sub>3</sub> were modelled by the 3-21G basis set.

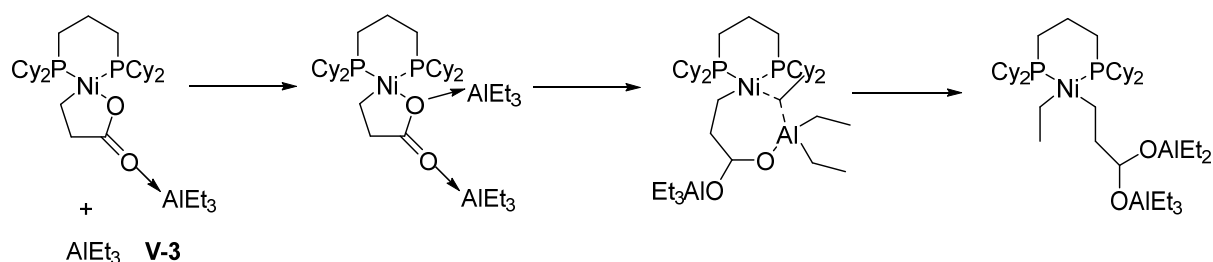
The reaction is initiated by the coordination of the Lewis acid to the acyl moiety of [(dcpp)nickelalactone] **V-1**. However, the transition state for the direct cleavage of [(dcpp)nickelalactone] **V-1** and the generation of a nickel propanoate intermediate lies very high in energy and would not be achievable under the mild reaction conditions reported before.



**Scheme 5.5:** Coordination of AlEt<sub>3</sub> **V-3** to [(dcpp)nickelalactone] **V-1**, further transmetalation is highly unfavorable.



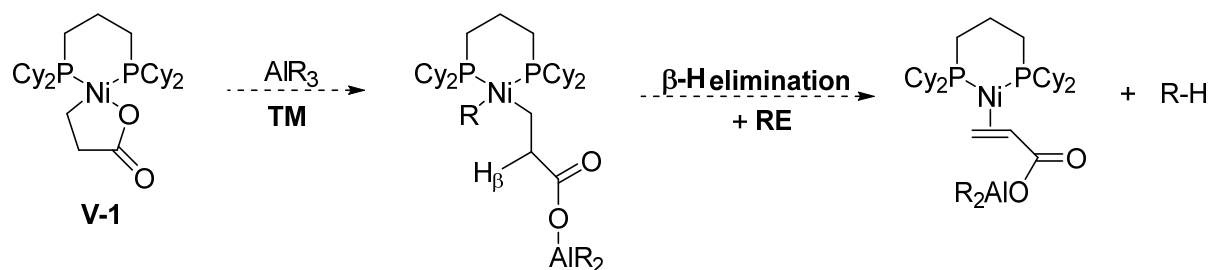
Upon coordination of an additional AlEt<sub>3</sub> **V-3** molecule on the second oxygen atom of [(dcpp)nickelalactone] **V-1**, the transition state for lactone ring opening lies significantly lower in energy, in good agreement with the reaction conditions. This also rationalize the large excess of trialkylaluminium derivatives required to perform the reactions efficiently.



**Scheme 5.6:** Coordination of a second AlEt<sub>3</sub> molecule **V-3** to the [(dcpp)nickelalactone-AlEt<sub>3</sub>] adduct induces transmetalation and formation of a nickel propanoate complex.

#### 5.1.4 Reactivity of tri(*tert*-butyl)aluminium **V-8**

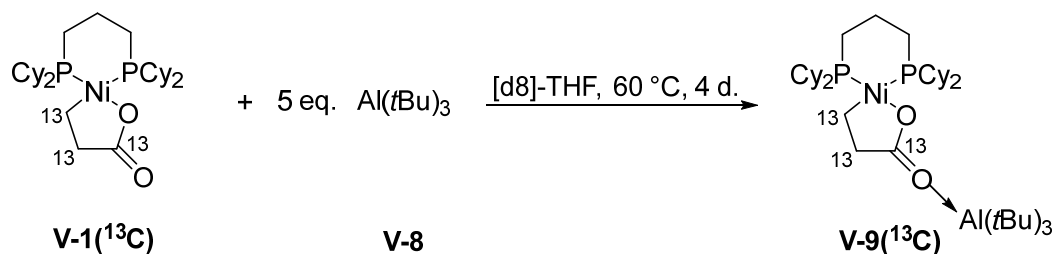
It would be even more interesting to induce β-hydride elimination on the propanoate fragment to generate acrylate derivatives as shown in **Scheme 5.7**. In this sense, the use of bulky substituents could prevent the coplanar configuration between the nickel center, the α and the β carbons of the transferred alkyl chain required for β-hydride elimination. Therefore, the reactivity of tri(*tert*-butyl)aluminium **V-8** was investigated.



**Scheme 5.7:** Possible synthesis of acrylate derivatives using AlR<sub>3</sub> compounds with substituents that do not fulfill the conditions for β-H elimination.

When <sup>13</sup>C[(dcpp)nickelalactone] **V-1**(<sup>13</sup>C) is reacted with only 1.5 eq. of Al(*t*Bu)<sub>3</sub> **V-8** in [d<sub>8</sub>]-THF at 60 °C, a new compound is observed, giving rise to two multiplets in <sup>31</sup>P{<sup>1</sup>H} NMR between δ = 12.9 ppm and δ = 13.6 ppm and between δ = 35.0 ppm and δ = 35.5 ppm. The <sup>31</sup>P{<sup>1</sup>H} NMR spectrum of the reaction is presented in **Figure 5.3**. By increasing the amount of Al(*t*Bu)<sub>3</sub> **V-8** to 5 eq., 28 % yield of product are measured after 8 h. at 60 °C. It seems that an equilibrium is reached since the yield does not further increase upon time. Fortunately, the complex could be crystallized in THF at -30 °C. X-ray diffraction analysis reveals a [(dcpp)nickelalactone-Al(*t*-Bu)<sub>3</sub>] adduct **V-9** in agreement with a <sup>31</sup>P{<sup>1</sup>H} NMR chemical shift close to the one reported for free <sup>13</sup>C[(dcpp)nickelalactone] **V-1**(<sup>13</sup>C). Curiously, switching the solvent from THF to non-coordinating toluene does not produce more <sup>13</sup>C[(dcpp)nickelalactone-AlR<sub>3</sub>] adduct **V-9**(<sup>13</sup>C). On the other hand, adding stronger coordinating agents such as pyridine or the Dipp carbene, does not break down the adduct either.

No adduct had been previously observed by NMR spectroscopy for the reactions with AlEt<sub>3</sub> **V-3** and Al(*n*Bu)<sub>3</sub> **V-5**. The bulkier the alkyl substituents get, the slower the reaction proceeds disclosing intermediates.



**Scheme 5.8:** Reaction between <sup>13</sup>C[(dcpp)nickelalactone] **V-1**(<sup>13</sup>C) and eq. of Al(*t*Bu)<sub>3</sub> **V-8** in [d<sub>8</sub>]-THF.

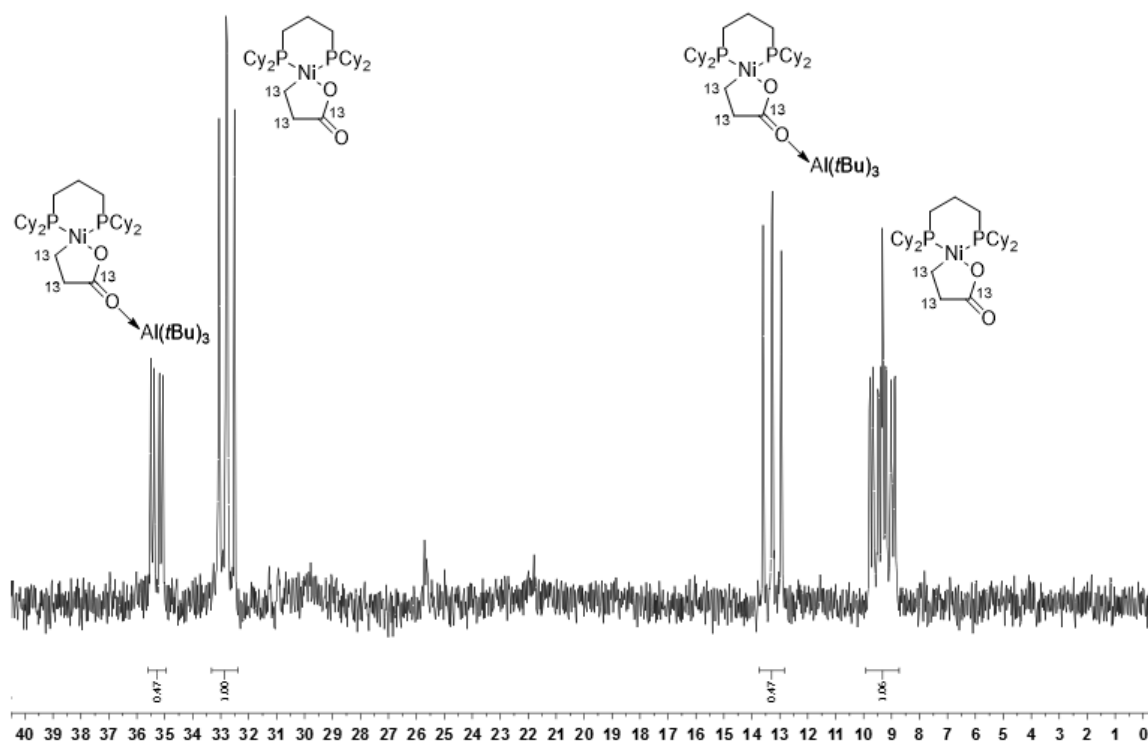


**Figure 5.3:**  $^{31}\text{P}\{^1\text{H}\}$  NMR spectrum of the reaction between  $^{13}\text{C}$ [(dcpp)nickelalactone] V-1( $^{13}\text{C}$ ) and 1.5 eq. of  $\text{Al}(t\text{Bu})_3$  V-8 after 4 d. at 60 °C in  $[\text{d}_8]\text{-THF}$ .

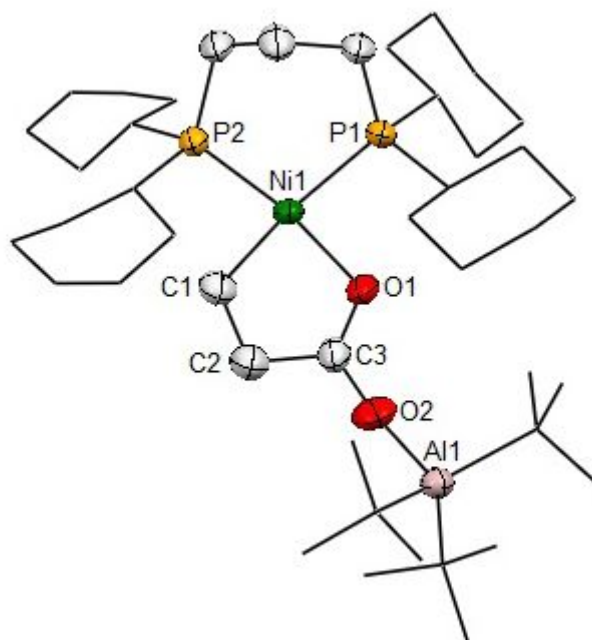
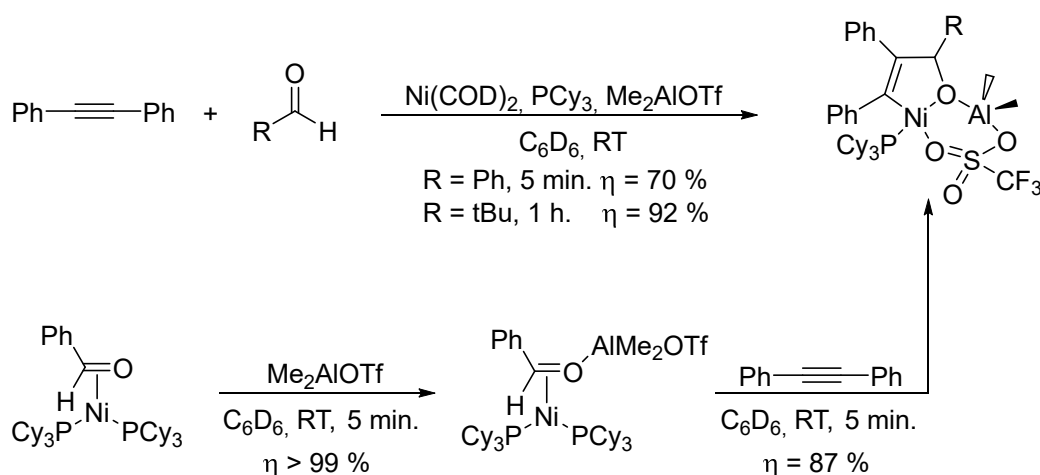


**Figure 5.4:** Molecular structure of the  $^{13}\text{C}$ [(dcpp)nickelalactone- $\text{Al}(t\text{-Bu})_3$ ] adduct V-9( $^{13}\text{C}$ ) determined by single crystal X-ray diffraction. Hydrogen atoms are omitted for clarity. Selected bond length [ $\text{\AA}$ ] and angles [ $^\circ$ ]:  $\text{Ni}_1\text{-C}_1$  1.966(3),  $\text{Ni}_1\text{-O}_1$  1.966(3),  $\text{C}_3\text{-O}_2$  1.246(4),  $\text{O}_2\text{-Al}_1$  1.831(2),  $\text{P}_1\text{-Ni}_1\text{-P}_2$  98.97(3),  $\text{C}_1\text{-Ni}_1\text{-O}_1$  83.95(12),  $\text{C}_3\text{-O}_2\text{-Al}_1$  150.3(3).

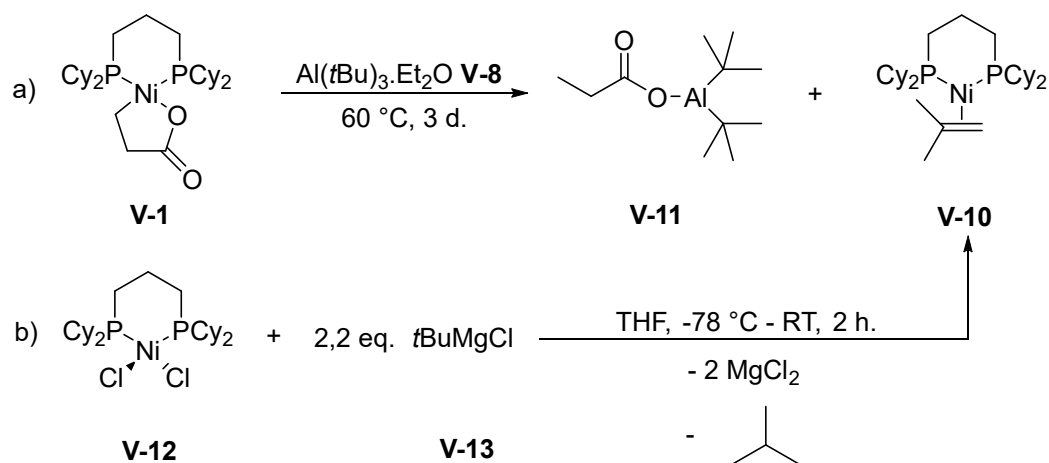
**Figure 5.4** shows the crystal structure of <sup>13</sup>C[(dcpp)nickelalactone-Al(*t*-Bu)<sub>3</sub>] **V-9**(<sup>13</sup>C). The adduct crystallizes in the space group C2/c. The aluminium is coordinated to the metallalactone through the oxygen of the carbonyl. The geometry around the oxygen atom is slightly bent as evidenced by the C<sub>3</sub>-O<sub>2</sub>-Al<sub>1</sub> angle that measures 150.3(3) °. The Al<sub>1</sub>-O<sub>2</sub> bond is particularly elongated with 1.831(2) Å. In comparison the Al-O bond in Ogoshi's oxanickelacycle-AlMe<sub>2</sub>OTf complex obtained through the oxidative coupling between diphenylacetylene and *tert*-butanal at a PCy<sub>3</sub> substituted nickel center measures 1.799(3) Å. In the opened intermediate [(PCy<sub>3</sub>)<sub>2</sub>Ni(benzaldehyde)-AlMe<sub>2</sub>OTf] adduct, the length of the Al-O bond reaches 1.780(8) Å. [3] Otherwise, the adduct presents structural parameters close to the ones determined for free [(dcpp)nickelalactone] **V-1**. The P<sub>1</sub>-Ni<sub>1</sub>-P<sub>2</sub> bite angles of both complexes (**V-1** and **V-9**) are comparable. Though, the Ni<sub>1</sub>-O<sub>1</sub> and C<sub>3</sub>-O<sub>1</sub> bonds are slightly elongated by 0.06 Å and 0.03 Å respectively. As expected the aluminium derivative withdraws electron density from the nickelalactone and weakens the bonds of the cycle.



**Scheme 5.9:** Ogoshi's oxidative coupling between diphenylacetylene and aldehydes in the presence of Ni(0)/PCy<sub>3</sub> and AlMe<sub>2</sub>OTf. [3]

The reaction in neat Al(*t*Bu)<sub>3</sub> **V-8** (60.8 eq.) at 60 °C does not show any Lewis adduct but a new AB system in <sup>31</sup>P{<sup>1</sup>H} NMR between δ = 20.6 ppm and δ = 21.3 ppm (<sup>2</sup>J<sub>P,P</sub> = 32.78 Hz) attributed to [(dcpp)Ni(2-methylpropene)] **V-10**, as shown in **Figure 5.5**. The NMR yield of the nickel-alkene complex reaches 27 % after 1 d. and 6 h. and increases up to 36 % after 3 d. [(dcpp)Ni(2-methylpropene)] **V-10** has been independently prepared starting from [(dcpp)NiCl<sub>2</sub>] **V-12** via two consecutive transmetallations through *t*BuMgCl **V-13**, as depicted in **Scheme 5.10**. Comparison of the NMR spectra unambiguously confirms the synthesis of the

alkene complex. Hence the *t*Bu group considerably slows down the reaction but it does not prevent β-hydride elimination from the alkyl moiety.



**Scheme 5.10:** a) Reaction between [(dcp)nickelalactone] **V-1** and Al(*t*Bu)<sub>3</sub> **V-8** generating [(dcp)Ni(2-methylpropene)] **V-10**. b) Reaction scheme of the independent synthesis of [(dcp)Ni(2-methylpropene)] **V-10**.

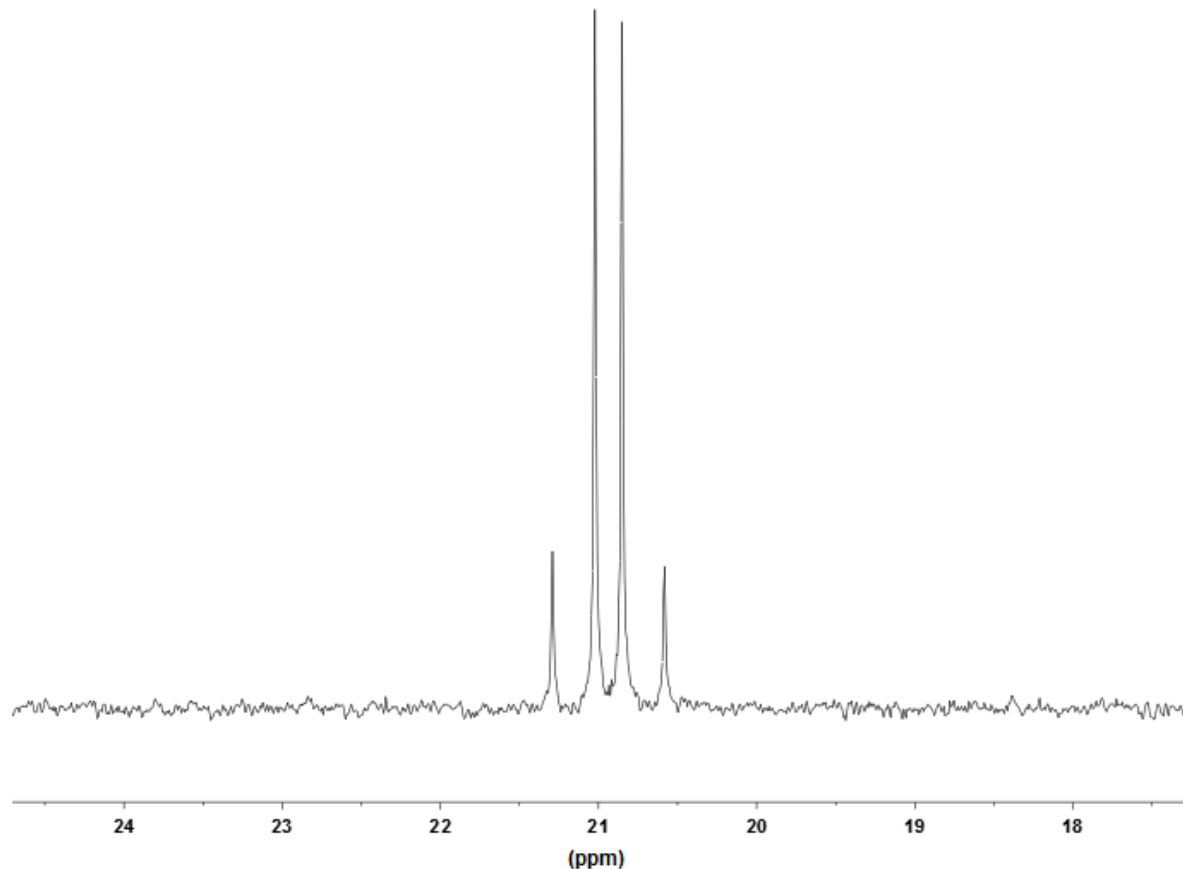
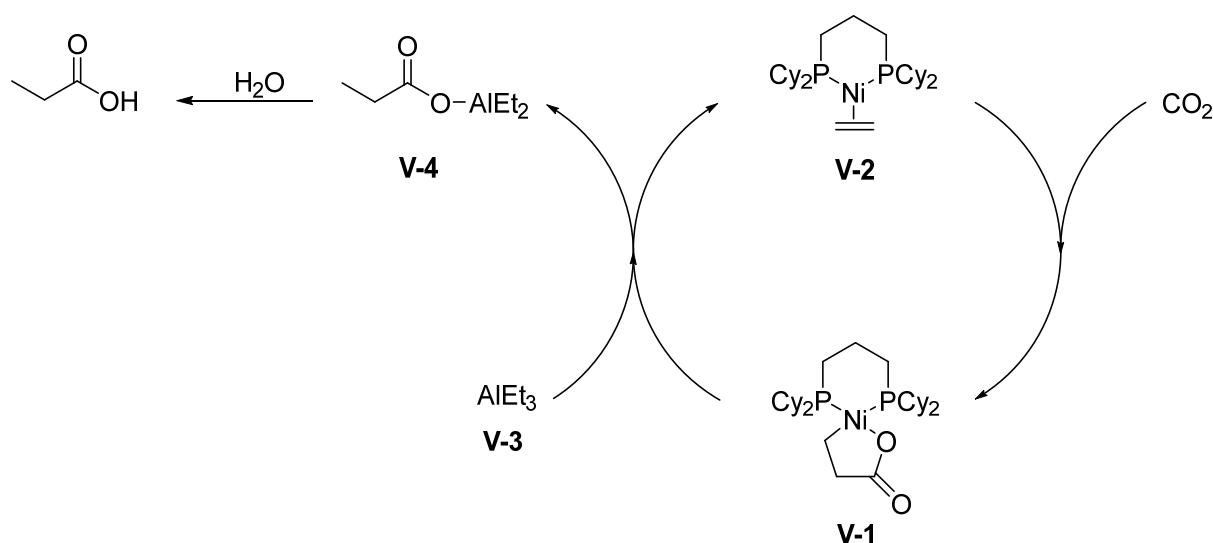


**Figure 5.5:** <sup>31</sup>P{<sup>1</sup>H} NMR spectrum of [(dcp)Ni(2-methylpropene)] **V-10** in THF at RT.

## 5.2 Preliminary catalytic investigations

In light of the stoichiometric investigations presented above, the catalytic production of propanoic acid derivatives from the oxidative coupling between ethylene and CO<sub>2</sub> has been considered. Commercially available AlEt<sub>3</sub> **V-3** has been chosen as transmetallating reagent. **Scheme 5.11** shows the presumed mechanism of this reaction. During the first step [(dcpp)nickelalactone] **V-1** is generated from the oxidative coupling between [(dcpp)Ni(C<sub>2</sub>H<sub>4</sub>)] **V-2** and CO<sub>2</sub>. Afterwards, the reaction between [(dcpp)nickelalactone] **V-1** and AlEt<sub>3</sub> **V-3** releases diethylaluminium propanoate **V-4** and regenerates directly the catalytic intermediate [(dcpp)Ni(C<sub>2</sub>H<sub>4</sub>)] **V-2**, without any need of additional ethylene. THF will be the solvent of choice. Aromatic solvents must be avoided because they promote the direct reaction between AlEt<sub>3</sub> **V-3** and CO<sub>2</sub>. Besides CO<sub>2</sub> has a greater solubility in THF compared to benzene or toluene, which facilitates the formation of [(dcpp)nickelalactone] **V-1**.



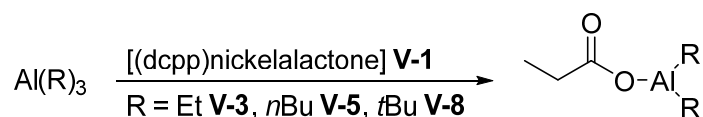
**Scheme 5.11:** Proposed catalytic cycle for the nickel mediated production of propanoic acid from ethylene, CO<sub>2</sub> and AlEt<sub>3</sub> **V-3**.

Unfortunately, a catalytic test under 8 bar of CO<sub>2</sub> with 10 mol% of [(dcpp)nickelalactone] **V-1** did not produce the expected diethylaluminium propanoate **V-4**. Instead, like for pinacolborane, <sup>31</sup>P{<sup>1</sup>H} NMR revealed the formation of [(dcpp)Ni(CO)<sub>2</sub>] **V-14**, which poisons the catalysis.

Until the right conditions are found to shut down the reduction of CO<sub>2</sub> into CO and to preferentially regenerate the metallalactone under mild conditions, the catalytic production of propanoic acid derivatives from ethylene and CO<sub>2</sub> cannot be achieved.

### 5.3 Conclusion and perspectives

This is the first report of the activation of a nickelalactone through an aluminium derivative. The reactions between [(dcpp)nickelalactone] **V-1** and trialkylaluminium derivatives with  $\beta$ -hydrogens (**V-3**, **V-5**, **V-8**) lead to the formation of propanoic acid derivatives.



**Scheme 5.12:** Synthesis of propanoates from [(dcpp)nickelalactone] **V-1** and trialkylaluminium derivatives (**V-3**, **V-5**, **V-8**).

AlR<sub>3</sub> compounds are good transmetallating reagents for the nickelalactone and favor  $\beta$ -hydride elimination over reductive elimination. Unfortunately, the  $\beta$ -hydride elimination on the transferred alkyl group is more favored than the elimination on the propanoate moiety that would generate acrylates. The steric properties of the aluminium derivatives could not be tuned in order to reverse the reactivity. Overall, these results stand in contrast to the reactivity of pinacolborane, which preferentially leads to reductive elimination on the nickel center and generates propanol derivatives after further reductions.

More extensive investigations will be required in order to cleanly switch the reactivity towards the synthesis of acrylates. A first empirical approach would consist in varying not only the steric but also the electronic properties of the trialkylaluminium reagents. Derivatives without accessible  $\beta$ -hydrogens, such as AlMe<sub>3</sub>, Al(neopentyl)<sub>3</sub>, Al(CF<sub>3</sub>)<sub>3</sub> or Al(Ph)<sub>3</sub>, could be tested in this sense. Aluminium halides or mixed aluminium alkyl halides could also come into consideration. The second approach, based on the DFT calculations discussed above, would moreover substitute dcpp for ligands with smaller bite angles and less bulky substituents in order to favor a double coordination of the trialkylaluminium derivative, which induces the lactone ring opening and its subsequent reactivity.

## 5.4 Experimental part

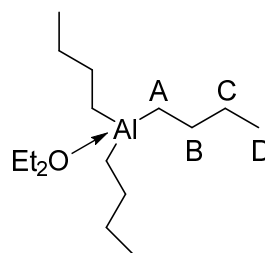
### 5.4.1 General Remarks

All reactions were carried out under an atmosphere of dry argon using standard Schlenk techniques or in a nitrogen-filled MBraun LabStar glovebox. THF and toluene were taken from an MBraun SPS-800 solvent purification system, freeze-pump-thaw degassed and stored over 4 Å molecular sieves. [d<sub>8</sub>]-THF and C<sub>6</sub>D<sub>6</sub> were degassed and stored over 4 Å molecular sieves.

[(tmeda)nickelalactone]<sup>[4]</sup> was synthesized according to a published procedure. All the other chemicals were purchased in reagent grade purity from Acros, Cytech and Sigma-Aldrich and were used without further purification. CO<sub>2</sub> was purchased from Air Liquide.

### 5.4.2 Synthesis of trialkylaluminium derivatives

#### 5.4.2.1 Synthesis of Al(*n*Bu)<sub>3</sub>.Et<sub>2</sub>O V-5

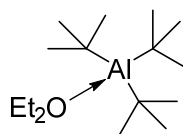


AlCl<sub>3</sub> (1.333 mg, 1.00×10<sup>-2</sup> mol, 1 eq.) is solubilized in 25 mL of Et<sub>2</sub>O and *n*BuMgCl (*C* = 2.0 mol.L<sup>-1</sup> in Et<sub>2</sub>O, *V* = 15.0 mL, 3.00×10<sup>-2</sup> mol, 3 eq.) is slowly added at -78 °C. The solution is stirred for 1 h. at -78 °C and allowed to come back to RT over 3 h. MgCl<sub>2</sub> precipitates out of the solution. The volatiles are removed under vacuum and the salts are washed two times with pentane to extract the product. If the collected solution is not clear at this point, additional filtration is necessary. The volatiles are then removed under reduced pressure and Al(*n*Bu)<sub>3</sub>.Et<sub>2</sub>O V-5 is gathered as a colorless liquid in 82 % yield (2.245 g).

<sup>1</sup>H NMR (300 MHz, C<sub>6</sub>D<sub>6</sub>): δ 0.19 (t, <sup>3</sup>*J*<sub>H,H</sub> = 7.2 Hz, 6H, CH<sub>2</sub> A), 0.68 (t, <sup>3</sup>*J*<sub>H,H</sub> = 7.2 Hz, 6H, CH<sub>3</sub> (Et<sub>2</sub>O)), 1.12 (t, <sup>3</sup>*J*<sub>H,H</sub> = 7.2 Hz, 9H, CH<sub>3</sub> D), 1.65 (m, 12H, CH<sub>2</sub> B + C), 3.30 (q, <sup>3</sup>*J*<sub>H,H</sub> = 7.2 Hz, 4H, CH<sub>2</sub> (Et<sub>2</sub>O)) ppm.

<sup>13</sup>C NMR (75 MHz, C<sub>6</sub>D<sub>6</sub>): δ 10.0 (CH<sub>2</sub> A), 13.1 (CH<sub>3</sub> (Et<sub>2</sub>O)), 14.11 (CH<sub>3</sub> D), 29.0 (CH<sub>2</sub> B or C), 29.5 (CH<sub>2</sub> B or C), 65.9 (CH<sub>2</sub> (Et<sub>2</sub>O)) ppm.

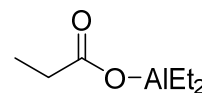


5.4.2.2 Synthesis of Al(*t*Bu)<sub>3</sub>.Et<sub>2</sub>O **V-8** <sup>[5]</sup>

AlCl<sub>3</sub> (1.333 mg, 1.00×10<sup>-2</sup> mol, 1 eq.) is solubilized in 25 mL of Et<sub>2</sub>O and *t*BuMgCl (*C* = 2.0 mol.L<sup>-1</sup> in Et<sub>2</sub>O, *V* = 15.0 mL, 3.00×10<sup>-2</sup> mol, 3 eq.) is slowly added at -78 °C. The solution is stirred for 1 h. at -78 °C and allowed to come back to RT over 2 h. 30 min. MgCl<sub>2</sub> precipitates out of the solution. The volatiles are removed under vacuum and the salts are washed two times with pentane to extract the product. If the collected solution is not clear at this point, additional filtration is necessary. The volatiles are then removed under reduced pressure and Al(*t*Bu)<sub>3</sub>.Et<sub>2</sub>O **V-8** is gathered as a colorless oily liquid in 80 % yield (2.168 g).

<sup>1</sup>H NMR (300 MHz, C<sub>6</sub>D<sub>6</sub>): δ 1.20 (s, 27H, C(CH<sub>3</sub>)<sub>3</sub>), 0.62 (t, <sup>3</sup>*J*<sub>H,H</sub> = 7.2 Hz, 6H, CH<sub>3</sub>(Et<sub>2</sub>O)), 3.47 (q, <sup>3</sup>*J*<sub>H,H</sub> = 7.2 Hz, 4H, CH<sub>2</sub>(Et<sub>2</sub>O)) ppm.

<sup>13</sup>C NMR (75 MHz, C<sub>6</sub>D<sub>6</sub>): δ 15.6 (CH<sub>3</sub>(Et<sub>2</sub>O)), 32.9 (C(CH<sub>3</sub>)<sub>3</sub>), 65.9 (CH<sub>2</sub>(Et<sub>2</sub>O)), 74.1 (C(CH<sub>3</sub>)<sub>3</sub>) ppm.

5.4.3 Synthesis of diethylaluminium propanoate **V-4** <sup>[1, 2]</sup>

AlEt<sub>3</sub> **V-3** 25 wt% in toluene (21.3 μl, 3.97×10<sup>-5</sup> mol, 1 eq.) is dissolved in 0,6 ml of C<sub>6</sub>D<sub>6</sub> in a J. Young tube. The tube is freeze-pump-thaw degassed and 1 bar of CO<sub>2</sub> is applied to it for 5 min at RT. The tube is then heated for 1 h. at 50 °C, the solution remains colorless.

<sup>1</sup>H NMR (300 MHz, C<sub>6</sub>D<sub>6</sub>): δ 0.27 (q, <sup>3</sup>*J*<sub>H,H</sub> = 8.1 Hz, 4H, CH<sub>2</sub> ethyl), 0.71 (t, <sup>3</sup>*J*<sub>H,H</sub> = 7.5 Hz, 3H, CH<sub>3</sub>), 1.33 (t, <sup>3</sup>*J*<sub>H,H</sub> = 8.1 Hz, 6H, CH<sub>3</sub> ethyl), 1.91 (q, <sup>3</sup>*J*<sub>H,H</sub> = 7.5 Hz, 2H, CH<sub>2</sub>) ppm.

<sup>13</sup>C NMR (75 MHz, C<sub>6</sub>D<sub>6</sub>): δ -1.0 (CH<sub>2</sub> ethyl), 9.0 (CH<sub>3</sub>), 9.1 (CH<sub>3</sub> ethyl), 30.5 (CH<sub>2</sub>), 184.4 (C=O) ppm.

<sup>1</sup>H NMR (300 MHz, [d<sub>8</sub>]-THF): δ -0.16 (q, <sup>3</sup>*J*<sub>H,H</sub> = 8.1 Hz, 4H, CH<sub>2</sub> ethyl), 0.96 (t, <sup>3</sup>*J*<sub>H,H</sub> = 8.1 Hz, 6H, CH<sub>3</sub> ethyl), 1.14 (t, <sup>3</sup>*J*<sub>H,H</sub> = 7.5 Hz, 3H, CH<sub>3</sub>), 2.55 (q, <sup>3</sup>*J*<sub>H,H</sub> = 7.5 Hz, 2H, CH<sub>2</sub>) ppm.

<sup>13</sup>C NMR (75 MHz, [d<sub>8</sub>]-THF): δ -0.9 (CH<sub>2</sub> ethyl), 8.7 (CH<sub>3</sub>), 8.8 (CH<sub>3</sub> ethyl), 30.0 (CH<sub>2</sub>), 184.8 (C=O) ppm.

## 5.4.4 Blank tests

### 5.4.4.1 Reacting AlEt<sub>3</sub> V-3 with CO<sub>2</sub> in [d<sub>8</sub>]-THF

AlEt<sub>3</sub> V-3 25 wt% in toluene (21.3 μl, 3.97×10<sup>-5</sup> mol, 1 eq.) is dissolved in 0.6 ml of [d<sub>8</sub>]-THF in a J. Young tube. The tube is freeze-pump-thaw degassed and 1 bar of CO<sub>2</sub> is applied to it for 2 min. at RT. After 1 d. at RT no reaction is observed and the solution remains colorless. The Young tube is re-degassed and 6 bar of CO<sub>2</sub> are applied to it for 2 min. After 1 d. at RT no reaction is observed as well as after 1 d. at 60 °C.

### 5.4.4.2 Reacting AlEt<sub>3</sub> V-3 with [(dcp)Ni(C<sub>2</sub>H<sub>4</sub>)] V-2 in [d<sub>8</sub>]-THF

[(dcp)Ni(C<sub>2</sub>H<sub>4</sub>)] V-2 (15.0 mg, 2.87×10<sup>-5</sup> mol, 1 eq.) is suspended in 0.6 ml of [d<sub>8</sub>]-THF in a J. Young tube and AlEt<sub>3</sub> V-3 25 wt% in toluene (23.2 μl, 4.30×10<sup>-5</sup> mol, 1.5 eq.) is added. After 1 d. at RT or 1 d. at 60 °C, besides the almost insoluble [(dcp)Ni(C<sub>2</sub>H<sub>4</sub>)] V-2, traces of another compound are detected by <sup>31</sup>P{<sup>1</sup>H}-NMR spectroscopy at δ = 63.3 ppm. <sup>1</sup>H-NMR just shows AlEt<sub>3</sub> V-3.

## 5.4.4 Stoichiometric Reactions

### 5.4.4.1 Reacting [(dcp)nickelalactone] V-1 with AlEt<sub>3</sub> V-3 in [d<sub>8</sub>]-THF

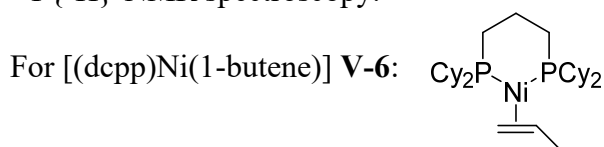
[(dcp)nickelalactone] V-1 (15.0 mg, 2.64×10<sup>-5</sup> mol, 1 eq.) is dissolved in 0,6 mL of [d<sub>8</sub>]-THF in a J. Young tube and reacted with AlEt<sub>3</sub> V-3 25 wt% in toluene (21.3 μL, 3.97×10<sup>-5</sup> mol, 1.5 eq.). After 1 d. at RT, formation of diethylaluminium propanoate CH<sub>3</sub>CH<sub>2</sub>C(O)OAlEt<sub>2</sub> V-4 and 6 % of [(dcp)Ni(C<sub>2</sub>H<sub>4</sub>)] V-2 is observed respectively through <sup>1</sup>H- and <sup>31</sup>P{<sup>1</sup>H}-NMR spectroscopy.

### 5.4.4.2 Reacting <sup>13</sup>C[(dcp)nickelalactone] V-1(<sup>13</sup>C) in neat AlEt<sub>3</sub> V-3

<sup>13</sup>C[(dcp)nickelalactone] V-1(<sup>13</sup>C) (15.0 mg, 2.63×10<sup>-5</sup> mol, 1 eq.) is reacted with 0.8 mL of AlEt<sub>3</sub> V-3 (25 wt% in toluene, 56.5 eq.) in a J. Young tube. After 30 min. at RT, full conversion exclusively to diethylaluminium propanoate CH<sub>3</sub>CH<sub>2</sub>C(O)OAlEt<sub>2</sub> V-4 and [(dcp)Ni(C<sub>2</sub>H<sub>4</sub>)] V-2 is observed respectively through <sup>1</sup>H- and <sup>31</sup>P{<sup>1</sup>H}-NMR spectroscopy.

#### 5.4.4.3 Reacting <sup>13</sup>C[(dcpp)nickelalactone] **V-1**(<sup>13</sup>C) with Al(*n*Bu)<sub>3</sub>.Et<sub>2</sub>O **V-5** in [d<sub>8</sub>]-THF

<sup>13</sup>C[(dcpp)nickelalactone] **V-1** (15.0 mg, 2.63×10<sup>-5</sup> mol, 1 eq.) is reacted with Al(*n*Bu)<sub>3</sub> **V-5** (139.3 mg, 5.11×10<sup>-4</sup> mol, 19 eq.) in a J. Young tube. 0.25 mL of [d<sub>8</sub>]-THF are added to have enough solvent in the NMR tube. Full conversion of <sup>13</sup>C[(dcpp)nickelalactone] **V-1**(<sup>13</sup>C) is achieved after 1 d. at 60 °C. Di(*n*-butyl)aluminium propanoate CH<sub>3</sub>CH<sub>2</sub>C(O)OAl(*n*Bu)<sub>2</sub> **V-7** and [(dcpp)Ni(1-butene)] **V-6** are the main products observed respectively through <sup>1</sup>H- and <sup>31</sup>P{<sup>1</sup>H}-NMR spectroscopy.



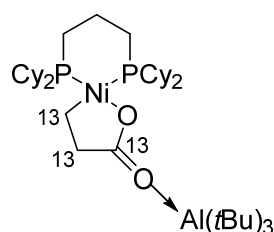
<sup>31</sup>P{<sup>1</sup>H} NMR (121 MHz, [d<sub>8</sub>]-THF): δ 22.7 - 23.6 (AB system, <sup>2</sup>J<sub>P,P</sub> = 31.0 Hz, 2P) ppm.

Crystals for X-ray diffraction analysis had been previously grown from the reaction between [(dcpp)NiCl<sub>2</sub>] **V-11** and 10 eq. of PhZnCl in the presence of butyl bromide in THF at RT.

#### 5.4.4.4 Reacting <sup>13</sup>C[(dcpp)nickelalactone] **V-1**(<sup>13</sup>C) with Al(*t*Bu)<sub>3</sub>.Et<sub>2</sub>O **V-8** in [d<sub>8</sub>]-THF

<sup>13</sup>C[(dcpp)nickelalactone] **V-1**(<sup>13</sup>C) (15.0 mg, 2.64×10<sup>-5</sup> mol, 1 eq.) is dissolved in 0.8 mL of [d<sub>8</sub>]-THF in a J. Young tube and reacted with Al(*t*Bu)<sub>3</sub> **V-8** (C = 2.0 mol.L<sup>-1</sup> in THF, 66.1 μL, 1.32×10<sup>-4</sup> mol, 5 eq.) at 60 °C. After 8 h. <sup>31</sup>P{<sup>1</sup>H} NMR shows the formation of the <sup>13</sup>C[(dcpp)nickelalactone-Al(*t*Bu)<sub>3</sub>] adduct **V-9**(<sup>13</sup>C) in 28 % yield. Longer reaction times do not increase the yield significantly (29 % after 23 h.).

For <sup>13</sup>C[(dcpp)nickelalactone-Al(*t*Bu)<sub>3</sub>] **V-9**(<sup>13</sup>C):

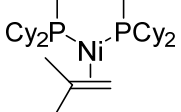


<sup>31</sup>P{<sup>1</sup>H} NMR (121 MHz, [d<sub>8</sub>]-THF): δ 12.9 - 13.6 (m, 1P), 35.06 - 35.50 (m, 1P) ppm.

#### 5.4.4.5 Reacting [(dcpp)nickelalactone] **V-1** in neat Al(*t*Bu)<sub>3</sub>.Et<sub>2</sub>O **V-8**

[(dcpp)nickelalactone] **V-1** (15.0 mg,  $2.64 \times 10^{-5}$  mol, 1 eq.) is reacted with Al(*t*Bu)<sub>3</sub> **V-8** ( $C = 2.0 \text{ mol.L}^{-1}$  in THF, 0.8 mL, 60.8 eq.) in a J. Young tube. After 1 d. at 60 °C, 27 % of [(dcpp)Ni(2-methylpropene)] **V-10** are detected by <sup>31</sup>P{<sup>1</sup>H} NMR. The yield increases to 36 % after 3 d. at 60 °C.

For [(dcpp)Ni(2-methylpropene)] **V-10**:



<sup>31</sup>P{<sup>1</sup>H} NMR (121 MHz, [d<sub>8</sub>]-THF): δ 20.6 - 21.3 (AB system, <sup>2</sup>J<sub>P,P</sub> = 32.8 Hz, 2P) ppm.

## 5.5 References

- [1] W. K. Johnson, J. C. Wygant, 3,057,900, Oct. 09, 1962.
- [2] J. Weidlein, *J. Organomet. Chem.*, **1969**, *16*, P33 - P35.
- [3] M. Ohashi, H. Saijo, T. Arai, S. Ogoshi, *Organomet.*, **2010**, *29*, 6534 - 6540.
- [4] R. Fischer, B. Nestler, H. Schütz, *Z. Anorg. All. Chem.*, **1989**, *577*, 111 - 114.
- [5] H. Lehmkuhl, *Angew. Chem.*, **1964**, *76*, 817.

Activation of CO<sub>2</sub> with chelating bis-carbene  
nickel complexes



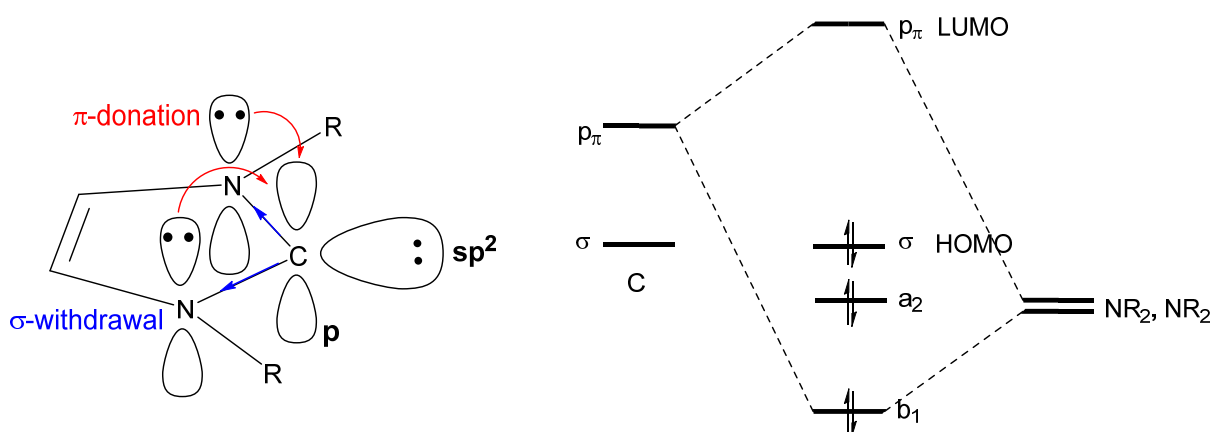
## 6 Synthesis and reactivity of (bis-NHC)nickel complexes

### 6.1 State of the art

#### 6.1.1 *N*-heterocyclic carbenes

The isolation of the first crystalline *N*-heterocyclic carbene (NHC) by Arduengo in 1991 <sup>[1]</sup> opened this research field. Since then, a large variety of NHC compounds has been developed and their application are ever growing.

A classic free NHC consist in an imidazole moiety, in which the central carbon atom bears a lone pair and an empty orbital. NHCs have a singlet ground state. The HOMO is an  $sp^2$  hybridized lone pair in the plane of the heterocycle whereas the LUMO is an unoccupied out of plane p-orbital. The two electronegative nitrogen atoms on both sides of the carbene center stabilize the molecule electronically in creating a push-pull environment. The nitrogen atoms give electron density from their lone pair into the empty p-orbital, while they inductively withdraw electron density from the filled  $sp^2$  hybridized orbital, as depicted in **Scheme 6.1**. The cyclic structure of a NHC further enforces a bent geometry which favors the singlet ground state. Bulky substituents can be attached to the nitrogen atoms to kinetically stabilize the free carbene and especially avoid dimerization reactions generating olefins. <sup>[2, 3, 4]</sup>



**Scheme 6.1:** Structure of a NHC and orbital interactions.

Molecular orbital diagram of a NHC.



NHCs are nucleophiles, which have been commonly employed as ligands for transition metal complexes. They are stronger two electron  $\sigma$ -donors than tertiary phosphines and weak  $\pi$ -donors and -acceptors. As a consequence, the metal-ligand bonds are particularly stable. Therefore, NHC-metal complexes usually have a good thermal stability, are often resistant to oxidation and do not tend to ligand dissociation.<sup>[5]</sup> Furthermore, they are highly active in numerous homogeneous catalytic reactions.<sup>[2, 5, 6, 7]</sup> Grubbs' second generation ruthenium catalysts for olefin metathesis are probably the most famous NHC-based complexes.<sup>[8]</sup> C-C and C-heteroatoms cross-coupling reactions have also been widely promoted by palladium-NHC complexes designed by Herrmann,<sup>[9, 10, 11]</sup> Nolan<sup>[12, 13]</sup> and Organ<sup>[14]</sup> among others. In addition, very efficient hydrosilylations as well as hydrogenation reactions catalyzed by NHC complexes have been reported.<sup>[6, 7]</sup>

### 6.1.2 Chelating (bis-NHC)nickel complexes

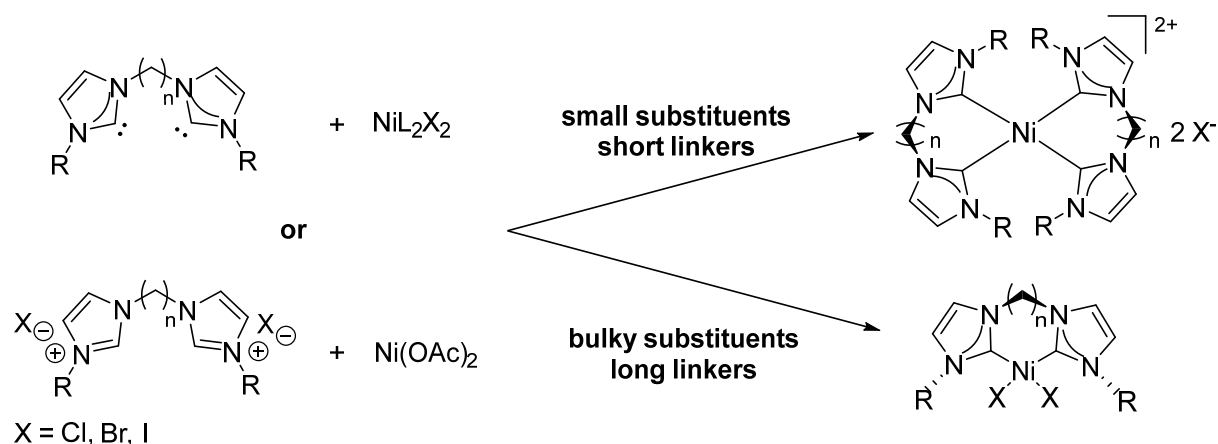
Chelating bis-phosphine ligands are commonly used for efficient homogeneous catalysis. It is therefore of interest to investigate the reactivity of stronger  $\sigma$  donating analogous chelating bis-NHC ligands. Chelating bis-NHC ligands are composed of two carbene moieties linked together through a spacer. The chemistry of their corresponding complexes has been far less explored. In particular, (bis-NHC) nickel complexes are still relatively rare.

#### 6.1.2.1 Chelating [(bis-NHC)nickel(II)] complexes

The investigations on (bis-NHC) nickel complexes started with the ambition of synthesizing analogues of cis chelated [(bis-NHC)Pd(II)dihalides]. The reactions between bis-imidazolium salts or free carbenes and appropriate nickel precursors led surprisingly to two different types of (bis-NHC)Ni(II) complexes. The length of the bridge and the size of the substituents on the nitrogen atoms had a great influence on the outcome of the reaction, as shown in **Scheme 6.2**.<sup>[15]</sup>

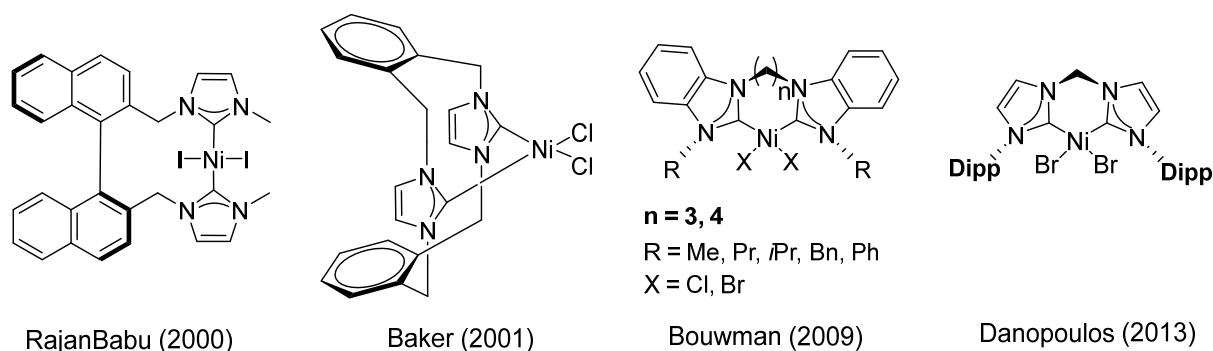
When small spacers or small substituents were used, cationic [(bis-NHC)<sub>2</sub>Ni]<sup>2+</sup> 2[X]<sup>-</sup> (X = halide) complexes were obtained. Hermann and Green independently described the first synthesis of these homoleptic complexes bearing two chelating bis-NHC ligands in 1999.<sup>[16, 17]</sup> They favored methyl linkers and alkyl groups such as methyl, isopropyl, cyclohexyl or *tert*-butyl moieties. Later, Huynh<sup>[15]</sup> and Foley<sup>[18]</sup> respectively reported related benzimidazole

derived and *N*-benzyl substituted cationic complexes, which successfully catalyzed either Kumada or Heck and Suzuki-Miyaura cross-coupling reactions.



**Scheme 6.2:** Synthesis of [(bis-NHC)Ni(II)] complexes. The outcome of the reaction is controlled by the size of the R substituents and the length of the spacer.

On the other hand, long spacers or bulky substituents preferentially gave the expected neutral [(bis-NHC)NiX<sub>2</sub>] complexes. The first example was provided by RajanBabu in 2000 who used the chiral binaphthyl backbone as a linker between both NHC units. The large size of the chelate ring enforced an unusual *trans* coordination on the nickel center.<sup>[19]</sup> Subsequently in 2001 Baker reported an *ortho*-cyclophane linked [(bis-NHC)NiCl<sub>2</sub>] complex with *cis* geometry.<sup>[20]</sup> Interestingly, by using longer classic spacers, as propyl or butyl bridges, Bouwman<sup>[21, 22]</sup> and Huynh<sup>[15]</sup> also managed to access *cis* chelated [(bis-NHC)NiX<sub>2</sub>] (X = Cl, Br) complexes, which turned out to catalyze Kumada cross-couplings as well as the vinyl polymerization of norbornene. Switching the *N*-substituent from small alkyl groups to bulkier Dipp moieties, as shown by Danopoulos, also led preferentially to neutral *cis* chelated bis-NHC dihalide nickel(II) complexes.<sup>[23]</sup> **Scheme 6.3** presents some of the aforementioned [(bis-NHC)NiX<sub>2</sub>] complexes.

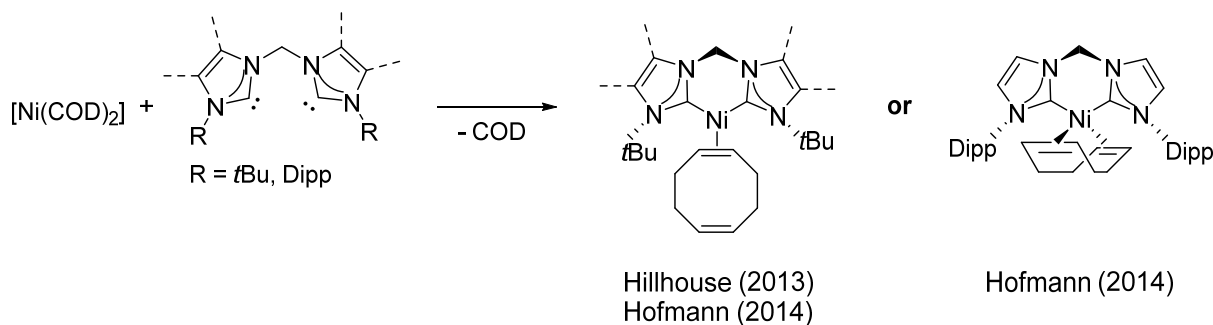


**Scheme 6.3:** Examples of [(bis-NHC)NiX<sub>2</sub>] complexes.

Besides, these two families of nickel(II) complexes, there are scarce examples of other [(bis-NHC)Ni(II)] compounds. Green described the synthesis of an ethyl bridged [(bis-NHC)nickel(II)-dimethyl] complex. The ligand substitution between [Ni(bipy)Me<sub>2</sub>] and the free carbene gave the targeted compound in 73 % yield. [24] In addition, Cao and Shi reported [(LDipp)Ni(carbonate)] complexes with varying linkers, which were active in the Kumada cross-coupling reaction. [25]

### 6.1.2.2 Chelating [(bis-NHC)Ni(0)] complexes

More recently, chelating [(bis-NHC)Ni(0)]-complexes have been reported. They were first obtained through ligand substitution reactions between [Ni(COD)<sub>2</sub>] and free bis-carbenes. During his investigations on bent nickel(imido) complexes in 2013, Hillhouse isolated the square planar [3,3'-methylenebis(1-*tert*-butyl-4,5-dimethylimidazoliylidene)Ni(η<sup>2</sup>-COD)] complex in excellent yield. [26] Afterwards Hofmann managed to obtain analogous [(*Li*tBu)Ni(COD)] and [(LDipp)Ni(COD)] complexes although in moderate yields. [27]



**Scheme 6.4:** Synthesis of [(bis-NHC)Ni(COD)] complexes through ligand substitution from [Ni(COD)<sub>2</sub>].

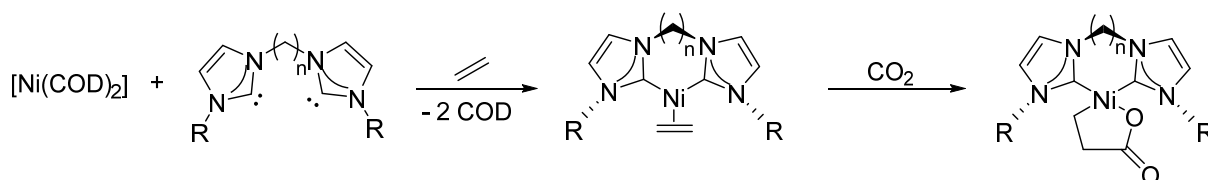
We can note that the reduction of [(bis-NHC)Ni(II)] complexes with two equivalents of reducing agents such as  $\text{KC}_8$  or  $\text{K}(\text{BEt}_3\text{H})$  also generates Ni(0) carbene complexes. Kubiak synthesized in 2014 the first Ni(0) tetracarbene from  $[(\text{bis-NHC})_2\text{Ni}]^{2+} 2[\text{Br}]^-$  by using this procedure.<sup>[28]</sup> Subsequently, Driess managed to isolate mixed chelating [silylene-carbeneNi(0)] complexes.<sup>[29]</sup>

### 6.1.3 Research objectives

This literature survey shows that it is still difficult to control the synthesis of desired [(bis-NHC)Ni(0)]-fragments and to a lesser extend of [(bis-NHC)Ni(II)] complexes. As a result, the oxidative coupling between ethylene and  $\text{CO}_2$  has never been investigated for chelating bis-carbene transition metal complexes. This reaction requires the synthesis of to date unknown [(bis-NHC)Ni(alkenes)] or [bis-NHC)Ni(alkynes)] and [(bis-NHC)nickelalactones].

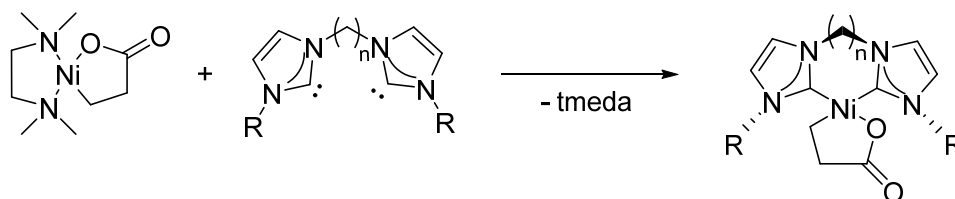
Taking into account the knowledge about bis-NHC nickel complexes, two strategies were developed to get access to targeted [(bis-NHC)nickelalactones]. These were also strongly inspired by the related diamine and bis-phosphine chemistry presented in **Chapter 3, 4 and 5**, which is well understood and has already been more extensively studied.

The first approach consists in oxidatively coupling unsaturated chelating [(bis-NHC)Ni(0)] complexes with  $\text{CO}_2$  to afford chelating [(bis-NHC)nickelalactones]. The synthesis of (bis-NHC)nickel dihalide complexes with small spacers is still out of reach (**6.1.2.1**). Therefore [(bis-NHC)Ni(alkenes)] will be preferentially generated directly from Ni(0) precursors rather than from two electron reduction of nickel(II) complexes. Following Hillhouse's<sup>[26]</sup> and Hofmann's<sup>[27]</sup> procedures, unsaturated [(bis-NHC)Ni]-complexes can be obtained starting from  $[\text{Ni}(\text{COD})_2]$  **VI-8** through a double ligand substitution. The first COD moiety will be displaced by the free carbene and the second one by the chosen alkenes or alkynes. In a second step, the unsaturated Ni(0) complexes can be reacted under a  $\text{CO}_2$  atmosphere to finally produce the chelating [(bis-NHC)nickelalactones].



**Scheme 6.5:** Synthesis of [(bis-NHC)nickelalactones] through oxidative coupling with ethylene and  $\text{CO}_2$ .

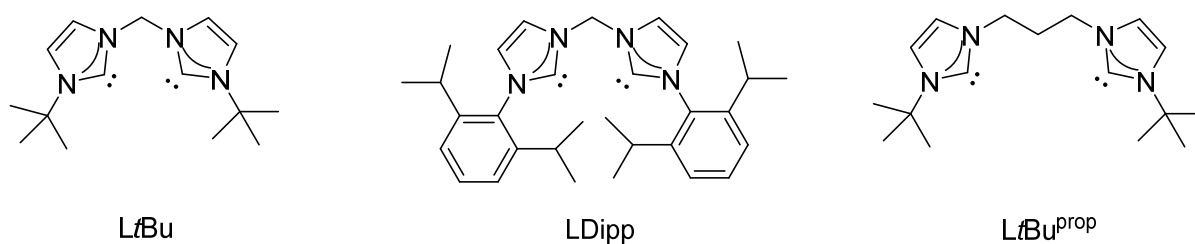
The second more straightforward approach uses preformed [(tmeda)nickelalactone] **VI-17** and relies on the ligand substitution of the diamine by stronger coordinating bis-NHCs, as depicted in **Scheme 6.6**. A study released by Walther in 2006 showed that a pyridine ligand of [(dipyridine)nickelalactone] could be easily displaced by a NHC to give the corresponding [(pyridine)(NHC)nickelalactone]. However, these complexes dimerize easily in DMF upon loss of the labile pyridine ligand.<sup>[30]</sup> Nevertheless, this result seemed encouraging enough to extend this methodology to chelating bis-carbenes.



**Scheme 6.6:** Synthesis of [(bis-NHC)nickelalactones] through ligand substitution.

## 6.2 Synthesis of [(bis-NHC)Ni(alkene)] and [(bis-NHC)Ni(alkyne)] complexes

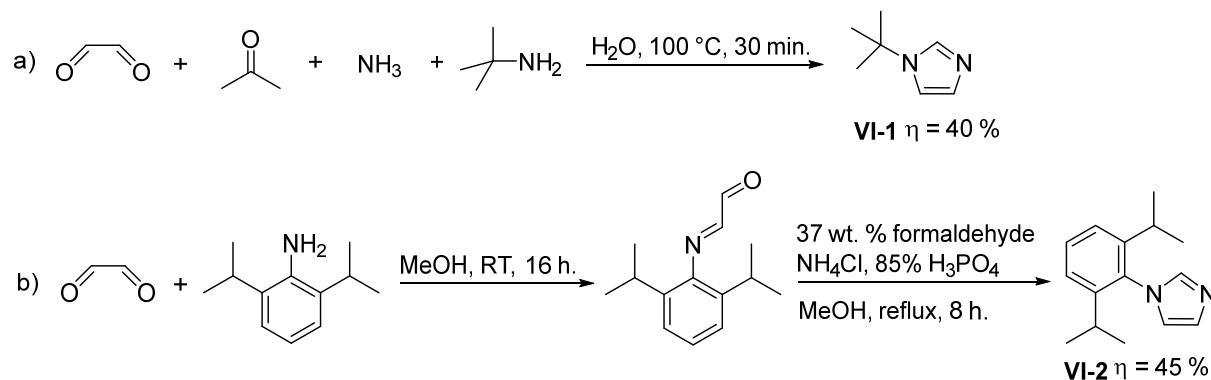
According to the first strategy presented in **6.1.3**, the starting point of this research project was the synthesis of new unsaturated chelating [(bis-NHC)Ni]-complexes. For this study 1,1'-di-*tert*-butyl-3,3'-methylenedimidazoline-2,2'-diylidene (**LtBu**), 1,1'-di-(2,6-diisopropylphenyl) butyl-3,3'-methylenedimidazoline-2,2'-diylidene (**LDipp**) and 1,1'-di-*tert*-butyl-3,3'-propylenedimidazoline-2,2'-diylidene (**LtBu**)<sup>prop</sup> were chosen as ligands.



**Scheme 6.7:** Ligands selected for the following investigations.

## 6.2.1 Synthesis of bis-NHC precursors

Prior to the coordination chemistry, substituted imidazoles and their corresponding imidazolium salts were generated. *N*-*tert*-butylimidazole **VI-1**<sup>[31]</sup> and *N*-(2,6-diisopropylphenyl)imidazole **VI-2**<sup>[32]</sup> were synthesized according to published procedures. Glyoxal, formaldehyde, ammonia and primary amines are reacted in polar solvents to afford the substituted imidazoles **VI-1** and **VI-2**. **Scheme 6.8** presents the reaction conditions.



**Scheme 6.8:** a) Streubel's procedure for the synthesis of *N*-*tert*-butylimidazole **VI-1**.<sup>[31]</sup> b) Zhang's procedure for the synthesis of *N*-(2,6-diisopropylphenyl)imidazole **VI-2**.<sup>[32]</sup>

Afterwards, the bis-imidazolium salts *LtBu*H<sub>2</sub>Br<sub>2</sub> **VI-5**, *LDipp*H<sub>2</sub>Br<sub>2</sub> **VI-6** and *LtBu*<sup>(prop)</sup>H<sub>2</sub>Br<sub>2</sub> **VI-7** were synthesized through S<sub>N</sub>2 reactions performed under pressure between the imidazoles and either dibromomethane **VI-3** or dibromopropane **VI-4**.<sup>[33]</sup> **Table 6.1** gives the optimized conditions for each carbene precursor.



The procedure reported by Hofmann *et al.* [27] for the [(*Lt*Bu)Ni(COD)] and [(LDipp)Ni(COD)] complexes was used as a guideline for the development of the new ethylene complexes. However, their synthesis' require a long and complicated work-up involving water and provide the products in low to moderate yields (34 % and 50% respectively). Indeed, the limited solubility of the nickel alkene complexes in common organic solvents renders the salts' separation difficult at the end of the reaction. Therefore, it proved to be essential to carry out the deprotonation in Et<sub>2</sub>O to precipitate and to remove KBr before adding the nickel precursor. In this way, the products' purification is restricted to the removal of the volatiles under vacuum and the extraction of free COD with pentane without important losses.

[(*Lt*Bu)Ni(C<sub>2</sub>H<sub>4</sub>)] **VI-9** is isolated as a brown product in 75 % yield. The ethylenic protons are strongly shifted upfield in <sup>1</sup>H NMR, resonating as an AA'XX' system between  $\delta = 0.99$  ppm and  $\delta = 1.18$  ppm. The methylene protons are diastereotopic, probably due to conformational rigidity, and give rise to two doublets. The ethylenic carbons appear at  $\delta = 27.7$  ppm in <sup>13</sup>C NMR, which rather corresponds to the chemical shift of an alkane. The carbenic center is located downfield at  $\delta = 203.7$  ppm as expected. Single crystals for X-ray diffraction analysis were grown from a THF solution at -25 °C. The solid state structure has a distorted square planar geometry with a bite angle of 91.45(14) °. The six-membered chelate ring adopts a boat shape conformation. The distance between the ethylenic C<sub>1</sub> and C<sub>2</sub> carbons of 1.419(5) Å lies between a single and a double C-C bond. This evidences a very strong  $\pi$ -back donation from the nickel center to the coordinated olefin in this complex.

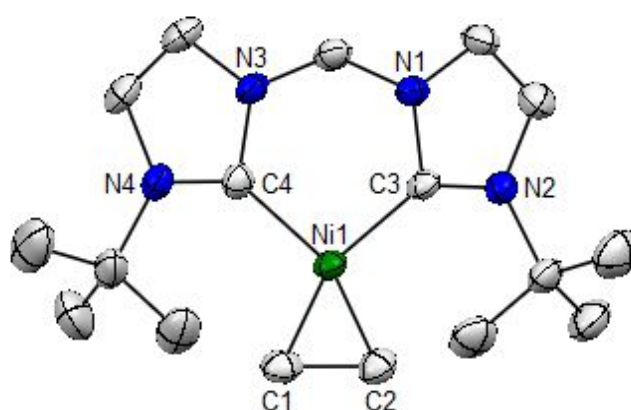


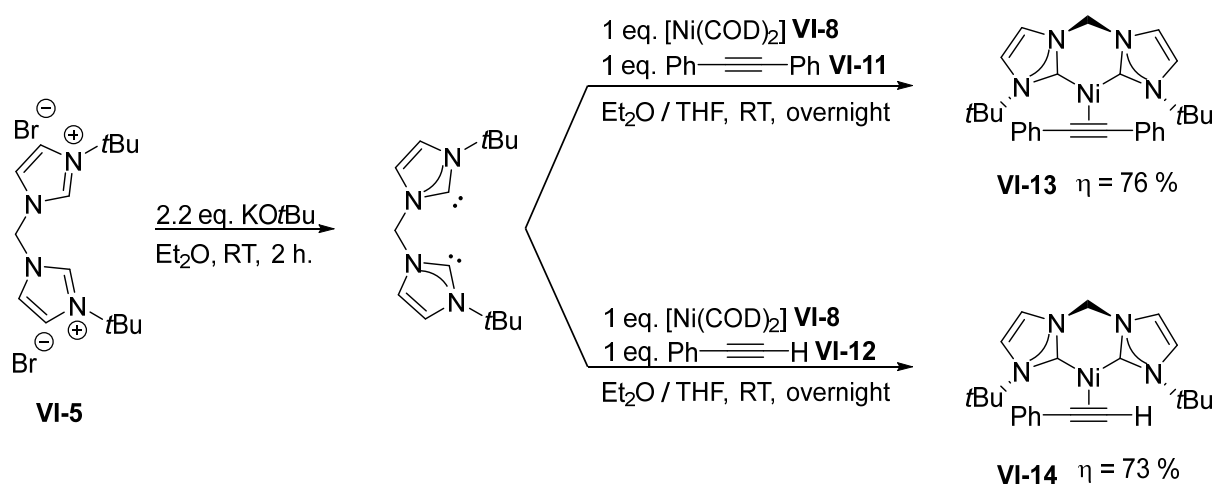
**Figure 6.1:** Molecular structure of [(*Lt*Bu)Ni(C<sub>2</sub>H<sub>4</sub>)] **VI-9** determined by single crystal X-ray diffraction. Hydrogen atoms are omitted for clarity. Selected bond lengths [Å] and angles [°]: Ni<sub>1</sub>-C<sub>1</sub> 1.953(4), Ni<sub>1</sub>-C<sub>2</sub> 1.947(3), Ni<sub>1</sub>-C<sub>3</sub> 1.923(3), Ni<sub>1</sub>-C<sub>4</sub> 1.903(3), C<sub>1</sub>-C<sub>2</sub> 1.419(5), C<sub>1</sub>-Ni<sub>1</sub>-C<sub>2</sub> 42.66(15), C<sub>3</sub>-Ni<sub>1</sub>-C<sub>4</sub> 91.45(14).



By switching the substituents on the nitrogen atoms to the bulkier Dipp units, [(LDipp)Ni(C<sub>2</sub>H<sub>4</sub>)] **VI-10** could be obtained as a red powder in 71 % yield. The <sup>1</sup>H and <sup>13</sup>C NMR chemical shifts of the ethylene moiety are here again extremely shifted upfield. The olefinic protons resonate at  $\delta = 0.14$  ppm as a singlet and the corresponding carbons at  $\delta = 25.2$  ppm. In this complex both methylene protons are also equivalent owing to fast geometry fluctuations in solution. The quaternary carbene atoms appear at  $\delta = 200.1$  ppm.

### 6.2.3 Synthesis of [(bis-NHC)Ni(alkyne)] complexes

The methodology has also been extended to alkyne complexes. In this way symmetric [(*Li*tBu)Ni(diphenylacetylene)] **VI-13** and asymmetric [(*Li*tBu)Ni(phenylacetylene)] **VI-14** have been synthesized in 76 % and 73 % yield respectively.



**Scheme 6.11:** Synthesis of [(*Li*tBu)Ni(diphenylacetylene)] **VI-13** and [(*Li*tBu)Ni(phenylacetylene)] **VI-14**.

NMR spectroscopy shows that the acetylene moiety in these complexes is strongly shifted downfield towards the olefinic area. The <sup>13</sup>C shift of the triple bond in [(*Li*tBu)Ni(diphenylacetylene)] **VI-13** is located at  $\delta = 138.7$  ppm. The acetylenic carbons in [(*Li*tBu)Ni(phenylacetylene)] **VI-14** are found at  $\delta = 124.1$  ppm and  $\delta = 138.49$  ppm and the corresponding proton appears at  $\delta = 6.49$  ppm. This points towards a strong  $\pi$ -back donation that highly weakens the triple bond of the alkyne. In addition, both complexes could be crystallized from THF solutions either at RT or at  $-30$  °C. The geometric parameters determined by X-ray diffraction back up the NMR results. The Ni-C<sub>acetylene</sub> bonds are about 4 Å shorter than

the Ni-C<sub>NHC</sub> bonds due to the back bonding. The acetylenic C<sub>1</sub>-C<sub>2</sub> bonds measure 1.280(8) Å and 1.292(6) Å respectively and are closer to a C-C double bond than to a triple bond. The C<sub>18</sub>-C<sub>1</sub>-C<sub>2</sub> (147.0(7) °) and C<sub>24</sub>-C<sub>2</sub>-C<sub>1</sub> (145.1(7) °) angles in [(*Li*T*Bu*)Ni(diphenylacetylene)] **VI-13** and H<sub>1</sub>-C<sub>1</sub>-C<sub>2</sub> (144.8 °) and C<sub>18</sub>-C<sub>2</sub>-C<sub>1</sub> (140.9(4) °) in [(*Li*T*Bu*)Ni(phenylacetylene)] **VI-14** show that the alkynes are bent. The complexes can therefore also be described as metallacyclopropenes.

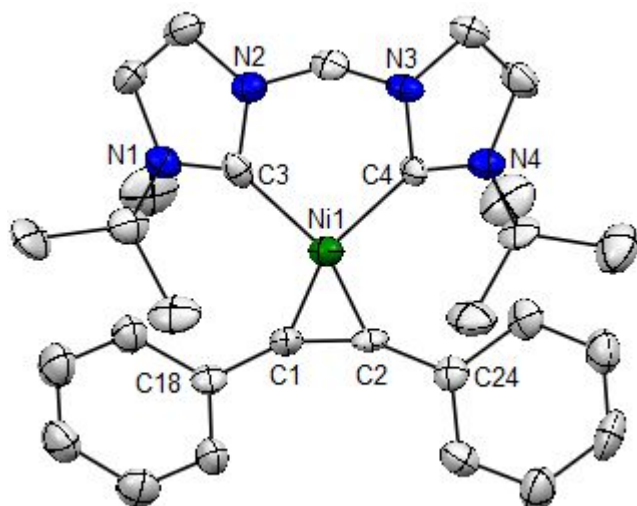


**Figure 6.2:** Molecular structure of [(*Li*T*Bu*)Ni(diphenylacetylene)] **VI-13** determined by single crystal X-ray diffraction. Hydrogen atoms are omitted for clarity.

Selected bond lengths [Å] and angles [°]: Ni<sub>1</sub>-C<sub>1</sub> 1.859(6), Ni<sub>1</sub>-C<sub>2</sub> 1.866(7), Ni<sub>1</sub>-C<sub>3</sub> 1.896(7), Ni<sub>1</sub>-C<sub>4</sub> 1.901(7), C<sub>1</sub>-C<sub>2</sub> 1.280(8), C<sub>1</sub>-Ni<sub>1</sub>-C<sub>2</sub> 40.2(3), C<sub>3</sub>-Ni<sub>1</sub>-C<sub>4</sub> 90.1(3), C<sub>18</sub>-C<sub>1</sub>-C<sub>2</sub> 147.0(7), C<sub>24</sub>-C<sub>2</sub>-C<sub>1</sub> 145.1(7).

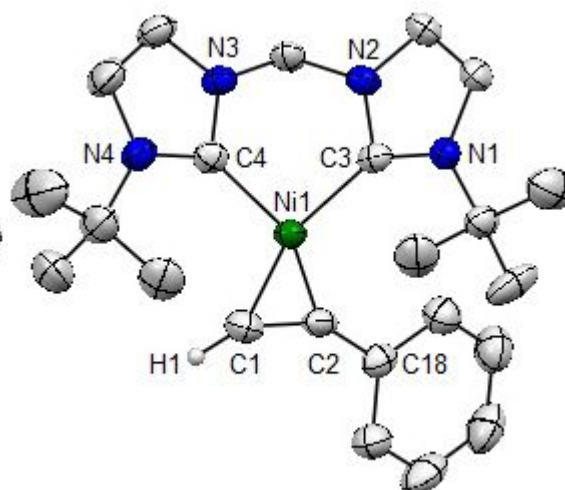


**Figure 6.3:** Molecular structure of [(*Li*T*Bu*)Ni(phenylacetylene)] **VI-14** determined by single crystal X-ray diffraction. Hydrogen atoms are omitted for clarity. Selected bond lengths [Å] and angles [°]: Ni<sub>1</sub>-C<sub>1</sub> 1.868(5), Ni<sub>1</sub>-C<sub>2</sub> 1.880(4), Ni<sub>1</sub>-C<sub>3</sub> 1.917(4), Ni<sub>1</sub>-C<sub>4</sub> 1.923(4), C<sub>1</sub>-C<sub>2</sub> 1.292(6), C<sub>1</sub>-H<sub>1</sub> 0.9500, C<sub>1</sub>-Ni<sub>1</sub>-C<sub>2</sub> 40.32(19), C<sub>3</sub>-Ni<sub>1</sub>-C<sub>4</sub> 90.54(18), H<sub>1</sub>-C<sub>1</sub>-C<sub>2</sub> 144.8, C<sub>18</sub>-C<sub>2</sub>-C<sub>1</sub> 140.9(4).

## 6.3 Ligand substitution reactions

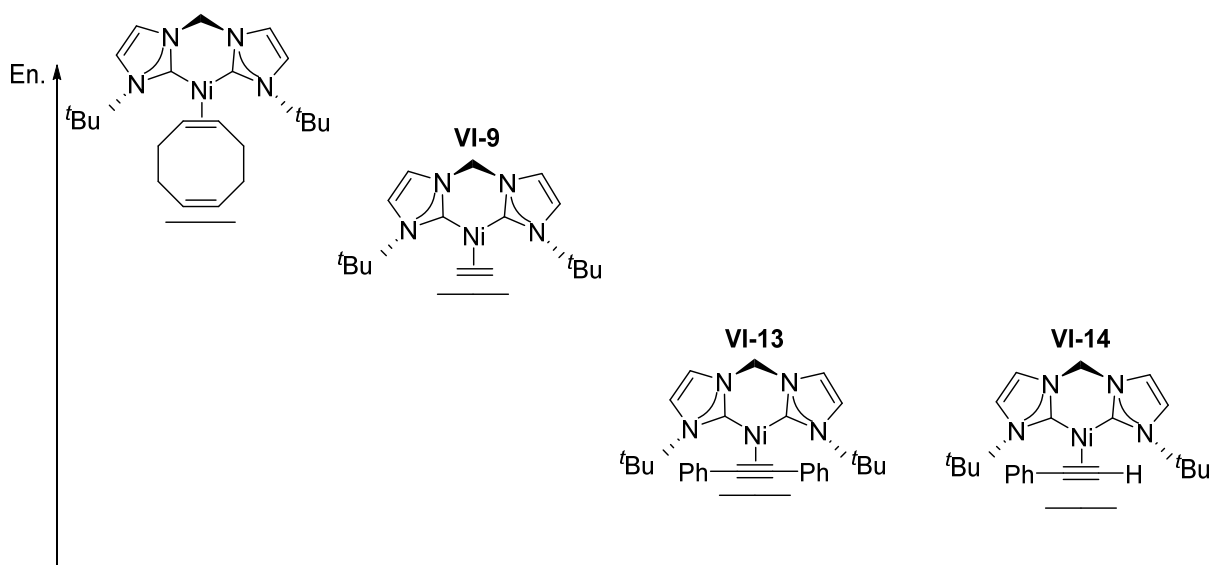
### 6.3.1 Relative stability of unsaturated [(bis-NHC)Ni]-complexes

The relative stability of the various nickel alkene and alkyne complexes has been probed and the experimental results are summarized in **Scheme 6.12**.

First of all, the synthesis of [(*Lt*Bu)Ni(C<sub>2</sub>H<sub>4</sub>)] **VI-9** and [(LDipp)Ni(C<sub>2</sub>H<sub>4</sub>)] **VI-10** from [Ni(COD)<sub>2</sub>] **VI-8** shows that these complexes are more stable than Hofmann's [(*Lt*Bu)Ni(COD)]<sup>[27]</sup> and [(LDipp)Ni(COD)]<sup>[27]</sup> complexes. The electron donating alkyl chain of 1,5-cyclooctadiene as well as the *cis*-disubstituted geometry of the olefin, enhancing the electronic density at the Ni(0) center, are responsible for the weaker interaction between the metal and the ligand in the later complexes.

Furthermore, [(*Lt*Bu)Ni(C<sub>2</sub>H<sub>4</sub>)] **VI-9** is instantaneously converted to the corresponding [(*Lt*Bu)Ni(alkyne)] **VI-13** and **VI-14** complexes upon addition of diphenylacetylene **VI-11** or phenylacetylene **VI-12**. In general, alkynes are more electron rich than alkenes and tend to bind more tightly to transition metals. Therefore, harsher conditions can be expected to carry out the oxidative coupling with CO<sub>2</sub> on more stable [(bis-NHC)Ni(alkyne)] complexes.

Moreover, diphenylacetylene **VI-11** can slowly be displaced by phenylacetylene **VI-12** at 60 °C. [(*Lt*Bu)Ni(phenylacetylene)] **VI-14** might be more stable because less sterically hindered.

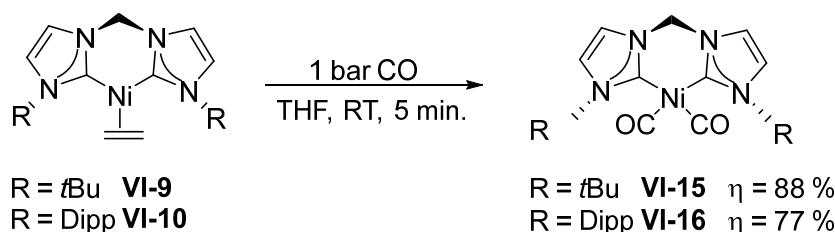


**Scheme 6.12:** Relative stability of unsaturated [(*Lt*Bu)Ni]-complexes.

### 6.3.2 Synthesis of [(bis-NHC)Ni(CO)<sub>2</sub>] complexes

To date a single [(bis-NHC)Ni(CO)<sub>2</sub>] complex has been reported by Danopoulos.<sup>[23]</sup> [(LDipp)Ni(CO)<sub>2</sub>] **VI-16** was synthesized through the reduction of [(LDipp)NiBr<sub>2</sub>] with an excess of Na/Hg under 100 psi (6.9 bar) of carbon monoxide. However, the product was obtained in low yield and could be characterized only crystallographically. The [(bis-NHC)Ni(C<sub>2</sub>H<sub>4</sub>)] complexes **VI-9** and **VI-10** have therefore been reacted with carbon monoxide to develop a milder, cleaner and more efficient route to the [(bis-NHC)Ni(CO)<sub>2</sub>] complexes and to typically gain information about the strength of the  $\pi$ -back donation in these new compounds.

When 1 bar of carbon monoxide is applied to [(*l*tBu)Ni(C<sub>2</sub>H<sub>4</sub>)] **VI-9** and [(LDipp)Ni(C<sub>2</sub>H<sub>4</sub>)] **VI-10**, new carbonyl complexes are formed within 5 min. at RT in good yields.



**Scheme 6.13:** Synthesis of [(*l*tBu)Ni(CO)<sub>2</sub>] **VI-15** and [(LDipp)Ni(CO)<sub>2</sub>] **VI-16**.

[(*l*tBu)Ni(CO)<sub>2</sub>] **VI-15** could be isolated as an orange powder in 88 % yield. A new resonance in <sup>13</sup>C NMR next to the carbenic center, at  $\delta = 204.2$  ppm, proves the coordination of the CO ligand. In addition, two strong absorption bands at 1874 cm<sup>-1</sup> and 1952 cm<sup>-1</sup> attributed to the CO stretches are observed by FTIR spectroscopy. [(*l*tBu)Ni(CO)<sub>2</sub>] **VI-15** could be crystallized at -30 °C in Et<sub>2</sub>O. The nickel is in a tetrahedral environment with a bite angle of 95.39(14) °. The Ni-C<sub>CO</sub> bonds are shorter than the Ni-C<sub>NHC</sub> bonds due to the  $\pi$ -back bonding. The effect of the  $\pi$ -back donation is further observable in the C<sub>1</sub>-O<sub>1</sub> (1.167(5) °) and C<sub>2</sub>-O<sub>2</sub> (1.159(4) °) carbonyl bonds lengths lying in between C-O double and triple bonds. The bonding parameters are overall comparable to Danopoulos' [(LDipp)Ni(CO)<sub>2</sub>] **VI-16** structure.<sup>[23]</sup>

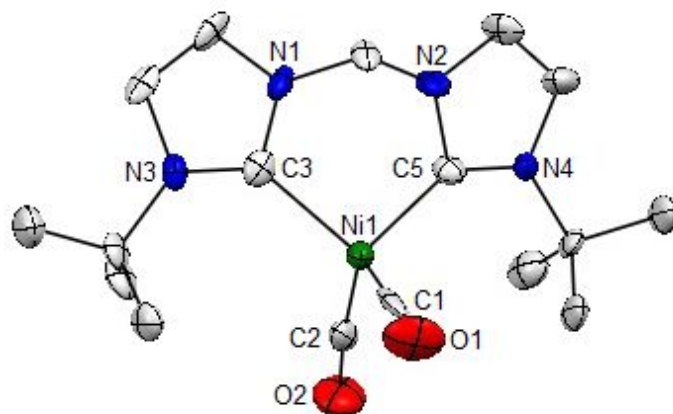


**Figure 6.4:** Molecular structure of  $[(LtBu)Ni(CO)_2]$  **VI-15** determined by single crystal X-ray diffraction. Hydrogen atoms are omitted for clarity. Selected bond lengths [Å] and angles [°]: Ni<sub>1</sub>-C<sub>1</sub> 1.755(4), Ni<sub>1</sub>-C<sub>2</sub> 1.755(4), Ni<sub>1</sub>-C<sub>3</sub> 2.009(3), Ni<sub>1</sub>-C<sub>5</sub> 1.996(3), C<sub>1</sub>-O<sub>1</sub> 1.167(5), C<sub>2</sub>-O<sub>2</sub> 1.159(4), C<sub>1</sub>-Ni<sub>1</sub>-C<sub>2</sub> 110.89(17), C<sub>3</sub>-Ni<sub>1</sub>-C<sub>5</sub> 95.39(14).

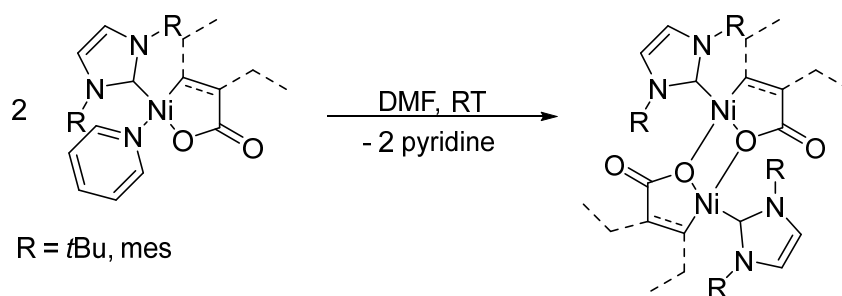
$[(LDipp)Ni(CO)_2]$  **VI-16** could also be easily obtained by ligand substitution as a brown powder in 77 % yield. The compound has been characterized spectroscopically and shows very close features to  $[(LtBu)Ni(CO)_2]$  **VI-16**. The carbonyls appear at  $\delta = 204.3$  ppm by  $^{13}C$  NMR. Two strong C-O absorption bands are found at  $1892\text{ cm}^{-1}$  and  $1960\text{ cm}^{-1}$  in the IR spectrum.

Comparison between the C-O stretching frequencies of  $[(dcp)Ni(CO)_2]$  **IV-26**,  $[(LtBu)Ni(CO)_2]$  **VI-15** and  $[(LDipp)Ni(CO)_2]$  **VI-16** confirms that NHCs are stronger  $\sigma$ -donor ligands than phosphines. The absorption bands are shifted by  $20\text{ cm}^{-1}$  to  $40\text{ cm}^{-1}$  to lower frequencies in the bis-carbene complexes.

## 6.4 Synthesis and reactivity of [(bis-NHC)nickelalactones]

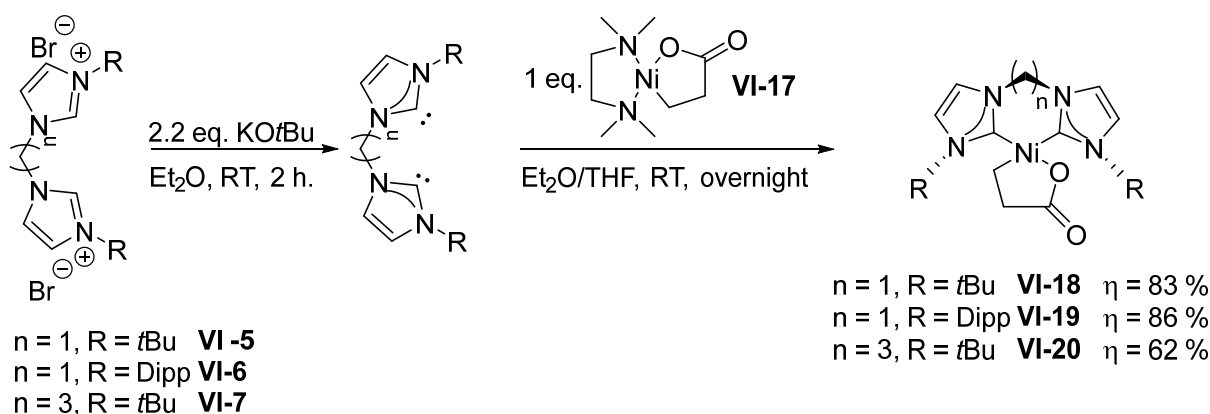
### 6.4.1 Synthesis of [(bis-NHC)nickelalactones] through ligand substitution

Chelating diamine and bis-phosphine nickelalactones are well known and have been thoroughly studied for a long time. Nevertheless, carbene nickelalactones remain nearly unexplored. A single example bearing a mono-carbene and a pyridine ligand was reported by Walther in 2006 as shown in **Scheme 6.14**.<sup>[30]</sup>



**Scheme 6.14:** [(pyridine)(NHC)nickelalactones] reported by Walther. The nickelalactones dimerize readily in DMF.

[(Bis-NHC)nickelalactones] can be efficiently synthesized through ligand substitution from [(tmeda)nickelalactone] **VI-17**. The methodology is similar to the one described in 6.2.2 for the synthesis of [(bis-NHC)Ni(0)-alkene] and [(bis-NHC)Ni(0)-alkynes] complexes. Deprotonation of the (bis-NHC) $\text{H}_2\text{Br}_2$  imidazolium salts **VI-5**, **VI-6** and **VI-7** with 2.2 eq. of  $\text{KO}^t\text{Bu}$  affords the free carbenes, which then easily displace the diamine in presence of [(tmeda)nickelalactone] **VI-17**. It is important to carry out the first step of the reaction in  $\text{Et}_2\text{O}$  to directly precipitate and remove  $\text{KBr}$ . THF is added for the second step to help solubilizing [(tmeda)nickelalactone] **VI-17**. Simple successive washings with THF,  $\text{Et}_2\text{O}$  and pentane afford clean [(bis-NHC)nickelalactones] in good yields. In this way, [(*Lt*Bu)nickelalactone] **VI-18**, [(LDipp)nickelalactone] **VI-19** and [(*Lt*Bu)<sup>prop</sup>nickelalactone] **VI-20** could be obtained. The lactones have poor solubility in most common organic solvents like Walther's derivatives<sup>[30]</sup> and turned out to be very stable compounds insensitive towards water and oxygen.



**Scheme 6.15:** Synthesis of [(*Lt*Bu)nickelalactone] **VI-18**, [(LDipp)nickelalactone] **VI-19** and [(*Lt*Bu)<sup>prop</sup>nickelalactone] **VI-20**.

[(*Lt*Bu)nickelalactone] **VI-18** is obtained as a beige product in 83 % yield. Despite its limited solubility, NMR data could be recorded in CD<sub>3</sub>CN. The <sup>1</sup>H NMR reveals two inequivalent Ni-CH<sub>2</sub> protons at δ = 0.47 ppm and δ = 0.74 ppm and two protons in α of the ester at δ = 2.03 ppm. <sup>13</sup>C NMR confirms the coordination of the bis-carbene to the nickel center with two quaternary carbons at δ = 180.6 ppm and δ = 186.1 ppm as well as the presence of a C=O bond at δ = 189.6 ppm. The presence of the lactone is further evidenced by FTIR spectroscopy displaying an absorption band at 1619 cm<sup>-1</sup>. Single crystals for X-ray diffraction analysis have been grown from an acetonitrile solution at RT. [(*Lt*Bu)nickelalactone] **VI-18** crystallizes in the space group P2<sub>1</sub>/n and the geometry around the nickel center is square planar. The bite angle C<sub>4</sub>Ni<sub>1</sub>C<sub>5</sub> (86.89(17) °) is significantly smaller compared to [(dcp)nickelalactone] **IV-4** (99.66(2) °). The chelate ring adopts a boat shape conformation. The Ni<sub>1</sub>C<sub>1</sub> (1.942(4) Å) and Ni<sub>1</sub>O<sub>1</sub> (1.909(3) Å) bond lengths are otherwise comparable to [(dcp)nickelalactone] **IV-4** (Ni<sub>1</sub>-C<sub>3</sub> 1.968(3) Å and Ni<sub>1</sub>-O<sub>1</sub> 1.9074(18) Å). The particularly elongated Ni<sub>1</sub>O<sub>1</sub> bond should ease the cleavage of the lactone.

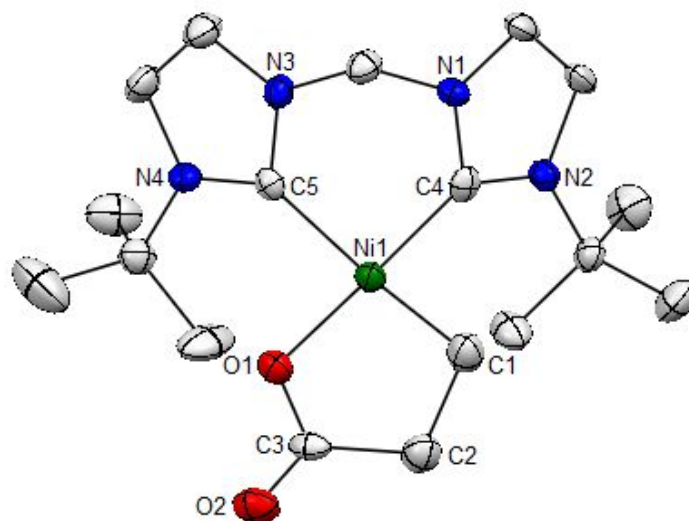


**Figure 6.5:** Molecular structure of [(*Lt*Bu)nickelalactone] **VI-18** determined by single crystal X-ray diffraction. Hydrogen atoms are omitted for clarity. Selected bond lengths [Å] and angles [°]: Ni<sub>1</sub>-O<sub>1</sub> 1.909(3), Ni<sub>1</sub>-C<sub>1</sub> 1.942(4), C<sub>3</sub>-O<sub>2</sub> 1.228(5), Ni<sub>1</sub>-C<sub>4</sub> 1.860(4), Ni<sub>1</sub>-C<sub>5</sub> 1.957(4), C<sub>4</sub>-Ni<sub>1</sub>-C<sub>5</sub> 86.89(17), C<sub>1</sub>-Ni<sub>1</sub>-O<sub>1</sub>. 84.73(16).

Afterwards, different parameters of the [(bis-NHC)nickelalactone] have been successively varied. First of all, the substituents on the nitrogen atoms have been replaced by bulkier Dipp moieties. By following the same methodology, [(LDipp)nickelalactone] **VI-19** can be isolated

as a beige product in 86 % yield.  $^1\text{H}$  NMR in MeOD reveals Ni-CH<sub>2</sub> protons as a triplet at  $\delta = 0.17$  ppm and CH<sub>2</sub> protons in  $\alpha$  of the ester as a second triplet at  $\delta = 1.52$  ppm.  $^{13}\text{C}$  NMR displays the quaternary carbene carbon atoms at  $\delta = 176.7$  ppm and  $\delta = 186.0$  ppm and the C=O at  $\delta = 194.3$  ppm. FTIR spectroscopy shows an absorption band at  $1562\text{ cm}^{-1}$ .

Next, the spacer between both NHC units has been modulated. The methyl chain has been switch for a longer propyl chain. [(*LtBu*)<sup>prop</sup>nickelalactone] **VI-20** is gathered as beige product in 62 % yield. The spectroscopic features resemble the ones previously reported for the other nickelalactones. Among others the acyl resonates at  $\delta = 189.2$  ppm in  $^{13}\text{C}$  NMR and vibrates at  $1615\text{ cm}^{-1}$  in IR spectroscopy. Single crystals for X-ray diffraction have been grown from a THF solution layered with Et<sub>2</sub>O and pentane at RT. The octagon formed by the propyl spacer between both NHC units is largely distorted. The C<sub>4</sub>-Ni<sub>1</sub>-C<sub>5</sub> bite angle, which measures  $98.46(8)^\circ$ , is over  $10^\circ$  larger than the one of [(*LtBu*)nickelalactone] **VI-18** and very close to the one of [(*dcpp*)nickelalactone] **IV-4**. The Ni<sub>1</sub>-O<sub>1</sub> bond ( $1.9237(15)\text{ \AA}$ ) is comparable to the analogous methyl bridged complex.

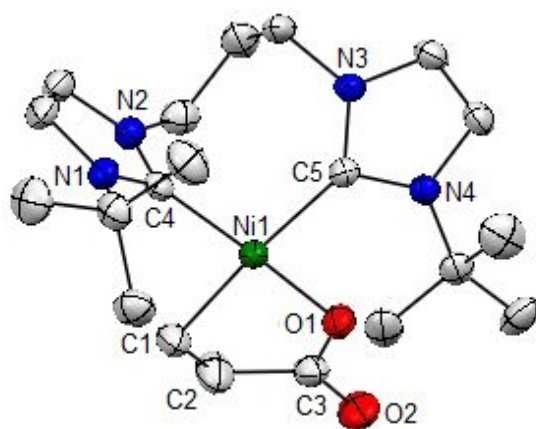
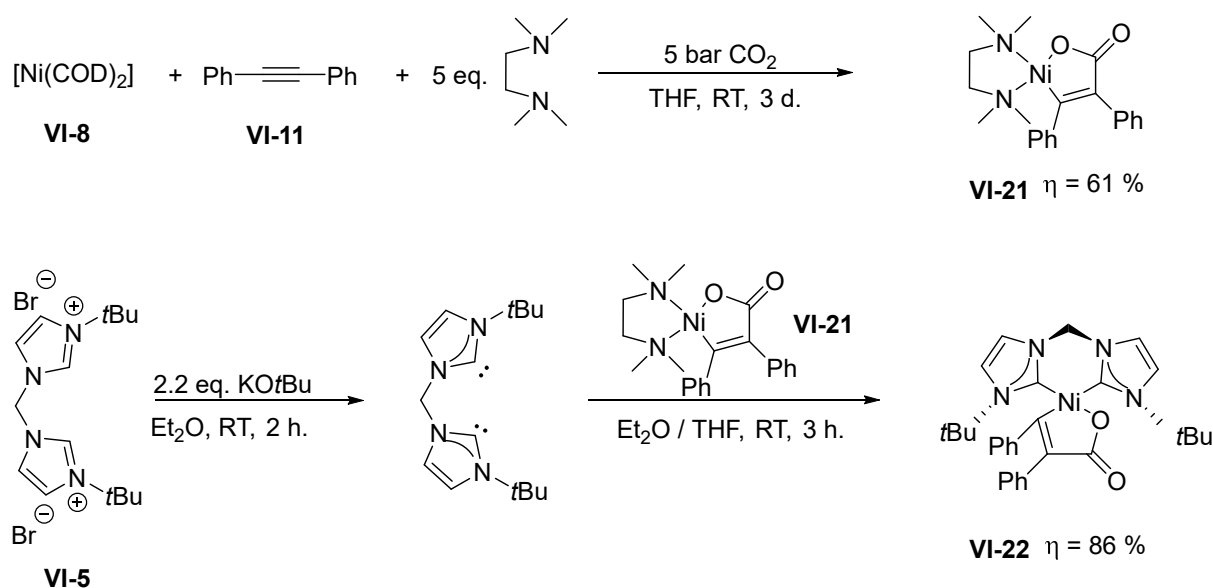


**Figure 6.6:** Molecular structure of [(*LtBu*)<sup>prop</sup>nickelalactone] **VI-20** determined by single crystal X-ray diffraction. Hydrogen atoms are omitted for clarity. Selected bond lengths [ $\text{\AA}$ ] and angles [ $^\circ$ ]: Ni<sub>1</sub>-O<sub>1</sub>  $1.9237(15)$ , Ni<sub>1</sub>-C<sub>1</sub>  $1.961(2)$ , C<sub>3</sub>-O<sub>2</sub>  $1.239(3)$ , Ni<sub>1</sub>-C<sub>4</sub>  $1.853(2)$ , Ni<sub>1</sub>-C<sub>5</sub>  $1.966(2)$ , C<sub>4</sub>-Ni<sub>1</sub>-C<sub>5</sub>  $98.46(8)$ , C<sub>1</sub>-Ni<sub>1</sub>-O<sub>1</sub>  $84.19(8)$ .

Finally, an unsaturated nickelalactone has been synthesized. Starting material, [(*tmeda*)nickela-2-oxacyclopenten-4,5-diphenyl-3-one] **VI-21**, was obtained by reacting [Ni(COD)<sub>2</sub>] **VI-8**, diphenylacetylene **VI-11** and *tmeda* under 5 bar of CO<sub>2</sub> according to Hoberg's procedure.<sup>[34]</sup> The diamine in this Ni(II) complex is also easily displaced by the free *LtBu* carbene yielding



86 % of the nearly insoluble yellow diphenyl substituted [(*Lt*Bu)oxanickelacyclopentenone] **VI-22**.



**Scheme 6.16:** Two step synthesis of [*Lt*Bu]nickela-2-oxacyclopenten-4,5-diphenyl-3-one **VI-22**.

$^{13}\text{C}$  NMR could be recorded in  $\text{CD}_3\text{CN}$  but the quaternary carbon centers are very weak. The olefinic carbons are found in their typical area at  $\delta = 141.6$  ppm and  $\delta = 142.0$  ppm. Due to the lack of nearby protons, it is difficult to unambiguously assign the carbon in  $\alpha$  of the nickel and the one in  $\alpha$  of the ester by means of HSQC and HMBC experiments. The carbene centers appear classically at  $\delta = 176.0$  ppm and  $\delta = 176.5$  ppm alongside the ester at  $\delta = 179.4$  ppm. Vibrational spectroscopy confirms the presence of the C=O bond with an absorption band at  $1604 \text{ cm}^{-1}$ . The substituted oxanickelacyclopentenone **VI-22** could be crystallized from an acetonitrile solution at RT. The C<sub>2</sub>-C<sub>3</sub> bond measures  $1.357(3) \text{ \AA}$  and clearly lies in the range of a double bond. The bite angle C<sub>4</sub>-Ni<sub>1</sub>-C<sub>5</sub> ( $86.31(8)^\circ$ ) is comparable to the one determined for [(*Lt*Bu)nickelalactone] **VI-9** ( $86.9(2)^\circ$ ) and the Ni<sub>1</sub>-O<sub>1</sub> bond is shorter by  $0.025(2) \text{ \AA}$ .

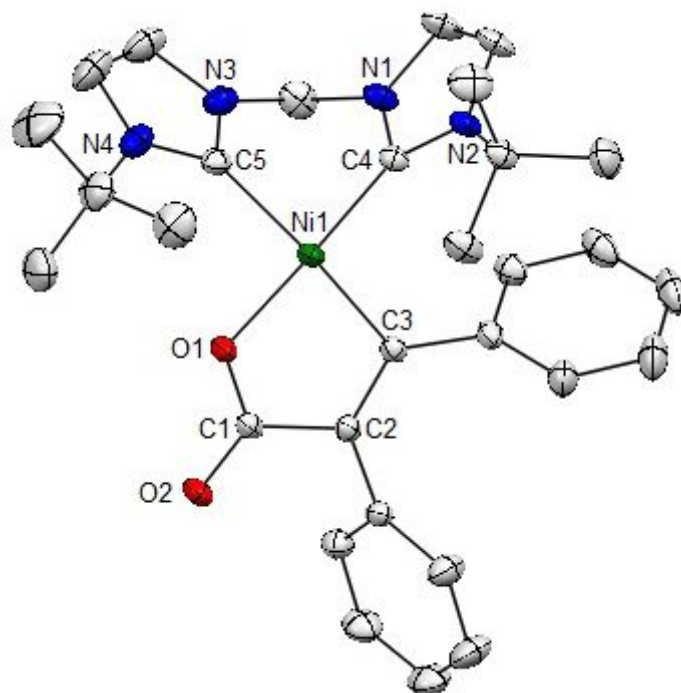
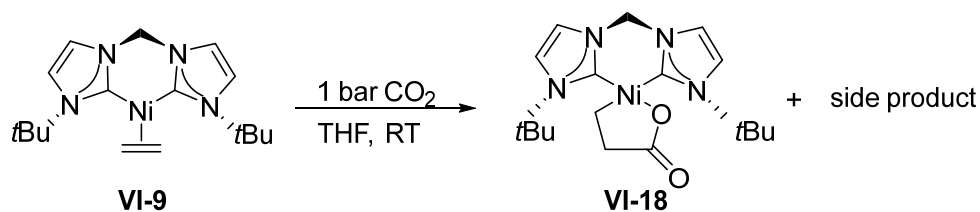


**Figure 6.7:** Molecular structure of [(*t*Bu)nickela-2-oxacyclopenten-4,5-diphenyl-3-one] **VI-27** determined by single crystal X-ray diffraction. Hydrogen atoms are omitted for clarity. Selected bond lengths [Å] and angles [°]: Ni<sub>1</sub>-O<sub>1</sub> 1.8837(14), Ni<sub>1</sub>-C<sub>3</sub> 1.9520(19), C<sub>2</sub>-C<sub>3</sub> 1.357(3), C<sub>1</sub>-O<sub>2</sub> 1.236(2), Ni<sub>1</sub>-C<sub>4</sub> 1.8658(19), Ni<sub>1</sub>-C<sub>5</sub> 1.954(2), C<sub>4</sub>-Ni<sub>1</sub>-C<sub>5</sub> 86.31(8), C<sub>3</sub>-Ni<sub>1</sub>-O<sub>1</sub> 84.87(7).

### 6.4.2 Synthesis of [(bis-NHC)nickelalactones] through oxidative coupling

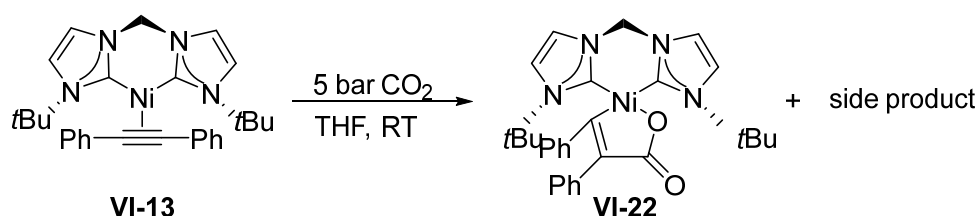
The [(bis-NHC)nickelalactones] can alternatively be synthesized through the oxidative coupling between [(bis-NHC)Ni-(alkene)] or [(bis-NHC)Ni-(alkyne)] complexes and CO<sub>2</sub>. Upon addition of 1 bar of CO<sub>2</sub> to [(*t*Bu)Ni(C<sub>2</sub>H<sub>4</sub>)] **VI-9** in THF, a beige insoluble product is formed. THF is essential to efficiently solubilize CO<sub>2</sub>. By comparison with the previously isolated complexes, [(*t*Bu)nickelalactone] **VI-9** was undoubtedly identified.



**Scheme 6.17:** Oxidative coupling between [(*t*Bu)Ni(C<sub>2</sub>H<sub>4</sub>)] **VI-9** and CO<sub>2</sub>.

Unfortunately, a symmetric side product characterized in  $^1\text{H}$  NMR by a singlet at  $\delta = 1.88$  ppm presumably for its *t*Bu group is also produced during the reaction. The formation of the  $[\text{L}t\text{Bu-CO}_2]$ -adduct,  $[(\text{L}t\text{Bu})\text{Ni}(\text{carbonate})]$  or  $[(\text{L}t\text{Bu})\text{Ni}(\text{oxalate})]$  complexes has been envisaged. Shi recently reported the synthesis of various alkane bridged  $[(\text{LDipp})\text{Ni}(\text{carbonate})]$  complexes in moderate yields by the reactions between bis-NHC imidazolium salts,  $\text{NiCl}_2$  and  $\text{K}_2\text{CO}_3$  in acetonitrile.<sup>[25]</sup> However,  $[(\text{L}t\text{Bu})\text{Ni}(\text{carbonate})]$  **VI-24** could not be synthesized by following this procedure. Nevertheless,  $[(\text{L}t\text{Bu})\text{Ni}(\text{carbonate})]$  **VI-24** was alternatively obtained through deprotonation of the imidazolium salt  $\text{L}t\text{BuH}_2\text{Br}_2$  **VI-5** followed by addition to  $[\text{Ni}(\text{CO}_3)]$  **VI-23**. The  $^1\text{H}$  NMR does not match the one of the unknown symmetric product. So far the other two potential side products were not independently synthesized yet.

Additionally,  $[(\text{LDipp})\text{nickelalactone}]$  **VI-19** is also obtained from  $[(\text{LDipp})\text{Ni}(\text{C}_2\text{H}_4)]$  **VI-10** under 1 bar of  $\text{CO}_2$ . Furthermore, by applying 1 bar of  $\text{CO}_2$  to  $[(\text{L}t\text{Bu})\text{Ni}(\text{diphenylacetylene})]$  **VI-13** in THF, no reaction is observed. Though by increasing the pressure to 5 bar of  $\text{CO}_2$ ,  $[(\text{L}t\text{Bu})\text{nickela-2-oxacyclopenten-4,5-diphenyl-3-one}]$  **VI-22** is formed. The nickelalactone as well as the side product with the *t*Bu group at  $\delta = 1.88$  ppm were identified by  $^1\text{H}$  NMR in  $\text{CD}_3\text{CN}$ . The need of harsher conditions is in good agreement with the fact that  $[(\text{bis-NHC})\text{Ni}(\text{alkyne})]$  complexes are more stable than alkene complexes and require a higher activation energy to perform the same transformation.



**Scheme 6.18:** Oxidative coupling between  $[(\text{L}t\text{Bu})\text{Ni}(\text{diphenylacetylene})]$  **VI-13** and  $\text{CO}_2$ . Higher pressures are required to achieve the reaction.

Unlike for chelating bis-phosphines, very mild conditions (1 - 5 bar of  $\text{CO}_2$ , RT) efficiently promote the oxidative coupling between  $[(\text{bis-NHC})\text{Ni}(\text{alkene})]$  or  $[(\text{bis-NHC})\text{Ni}(\text{alkyne})]$  complexes and  $\text{CO}_2$ . However, a still unidentified side product is simultaneously generated. Preliminary DFT calculations at the  $\text{wB97XD}(\text{THF})/\text{TZVP}$  level of theory have been performed for the LMe ligand and support the experimental findings. The  $\Delta G^\ddagger$  of the transition state measures  $20.83 \text{ kcal}\cdot\text{mol}^{-1}$  and is in good agreement with the mild reaction conditions. Moreover, the coupling is exergonic by  $10.98 \text{ kcal}\cdot\text{mol}^{-1}$ . Indeed  $[(\text{L}t\text{Bu})\text{nickelalactone}]$  **VI-18**

is more stable than  $[(\text{Li}t\text{Bu})\text{Ni}(\text{C}_2\text{H}_4)]$  **VI-9** and cannot be reverted into the latter upon heating. **Figure 6.8** shows comparatively the energy profiles of the oxidative coupling for the dcpp and the LMe ligands.

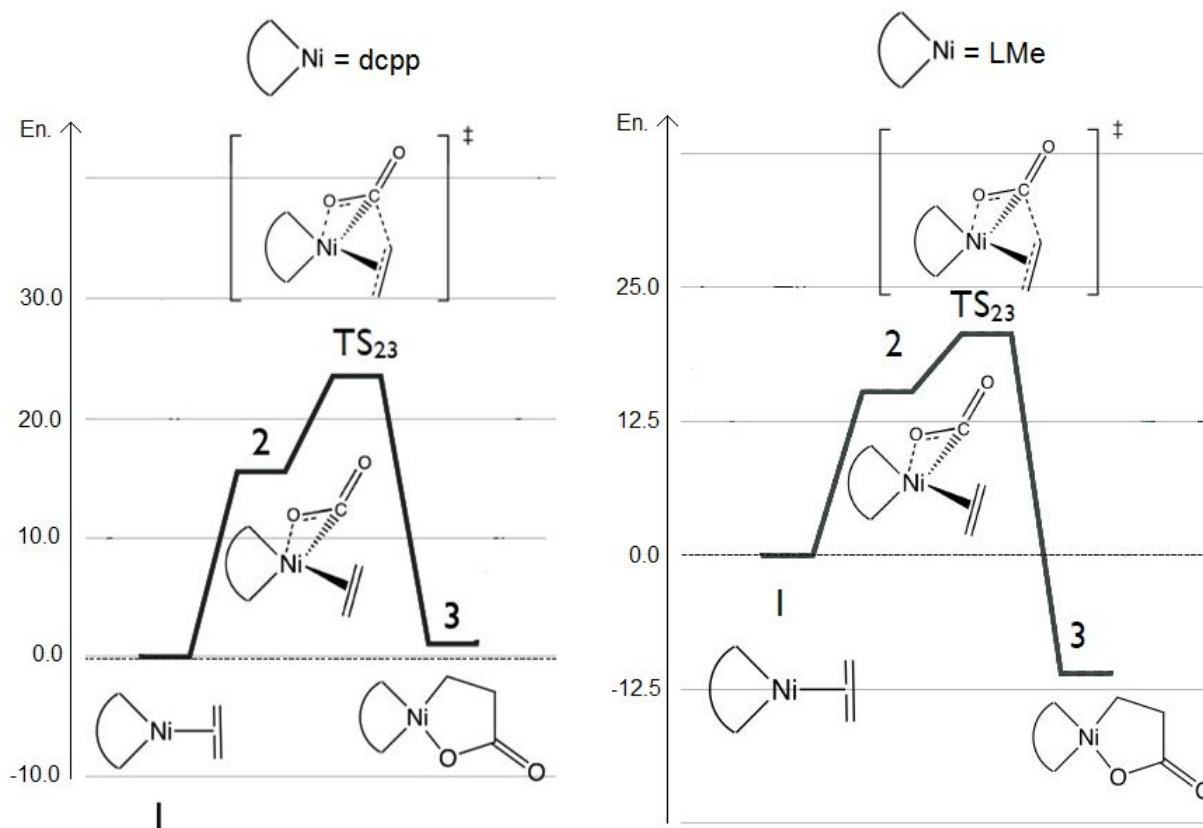


**Figure 6.8:** Comparison between the energy profiles of the oxidative coupling for the dcpp and LMe ligands at the wB97XD(THF)/TZVP level of theory.

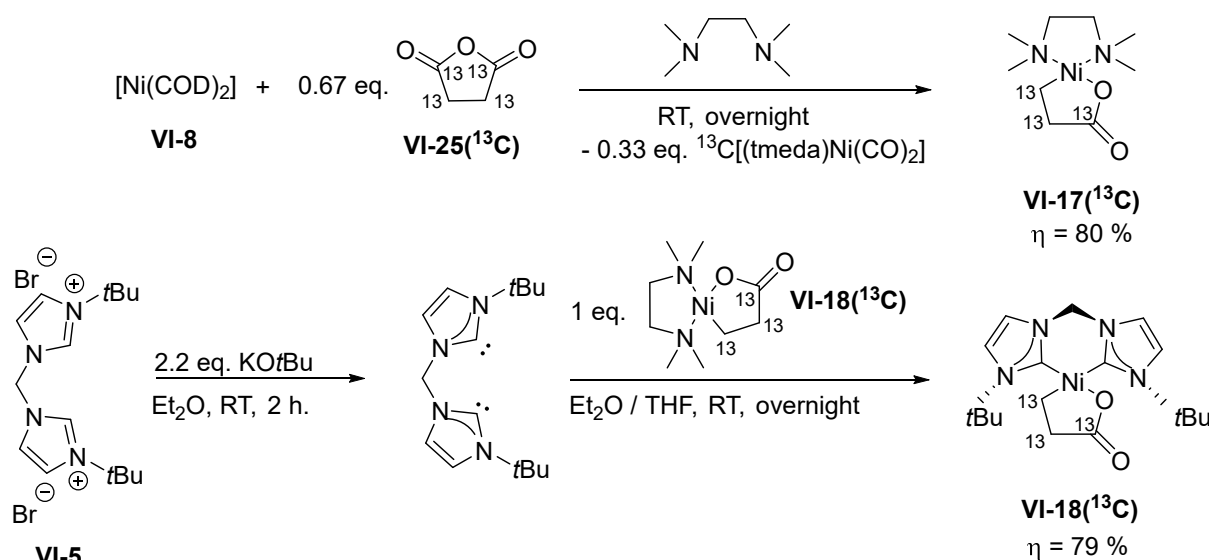
### 6.4.3 Reactivity of [(bis-NHC)nickelalactones]

A new family of [(bis-NHC)nickelalactones] **VI-18**, **VI-19**, **VI-20** and **VI-22**, that can either be accessed by ligand substitution or by oxidative coupling between unsaturated nickel complexes and  $\text{CO}_2$ , has been developed. The next step was thus to explore their reactivity, especially towards the synthesis of acrylates and alcoholates.

Limbach's <sup>[35, 36]</sup> and Vogt's <sup>[37]</sup> procedures to generate acrylates, employing either sodium phenoxide or a combination of LiI and  $\text{Et}_3\text{N}$ , have been tested on [(*Li*tBu)nickelalactone] **VI-18** without any success. The approach described in **Chapter 4** and **5** using various transmetallating reagents also proved to be inconclusive so far. Rapidly limitations were encountered, first of all

because of the poor solubility of [(bis-NHC)nickelalactones] in the organic solvents commonly used for these reactions. Moreover, the thermodynamic stability of these complexes could be deleterious. Indeed, calculations show that [(bis-NHC)nickelalactones] may be more readily accessible than [(bis-phosphine)nickelalactones], but that does not mean that further steps would be more favorable as well. Finally, the loss of the phosphorus probe made the monitoring of the reactions very difficult.

In order to better understand that chemistry,  $^{13}\text{C}$ [(*Lt*Bu)nickelalactone] **VI-18**( $^{13}\text{C}$ ) was synthesized in a two-step procedure described in **Scheme 6.22**. Starting from  $^{13}\text{C}$  labelled succinic anhydride **VI-25**( $^{13}\text{C}$ ),  $^{13}\text{C}$ [(tmeda)nickelalactone] **VI-17**( $^{13}\text{C}$ ) could be obtained in 80 % yield following Fischer's procedure.<sup>[48]</sup> Deprotonation of the *Lt*BuH<sub>2</sub>Br<sub>2</sub> imidazolium salt **VI-5** and subsequent reaction with  $^{13}\text{C}$ [(tmeda)nickelalactone] **VI-17**( $^{13}\text{C}$ ) afforded  $^{13}\text{C}$ [(*Lt*Bu)nickelalactone] **VI-18**( $^{13}\text{C}$ ) in 79 % yield.



**Scheme 6.19:** Two step synthesis of  $^{13}\text{C}$ [(*Lt*Bu)nickelalactone] **VI-18**( $^{13}\text{C}$ ).

With the  $^{13}\text{C}$  NMR probe in hand and by optimizing the reaction conditions, new advances in the synthesis of acrylates or alcoholates from (bis-NHC)nickelalactones can be expected.

## 6.5 Conclusion and perspectives

The development of robust procedures led to the efficient synthesis of new [(bis-NHC)Ni(0)] and [(bis-NHC)Ni(II)]-complexes in good yields.

In this way, starting from [Ni(COD)<sub>2</sub>] **VI-8** through successive ligand substitutions, the family of [(bis-NHC)Ni-(alkene)] complexes could be extended to so far unreported ethylene compounds [(*Lt*Bu)Ni(C<sub>2</sub>H<sub>4</sub>)] **VI-9** and [(LDipp)Ni(C<sub>2</sub>H<sub>4</sub>)] **VI-10**. Furthermore, the first [(bis-NHC)Ni-(alkyne)] complexes [(*Lt*Bu)Ni(diphenylacetylene)] **VI-13** and [(*Lt*Bu)Ni(phenylacetylene)] **VI-14** were described. The unsaturated [(bis-NHC)Ni(0)]-complexes were then successfully converted into the [(*Lt*Bu)Ni(CO)<sub>2</sub>] **VI-15** and [(LDipp)Ni(CO)<sub>2</sub>] **VI-16** compounds upon addition of carbon monoxide. Despite their high sensitivity, [(bis-NHC)Ni(0)]-complexes could constitute a good entry point in catalytic cycles. It would be interesting to extend the scope of available [(bis-NHC)Ni(0)]-complexes and to explore their reactivity for example towards the catalytic formation of benzonitriles<sup>[39 - 44]</sup> or the arylocyanation of alkynes.<sup>[45 - 48]</sup>

In addition, the first [(bis-NHC)nickelalactones], [(*Lt*Bu)nickelalactone] **VI-18**, [(LDipp)nickelalactone] **VI-19**, [(*Lt*Bu)<sup>prop</sup>nickelalactone] **VI-20** and [(*Lt*Bu)nickela-2-oxacyclopenten-4,5-diphenyl-3-one] **VI-22** have been synthesized in good yields through ligand substitution from [(tmeda)nickelalactone] **VI-17**. They are also easily accessible through oxidative coupling between unsaturated [(bis-NHC)Ni(0)]-complexes, [(*Lt*Bu)Ni(C<sub>2</sub>H<sub>4</sub>)] **VI-9**, [(Dipp)Ni(C<sub>2</sub>H<sub>4</sub>)] **V-10** and [(*Lt*Bu)Ni(diphenylacetylene)] **VI-13**, and CO<sub>2</sub> under mild conditions. However, more efforts are still required to convert them efficiently into valuable chemicals such as acrylates or alcoholates.

## 6.6 Experimental part

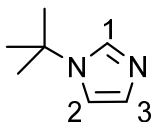
### 6.6.1 General Remarks

All reactions were carried out under an atmosphere of dry argon using standard Schlenk techniques or in a nitrogen-filled MBraun LabStar glovebox. Acetonitrile, diethyl ether, THF and pentane were taken from a MBraun SPS-800 solvent purification system. Acetonitrile, methanol and water were degassed by bubbling argon and all the other solvents were degassed by using the freeze-pump-thaw procedure. [d8]-THF, CD<sub>3</sub>CN and MeOD were degassed and stored over 4 Å molecular sieves.

*N*-(2,6-diisopropylphenyl)imidazole<sup>[32]</sup> **VI-2**, and [(tmeda)nickelalactone]<sup>[38]</sup> **VI-22** were synthesized according to published procedures. All the other chemicals were purchased in reagent grade purity from Acros and Sigma-Aldrich and were used without further purification. CO, CO<sub>2</sub> and ethylene were purchased from Air Liquide.

### 6.6.2 Synthesis of imidazoles and corresponding imidazolium salts

#### 6.6.2.1 *N*-*tert*-butylimidazole **VI-1**

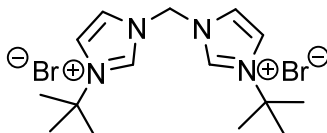


*N*-*tert*-butylimidazole **VI-1** was prepared according to a modified published procedure.<sup>[31]</sup> Distilled water (200 mL) was placed in a 500 mL three necked flask connected to two dropping funnels and a water condenser. One dropping funnel was filled with 37 % formaldehyde (29.8 mL, 0.4 mol, 1 eq.) and 40 % glyoxal (46 mL, 0.4 mol, 1 eq.), the other with *tert*-butylamine (42.4 mL, 0.4 mol, 1 eq.) and 30 % aqueous ammonia (25.6 mL, 0.4 mol, 1 eq.). The water was heated until boiling and then both solutions were added simultaneously drop by drop. After complete addition, the brown reaction mixture was stirred for further 30 min. at 100 °C. The organic products were extracted with 2 × 200 mL of CH<sub>2</sub>Cl<sub>2</sub>. The organic fractions were dried over Na<sub>2</sub>SO<sub>4</sub> and CH<sub>2</sub>Cl<sub>2</sub> was removed by rotary evaporator. The remaining mixture was purified by vacuum transfer. *N*-*tert*-butylimidazole **VI-1** is obtained as a pale yellow liquid in 40 % yield (19.90 g) by heating up to 85 - 100 °C.

<sup>1</sup>H NMR (300 MHz, CDCl<sub>3</sub>): δ 1.47 (s, 9H, CH<sub>3</sub>), 6.97 (s, 2H, HC=CH), 7.53 (s, 1H, N-CH-N) ppm.

$^{13}\text{C}\{^1\text{H}\}$  NMR (75 MHz,  $\text{CDCl}_3$ ):  $\delta$  30.5 ( $\text{CCH}_3$ ), 54.6 ( $\text{CCH}_3$ ), 116.2 ( $\text{C}_2$ ), 128.9 ( $\text{C}_3$ ), 134.2 ( $\text{C}_1$ ) ppm.

#### 6.6.2.2 (*LtBu*) $\text{H}_2\text{Br}_2$ **VI-5**

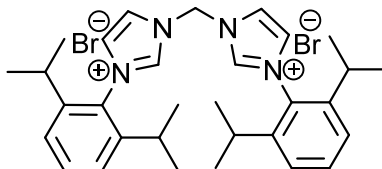


*N*-*tert*-butylimidazole **VI-1** (4 g,  $3.22 \times 10^{-2}$  mol, 1 eq.) is diluted in 13 mL of THF in a Fischer-Porter and dibromomethane **VI-3** (1.10 mL,  $1.61 \times 10^{-2}$  mol, 0.5 eq.) is added to the colorless solution. The reaction mixture is heated for 5 d. at 130 °C; a white to brownish precipitate appears. The solution is filtered away, the product is washed with THF until it becomes white and dried overnight at 100 °C under vacuum. (*LtBu*) $\text{H}_2\text{Br}_2$  **VI-5** is gathered as a white powder in 94 % yield (6.42 g).

$^1\text{H}$  NMR (300 MHz,  $[\text{d}_6]\text{-DMSO}$ ):  $\delta$  1.54 (s, 18H,  $\text{CH}_3$ ), 6.58 (s, 2H,  $\text{N-CH}_2\text{-N}$ ), 8.11 (d,  $^3J_{\text{H,H}} = 1.9$  Hz, 4H,  $\text{HC=CH}$ ), 9.73 (s, 2H,  $\text{N=CH-N}$ ) ppm.

$^{13}\text{C}\{^1\text{H}\}$  NMR (75 MHz,  $[\text{d}_6]\text{-DMSO}$ ):  $\delta$  28.8 ( $\text{CCH}_3$ ), 57.6 ( $\text{CCH}_3$ ), 60.3 ( $\text{N-CH}_2\text{-N}$ ), 120.9 ( $\text{CH imi}$ ), 122.5 ( $\text{CH imi}$ ), 136.4 ( $\text{N=CH-N}$ ) ppm.

#### 6.2.2.3 (LDipp) $\text{H}_2\text{Br}_2$ **VI-6**



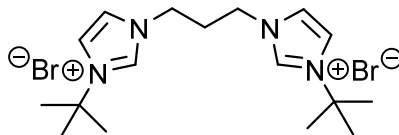
*N*-(2,6-diisopropylphenyl)imidazole **VI-2** (4 g,  $1.75 \times 10^{-2}$  mol, 1 eq.) is diluted in 8 mL of THF in a Fischer-Porter and dibromomethane **VI-3** (0.6 mL,  $8.75 \times 10^{-3}$  mol, 0.5 eq.) is added to the colorless solution. The reaction mixture is heated for 3 d. at 150 °C; a white to brownish precipitate appears. The solution is filtered away, the product is carefully washed with acetone and then THF until it becomes white and dried overnight at 100 °C under vacuum. (LDipp) $\text{H}_2\text{Br}_2$  **VI-6** is gathered as a white powder in 60 % yield (3.33 g).

$^1\text{H}$  NMR (300 MHz,  $[\text{d}_6]\text{-DMSO}$ ):  $\delta$  1.05 (d,  $^3J_{\text{H,H}} = 6.6$  Hz, 24H,  $\text{CH}(\text{CH}_3)_2$ ), 2.19 (sept,  $^3J_{\text{H,H}} = 6.6$  Hz, 4H,  $\text{CH}(\text{CH}_3)_2$ ), 6.94 (s, 2H,  $\text{N-CH}_2\text{-N}$ ), 7.41 (d,  $^3J_{\text{H,H}} = 7.8$  Hz, 4H,  $\text{CH meta}$ ), 7.58 (t,  $^3J_{\text{H,H}} = 7.8$  Hz, 2H,  $\text{CH para}$ ), 8.22 (s, 2H,  $\text{HC=CH}$ ), 8.44 (s, 2H,  $\text{HC=CH}$ ), 10.07 (s, 2H,  $\text{N=CH-N}$ ) ppm.



$^{13}\text{C}\{^1\text{H}\}$  NMR (75 MHz, [d6]-DMSO):  $\delta$  23.6 (CH<sub>3</sub>), 27.8 (CH(CH<sub>3</sub>)<sub>2</sub>), 58.5 (N-CH<sub>2</sub>-N), 123.0 (CH imi), 124.4 (CH meta), 125.5 (CH imi), 129.9 (C ipso), 131.5 (CH para), 138.9 (N=CH-N), 144.6 (C ortho) ppm.

#### 6.6.2.4 (LtBu)<sup>prop</sup>H<sub>2</sub>Br<sub>2</sub> VI-7



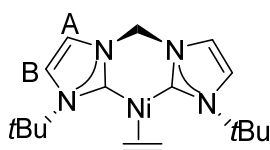
*N*-tert-butylimidazole VI-1 (4.0 g,  $3.22 \times 10^{-2}$  mol, 1 eq.) is diluted in 15 mL of THF in a Fischer-Porter and 1,3-dibromopropane VI-4 (1.64 mL,  $1.61 \times 10^{-2}$  mol, 0,5 eq.) is added to the colorless solution. The reaction mixture is heated for 3 d. at 130 °C; a white to brownish precipitate appears. The solution is filtered away, the product is washed with acetone until it becomes white and dried overnight at 100 °C under vacuum. (LtBu)<sup>prop</sup>H<sub>2</sub>Br<sub>2</sub> VI-7 is gathered as a white powder in 73 % yield (5.317 g).

$^1\text{H}$  NMR (300 MHz, [d6]-DMSO):  $\delta$  1.51 (s, 18H, CH<sub>3</sub>), 3.50 (quint,  $^3J_{\text{H,H}} = 6.6$  Hz, 2H, CH<sub>2</sub>-CH<sub>2</sub>-CH<sub>2</sub>), 4.20 (t,  $^3J_{\text{H,H}} = 6.6$  Hz, 4H, N-CH<sub>2</sub>), 7.83 (s, 2H, HC=CH), 7.98 (s, 2H, HC=CH), 9.37 (s, 2H, N=CH-N) ppm.

$^{13}\text{C}\{^1\text{H}\}$  NMR (75 MHz, [d6]-DMSO):  $\delta$  29.0 (CCH<sub>3</sub>), 29.2 (N-CH<sub>2</sub>-CH<sub>2</sub>-CH<sub>2</sub>-N), 46.1 (N-CH<sub>2</sub>), 59.6 (CCH<sub>3</sub>), 120.3 (CH imi), 122.6 (CH imi), 134.9 (N=CH-N) ppm.

### 6.6.3 Synthesis of [(bis-NHC)Ni(0)-alkene] and [-alkyne] complexes

#### 6.6.3.1 [(LtBu)Ni(C<sub>2</sub>H<sub>4</sub>)] VI-9



Di-tert-butyl-methylene-imidazolium dibromide LtBuH<sub>2</sub>Br<sub>2</sub> VI-5 (400.0 mg,  $9.47 \times 10^{-4}$  mol, 1 eq.) and KOtBu (233.9 mg,  $2.08 \times 10^{-3}$  mol, 2.2 eq.) are mixed together in a Schlenk flask and suspended in 40 mL of Et<sub>2</sub>O. The reaction mixture is stirred for 2 h. at RT before it is filtered in the glovebox to remove precipitated KBr. [Ni(COD)<sub>2</sub>] VI-8 (261.5 mg,  $9.47 \times 10^{-4}$  mol, 1 eq.) is added to the yellow solution and 10 mL of THF are used to rinse the walls of the Schlenk and to help solubilizing [Ni(COD)<sub>2</sub>] VI-8. The solution is freeze-pump-thaw degassed without any previous stirring and 1 bar of ethylene is applied to the Schlenk. The reaction turns bright orange and is stirred overnight at RT. The gas and the solvent are removed under reduced

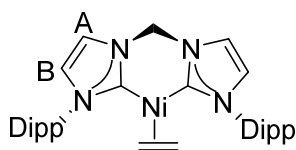
pressure. The residue is washed with  $3 \times 15$  mL of pentane and dried overnight at  $70\text{ }^{\circ}\text{C}$  under vacuum.  $[(\text{LtBu})\text{Ni}(\text{C}_2\text{H}_4)]$  **VI-9** is gathered as a brown product in 75% yield (247.6 mg). Crystals for X-Ray diffraction analysis were grown from a THF solution at  $-25\text{ }^{\circ}\text{C}$ .

**$^1\text{H}$  NMR** (300 MHz, [d8]-THF):  $\delta$  1.06 + 1.20 (AA'BB',  $^3J_{\text{A,A}'} = ^3J_{\text{B,B}'} = 10.4$  Hz,  $^3J_{\text{A,B}'} = 12.3$  Hz,  $^2J_{\text{A,B}} = -2.9$  Hz, 4H,  $\text{H}_2\text{C}=\text{CH}_2$ )\*, 1.68 (s, 18H,  $\text{CCH}_3$ ), 5.63 (d,  $^2J_{\text{H,H}} = 12.3$  Hz, 1H, N- $\text{CH}_2$ -N), 5.97 (d,  $^2J_{\text{H,H}} = 12.3$  Hz, 1H, N- $\text{CH}_2$ -N), 6.94 (d,  $^3J_{\text{H,H}} = 2.1$  Hz, 2H, CH imi B), 7.00 (d,  $^3J_{\text{H,H}} = 2.1$  Hz, 2H, CH imi A) ppm.

**$^{13}\text{C}\{1\text{H}\}$  NMR** (75 MHz, [d8]-THF):  $\delta$  27.7 ( $\text{H}_2\text{C}=\text{CH}_2$ ), 31.0 ( $\text{CCH}_3$ ), 57.2 ( $\text{CCH}_3$ ), 62.9 (N- $\text{CH}_2$ -N), 115.8 (CH imi B), 118.0 (CH imi A), 203.7 (N=C-N) ppm.

\* The coupling constants of the AA'BB' system were determined through simulations performed with TOPSPIN ("module daisy") at 300 MHz and 500 MHz. The simulated spectra can be found in the appendices (7.2).

#### 6.6.3.2 $[(\text{LDipp})\text{Ni}(\text{C}_2\text{H}_4)]$ **VI-10**

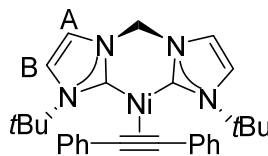


Di-isopropylphenyl-methylene-imidazolium dibromide LDippH<sub>2</sub>Br<sub>2</sub> **VI-6** (400 mg,  $6.34 \times 10^{-4}$  mol, 1 eq.) and KO $t$ Bu (156.6 mg,  $1.40 \times 10^{-3}$  mol, 2.2 eq) are mixed together in a Schlenk flask and suspended in 40 mL of Et<sub>2</sub>O. The reaction mixture is stirred for 2 h. at RT before it is filtered in the glovebox to remove precipitated KBr.  $[\text{Ni}(\text{COD})_2]$  **VI-8** (175.1 mg,  $6.34 \times 10^{-4}$  mol, 1 eq.) is added to the brown solution and 10 mL of THF are used to rinse the walls of the Schlenk and to help solubilizing  $[\text{Ni}(\text{COD})_2]$  **VI-8**. The solution is freeze-pump-thaw degassed without any previous stirring and 1 bar of ethylene is applied to the Schlenk. The solution turns red and is stirred overnight at RT. The gas and the solvent are removed under reduced pressure. The residue is washed with  $3 \times 15$  mL of pentane and dried overnight at  $70\text{ }^{\circ}\text{C}$  under vacuum.  $[(\text{LDipp})\text{Ni}(\text{C}_2\text{H}_4)]$  **VI-10** is gathered as a red product in 71 % (250.7 mg) yield.

**$^1\text{H}$  NMR** (300 MHz, [d8]-THF):  $\delta$  0.14 (s, 4H,  $\text{H}_2\text{C}=\text{CH}_2$ ), 1.02 (d,  $^3J_{\text{H,H}} = 6.9$  Hz, 12H,  $\text{CH}_3$ ), 1.08 (d,  $^3J_{\text{H,H}} = 6.9$  Hz, 12H,  $\text{CH}_3$ ), 2.78 (sept,  $^3J_{\text{H,H}} = 6.9$  Hz, 4H,  $\text{CH}(\text{CH}_3)_2$ ), 5.90 (s, 2H, N- $\text{CH}_2$ -N), 6.89 (d,  $^3J_{\text{H,H}} = 1.8$  Hz, 2H, CH imi B), 7.09 - 7.11 (m, 4H, CH meta), 7.22 (d,  $^3J_{\text{H,H}} = 1.8$  Hz, 2H, CH imi A), 7.21 - 7.26 (m, 2H, CH para) ppm.

$^{13}\text{C}\{^1\text{H}\}$  NMR (75 MHz, [d8]-THF):  $\delta$  23.8 ( $\text{CH}_3$ ), 24.9 ( $\text{CH}_3$ ), 25.2 ( $\text{H}_2\text{C}=\text{CH}_2$ ), 28.8 ( $\text{CH}(\text{CH}_3)_2$ ), 63.1 ( $\text{N}-\text{CH}_2-\text{N}$ ), 118.9 ( $\text{CH}$  imi A), 121.8 ( $\text{CH}$  imi B), 123.3 ( $\text{CH}$  meta), 128.8 ( $\text{CH}$  para), 139.7 ( $\text{C}$  ipso), 146.3 ( $\text{C}$  ortho), 200.1 ( $\text{N}=\text{C}-\text{N}$ ) ppm.

### 6.6.3.3 [(*tert*-Bu)Ni(Ph-C $\equiv$ C-Ph)] VI-13

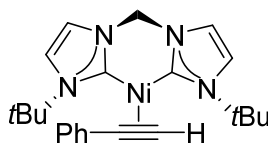


Di-*tert*-butyl-methylene-imidazolium dibromide  $\text{LiBuH}_2\text{Br}_2$  VI-5 (200.0 mg,  $4.74 \times 10^{-4}$  mol, 1 eq.) and  $\text{KO}t\text{Bu}$  (117.0 mg,  $1.04 \times 10^{-3}$  mol, 2.2 eq.) are mixed together in a Schlenk flask and suspended in 20 mL of  $\text{Et}_2\text{O}$ . The reaction mixture is stirred for 2 h. at RT before it is filtered in the glovebox to remove precipitated  $\text{KBr}$ .  $[\text{Ni}(\text{COD})_2]$  VI-8 (130.7 mg,  $4.74 \times 10^{-4}$  mol, 1 eq.) and diphenylacetylene VI-11 (84.4 mg,  $4.74 \times 10^{-4}$  mol, 1 eq.) are added to the yellow solution and 5 mL of THF are used to rinse the walls of the Schlenk and to help solubilizing  $[\text{Ni}(\text{COD})_2]$  VI-8. The reaction turns red and is stirred overnight at RT. The solvent is removed under reduced pressure and the remaining red residue is washed with  $3 \times 8$  mL of pentane and dried overnight at  $70^\circ\text{C}$  under vacuum.  $[(\text{tert}\text{-Bu})\text{Ni}(\text{Ph}-\text{C}\equiv\text{C}-\text{Ph})]$  VI-13 is gathered as a red product in 76 % yield (179.7 mg). Crystals for X-ray diffraction analysis were grown from a saturated THF solution at RT.

$^1\text{H}$  NMR (300 MHz, [d8]-THF):  $\delta$  1.60 (s, 18H,  $\text{CCH}_3$ ), 5.79 (d,  $^2J_{\text{H,H}} = 12.3$  Hz, 1H,  $\text{N}-\text{CH}_2-\text{N}$ ), 6.39 (d,  $^2J_{\text{H,H}} = 12.3$  Hz, 1H,  $\text{N}-\text{CH}_2-\text{N}$ ), 6.78 - 6.84 (m, 2H,  $\text{CH}$  para), 6.96 - 7.01 (m, 4H,  $\text{CH}$  meta), 7.01 (d,  $^3J_{\text{H,H}} = 1.8$  Hz, 2H,  $\text{CH}$  imi B), 7.13 (d,  $^3J_{\text{H,H}} = 1.8$  Hz, 2H,  $\text{CH}$  imi A), 7.17 - 7.21 (m, 4H,  $\text{CH}$  ortho) ppm.

$^{13}\text{C}\{^1\text{H}\}$  NMR (75 MHz, [d8]-THF):  $\delta$  31.1 ( $\text{CCH}_3$ ), 57.6 ( $\text{CCH}_3$ ), 62.9 ( $\text{N}-\text{CH}_2-\text{N}$ ), 117.0 ( $\text{CH}$  imi B), 118.9 ( $\text{CH}$  imi A), 122.9 ( $\text{CH}$  para), 127.5 ( $\text{CH}$  meta), 128.5 ( $\text{CH}$  ortho), 138.7 ( $\text{C}\equiv\text{C}$ ), 140.7 ( $\text{C}-\text{Ph}$ ), 200.9 ( $\text{N}=\text{C}-\text{N}$ ) ppm.

### 6.6.3.4 [(*tert*-Bu)Ni(Ph-C $\equiv$ C-H)] VI-14



Di-*tert*-butyl-methylene-imidazolium dibromide  $\text{LiBuH}_2\text{Br}_2$  VI-5 (200.0 mg,  $4.74 \times 10^{-4}$  mol, 1 eq.) and  $\text{KO}t\text{Bu}$  (117.0 mg,  $1.04 \times 10^{-3}$  mol, 2.2 eq.) are mixed together in a Schlenk flask and suspended in 20 mL of  $\text{Et}_2\text{O}$ . The reaction mixture is stirred for 2 h. at RT before it is filtered

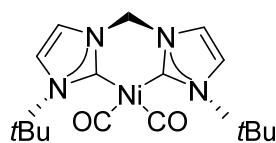
in the glovebox to remove precipitated KBr.  $[\text{Ni}(\text{COD})_2]$  **VI-8** (130.7 mg,  $4.74 \times 10^{-4}$  mol, 1 eq.) and phenylacetylene **VI-12** (52.0  $\mu\text{L}$ ,  $4.74 \times 10^{-4}$  mol, 1 eq.) are added to the yellow solution and 5 mL of THF are used to rinse the walls of the Schlenk and to help solubilizing  $[\text{Ni}(\text{COD})_2]$  **VI-8**. The reaction turns brown and is stirred overnight at RT. The solvent is removed under reduced pressure and the remaining brown residue is washed with  $3 \times 8$  mL of pentane and dried overnight at 70 °C under vacuum.  $[(\text{tBu})\text{Ni}(\text{Ph-C}\equiv\text{C-H})]$  **VI-14** is gathered as a brown product in 73 % yield (146.6 mg). Crystals for X-Ray diffraction analysis were grown from a THF solution at -30 °C.

$^1\text{H NMR}$  (300 MHz, [d8]-THF):  $\delta$  1.57 (s, 9H,  $\text{CCH}_3$ ), 1.83 (s, 9H,  $\text{CCH}_3$ ), 5.70 (d,  $^2J_{\text{H,H}} = 12.3$  Hz, 1H, N- $\text{CH}_2$ -N), 6.14 (d,  $^2J_{\text{H,H}} = 12.3$  Hz, 1H, N- $\text{CH}_2$ -N), 6.49 (s, 1H,  $\text{C}\equiv\text{C-H}$ ), 6.78 - 6.84 (m, 1H, CH para), 6.94 - 7.01 (m, 2H, CH meta), 6.98 (d,  $^3J_{\text{H,H}} = 2.1$  Hz, 1H, CH imi), 7.00 (d,  $^3J_{\text{H,H}} = 2.1$  Hz, 1H, CH imi), 7.05 (d,  $^3J_{\text{H,H}} = 2.1$  Hz, 1H, CH imi), 7.10 (d,  $^3J_{\text{H,H}} = 2.1$  Hz, 1H, CH imi), 7.10 - 7.14 (m, 2H, CH ortho) ppm.

$^{13}\text{C}\{^1\text{H}\}$  NMR (75 MHz, [d8]-THF):  $\delta$  31.0 ( $\text{CCH}_3$ ), 31.1 ( $\text{CCH}_3$ ), 57.6 ( $\text{CCH}_3$ ), 57.8 ( $\text{CCH}_3$ ), 62.8 (N- $\text{CH}_2$ -N), 116.3 (CH imi), 117.0 (CH imi), 118.1 (CH imi), 118.7 (CH imi), 122.9 (CH para), 124.1 ( $\equiv\text{C-H}$ ), 127.5 (CH meta), 128.8 (CH ortho), 138.5 (Ph-C), 140.3 (C ipso), 200.9 (N=C-N), 201.9 (N=C-N) ppm.

## 6.6.4 Synthesis of [(bis-NHC)Ni(0)-carbonyl] complexes

### 6.6.4.1 $[(\text{tBu})\text{Ni}(\text{CO})_2]$ **VI-15**



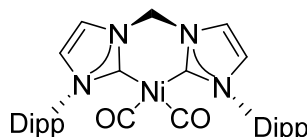
$[(\text{tBu})\text{Ni}(\text{C}_2\text{H}_4)]$  **VI-9** (100 mg,  $3.04 \times 10^{-4}$  mol, 1 eq.) is dissolved in 4 mL of THF. The brown solution is freeze-pump-thaw degassed and 1 bar of CO is applied to the Schlenk. The reaction is stirred for 15 min. at RT. The solution turns yellow and a yellow to orange precipitate falls out. The gas and the solvent are removed under reduced pressure.  $[(\text{tBu})\text{Ni}(\text{CO})_2]$  **VI-15** is gathered as an orange powder in 88 % yield (92.3 mg). Crystals for X-Ray diffraction analysis were grown from an  $\text{Et}_2\text{O}$  solution at -30 °C.

$^1\text{H NMR}$  (300 MHz, [d8]-THF):  $\delta$  1.79 (s, 18H,  $\text{CCH}_3$ ), 5.64 (s, 2H, N- $\text{CH}_2$ -N), 7.12 (d,  $^3J_{\text{H,H}} = 1.8$  Hz, 2H, CH imi), 7.14 (d,  $^3J_{\text{H,H}} = 1.8$  Hz, 2H, CH imi) ppm.

$^{13}\text{C}\{^1\text{H}\}$  NMR (75 MHz, [d8]-THF):  $\delta$  30.2 (CCH<sub>3</sub>), 58.2 (CCH<sub>3</sub>), 63.1 (N-CH<sub>2</sub>-N), 117.4 (CH imi), 118.4 (CH imi), 199.3 (N=C-N), 204.2 (C=O) ppm.

IR (cm<sup>-1</sup>):  $\nu$  (C=O) = 1952 (s); 1874 (s).

#### 6.6.4.2 [(LDipp)Ni(CO)<sub>2</sub>] VI-16



[(LDipp)Ni(C<sub>2</sub>H<sub>4</sub>)] VI-10 (100 mg, 1.80×10<sup>-4</sup> mol, 1 eq.) is dissolved in 4 mL of THF. The red solution is freeze-pump-thaw degassed and 1 bar of CO is applied to the Schlenk. The reaction mixture rapidly turns yellow-brownish. The gas and the solvent are removed under reduced pressure. [(LDipp)Ni(CO)<sub>2</sub>] VI-16 is gathered as a brown powder in 77 % yield (81.0 mg).

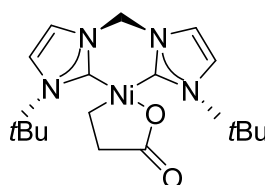
$^1\text{H}$  NMR (300 MHz, [d8]-THF):  $\delta$  1.01 (d,  $^3J_{\text{H,H}} = 6.9$  Hz, 12H, CH<sub>3</sub>), 1.15 (d,  $^3J_{\text{H,H}} = 6.9$  Hz, 12H, CH<sub>3</sub>), 2.67 (sept,  $^3J_{\text{H,H}} = 6.9$  Hz, 4H, CH(CH<sub>3</sub>)<sub>2</sub>), 5.85 (s, 2H, N-CH<sub>2</sub>-N), 7.05 (d,  $^3J_{\text{H,H}} = 1.8$  Hz, 2H, CH imi), 7.15 - 7.18 (m, 4H, CH meta), 7.26 - 7.31 (m, 2H, CH para), 7.37 (d,  $^3J_{\text{H,H}} = 1.8$  Hz, 2H, CH imi) ppm.

$^{13}\text{C}\{^1\text{H}\}$  NMR (75 MHz, [d8]-THF):  $\delta$  23.3 (CH<sub>3</sub>), 25.3 (CH<sub>3</sub>), 28.6 (CH(CH<sub>3</sub>)<sub>2</sub>), 63.4 (N-CH<sub>2</sub>-N), 119.7 (CH imi), 123.1 (CH imi), 123.8 (CH meta), 129.3 (CH para), 138.4 (C ipso), 146.6 (C ortho), 204.3 (C=O), 205.0 (N=C-N) ppm.

IR (cm<sup>-1</sup>):  $\nu$  (C=O) = 1960 (s); 1891 (s).

### 6.6.5 Synthesis of [(bis-NHC)nickelalactones]

#### 6.6.5.1 [(*t*Bu)Ni(CH<sub>2</sub>CH<sub>2</sub>COO- $\kappa$ C, $\kappa$ O)] VI-18



Di-*tert*-butyl-methylene-imidazolium dibromide *t*BuH<sub>2</sub>Br<sub>2</sub> VI-5 (400 mg, 9.47×10<sup>-4</sup> mol, 1 eq.) and KO*t*Bu (233.9 mg, 2.08×10<sup>-3</sup> mol, 2.2 eq.) are mixed together in a Schlenk flask and suspended in 40 mL of Et<sub>2</sub>O. The reaction mixture is stirred for 2 h. at RT before it is filtered in the glovebox to remove precipitated KBr. [(tmeda)nickelalactone] VI-17 (234.0 mg, 9.47×10<sup>-4</sup> mol, 1 eq.) is added to the yellow solution and 10 mL of THF are used to rinse the

walls of the Schlenk and to help solubilizing the reagent. The reaction is stirred overnight at RT, a beige product falls out of the solution. The supernatant is removed through a cannula and the residue is washed with  $1 \times 15$  mL of THF,  $1 \times 15$  mL of Et<sub>2</sub>O and  $3 \times 15$  mL of pentane. The product is dried overnight at 60 °C under vacuum. [(*Lt*Bu)Ni(CH<sub>2</sub>CH<sub>2</sub>COO-κC,κO)] **VI-23** is gathered as a beige product in 83 % yield (307.5 mg). It is nearly insoluble in THF, Et<sub>2</sub>O and hydrocarbons and has a limited solubility in CH<sub>2</sub>Cl<sub>2</sub> and CH<sub>3</sub>CN. Crystals for X-Ray diffraction analysis were grown from an acetonitrile solution at RT.

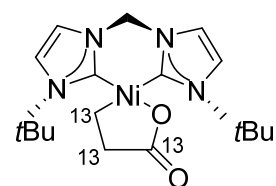
Note: In DMF, formation of [(*Lt*Bu)Ni(carbonate)] **VI-24** and of the product giving rise to a singlet at  $\delta = 1.88$  ppm in <sup>1</sup>H NMR is observed. [(*Lt*Bu)Ni(carbonate)] **VI-24** crystals were grown from the DMF solution at -30 °C. The crystallographic data are available in the appendices.

<sup>1</sup>H NMR (300 MHz, CD<sub>3</sub>CN):  $\delta$  0.47 (m, 1H, Ni-CH<sub>2</sub>), 0.74 (m, 1H, Ni-CH<sub>2</sub>), 1.75 (s, 9H, CCH<sub>3</sub>), 1.85 (s, 9H, CCH<sub>3</sub>), 2.03 (m, 2H, O-C(O)-CH<sub>2</sub>), 5.96 (d, <sup>2</sup>J<sub>H,H</sub> = 12.9 Hz, 1H, N-CH<sub>2</sub>-N), 6.99 (d, <sup>3</sup>J<sub>H,H</sub> = 2.1 Hz, 1H, CH imi), 7.04 (d, <sup>3</sup>J<sub>H,H</sub> = 2.1 Hz, 1H, CH imi), 7.12 (d, <sup>2</sup>J<sub>H,H</sub> = 12.9 Hz, 1H, N-CH<sub>2</sub>-N), 7.20 (d, <sup>3</sup>J<sub>H,H</sub> = 2.1 Hz, 1H, CH imi), 7.23 (d, <sup>3</sup>J<sub>H,H</sub> = 2.1 Hz, 1H, CH imi) ppm.

<sup>13</sup>C{<sup>1</sup>H} NMR (75 MHz, CD<sub>3</sub>CN):  $\delta$  9.6 (Ni-CH<sub>2</sub>), 31.2 (CCH<sub>3</sub>), 31.8 (CCH<sub>3</sub>), 37.8 (O-C(O)-CH<sub>2</sub>), 58.7 (CCH<sub>3</sub>), 58.75 (CCH<sub>3</sub>), 64.1 (N-CH<sub>2</sub>-N), 118.6 (CH imi), 119.6 (CH imi), 120.6 (CH imi), 121.3 (CH imi), 180.6 (N=C-N), 186.1 (N=C-N), 189.6 (C=O) ppm.

IR (cm<sup>-1</sup>):  $\nu$  (C=O) = 1619 (m).

#### 6.6.5.2 <sup>13</sup>C[(*Lt*Bu)Ni(CH<sub>2</sub>CH<sub>2</sub>COO-κC,κO)] **VI-18**(<sup>13</sup>C)

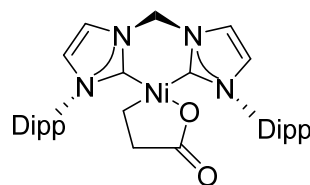


<sup>13</sup>C[(*Lt*Bu)Ni(CH<sub>2</sub>CH<sub>2</sub>COO-κC,κO)] **VI-18**(<sup>13</sup>C) was synthesized following the same procedure by using <sup>13</sup>C[(*tmeda*)nickelalactone] **VI-18**(<sup>13</sup>C). Starting from 371.6 mg ( $8.80 \times 10^{-4}$  mol, 1 eq.) of di-*tert*-butyl-methylene-imidazolium dibromide *Lt*BuH<sub>2</sub>Br<sub>2</sub> **VI-5**, <sup>13</sup>C[(*Lt*Bu)Ni(CH<sub>2</sub>CH<sub>2</sub>COO-κC,κO)] **VI-18**(<sup>13</sup>C) was isolated as a beige product in 79 % yield (274 mg).

**$^1\text{H}$  NMR** (300 MHz,  $\text{CD}_3\text{CN}$ ):  $\delta$  0.20 - 0.30 + 0.63 - 0.73 (m, 1H,  $\text{Ni-}^{13}\text{CH}_2$ ), 0.47 - 0.58 + 0.86 - 1.00 (m, 1H,  $\text{Ni-}^{13}\text{CH}_2$ ), 1.75 (s, 9H,  $\text{CCH}_3$ ), 1.85 (s, 9H,  $\text{CCH}_3$ ), 1.94 (m, 2H,  $\text{O-C(O)-}^{13}\text{CH}_2$ ), 5.96 (d,  $^2J_{\text{H,H}} = 12.9$  Hz, 1H,  $\text{N-CH}_2\text{-N}$ ), 6.99 (d,  $^3J_{\text{H,H}} = 2.1$  Hz, 1H,  $\text{CH imi}$ ), 7.04 (d,  $^3J_{\text{H,H}} = 2.1$  Hz, 1H,  $\text{CH imi}$ ), 7.13 (d,  $^2J_{\text{H,H}} = 12.9$  Hz, 1H,  $\text{N-CH}_2\text{-N}$ ), 7.20 (d,  $^3J_{\text{H,H}} = 2.1$  Hz, 1H,  $\text{CH imi}$ ), 7.23 (d,  $^3J_{\text{H,H}} = 2.1$  Hz, 1H,  $\text{CH imi}$ ) ppm.

**$^{13}\text{C}\{^1\text{H}\}$  NMR** (75 MHz,  $\text{CD}_3\text{CN}$ ):  $\delta$  9.6 (dd,  $^1J_{\text{C,C}} = 32.2$  Hz,  $^2J_{\text{C,C}} = 1.4$  Hz,  $\text{Ni-}^{13}\text{CH}_2$ ), 31.3 ( $\text{CCH}_3$ ), 31.8 ( $\text{CCH}_3$ ), 37.8 (dd,  $^1J_{\text{C,C}} = 51.6$  Hz,  $^1J_{\text{C,C}} = 32.2$  Hz,  $\text{O-C(O)-}^{13}\text{CH}_2$ ), 58.7 ( $\text{CCH}_3$ ), 58.8 ( $\text{CCH}_3$ ), 64.1 ( $\text{N-CH}_2\text{-N}$ ), 118.6 ( $\text{CH imi}$ ), 119.6 ( $\text{CH imi}$ ), 120.6 ( $\text{CH imi}$ ), 121.3 ( $\text{CH imi}$ ), 187.2 ( $\text{N=C-N}$ ), 187.9 ( $\text{N=C-N}$ ), 189.6 (dd,  $^1J_{\text{C,C}} = 51.6$  Hz,  $^2J_{\text{C,C}} = 1.4$  Hz,  $\text{C=O}$ ) ppm.

#### 6.6.5.3 [(LDipp)Ni( $\text{CH}_2\text{CH}_2\text{COO-}\kappa\text{C},\kappa\text{O}$ )] **VI-19**



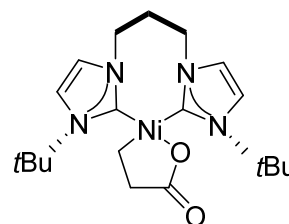
Di-isopropylphenyl-methylene-imidazolium dibromide  $\text{LDippH}_2\text{Br}_2$  **VI-6** (400 mg,  $6.34 \times 10^{-4}$  mol, 1 eq.) and  $\text{KO}t\text{Bu}$  (156.6 mg,  $1.40 \times 10^{-3}$  mol, 2.2 eq.) are mixed together in a Schlenk flask and suspended in 40 mL of  $\text{Et}_2\text{O}$ . The reaction mixture is stirred for 2 h. at RT before it is filtered in the glovebox to remove precipitated  $\text{KBr}$ . [(tmeda)nickelalactone] **VI-17** (156.7 mg,  $6.34 \times 10^{-4}$  mol, 1 eq.) is added to the brown solution and 10 mL of THF are used to rinse the walls of the Schlenk and to help solubilizing the reagent. The reaction is stirred overnight at RT; a beige product falls out of the solution. The supernatant is removed through a cannula and the residue is washed with  $1 \times 15$  mL of THF,  $1 \times 15$  mL of  $\text{Et}_2\text{O}$  and  $3 \times 15$  mL of pentane. The product is dried overnight at  $60^\circ\text{C}$  under vacuum. [(LDipp)Ni( $\text{CH}_2\text{CH}_2\text{COO-}\kappa\text{C},\kappa\text{O}$ )] **VI-19** is gathered as a beige product in 86 % yield (325.0 mg). It has poor solubility in common organic solvents.

**$^1\text{H}$  NMR** (300 MHz,  $\text{MeOD}$ ):  $\delta$  0.17 (t,  $^3J_{\text{H,H}} = 7.2$  Hz, 2H,  $\text{Ni-CH}_2$ ), 1.04 (d,  $^3J_{\text{H,H}} = 6.9$  Hz, 6H,  $\text{CH}_3$ ), 1.10 (d,  $^3J_{\text{H,H}} = 6.9$  Hz, 6H,  $\text{CH}_3$ ), 1.34 (d,  $^3J_{\text{H,H}} = 6.9$  Hz, 6H,  $\text{CH}_3$ ), 1.37 (d,  $^3J_{\text{H,H}} = 6.9$  Hz, 6H,  $\text{CH}_3$ ), 1.52 (t,  $^3J_{\text{H,H}} = 7.2$  Hz, 2H,  $\text{O-C(O)-CH}_2$ ), 2.61 (sept,  $^3J_{\text{H,H}} = 6.9$  Hz, 2H,  $\text{CH}(\text{CH}_3)_2$ ), 2.95 (sept,  $^3J_{\text{H,H}} = 6.9$  Hz, 2H,  $\text{CH}(\text{CH}_3)_2$ ), 6.35 (s, 2H,  $\text{N-CH}_2\text{-N}$ ), 7.02 (d,  $^3J_{\text{H,H}} = 1.8$  Hz, 1H,  $\text{CH imi}$ ), 7.05 (d,  $^3J_{\text{H,H}} = 2.1$  Hz, 1H,  $\text{CH imi}$ ), 7.18 - 7.28 (m, 4H,  $\text{CH meta}$ ), 7.31 - 7.44 (m, 2H,  $\text{CH para}$ ), 7.50 (d,  $^3J_{\text{H,H}} = 2.1$  Hz, 1H,  $\text{CH imi}$ ), 7.52 (d,  $^3J_{\text{H,H}} = 1.8$  Hz, 1H,  $\text{CH imi}$ ) ppm.

$^{13}\text{C}$ -NMR (75 MHz, MeOD):  $\delta$  7.7 (Ni-CH<sub>2</sub>), 23.7 (CH<sub>3</sub>), 23.8 (CH<sub>3</sub>), 25.6 (CH<sub>3</sub>), 25.9 (CH<sub>3</sub>), 29.6 (CH(CH<sub>3</sub>)<sub>2</sub>), 29.7 (CH(CH<sub>3</sub>)<sub>2</sub>), 38.5 (O-C(O)-CH<sub>2</sub>), 63.0 (N-CH<sub>2</sub>-N), 120.0 (CH imi), 121.4 (CH imi), 124.1 (CH meta), 124.9 (CH meta), 126.8 (CH imi), 127.2 (CH imi), 130.3 (CH para), 130.6 (CH para), 137.8 (C ipso), 138.2 (C ipso), 146.4 (C ortho), 146.5 (C ortho), 176.7 (N=C-N), 186.0 (N=C-N), 194.3 (C=O) ppm.

IR (cm<sup>-1</sup>):  $\nu$  (C=O) = 1562 (m).

#### 6.6.5.4 [(*Li*tBu)<sup>prop</sup>Ni(CH<sub>2</sub>CH<sub>2</sub>COO- $\kappa$ C, $\kappa$ O)] VI-20



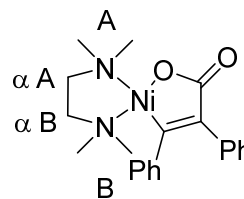
Di-*tert*-butyl-propylene-imidazolium dibromide *Li*tBu<sup>prop</sup>H<sub>2</sub>Br<sub>2</sub> VI-7 (200 mg, 4.44×10<sup>-4</sup> mol, 1 eq.) and KO*t*Bu (109.6 mg, 9.77×10<sup>-4</sup> mol, 2.2 eq.) are mixed together in a Schlenk flask and suspended in 20 mL of Et<sub>2</sub>O. The reaction mixture is stirred for 2 h. at RT before it is filtered in the glovebox to remove precipitated KBr. [(tmeda)nickelalactone] VI-17 (109.6 mg, 9.77×10<sup>-4</sup> mol, 1 eq.) is added to the colorless solution and 6 mL of THF are used to rinse the walls of the Schlenk and to help solubilizing the reagent. The reaction is stirred overnight at RT; a beige product falls out of the solution. The supernatant is removed through a cannula and the residue is washed with 1 × 7 mL of THF, 1 × 7 mL of Et<sub>2</sub>O and 3 × 7 mL of pentane. The product is dried overnight at 60 °C under vacuum. [(*Li*tBu)<sup>prop</sup>Ni(CH<sub>2</sub>CH<sub>2</sub>COO- $\kappa$ C, $\kappa$ O)] VI-20 is gathered as a beige product in 62 % yield (116.0 mg). It has poor solubility in common organic solvents. Crystals for X-Ray diffraction analysis were grown at RT from a THF solution first layered with Et<sub>2</sub>O, then with pentane.

$^1\text{H}$  NMR (500 MHz, CD<sub>3</sub>CN):  $\delta$  0.19 (m, 2H, Ni-CH<sub>2</sub>), 1.94 (s, 18H, CCH<sub>3</sub>), 1.96 (m, 2H, O-C(O)-CH<sub>2</sub>), 4.28 (m, 3H, N-CH<sub>2</sub>-CH<sub>2</sub>-CH<sub>2</sub>-N), 5.76 (m, 3H, N-CH<sub>2</sub>-CH<sub>2</sub>-CH<sub>2</sub>-N), 6.90 (br s, 2H, CH imi), 6.96 (d, <sup>3</sup>J<sub>H,H</sub> = 2.0 Hz, 2H, CH imi), 7.00 (d, <sup>3</sup>J<sub>H,H</sub> = 2.0 Hz, 2H, CH imi), 7.07 (br s, 2H, CH imi) ppm.

$^{13}\text{C}\{^1\text{H}\}$  NMR (125 MHz, CD<sub>3</sub>CN):  $\delta$  8.2 (Ni-CH<sub>2</sub>), 31.9 (CCH<sub>3</sub>), 38.5 (O-C(O)-CH<sub>2</sub>), 49.2 (N-CH<sub>2</sub>-CH<sub>2</sub>-CH<sub>2</sub>-N), 58.5 (CCH<sub>3</sub>), 119.2 (CH imi), 119.4 (CH imi), 122.2 (CH imi), 123.3 (CH imi), 179.3 (N=C-N), 189.2 (C=O) ppm.

IR (cm<sup>-1</sup>):  $\nu$  (C=O) = 1615 (m)



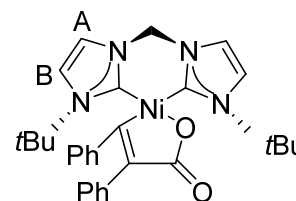
6.6.5.5 [(tmeda)Ni(C(Ph)=C(Ph)COO-κC,κO)] **VI-21**


[(tmeda)Ni(C(Ph)=C(Ph)COO-κC,κO)] **VI-21** was prepared according to a modified published procedure.<sup>[34]</sup> [Ni(COD)<sub>2</sub>] **VI-8** (500 mg, 1.81×10<sup>-3</sup> mol, 1 eq.) is mixed with diphenylacetylene **VI-11** (322.8 mg, 1.81×10<sup>-3</sup> mol, 1 eq.) in a Fischer-Porter and suspended in 10 mL of THF. Tmeda (1.36 mL, 9.06×10<sup>-3</sup> mol, 5 eq.) is added to the reaction mixture which is then freeze-pump-thaw degassed. The vessel is pressurized with 5 bar of CO<sub>2</sub> and reacted over the weekend at RT. The solution turns red and an orange precipitate falls out. The supernatant is filtered away and the remaining product is washed with 3 × 8 mL of Et<sub>2</sub>O and dried overnight under vacuum at RT. [(tmeda)Ni(C(Ph)=C(Ph)COO-κC,κO)] **VI-21** is gathered as an orange product in 61 % yield (435.5 mg). Crystals for X-Ray diffraction analysis were grown at -30 °C from a CD<sub>2</sub>Cl<sub>2</sub> solution.

<sup>1</sup>H NMR (300 MHz, CD<sub>2</sub>Cl<sub>2</sub>): δ 1.96 (s, 6H, N(CH<sub>3</sub>)<sub>2</sub> A), 2.24 (br s, 2H, N-CH<sub>2</sub> αB), 2.26 (br s, 2H, N-CH<sub>2</sub> αA), 2.64 (s, 6H, N(CH<sub>3</sub>)<sub>2</sub> B), 6.86 - 6.90 (m, 2H, CH ortho), 6.93 - 7.05 (m, 4H, CH meta), 7.06 - 7.09 (m, 4H, CH ortho + para) ppm.

<sup>13</sup>C{<sup>1</sup>H} NMR (75 MHz, CD<sub>2</sub>Cl<sub>2</sub>): δ 47.4 (N(CH<sub>3</sub>)<sub>2</sub> B), 48.7 (N(CH<sub>3</sub>)<sub>2</sub> A), 56.8 (N-CH<sub>2</sub> αB), 63.5 (N-CH<sub>2</sub> αA), 124.7 (CH para), 125.3 (CH para), 126.9 (CH meta), 127.6 (CH meta), 127.9 (CH ortho), 130.2 (CH ortho), 139.7 (C ipso), 147.2 (Ni-C(Ph)=C), 157.5 (O-C(O)-C(Ph)), 180.0 (C=O) ppm.

IR (cm<sup>-1</sup>): ν (C=O) = 1633 (m).

 6.6.5.6 [(*t*Bu)Ni(C(Ph)=C(Ph)COO-κC,κO)] **VI-22**


Di-*tert*-butyl-methylene-imidazolium dibromide *t*BuH<sub>2</sub>Br<sub>2</sub> **VI-5** (200 mg, 4.74×10<sup>-4</sup> mol, 1 eq.) and KO*t*Bu (117.0 mg, 1.04×10<sup>-3</sup> mol, 2.2 eq.) are mixed together in a Schlenk flask and suspended in 20 mL of Et<sub>2</sub>O. The reaction mixture is stirred for 2 h. at RT before it is filtered in the glovebox to remove precipitated KBr. [(tmeda)nickela-4,5-diphenyl-lactone] **VI-21**

(188.1 mg,  $4.74 \times 10^{-4}$  mol, 1 eq.) is added to the yellow solution and 6 mL of THF are used to rinse the walls of the Schlenk and to help solubilizing the reagent. The reaction is stirred overnight at RT; a yellow product falls out of the solution. The supernatant is removed through a cannula and the residue is washed with  $2 \times 8$  mL of Et<sub>2</sub>O and  $3 \times 8$  mL of pentane. The product is dried overnight at 60 °C under vacuum. [(*Li*Bu)Ni(C(Ph)=C(Ph)COO-κC,κO)] **VI-22** is gathered as a yellow product in 86 % yield (221.2 mg). It has poor solubility in common organic solvents. Crystals for X-ray diffraction analysis were grown from a saturated acetonitrile solution at RT.

**<sup>1</sup>H NMR** (300 MHz, CD<sub>3</sub>CN): δ 1.41 (s, 9H, CCH<sub>3</sub>), 1.84 (s, 9H, CCH<sub>3</sub>), 6.10 (d, <sup>2</sup>J<sub>H,H</sub> = 12.6 Hz, 1H, N-CH<sub>2</sub>-N), 6.48 – 6.51 (m, 2H, CH ortho), 6.73 (d, <sup>3</sup>J<sub>H,H</sub> = 2.1 Hz, 1H, CH imi B), 6.72 - 6.78 (m, 1H, CH para), 6.82 - 6.91 (m, 2H, CH ortho), 6.88 - 6.97 (m, 1H, CH para), 6.93 - 7.02 (m, 4H, CH meta), 7.12 (d, <sup>3</sup>J<sub>H,H</sub> = 1.8 Hz, 1H, CH imi A), 7.25 (d, <sup>3</sup>J<sub>H,H</sub> = 2.1 Hz, 1H, CH imi A), 7.35 (d, <sup>3</sup>J<sub>H,H</sub> = 1.8 Hz, 1H, CH imi B), 7.45 (d, <sup>2</sup>J<sub>H,H</sub> = 12.6 Hz, 1H, N-CH<sub>2</sub>-N) ppm.

**<sup>13</sup>C{<sup>1</sup>H} NMR** (75 MHz, CD<sub>3</sub>CN): δ 30.6 (CCH<sub>3</sub>), 31.3 (CCH<sub>3</sub>), 58.5 (CCH<sub>3</sub>), 59.2 (CCH<sub>3</sub>), 64.3 (N-CH<sub>2</sub>-N), 119.3 (CH imi A), 120.5 (CH imi B), 121.2 (CH imi B), 122.3 (CH imi A), 123.9 (CH para), 125.2 (CH para), 127.3 (CH meta), 127.6 (CH meta), 127.7 (CH ortho), 131.6 (CH ortho), 141.0 (Ni-C(Ph)), 141.6 (O-C(O)-C(Ph)), 142.0 (C ipso), 176.0 (N-C-N), 176.5 (C=O), 179.5 (N=C-N) ppm.

**IR** (cm<sup>-1</sup>): ν (C=O) = 1604 (m).

## 6.7 References

- [1] A. J. Arduengo, R. L. Harlow, M. Kline, *J. Am. Chem. Soc.*, **1991**, *113*, 361 - 363.
- [2] D. Bourissou, O. Guerret, F. P. Gabbaï, G. Bertrand, *Chem. Rev.*, **2000**, *100*, 39 - 91.
- [3] F. E. Hahn, M. C. Jahnke, *Angew. Chem. Int. Ed.*, **2008**, *47*, 3122 - 3172.
- [4] M. N. Hopkinson, C. Richter, M. Schedler, F. Glorius, *Nature*, **2014**, *510*, 485 - 495.
- [5] W. A. Herrmann, *Angew. Chem. Int. Ed.*, **2002**, *41*, 1290 - 1309.
- [6] S. Díez-González, N. Marion, S. P. Nolan, *Chem. Rev.*, **2009**, *109*, 3612 - 3676.
- [7] A. T. Normand, K. J. Cavell, *Eur. J. Inorg. Chem.*, **2008**, 2781 - 2800.
- [8] M. Scholl, S. Ding, C. W. Lee, R. H. Grubbs, *Org. Lett.*, **1999**, *1*, 953 - 956.
- [9] W. A. Herrmann, M. Elison, J. Fischer, C. Köcher, G. R. J. Artus, *Angew. Chem Int. Ed.*, **1995**, *34*, 2371 - 2374.
- [10] W. A. Herrmann, C. P. Reisinger, M. J. Spiegler, *J. Organomet. Chem.*, **1998**, *557*, 93 - 96.
- [11] C. W. K. Gstottmayr, V. P. W. Bohm, E. Herdtweck, M. Grosche, W. A. Herrmann, *Angew. Chem. Int. Ed.*, **2002**, *41*, 1363 - 1365.
- [12] O. Navarro, R. A. III Kelly, S. P. Nolan, *J. Am. Chem. Soc.*, **2003**, *125*, 16194 - 16195.
- [13] N. Marion, O. Navarro, J. Mei, E. D. Stevens, N. M. Scott, S. P. Nolan, *J. Am. Chem. Soc.*, **2006**, *128*, 4101 - 4111.
- [14] C. J. O'Brien, E. A. B. Kantchev, C. Valente, N. Hadei, G. A. Chass, A. Lough, A. C. Hopkinson, M. G. Organ, *Chem. Eur. J.*, **2006**, *12*, 4743 - 4748.
- [15] H. V. Huynh, R. Jothibas, *Eur. J. Inorg. Chem.*, **2009**, 1926 - 1931.
- [16] W. A. Herrmann, J. Schwarz, M. G. Gardiner, M. Spiegler, *J. Organomet. Chem.*, **1999**, *575*, 80 - 86.
- [17] R. E. Douthwaite, D. Haüssinger, M. L. H. Green, P. J. Silcock, P. T. Gomes, A. M. Martins, A. A. Danopoulos, *Organomet.*, **1999**, *18*, 4584 - 4590.
- [18] T. A. P. Paulose, S.-C. Wu, J. A. Olson, T. Chau, N. Theaker, M. Hassler, J. W. Quail, S. R. Foley, *Dalton Trans.*, **2012**, *41*, 251 - 260.

- [19] D. S. Clyne, J. Jin, E. Genest, J. C. Gallucci, T. V. RajanBabu, *Org. Lett.*, **2000**, *2*, 1125 - 1128.
- [20] M. V. Baker, B. W. Skelton, A. H. White, C. C. Williams, *J. Chem. Soc., Dalton. Trans.*, **2001**, 111 - 120.
- [21] J. Berding, M. Lutz, A. L. Spek, E. Bouwman, *Organomet.*, **2009**, *28*, 1845 - 1854.
- [22] J. Berding, M. Lutz, A. L. Spek, E. Bouwman, *Appl. Organomet. Chem.*, **2011**, *25*, 76 - 81.
- [23] A. Huffer, B. Jeffery, B. J. Waller, A. A. Danopoulos, *C. R. Chimie*, **2013**, *16*, 557 - 565.
- [24] R. E. Douthwaite, M. L. H. Green, P. J. Silcock, P. T. Gomes, *Organomet.*, **2001**, *20*, 2611 - 2615.
- [25] J. Guo, L. Lv, X. Wang, C. Cao, G. Pang, Y. Shi, *Inorg. Chem. Commun.*, **2013**, *31*, 74 - 78.
- [26] N. D. Harrold, G. L. Hillhouse, *Chem. Sci.*, **2013**, *4*, 4011 - 4015.
- [27] M. Brendel, C. Braun, F. Rominger, P. Hofmann, *Angew. Chem. Int. Ed.*, **2014**, *53*, 8741 - 8745.
- [28] M. H. Reineke, M. D. Sampson, A. L. Rheingold, C. P. Kubiak, *Inorg. Chem.*, **2015**, *54*, 3211 - 3217.
- [29] G. Tan, S. Enthaler, S. Inoue, B. Blom, M. Driess, *Angew. Chem. Int. Ed.*, **2015**, *54*, 2214 - 2218.
- [30] J. Langer, D. Walther, H. Görls, *J. Organomet. Chem.*, **2006**, *691*, 4874 - 4881.
- [31] S. Sauerbrey, P. K. Majhi, J. Daniels, G. Schnakenburg, G. M. Brändle, K. Scherer, R. Streubel, *Inorg. Chem.*, **2011**, *50*, 793 - 799.
- [32] J. Liu, J. Chen, J. Zhao, Y. Zhao, L. Li, H. Zhang, *Synthesis*, **2003**, *17*, 2661 - 2666.
- [33] T. Scherg, S. A. Schneider, G. D. Frey, J. Schwarz, E. Herdtweck, W. A. Herrmann, *Synlett*, **2006**, 2894 - 2907.
- [34] H. Hoberg, D. Schaefer, G. Burkhart, C. Krüger, M. J. Romao, *J. Organomet. Chem.*, **1984**, *266*, 203 - 224.
- [35] M. L. Lejkowski, R. Lindner, T. Kageyama, G. E. Bódizs, P. N. Plessow, I. B. Müller, A. Schäfer, F. Rominger, P. Hofmann, C. Futter, S. A. Schunk, M. Limbach, *Chem. Eur. J.*, **2012**, *18*, 14017 - 14025.

- [36] N. Huguet, I. Jevtovikj, A. Gordillo, M. L. Lejkowski, R. Lindner, M. Bru, A. Y. Khalimon, F. Rominger, S. A. Svhunk, P. Hofmann, M. Limbach, *Chem. Eur. J.*, **2014**, *20*, 16858 - 16862.
- [37] C. Hendriksen, E. A. Pidko, G. Yang, B. Schöffner, D. Vogt, *Chem. Eur. J.*, **2014**, *20*, 12037 – 12040.
- [38] R. Fischer, B. Nestler, H. Schütz, *Z. Anorg. All. Chem.*, **1989**, *577*, 111 - 114.
- [39] P. Anbarasan, T. Schareina, M. Beller, *Chem. Soc. Rev.*, **2011**, *40*, 5049 - 5067.
- [40] L. Cassar, *J. Organomet. Chem.*, **1973**, *54*, C57 – C58.
- [41] Y. Sakakibara, F. Okuda, A. Shimoyabashi, K. Kirino, M. Sakai, N. Uchino, K. Takagi, *Bull. Chem. Soc. Jpn.*, **1988**, *61*, 1985 - 1990.
- [42] Y. Sakakibara, Y. Ido, K. Sasaki, M. Sakai, N. Uchino, *Bull. Chem. Soc. Jpn.*, **1993**, *66*, 2776 - 2778.
- [43] V. Percec, J.-Y. Bae, D. H. Hill, *J. Org. Chem.*, **1995**, *60*, 6895 - 6903.
- [44] F. Burg, J. Egger, J. Deutsch, N. Guimond, *Org. Process Res. Dev.*, **2016**, *20*, 1540 - 1545.
- [45] Y. Nakao, S. Oda, T. Hiyama, *J. Am. Chem. Soc.*, **2004**, *126*, 13904 - 13905.
- [46] Y. Nakao, S. Oda, A. Yada, T. Hiyama, *Tetrahedron*, **2006**, *62*, 7567 - 7576.
- [47] Y. Nakao, A. Yada, S. Ebata, T. Hiyama, *J. Am. Chem. Soc.*, **2007**, *129*, 2428 - 2429.
- [48] Y.-Y. Ohnishi, Y. Nakao, H. Sato, Y. Nakao, T. Hiyama, S. Sakaki, *Organomet.*, **2009**, *28*, 2583 - 2594.

# Appendices



## 7 Appendices

### 7.1 Crystallographic data

Selected crystallographic data are summarized in the following tables.

The residual factors are defined as follows:

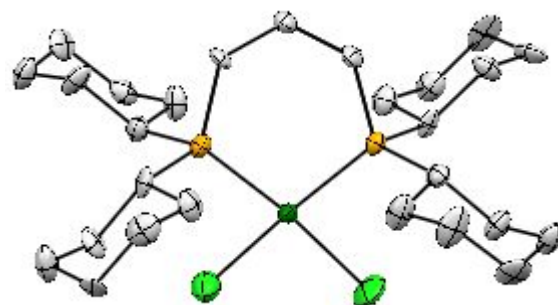
$$R_1 = \frac{\sum ||F_o| - |F_c||}{\sum |F_o|}$$

$$wR_2 = \sqrt{\frac{\sum [w(F_o^2 - F_c^2)]^2}{\sum [w(F_o^2)]^2}}$$



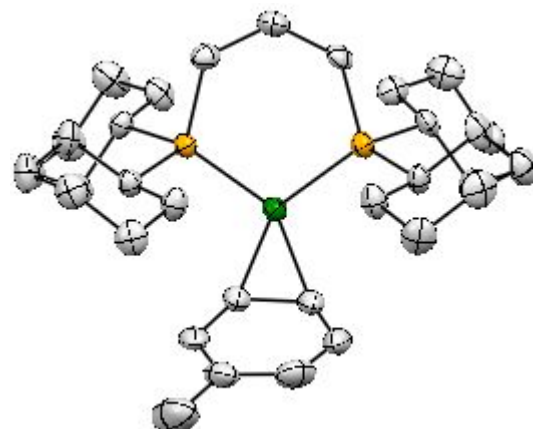
7.1.1 [(dcpp)NiCl<sub>2</sub>] II-3

ID	Florian4
Formula	C <sub>27</sub> H <sub>49</sub> Cl <sub>2</sub> NiP <sub>2</sub>
Molecular weight (g.mol <sup>-1</sup> )	565.21
Crystal system	monoclinic
Space group	<i>P n</i>
<i>a</i> (Å)	9.455(4)
<i>b</i> (Å)	8.841(4)
<i>c</i> (Å)	16.771(9)
$\alpha$ (°)	90
$\beta$ (°)	91.255(14)
$\gamma$ (°)	90
Volume (Å <sup>3</sup> )	1401.6(12)
<i>Z</i>	2
Calculated density (g.cm <sup>-3</sup> )	1.339
Absorption coefficient (mm <sup>-1</sup> )	1.011
<i>F</i> (000)	606
Crystal size (mm <sup>3</sup> )	0.251 x 0.121 x 0.060
Temperature (K)	193(2)
Wavelength (Å)	0.71073
Reflections collected	4941
Independent reflections ( <i>R</i> <sub>int</sub> )	2350 (0.0943)
Reflections used for refinement	2350
Refined parameters	299
GOF on <i>F</i> <sup>2</sup>	1.179
<i>R</i> <sub>1</sub> [ <i>I</i> > 2σ( <i>I</i> )]	0.0497
w <i>R</i> <sub>2</sub> [all data]	0.1721



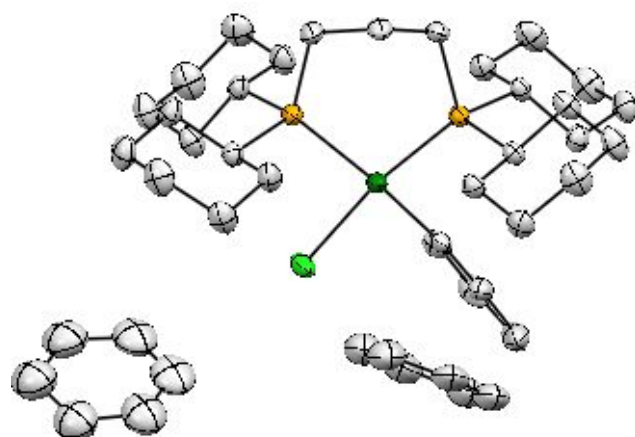
## 7.1.2 [(dcpp)Ni(toluene)] II-4

ID	Florian26_a
Formula	C <sub>34</sub> H <sub>58</sub> NiP <sub>2</sub>
Molecular weight (g.mol <sup>-1</sup> )	587.45
Crystal system	triclinic
Space group	P -1
a (Å)	8.9535(15)
b (Å)	11.0168(16)
c (Å)	17.829(3)
α (°)	76.369(6)
β (°)	85.353(6)
γ (°)	70.631(6)
Volume (Å <sup>3</sup> )	1612.4(5)
Z	2
Calculated density (g.cm <sup>-3</sup> )	1.210
Absorption coefficient (mm <sup>-1</sup> )	0.722
F(000)	640
Crystal size (mm <sup>3</sup> )	0.200 x 0.060 x 0.040
Temperature (K)	193(2)
Wavelength (Å)	0.71073
Reflections collected	21935
Independent reflections (Rint)	6060 (0.1175)
Reflections used for refinement	6060
Refined parameters	341
GOF on F <sup>2</sup>	0.976
R <sub>1</sub> [I>2σ(I)]	0.0577
wR <sub>2</sub> [all data]	0.1170



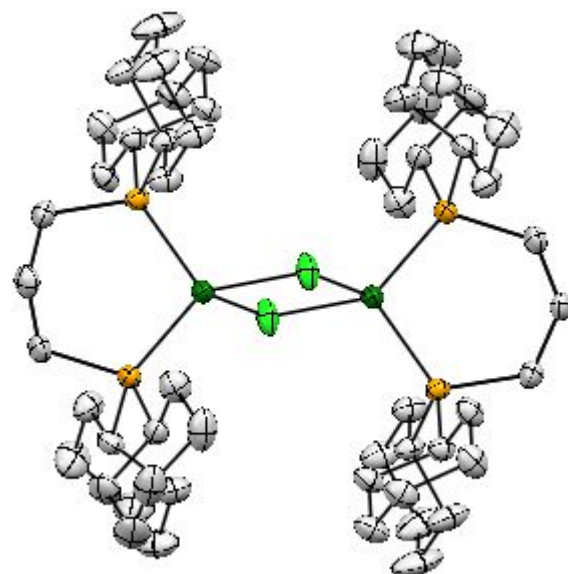
## 7.1.3 [(dcpp)Ni(Ph)(Cl)] II-14

ID	Florian9m
Formula	C <sub>45</sub> H <sub>67</sub> ClNiP <sub>2</sub>
Molecular weight (g.mol <sup>-1</sup> )	764.08
Crystal system	triclinic
Space group	<i>P</i> -1
a (Å)	8.9005(4)
b (Å)	10.6035(4)
c (Å)	23.4174(10)
α (°)	77.5586(15)
β (°)	87.0367(16)
γ (°)	77.3667(15)
Volume (Å <sup>3</sup> )	2105.88(15)
Z	2
Calculated density (g.cm <sup>-3</sup> )	1.205
Absorption coefficient (mm <sup>-1</sup> )	0.629
F(000)	824
Crystal size (mm <sup>3</sup> )	0.399 x 0.281 x 0.136
Temperature (K)	193(2)
Wavelength (Å)	0.71073
Reflections collected	62114
Independent reflections (Rint)	12855 (0.0345)
Reflections used for refinement	12855
Refined parameters	552
GOF on F <sup>2</sup>	1.067
R <sub>1</sub> [I > 2σ(I)]	0.0389
wR <sub>2</sub> [all data]	0.0893



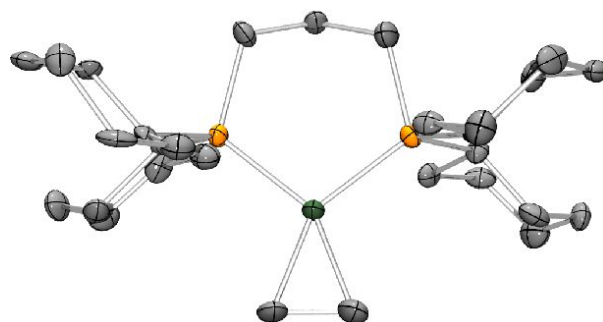
7.1.4 [(dcpp)NiCl]<sub>2</sub> II-16

ID	alexia1m
Formula	C <sub>54</sub> H <sub>100</sub> Cl <sub>2</sub> Ni <sub>2</sub> P <sub>4</sub>
Molecular weight (g.mol <sup>-1</sup> )	1061.54
Crystal system	triclinic
Space group	<i>P</i> -1
a (Å)	10.5873(8)
b (Å)	12.1027(9)
c (Å)	12.1731(9)
α (°)	108.590(4)
β (°)	101.906(4)
γ (°)	100.654(4)
Volume (Å <sup>3</sup> )	1392.78(18)
Z	1
Calculated density (g.cm <sup>-3</sup> )	1.266
Absorption coefficient (mm <sup>-1</sup> )	0.920
F(000)	574
Crystal size (mm <sup>3</sup> )	0.20 x 0.14 x 0.10
Temperature (K)	193(2)
Wavelength (Å)	0.71073
Reflections collected	41637
Independent reflections (Rint)	10582 (0.0441)
Reflections used for refinement	10582
Refined parameters	290
GOF on F <sup>2</sup>	1.035
R <sub>1</sub> [I>2σ(I)]	0.0389
wR <sub>2</sub> [all data]	0.0951



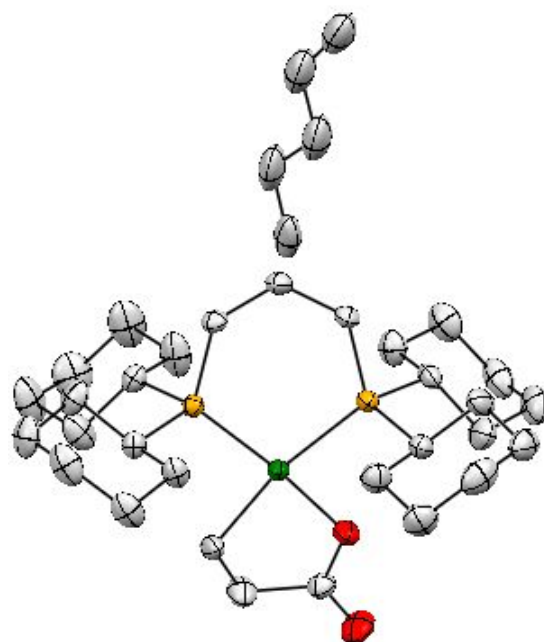
7.1.5 [(dcpp)Ni(C<sub>2</sub>H<sub>4</sub>)] **IV-3**

ID	mo_Alexia9_0m_a
Formula	C <sub>29</sub> H <sub>54</sub> NiP <sub>2</sub>
Molecular weight (g.mol <sup>-1</sup> )	523.37
Crystal system	monoclinic
Space group	P 2 <sub>1</sub> /n
a (Å)	9.4676(8)
b (Å)	9.0227(8)
c (Å)	16.3342(15)
α (°)	90
β (°)	91.063(3)
γ (°)	90
Volume (Å <sup>3</sup> )	1395.1(2)
Z	2
Calculated density (g.cm <sup>-3</sup> )	1.246
Absorption coefficient (mm <sup>-1</sup> )	0.825
F(000)	572
Crystal size (mm <sup>3</sup> )	0.200 x 0.100 x 0.050
Temperature (K)	193(2)
Wavelength (Å)	0.71073
Reflections collected	35460
Independent reflections (Rint)	2849 (0.1601)
Reflections used for refinement	2849
Refined parameters	299
GOF on F <sup>2</sup>	1.276
R <sub>1</sub> [I > 2σ(I)]	0.0788
wR <sub>2</sub> [all data]	0.1562



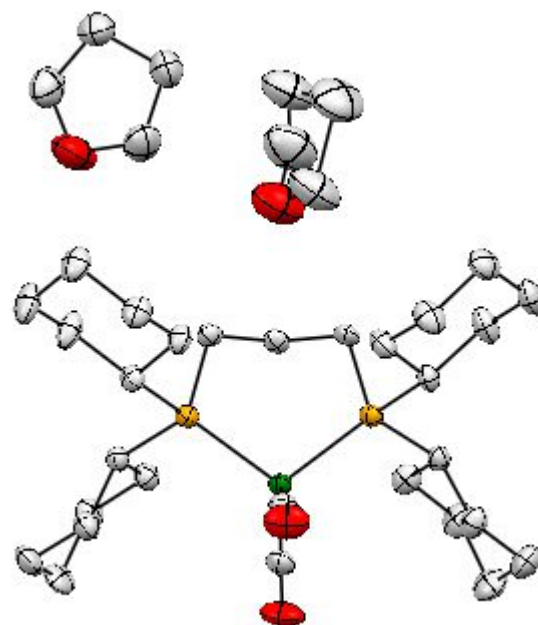
## 7.1.6 [(dcpp)nickelalactone] IV-4

ID	Alexia16
Formula	$C_{30}H_{54}NiO_2P_2, 0,5(C_5H_{12})$
Molecular weight ( $g \cdot mol^{-1}$ )	603.46
Crystal system	orthorhombic
Space group	$Pca2_1$
a (Å)	19.7359(5)
b (Å)	10.6777(3)
c (Å)	16.6426(4)
$\alpha$ (°)	90
$\beta$ (°)	90
$\gamma$ (°)	90
Volume (Å <sup>3</sup> )	3507.16(16)
Z	4
Calculated density ( $g \cdot cm^{-3}$ )	1.143
Absorption coefficient ( $mm^{-1}$ )	0.669
F(000)	1316
Crystal size (mm <sup>3</sup> )	0.18 x 0.18 x 0.02
Temperature (K)	193(2)
Wavelength (Å)	0.71073
Reflections collected	101184
Independent reflections (Rint)	14014 (0.0417)
Reflections used for refinement	14014
Refined parameters	412
GOF on F <sup>2</sup>	1.170
R <sub>1</sub> [ $I > 2\sigma(I)$ ]	0.0444
wR <sub>2</sub> [all data]	0.1565



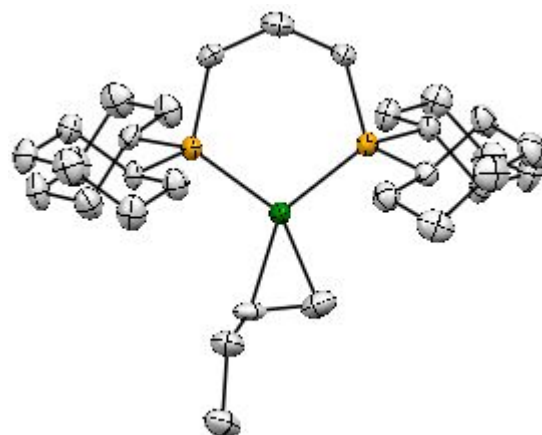
7.1.7 [(dcpp)Ni(CO)<sub>2</sub>] **IV-23**

ID	alexia14m_a
Formula	C <sub>33</sub> H <sub>58</sub> NiO <sub>3</sub> P <sub>2</sub>
Molecular weight (g.mol <sup>-1</sup> )	623.44
Crystal system	monoclinic
Space group	P 2/c
a (Å)	19.9301(9)
b (Å)	9.3949(4)
c (Å)	18.7119(6)
α (°)	90
β (°)	106.937(2)
γ (°)	90
Volume (Å <sup>3</sup> )	3351.7(2)
Z	4
Calculated density (g.cm <sup>-3</sup> )	1.236
Absorption coefficient (mm <sup>-1</sup> )	0.705
F(000)	1352
Crystal size (mm <sup>3</sup> )	0.200 x 0.180 x 0.060
Temperature (K)	193(2)
Wavelength (Å)	0.71073
Reflections collected	6769
Independent reflections (Rint)	6769 (?)
Reflections used for refinement	6769
Refined parameters	376
GOF on F <sup>2</sup>	1.180
R <sub>1</sub> [I > 2σ(I)]	0.0609
wR <sub>2</sub> [all data]	0.1199



## 7.1.8 [(dcpp)Ni(1-butene)] V-6

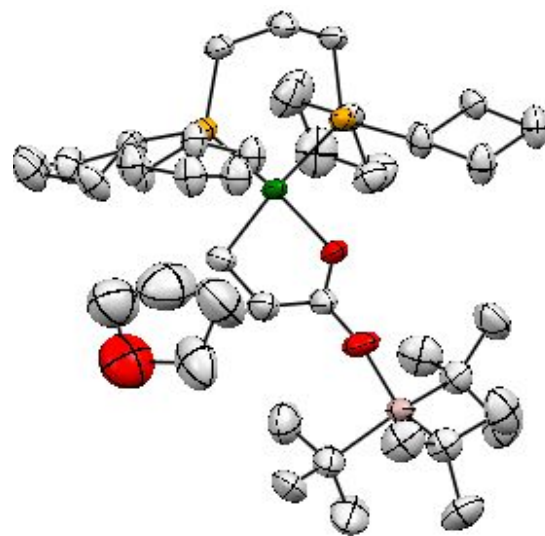
ID	alexia3m
Formula	C <sub>31</sub> H <sub>58</sub> NiP <sub>2</sub>
Molecular weight (g.mol <sup>-1</sup> )	551.42
Crystal system	triclinic
Space group	<i>P 1</i>
a (Å)	8.7517(8)
b (Å)	10.3122(8)
c (Å)	10.5977(14)
α (°)	115.549(7)
β (°)	97.376(7)
γ (°)	110.062(5)
Volume (Å <sup>3</sup> )	766.25(14)
Z	1
Calculated density (g.cm <sup>-3</sup> )	1.195
Absorption coefficient (mm <sup>-1</sup> )	0.755
F(000)	302
Crystal size (mm <sup>3</sup> )	0.25 x 0.11 x 0.06
Temperature (K)	193(2)
Wavelength (Å)	0.71073
Reflections collected	10678
Independent reflections (Rint)	5726 (0.0461)
Reflections used for refinement	5726
Refined parameters	309
GOF on F <sup>2</sup>	1.020
R <sub>1</sub> [I > 2σ(I)]	0.0500
wR <sub>2</sub> [all data]	0.1205





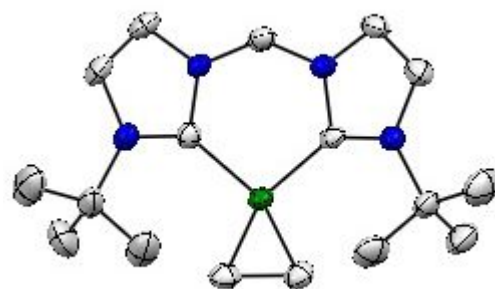
7.1.9 [(dcpp)nickelalactone-Al(*t*Bu)<sub>3</sub>] V-9

ID	Alexia43Bis_a
Formula	C <sub>44</sub> H <sub>85</sub> AlNiO <sub>2.50</sub> P <sub>2</sub>
Molecular weight (g.mol <sup>-1</sup> )	801.74
Crystal system	monoclinic
Space group	C 2/c
a (Å)	18.1565(15)
b (Å)	21.8169(16)
c (Å)	25.187(2)
α (°)	90
β (°)	110.893(4)
γ (°)	90
Volume (Å <sup>3</sup> )	9321.1(13)
Z	8
Calculated density (g.cm <sup>-3</sup> )	1.143
Absorption coefficient (mm <sup>-1</sup> )	0.537
F(000)	3520
Crystal size (mm <sup>3</sup> )	0.180 x 0.140 x 0.080
Temperature (K)	193(2)
Wavelength (Å)	0.71073
Reflections collected	69673
Independent reflections (Rint)	9470 (0.0535)
Reflections used for refinement	9470
Refined parameters	597
GOF on F <sup>2</sup>	1.021
R <sub>1</sub> [I > 2σ(I)]	0.0528
wR <sub>2</sub> [all data]	0.1387



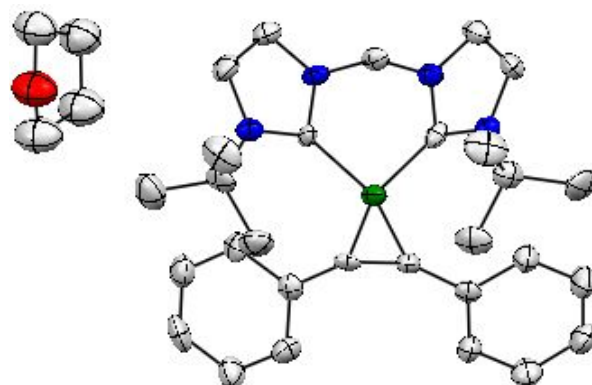
7.1.10 [(*Lt*Bu)Ni(C<sub>2</sub>H<sub>4</sub>)] VI-9

ID	Alexia29_b
Formula	C <sub>17</sub> H <sub>28</sub> N <sub>4</sub> Ni
Molecular weight (g.mol <sup>-1</sup> )	347.14
Crystal system	orthorhombic
Space group	<i>P n a 2<sub>1</sub></i>
a (Å)	14.3232(6)
b (Å)	10.9530(4)
c (Å)	11.4879(6)
α (°)	90
β (°)	90
γ (°)	90
Volume (Å <sup>3</sup> )	1802.24(14)
Z	4
Calculated density (g.cm <sup>-3</sup> )	1.279
Absorption coefficient (mm <sup>-1</sup> )	1.079
F(000)	744
Crystal size (mm <sup>3</sup> )	0.060 x 0.030 x 0.010
Temperature (K)	193(2)
Wavelength (Å)	0.71073
Reflections collected	30631
Independent reflections (Rint)	3650 (0.0528)
Reflections used for refinement	3650
Refined parameters	205
GOF on F <sup>2</sup>	1.022
R <sub>1</sub> [I > 2σ(I)]	0.0279
wR <sub>2</sub> [all data]	0.0608



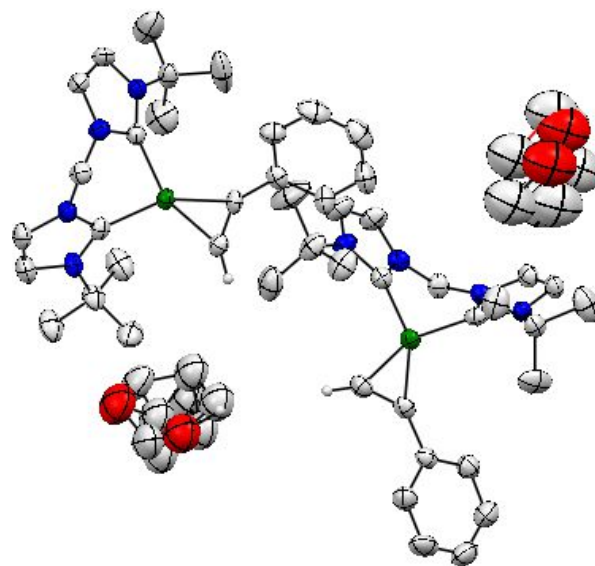
7.1.11 [(*Lt*Bu)Ni(PhC≡CPh)] VI-13

ID	Alexia35_a
Formula	C <sub>31</sub> H <sub>38</sub> N <sub>4</sub> NiO <sub>0.50</sub>
Molecular weight (g.mol <sup>-1</sup> )	533.36
Crystal system	monoclinic
Space group	P 2 <sub>1</sub> /n
a (Å)	11.833(3)
b (Å)	10.566(3)
c (Å)	22.554(6)
α (°)	90
β (°)	99.464(12)
γ (°)	90
Volume (Å <sup>3</sup> )	2781.5(14)
Z	4
Calculated density (g.cm <sup>-3</sup> )	1.274
Absorption coefficient (mm <sup>-1</sup> )	0.725
F(000)	1136
Crystal size (mm <sup>3</sup> )	0.340 x 0.040 x 0.020
Temperature (K)	193(2)
Wavelength (Å)	0.71073
Reflections collected	21431
Independent reflections (Rint)	4529 (0.2699)
Reflections used for refinement	4529
Refined parameters	408
GOF on F <sup>2</sup>	0.976
R <sub>1</sub> [I > 2σ(I)]	0.0740
wR <sub>2</sub> [all data]	0.1661



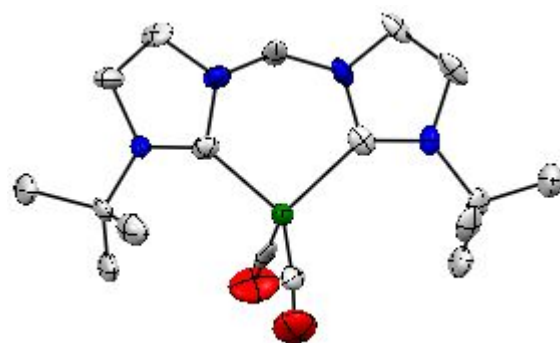
7.1.12 [(*Lt*Bu)Ni(PhC≡CH)] VI-14

ID	Alexia38_a
Formula	C <sub>27</sub> H <sub>38</sub> N <sub>4</sub> NiO
Molecular weight (g.mol <sup>-1</sup> )	493.32
Crystal system	monoclinic
Space group	C c
a (Å)	15.6787(19)
b (Å)	15.2754(17)
c (Å)	22.621(3)
α (°)	90
β (°)	103.238(5)
γ (°)	90
Volume (Å <sup>3</sup> )	5273.8(11)
Z	8
Calculated density (g.cm <sup>-3</sup> )	1.243
Absorption coefficient (mm <sup>-1</sup> )	0.761
F(000)	2112
Crystal size (mm <sup>3</sup> )	0.180 x 0.160 x 0.030
Temperature (K)	193(2)
Wavelength (Å)	0.71073
Reflections collected	40271
Independent reflections (Rint)	12173 (0.0477)
Reflections used for refinement	12173
Refined parameters	700
GOF on F <sup>2</sup>	0.984
R <sub>1</sub> [I > 2σ(I)]	0.0424
wR <sub>2</sub> [all data]	0.0934



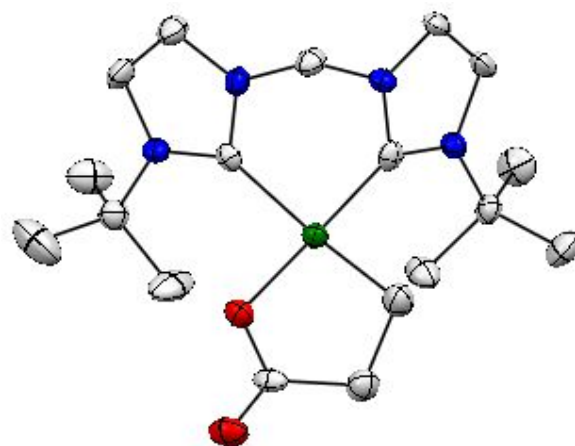
7.1.13 [(*Lt*Bu)Ni(CO)<sub>2</sub>] VI-15

ID	AO446
Formula	C <sub>17</sub> H <sub>24</sub> N <sub>4</sub> NiO <sub>2</sub>
Molecular weight (g.mol <sup>-1</sup> )	375.09
Crystal system	orthorhombic
Space group	P 2 <sub>1</sub> 2 <sub>1</sub> 2 <sub>1</sub>
a (Å)	9.5206(8)
b (Å)	12.9925(12)
c (Å)	14.7824(13)
α (°)	90
β (°)	90
γ (°)	90
Volume (Å <sup>3</sup> )	1828.5(3)
Z	4
Calculated density (g.cm <sup>-3</sup> )	1.363
Absorption coefficient (mm <sup>-1</sup> )	1.077
F(000)	792
Crystal size (mm <sup>3</sup> )	0.10 x 0.08 x 0.01
Temperature (K)	193(2)
Wavelength (Å)	0.71073
Reflections collected	22860
Independent reflections (Rint)	3883 (0.0655)
Reflections used for refinement	3883
Refined parameters	224
GOF on F <sup>2</sup>	1.081
R <sub>1</sub> [I > 2σ(I)]	0.0391
wR <sub>2</sub> [all data]	0.0897



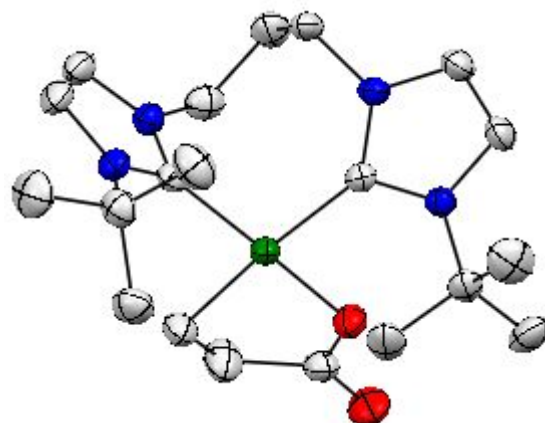
7.1.14 [(*Lt*Bu)nickelalactone] **VI-18**

ID	Alexia26
Formula	C <sub>18</sub> H <sub>28</sub> N <sub>4</sub> NiO <sub>2</sub>
Molecular weight (g.mol <sup>-1</sup> )	391.15
Crystal system	monoclinic
Space group	P 2 <sub>1</sub> /n
a (Å)	12.016(2)
b (Å)	11.0221(19)
c (Å)	14.146(3)
α (°)	90
β (°)	95.469(8)
γ (°)	90
Volume (Å <sup>3</sup> )	1865.0(6)
Z	4
Calculated density (g.cm <sup>-3</sup> )	1.393
Absorption coefficient (mm <sup>-1</sup> )	1.059
F(000)	832
Crystal size (mm <sup>3</sup> )	0.150 x 0.040 x 0.030
Temperature (K)	193(2)
Wavelength (Å)	0.71073
Reflections collected	30635
Independent reflections (Rint)	3280 (0.1930)
Reflections used for refinement	3280
Refined parameters	232
GOF on F <sup>2</sup>	1.011
R <sub>1</sub> [I > 2σ(I)]	0.0523
wR <sub>2</sub> [all data]	0.0997



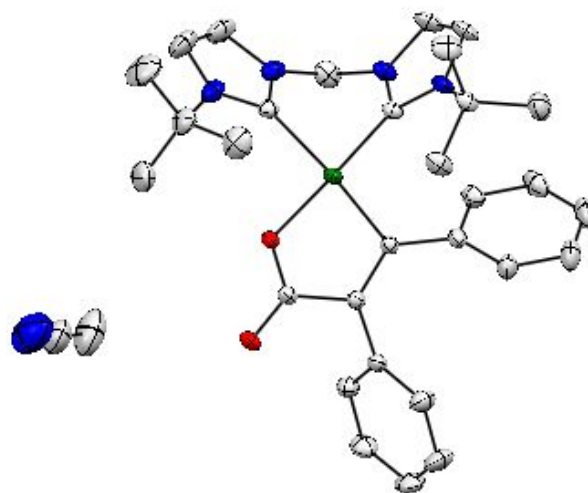
7.1.15 [(*Lt*Bu)<sup>prop</sup>nickelalactone] VI-20

ID	Alexia30_a
Formula	C <sub>20</sub> H <sub>32</sub> N <sub>4</sub> NiO <sub>2</sub>
Molecular weight (g.mol <sup>-1</sup> )	419.20
Crystal system	monoclinic
Space group	P 2 <sub>1</sub> /c
a (Å)	13.8222(6)
b (Å)	10.3392(4)
c (Å)	15.0732(6)
α (°)	90
β (°)	104.136(2)
γ (°)	90
Volume (Å <sup>3</sup> )	2088.89(15)
Z	4
Calculated density (g.cm <sup>-3</sup> )	1.333
Absorption coefficient (mm <sup>-1</sup> )	1.950
F(000)	896
Crystal size (mm <sup>3</sup> )	0.140 x 0.060 x 0.050
Temperature (K)	193(2)
Wavelength (Å)	0.71073
Reflections collected	30730
Independent reflections (Rint)	4761 (0.0551)
Reflections used for refinement	4761
Refined parameters	250
GOF on F <sup>2</sup>	1.021
R <sub>1</sub> [I > 2σ(I)]	0.0374
wR <sub>2</sub> [all data]	0.0948



7.1.16 [(*Lt*Bu)Ni(C(Ph)=C(Ph)C(O)O)- κC,κO] VI-22

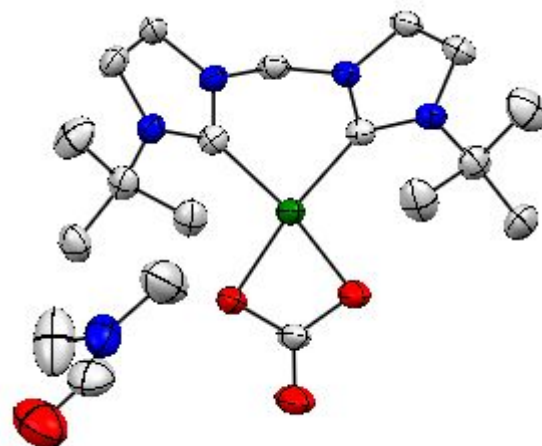
ID	Alexia37_a
Formula	C <sub>32</sub> H <sub>37</sub> N <sub>5</sub> NiO <sub>2</sub>
Molecular weight (g.mol <sup>-1</sup> )	582.37
Crystal system	monoclinic
Space group	P 2 <sub>1</sub>
a (Å)	7.857(3)
b (Å)	22.6159(9)
c (Å)	8.4121(3)
α (°)	90
β (°)	97.2912(13)
γ (°)	90
Volume (Å <sup>3</sup> )	1482.70(10)
Z	2
Calculated density (g.cm <sup>-3</sup> )	1.304
Absorption coefficient (mm <sup>-1</sup> )	0.691
F(000)	616
Crystal size (mm <sup>3</sup> )	0.360 x 0.220 x 0.180
Temperature (K)	193(2)
Wavelength (Å)	0.71073
Reflections collected	69849
Independent reflections (Rint)	9058 (0.0411)
Reflections used for refinement	9058
Refined parameters	395
GOF on F <sup>2</sup>	1.041
R <sub>1</sub> [I>2σ(I)]	0.0276
wR <sub>2</sub> [all data]	0.0583





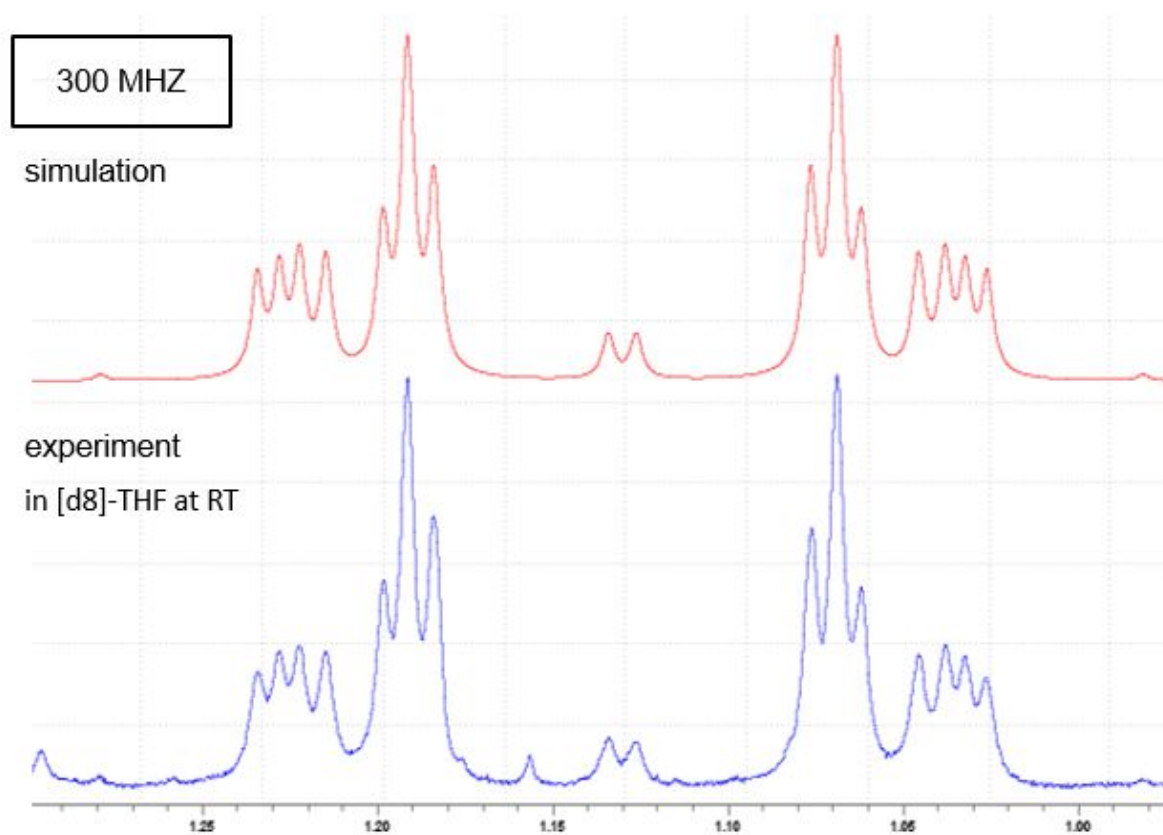
7.1.17 [(*Lt*Bu)Ni(CO<sub>3</sub>)] VI-28

ID	Alexia25_a
Formula	C <sub>19</sub> H <sub>31</sub> N <sub>5</sub> NiO <sub>4</sub>
Molecular weight (g.mol <sup>-1</sup> )	452.20
Crystal system	monoclinic
Space group	P 2 <sub>1</sub> /n
a (Å)	10.1966(4)
b (Å)	15.8385(6)
c (Å)	13.8130(5)
α (°)	90
β (°)	91.163(3)
γ (°)	90
Volume (Å <sup>3</sup> )	2230.32(15)
Z	4
Calculated density (g.cm <sup>-3</sup> )	1.347
Absorption coefficient (mm <sup>-1</sup> )	1.537
F(000)	960
Crystal size (mm <sup>3</sup> )	0.120 x 0.080 x 0.060
Temperature (K)	193(2)
Wavelength (Å)	0.71073
Reflections collected	11429
Independent reflections (Rint)	3751 (0.0875)
Reflections used for refinement	3751
Refined parameters	270
GOF on F <sup>2</sup>	1.008
R <sub>1</sub> [I > 2σ(I)]	0.0568
wR <sub>2</sub> [all data]	0.1352

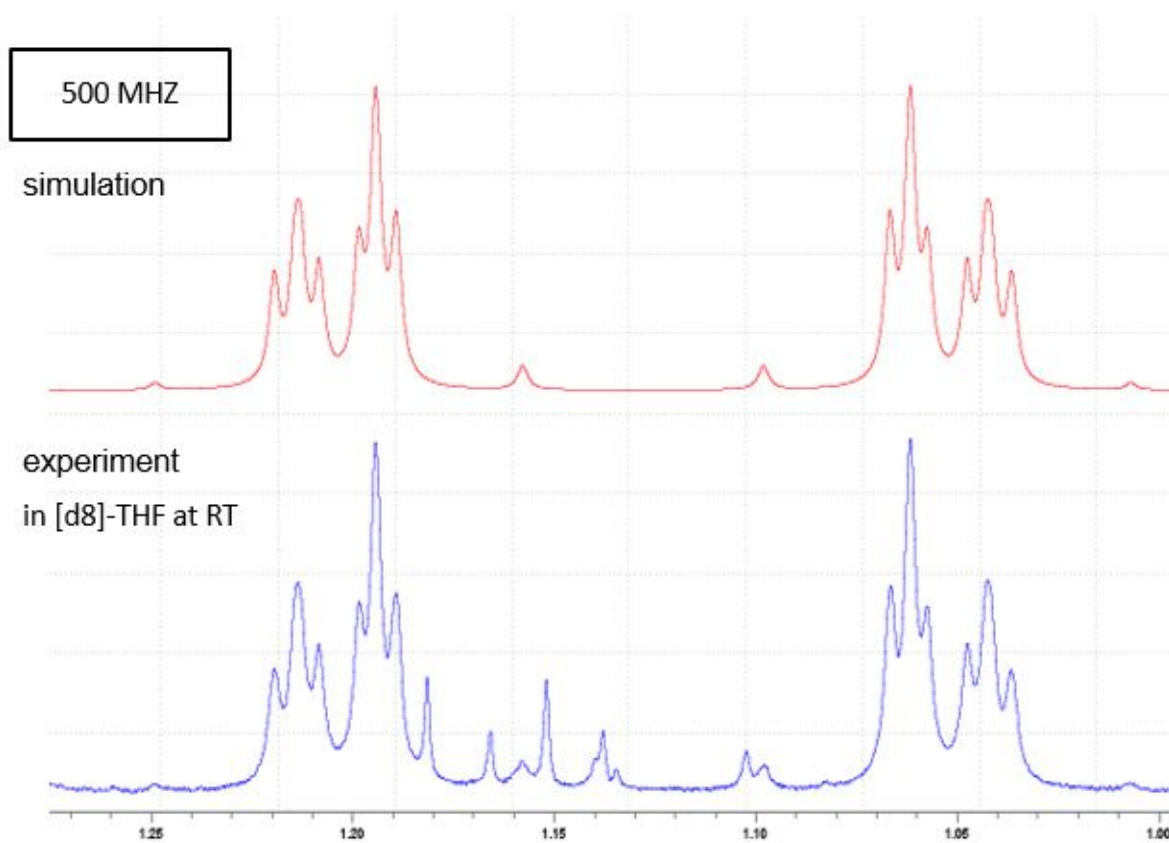


## 7.2 NMR simulations

The AA'BB' system of the ethylenic protons of [(*Lt*Bu)Ni(C<sub>2</sub>H<sub>4</sub>)] **VI-9** has been simulated at 300 MHz and 500 MHz with TOPSPIN, using the “module daisy”. The work was realized by Stéphane Massou and Marc Vedrenne of the NMR service (Toulouse). The simulated spectra were superimposed to the recorded <sup>1</sup>H NMR spectra of [(*Lt*Bu)Ni(C<sub>2</sub>H<sub>4</sub>)] **VI-9** and can be found below.



**Scheme 7.1:** <sup>1</sup>H NMR spectrum of the ethylenic protons of [(*Lt*Bu)Ni(C<sub>2</sub>H<sub>4</sub>)] **IV-9** at 300 MHz.



**Scheme 7.2:**  $^1\text{H}$  NMR spectrum of the ethylenic protons of  $[(\text{LiBu})\text{Ni}(\text{C}_2\text{H}_4)]$  **IV-9** at 500 MHz.

## 7.3 Résumé de la thèse

La thèse intitulée “Couplages de Negishi et Couplages Oxydants à Base de Complexes de Nickel” a été réalisée au Laboratoire Hétérochimie Fondamentale et Appliquée à Toulouse entre janvier 2014 et février 2017 sous la direction du Dr. Nicolas Mézailles et du Dr. Noël Nebra-Muñiz. Cette thèse est divisée en deux parties distinctes. La première partie décrit un couplage croisé de Negishi catalysé par des complexes de nickel substitués par des ligand bis-phosphines chelatants, suivie de l'étude mécanistique complète de ce système. La deuxième partie est dédiée à l'activation et la fonctionnalisation du CO<sub>2</sub> en produits chimiques à haute valeur ajoutée par des complexes de nickel coordonnés par des ligands phosphines ou NHC bidentes.

### 7.3.1 Couplage croisé de Negishi catalysé par des complexes bis-phosphines de nickel

#### 7.3.1.1 Introduction

Les couplages croisés constituent un outil majeur en chimie organique de synthèse pour la formation de nouvelles liaisons C-C et C-hétéroatomes<sup>[1]</sup> et trouvent de nombreuses applications dans des domaines aussi variés que l'industrie pharmaceutique<sup>[1, 2]</sup> et agrochimique, les polymères<sup>[3]</sup> ou les cristaux liquides.<sup>[4]</sup> En 2010, Richard Heck, Ei-ichi Negishi et Akira Suzuki ont été récompensés par le prix Nobel de Chimie pour leurs travaux novateurs dans ce domaine, qui reste toujours très actif en terme de recherche.

Un couplage croisé est une réaction entre un électrophile, généralement un halogénure d'aryle, et une espèce organométallique nucléophile, catalysée par un métal de transition, qui génère une nouvelle liaison C-C. Parmi les réactions de couplages croisés, la réaction de Negishi emploie des dérivés zinciques comme nucléophiles, qui présentent de multiples avantages. Ceux-ci sont en effet peu toxiques, tolèrent de nombreux groupements fonctionnels et permettent de mettre en oeuvre les réactions dans des conditions douces. Alors que la plupart des couplages sont catalysés par des complexes de palladium extrêmement efficaces,<sup>[5]</sup> dont on connaît bien le mode de fonctionnement, beaucoup moins de complexes de nickel ont été décrits pour cette même application. Les chercheurs sont actuellement confrontés à deux défis majeurs, qui sont d'une part la réduction de la charge catalytique<sup>[6]</sup> et d'autre part le couplage de dérivés peu chers mais plus difficiles à activer, tels que les chlorure d'aryles.<sup>[7, 8]</sup>

Ainsi, dans cette optique, de nouveaux complexes bis-phosphines de nickel ont été développés au cours de cette thèse et utilisés comme catalyseurs pour le couplage croisé de Negishi entre des chlorure d'aryles, abondants et peu chers, mais difficiles à activer, et des dérivés zinciques. Le ligand de choix est le 1,3-bis(dicyclohexyl)phosphino-propane (dcpp) **II-1**. En effet, les groupements alkyls fortement électro-donneurs ainsi que l'espaceur propane, conférant un grand angle de morsure et de la flexibilité aux complexes métalliques, stabilisent efficacement des espèces de Ni(0) (**Schéma 1**).

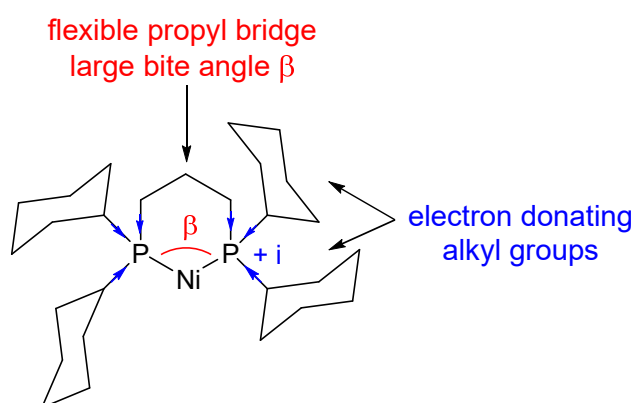


**Schéma 1:** Propriétés du système [(dcp)Ni].

La principale motivation de ce travail est le développement d'une nouvelle catalyse de couplage croisé efficace dans des conditions douces. De plus, beaucoup d'intérêt a été apporté à la compréhension du mécanisme de la réaction, afin de déterminer si la réaction suit un cycle Ni(0)/Ni(II) ou un cycle Ni(I)/Ni(III). La détermination du mécanisme permet de mieux appréhender la chimie du nickel et de pouvoir par la suite développer de nouveaux systèmes plus performants.

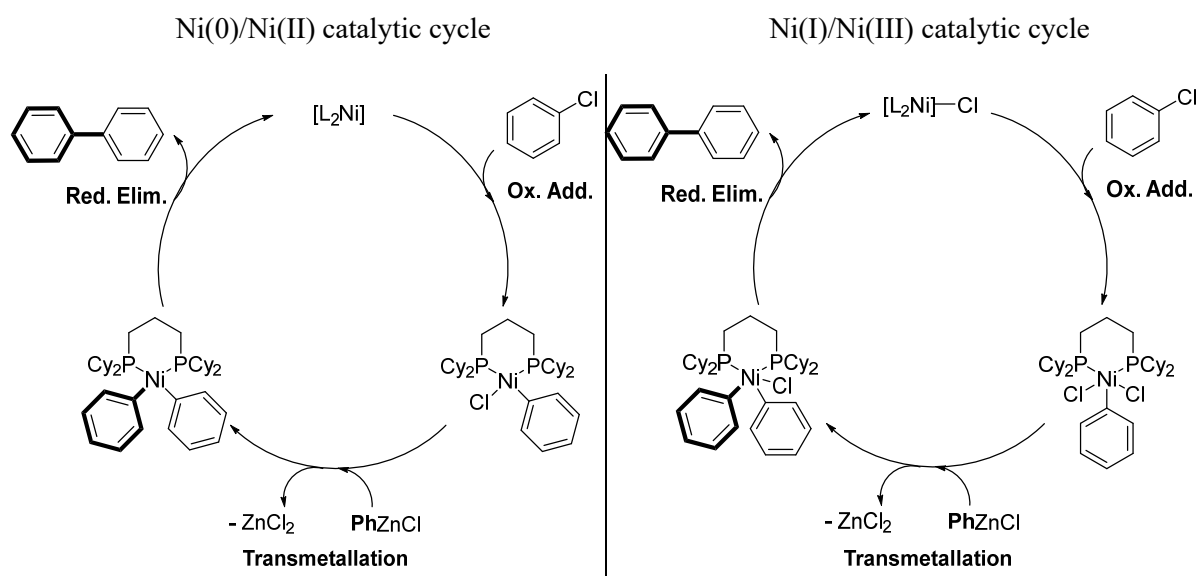


**Schéma 2:** Mécanismes généraux Ni(0)/Ni(II) et Ni(I)/Ni(III) de couplage croisé.

### 7.3.1.2 Synthèse du catalyseur [(dcp)Ni(toluène)] **II-4**

Le catalyseur sélectionné pour le couplage croisé de Negishi est le complexe de Ni(0), [(dcp)Ni(toluène)] **II-4**. Celui-ci est obtenu par réduction du complexe de Ni(II) [(dcp)NiCl<sub>2</sub>] **II-3** au moyen de 2 eq. de KC<sub>8</sub> dans du toluène. [(dcp)Ni(toluène)] **II-4** a pu être caractérisé par RMN et diffraction des rayons X (DRX) par Matthieu Demange.<sup>[9]</sup> La grande réactivité et l'importante solubilité de ce complexe, le qualifient comme réactif de choix pour les études catalytiques et mécanistiques menées par la suite.

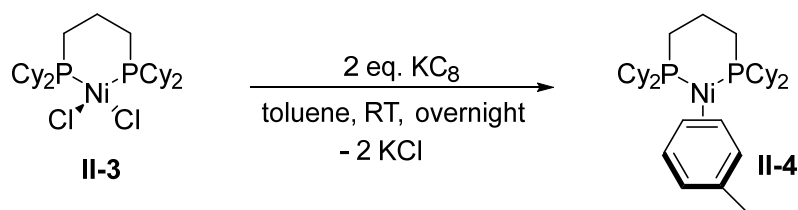


**Schéma 3:** Synthèse de [(dcp)Ni(toluène)] **II-4**.

### 7.3.1.3 Couplage croisé de Negishi catalysé par [(dcp)Ni(toluène)] **II-4**

L'activité de [(dcp)Ni(toluène)] **II-4** a tout d'abord été testée dans la réaction modèle entre le 4-chlorotoluène **II-7** et le chlorure de phenyl zinc **II-8** dans le THF à 60 °C, présentée dans le **Schéma 4**.

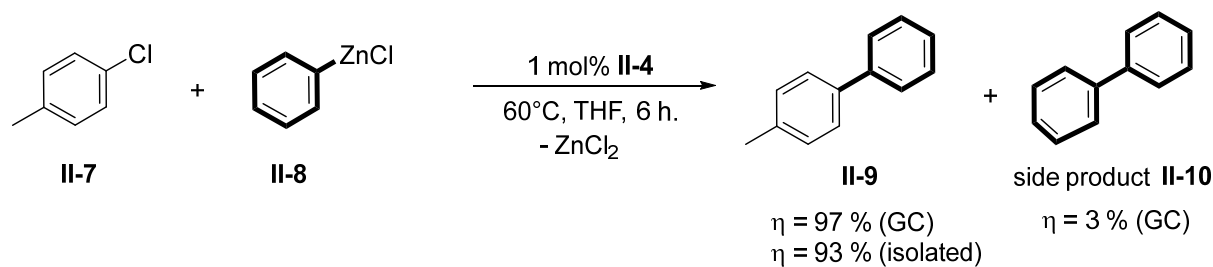


**Schéma 4:** Réaction modèle du couplage croisé de Negishi entre le 4-chlorotoluène **II-7** et PhZnCl **II-8** catalysée par 1 mol% de [(dcp)Ni(toluène)] **II-4** à 60 °C dans le THF.

En utilisant 1 mol% de catalyseur, le produit de couplage croisé **II-9** a été obtenu avec 97 % de rendement GC après seulement 6 h. 3 % de produit d'homocouplage **II-10** ont également été détectés par GC-MS. Après work-up 93 % de produit de couplage croisé **II-9** ont été isolés. La charge catalytique peut être abaissée à 0,2 mol%, et même jusqu'à 0,01 mol% sans observer de dégradation du catalyseur **II-4** après de longs temps réactionnels.

Ainsi, en suivant cette méthodologie de nombreux substrats aussi bien riches que pauvres en électrons ont pu être couplés avec succès à 0,2 mol% de [(dcp)Ni(toluène)] **II-4** avec d'excellents rendements. De plus, des chloropyridines et des électrophiles fortement encombrés en *ortho* du chlorure ou portant des fonctions amines particulièrement sensibles, et reconnus difficiles à coupler, ont tous fourni les produits de couplage croisés avec de bons rendements et des temps de réactions courts à 1 mol% de catalyseur **II-4**.

### 7.3.1.4 Etudes mécanistiques

Par la suite, des études stoechiométriques et catalytiques ainsi que des calculs DFT ont été effectués, afin d'élucider le mécanisme de ce couplage croisé. Tous les résultats pointent vers un cycle catalytique Ni(0)/Ni(II) induit par la présence du ligand bidenté dcp **II-1** fortement donneur. Les trois étapes élémentaires d'un couplage croisé, qui sont l'addition oxydante, la transmétallation et l'élimination réductrice, peuvent toutes être réalisées à température ambiante à partir de complexes dcp de nickel et génèrent exclusivement des espèces de Ni(0) et de Ni(II), parmi lesquelles [(dcp)Ni(Ph)(Cl)] **II-14** a pu être isolée et caractérisée. De plus, les calculs DFT au niveau B3PW91 confirment que l'addition oxydante ( $\Delta G^\ddagger = 12,9 \text{ kcal.mol}^{-1}$ ) et l'élimination réductrice ( $\Delta G^\ddagger = 13,2 \text{ kcal.mol}^{-1}$ ) ont des énergies d'activation particulièrement basses alors que la transmétallation ( $\Delta G^\ddagger = 21,8 \text{ kcal.mol}^{-1}$ ) et l'échange de ligands produit/substrat ( $\Delta G^\ddagger = 22,9 \text{ kcal.mol}^{-1}$ ) constituent les étapes cinétiquement

déterminantes de la réaction. L'état de repos du catalyseur est le produit d'addition oxydante  $[(dcpp)Ni(Ph)(Cl)]$  **II-14**. Le cycle catalytique de la réaction proposé à partir des études stoechiométriques et des calculs DFT est illustré dans le **Schéma 5**.

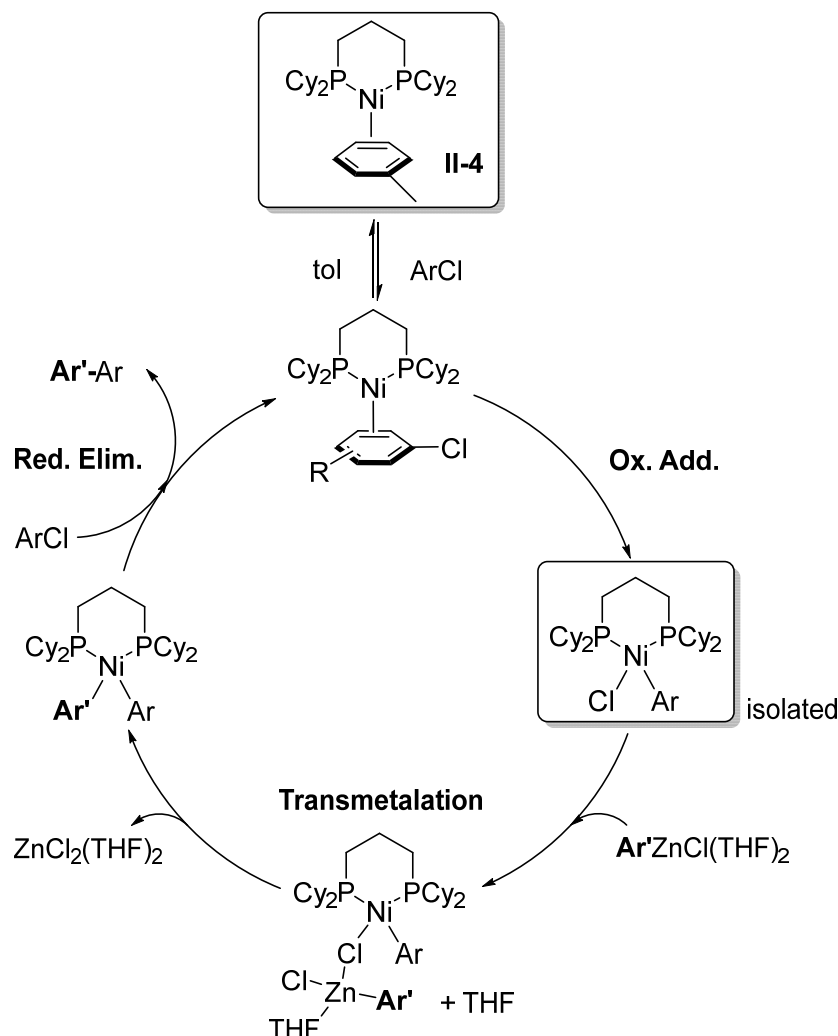


**Schéma 5:** Cycle catalytique proposé à partir des études stoechiométriques et des calculs DFT pour la réaction de couplage croisé catalysée par le complexe  $[(dcpp)Ni(\text{toluène})]$  **II-4** entre des chlorures d'aryles et des dérivés zinciques.

Afin d'apporter des preuves supplémentaires au mécanisme  $Ni(0)/Ni(II)$  et de pouvoir infirmer la participation d'espèces de  $Ni(I)$  au cycle catalytique, le complexe paramagnétique de  $Ni(I)$   $[(dcpp)NiCl]_2$  **II-16** a été synthétisé indépendamment par réduction de  $[(dcpp)NiCl_2]$  **II-3** avec 1 eq. de  $KC_8$  (**Schéma 6**), et caractérisé par RPE et DRX.



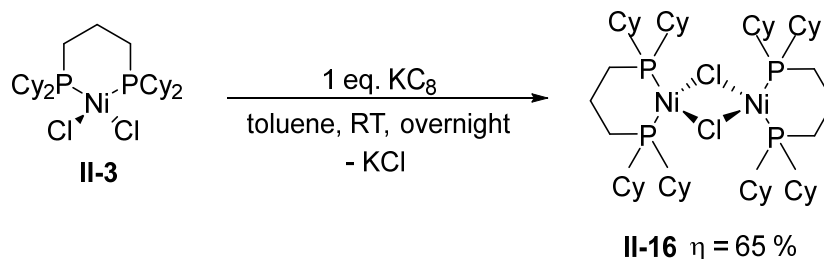


**Schéma 6:** Synthèse du complexe de Ni(I) [(dcpp)NiCl]<sub>2</sub> **II-16**.

Le complexe de Ni(I) [(dcpp)NiCl]<sub>2</sub> **II-16** ne réagit pas avec des chlorures d'aryles et génère préférentiellement des espèces diamagnétiques de Ni(II) et/ou de Ni(0) en présence de PhZnCl **II-8**. Par ailleurs, aucun processus redox, conduisant à la formation d'espèces de Ni(I) n'a pu être identifié lors des études stoechiométriques. De plus, lorsque la réaction modèle de Negishi entre le 4-chlorotoluène **II-7** et PhZnCl **II-8** est réalisée en présence d'1 mol% de [(dcpp)NiCl]<sub>2</sub> **II-16**, de mauvaises conversions et sélectivités ont été observées. En effet, après 72 h., seulement 7 % de produit de couplage **II-9** ont été obtenu à la faveur de 33 % de produit d'homocouplage **II-10**.

Ainsi la présence du ligand dcpp chélatant **II-1** inhibe un mécanisme de type Ni(I)/Ni(III), en faveur d'un mécanisme Ni(0)/Ni(II). Ce résultat est en contraste avec les autres études mécanistiques menées sur des catalyses de Negishi au nickel avec des ligands phosphines monodentes qui fonctionnent sur le modèle Ni(I)/Ni(III).<sup>[10, 11]</sup>

## 7.3.2 Activation et fonctionnalisation du CO<sub>2</sub> avec des complexes de nickel coordinés par des ligands bis-phosphines

### 7.3.2.1 Introduction

Le CO<sub>2</sub> est le principal gaz à effet de serre émis par les activités humaines et contribue au réchauffement et aux changements climatiques. Il devient donc important de pouvoir valoriser le CO<sub>2</sub>, notamment en l'incorporant dans de nouvelles réactions. Le CO<sub>2</sub> présente l'avantage d'être une ressource renouvelable non toxique et peu coûteuse. A ce jour seulement trois procédés industriels utilisent le CO<sub>2</sub> en tant que réactif pour la production d'urée, de carbonates et d'aspirine®. Il serait très intéressant et avantageux de pouvoir produire de l'acide acrylique

directement à partir d'éthylène et de CO<sub>2</sub>. En effet les dérivés d'acide acrylique représentent un marché de l'ordre de 5,4 Mtonnes.an<sup>-1</sup> essentiellement pour la production de polymères. [12]

Le couplage oxydant entre l'éthylène et le CO<sub>2</sub>, assisté par des métaux de transitions, et notamment le nickel, [13, 14] est connu depuis les années 1980. Ce couplage conduit à la formation de nickelalactones, qui restent cependant très difficiles à cliver. Une élimination β-H permettrait de produire directement de l'acide acrylique. Ce processus n'est néanmoins pas favorable cinétiquement et thermodynamiquement. [15] De nouvelles stratégies, impliquant l'utilisation d'électrophiles forts [16, 17, 18] ou de bases, [19] ont donc été mises place afin d'induire l'élimination β-H et de produire des acrylates. De premiers processus catalytiques ont pu être mis en place récemment. [20, 21, 22]

La transmétallation pourrait être une alternative intéressante afin de cliver la liaison Ni-O des nickelalactones et d'induire la formation de dérivés acryliques. Des travaux de Mori [23, 24] et Rovis [25] sur des composés zinciques, ont montrés que ceux-ci peuvent en effet ouvrir les nickelalactones, mais conduisent après élimination réductrice invariablement à des dérivés d'acides carboxyliques. Nous nous sommes donc tournés vers les boranes, afin de pouvoir favoriser l'élimination β-H par rapport à une élimination réductrice, dans le but de trouver une alternative pour la synthèse de dérivés d'acide acrylique.

### 7.3.2.2 Synthèse de [(dcpp)Ni(C<sub>2</sub>H<sub>4</sub>)] **IV-3**

[(dcpp)Ni(C<sub>2</sub>H<sub>4</sub>)] **IV-3** est obtenu par réactions de substitutions de ligands à partir de [Ni(COD)<sub>2</sub>] **IV-2**. Le premier ligand COD est déplacé rapidement à température ambiante par la bis-phosphine dcpp **IV-1**, puis le second COD est substitué sous pression d'éthylène, générant le complexe [(dcpp)Ni(C<sub>2</sub>H<sub>4</sub>)] **IV-3** avec un rendement isolé de 64 % (**Schéma 7**). [(dcpp)Ni(C<sub>2</sub>H<sub>4</sub>)] **IV-3** est très sensible à l'oxygène et possède une mauvaise solubilité à tous les solvant organiques usuels.

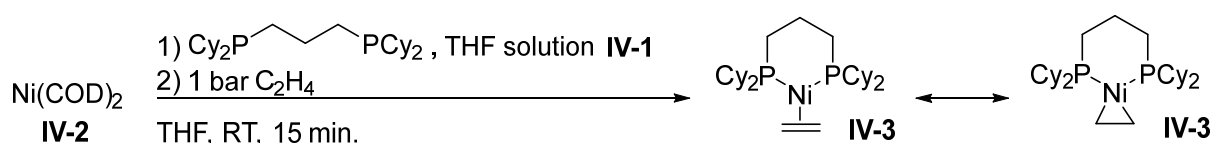


**Schéma 7:** Synthèse de [(dcpp)Ni(C<sub>2</sub>H<sub>4</sub>)] **IV-3** par réactions de substitutions de ligands à partir de [Ni(COD)<sub>2</sub>] **IV-2**.

Le complexe est caractérisé en RMN  $^{31}\text{P}\{^1\text{H}\}$  par un singulet à  $\delta = 25,5$  ppm. Les protons et les carbones éthyléniques sont très blindés et sortent à  $\delta = 1,52$  ppm en RMN  $^1\text{H}$  et à  $\delta = 31,9$  ppm en RMN  $^{13}\text{C}\{^1\text{H}\}$ , démontrant la richesse électronique du fragment  $[(\text{dcpp})\text{Ni}]$  et la forte rétro-donation du centre métallique vers l'oléfine coordonnée. La structure RX de  $[(\text{dcpp})\text{Ni}(\text{C}_2\text{H}_4)]$  **IV-3** montre que le complexe adopte une géométrie plan carrée distordue. L'angle de morsure mesure  $104,50(10)^\circ$  et la liaison éthylénique  $\text{C}_4\text{-C}_5 = 1,407(15)$  Å, ce qui se situe à mi-chemin entre une liaison C-C simple et une liaison C-C double. La **Figure 1** représente la structure RX résolue de  $[(\text{dcpp})\text{Ni}(\text{C}_2\text{H}_4)]$  **IV-3**.

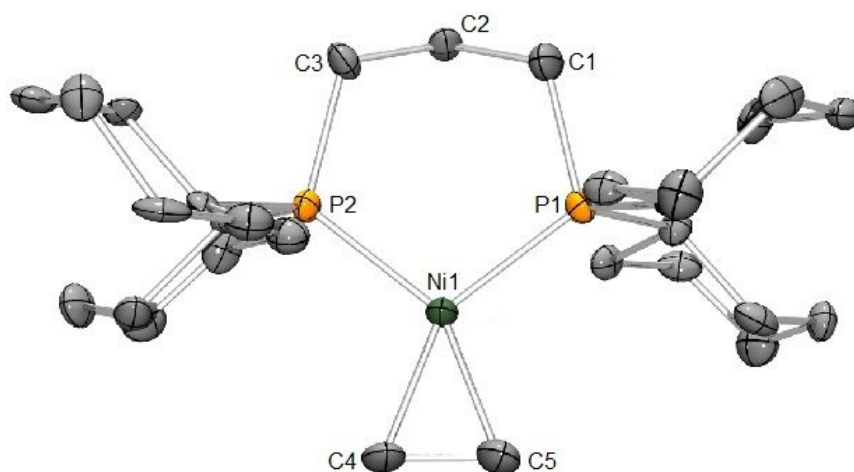


**Figure 1:** Structure moléculaire de  $[(\text{dcpp})\text{Ni}(\text{C}_2\text{H}_4)]$  **IV-3** déterminée par diffraction de rayons X sur monocristal. Les atomes d'hydrogènes sont omis par souci de clarté. Longueurs de liaisons [Å] et angles [ $^\circ$ ] sélectionnés:  $\text{C}_4\text{-C}_5$  1,407(15),  $\text{P}_1\text{-Ni}_1\text{-P}_2$  104,50(10).

### 7.3.2.3 Synthèse de $[(\text{dcpp})\text{nickelalactone}]$ **IV-4**

Tout d'abord  $[(\text{dcpp})\text{nickelalactone}]$  **IV-4** a essayé d'être obtenue par le couplage oxydant entre  $[(\text{dcpp})\text{Ni}(\text{C}_2\text{H}_4)]$  **IV-3** et  $\text{CO}_2$ . Lorsque  $[(\text{dcpp})\text{Ni}(\text{C}_2\text{H}_4)]$  **IV-3** est placé sous 1 bar de  $\text{CO}_2$ , aucune réaction n'est observée. En montant la pression à 6 bar de  $\text{CO}_2$ , de petites quantités d'un nouveau produit sont observées par RMN  $^{31}\text{P}\{^1\text{H}\}$  sous forme de doublets à  $\delta = 10,4$  ppm ( $^2J_{\text{P,P}} = 32,8$  Hz) et à  $\delta = 32,1$  ppm ( $^2J_{\text{P,P}} = 32,8$  Hz). Ces signaux sont attribués au produit de couplage oxydant  $[(\text{dcpp})\text{nickelalactone}]$  **IV-4**.

$[(\text{dcpp})\text{nickelalactone}]$  **IV-4** a donc été synthétisée alternativement par substitution de ligands à partir de  $[(\text{tmeda})\text{nickelalactone}]$  **IV-5** et a pu être isolée avec 68 % de rendement. La comparaison des spectres RMN  $^{31}\text{P}\{^1\text{H}\}$  permet de confirmer, que le produit obtenu par la première voie de synthèse correspond bien également à  $[(\text{dcpp})\text{nickelalactone}]$  **IV-4**.

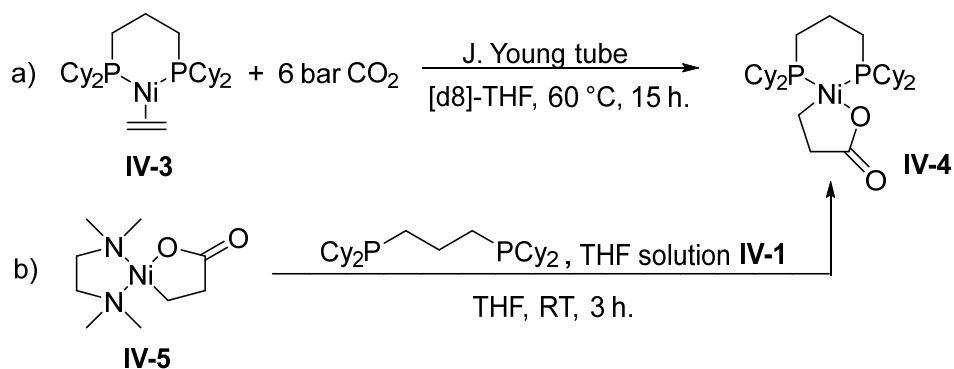


**Schéma 8:** Synthèse de [(dcpp)nickelalactone] **IV-4** par a) couplage oxydant à 6 bar de CO<sub>2</sub> and b) substitution de ligand à partir de [(tmeda)nickelalactone] **IV-5**.

Le complexe [(dcpp)nickelalactone] **IV-4** a été cristallisé par diffusion de pentane dans une solution de THF à température ambiante et la structure est présentée dans la **Figure 2**. [(dcpp)nickelalactone] **IV-4** adopte une géométrie plan carrée autour de l'atome central de nickel. L'angle de morsure P<sub>2</sub>-Ni<sub>1</sub>-P<sub>1</sub> mesure 99,66(2)° et est inférieur à celui de [(dcpp)Ni(C<sub>2</sub>H<sub>4</sub>)] **IV-3**, comme attendu. Les autres paramètres cristallographiques sont comparables en tous points aux nickelalactones connues dans la littérature. [13, 20, 26]

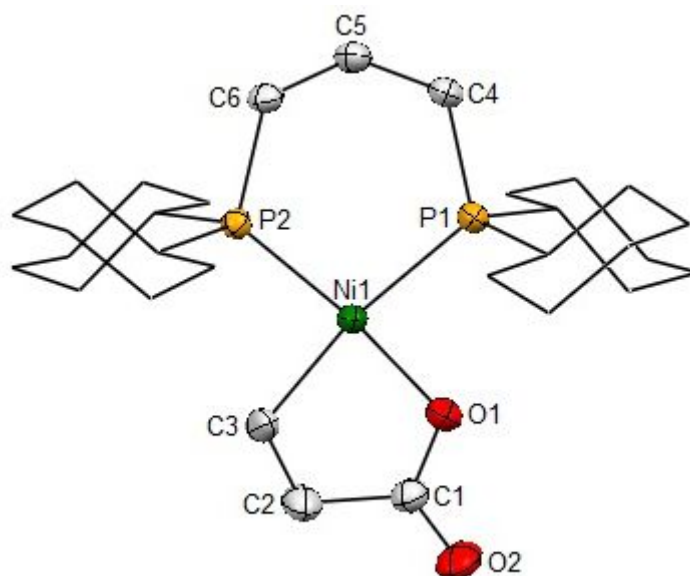


**Figure 2:** Structure moléculaire de [(dcpp)nickelalactone] **IV-4** déterminée par diffraction des rayons X sur monocristal. Les atomes d'hydrogène sont omis par souci de clarté. Longueurs de liaisons [Å] et angles [°] sélectionnés: Ni<sub>1</sub>-O<sub>1</sub> 1,9074(18), Ni<sub>1</sub>-C<sub>3</sub> 1,968(3), C<sub>1</sub>-O<sub>2</sub> 1,214(3), P<sub>1</sub>-Ni<sub>1</sub>-P<sub>2</sub> 99,66(2).

[(dcpp)nickelalactone] **IV-4** est stable à température ambiante sous atmosphère inerte pendant des mois, mais se dégrade complètement à 60 °C en l'espace de 3 j. en [(dcpp)Ni(C<sub>2</sub>H<sub>4</sub>)] **IV-3** et CO<sub>2</sub>.

### 7.3.2.4 Etude cinétique de l'équilibre entre [(dcpp)Ni(C<sub>2</sub>H<sub>4</sub>)] **IV-3** et [(dcpp)-nickelalactone] **IV-4**

La synthèse et l'étude de la stabilité de [(dcpp)nickelalactone] **IV-4** ont mis en évidence l'équilibre entre [(dcpp)Ni(C<sub>2</sub>H<sub>4</sub>)] **IV-3** et [(dcpp)nickelalactone] **IV-4**. Des études cinétiques ont été menées afin de déterminer l'ordre de la réaction et les paramètres d'activation. Pour cela une quantité connue de [(dcpp)nickelalactone] **IV-4** est chauffée à différentes températures comprises entre 55 °C et 90 °C avec PPh<sub>3</sub> comme standard interne. La décroissance de la concentration de [(dcpp)nickelalactone] **IV-4** est suivie par RMN <sup>31</sup>P{<sup>1</sup>H} (**Figure 3**).

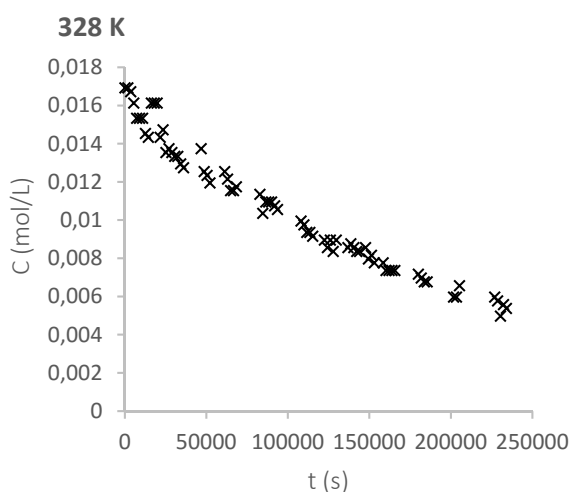


**Figure 3:** Profil cinétique de la réaction à 55 °C.

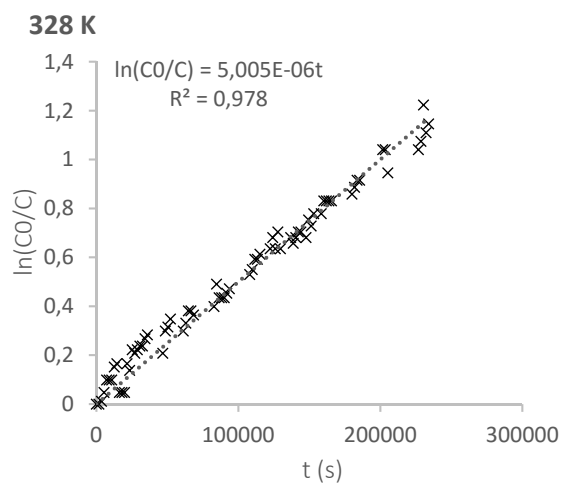


**Figure 4:**  $\ln([Nilactone]_0/[Nilactone])$  en fonction du temps pour la réaction dans le THF à 55 °C.

La réaction est d'ordre 1, comme le prouve le graphe  $\ln([Nilactone]_0/[Nilactone]) = f(t)$  (**Figure 4**) qui donne une droite. L'enthalpie libre de l'état de transition  $\Delta G^\ddagger$  peut être obtenue à partir des constantes de vitesse déterminées graphiquement et insérées dans l'équation de Eyring. Ainsi, un  $\Delta G^\ddagger = 27,39 \text{ kcal.mol}^{-1}$  moyen a été calculé. La variation de température donne de plus accès par l'intermédiaire d'un graphe de Eyring aux paramètres  $\Delta H^\ddagger$  et  $\Delta S^\ddagger$ , qui ont été évalués à

$\Delta H^\ddagger = 25,17 \text{ kcal.mol}^{-1}$  et  $\Delta S^\ddagger = -6,50 \text{ kcal.mol}^{-1}$ . Les paramètres d'activation de la décomposition de [(dcp)nickelalactone] **IV-4** en [(dcp)Ni(C<sub>2</sub>H<sub>4</sub>)] **IV-3** et CO<sub>2</sub> sont bien en accord avec les conditions expérimentales reportées précédemment.

### 7.3.2.5 Réactivité de [(dcp)nickelalactone] **IV-4** avec du pinacolborane **IV-8**

Afin de cliver [(dcp)nickelalactone] **IV-4** et de la convertir en dérivés acryliques, celle-ci a été mise en présence de boranes, agissant en tant qu'agents de transmétallation, comme alternative aux électrophiles [16, 17, 18] et bases fortes [19] couramment utilisés. Le pinacolborane **IV-8** est le réactif le plus approprié pour cette transformation de part son absence de réactivité avec l'éthylène et [(dcp)Ni(C<sub>2</sub>H<sub>4</sub>)] **IV-3**.

Lorsque [(dcp)nickelalactone] **IV-4** réagit avec du pinacolborane **IV-8**, il se forme un nouveau composé organométallique [(dcp)NiH]<sub>2</sub> **IV-9** en l'espace de 10 min. à température ambiante. Ce composé, connu de la littérature, se laisse facilement reconnaître par son déplacement chimique à  $\delta = 25,0 \text{ ppm}$  en RMN <sup>31</sup>P {<sup>1</sup>H} et par la présence d'un hydruure sous forme d'un quintet à  $\delta = -10,1 \text{ ppm}$  en RMN <sup>1</sup>H. De plus, ce composé a pu être cristallisé. Cependant, il n'a pas été possible à ce stade de la réaction de déterminer la ou les produits organiques formés simultanément et mis en évidence par RMN DOSY <sup>1</sup>H.

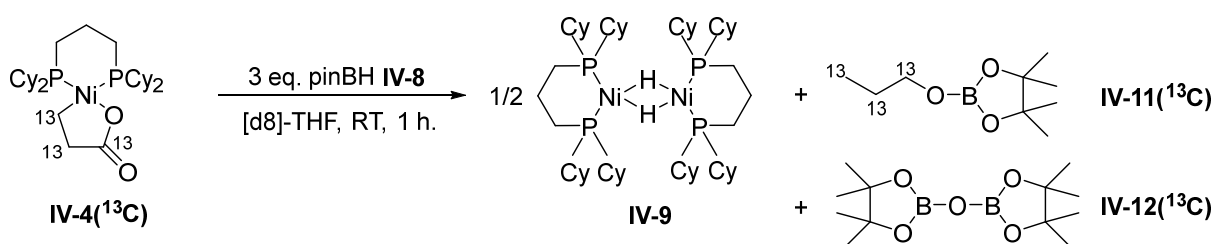


**Schéma 9:** Réaction entre <sup>13</sup>C[(dcp)nickelalactone] **IV-4**(<sup>13</sup>C) et 3 eq. de pinacolborane **IV-8**.

Pour cela, [(dcp)nickelalactone] **IV-4** a été marquée au <sup>13</sup>C. Ainsi, en optimisant les conditions réactionnelles, il s'avère qu'il faut au minimum 3 eq. de pinacolbrane **IV-8** pour convertir toute la [(dcp)nickelalactone] **IV-4**. La RMN <sup>13</sup>C, présentée dans la **Figure 5**, possède trois signaux attribués à la chaîne linéaire propyl du produit organique formé. De façon surprenante, aucun carbone associé à une fonction carbonyle n'a pu être repéré, ce qui signifie que l'ester a été réduit au cours de la réaction. Des expériences HSQC 1D <sup>1</sup>H donnent accès aux protons directement liés à des centres <sup>13</sup>C (**Figure 6**). En combinaison avec des expériences classiques

de RMN 2D, il est possible de les attribuer aux carbones correspondants de la chaîne propyle. Le spectre HSQC 1D  $^1\text{H}$  présente un signal supplémentaire, appartenant aux protons des groupements méthyles du pinacolborane **IV-8**, l'abondance naturelle de  $^{13}\text{C}$  n'étant plus négligeable au vu des huit carbones équivalents présents dans la molécule. Enfin, la RMN  $^{11}\text{B}$ , suggère la présence de deux unités borates par deux pics à  $\delta = 21,6$  ppm et  $\delta = 22,5$  ppm.

Ainsi l'analyse de la réaction par spectroscopie RMN, permet de conclure à la formation de propoxypinacolborane **IV-11** et de diboroxane pinBOBpin **IV-12** à l'issue de la réaction de [(dcpp)nickelalactone] **IV-4** avec 3 eq. de pinacolborane **IV-8**.

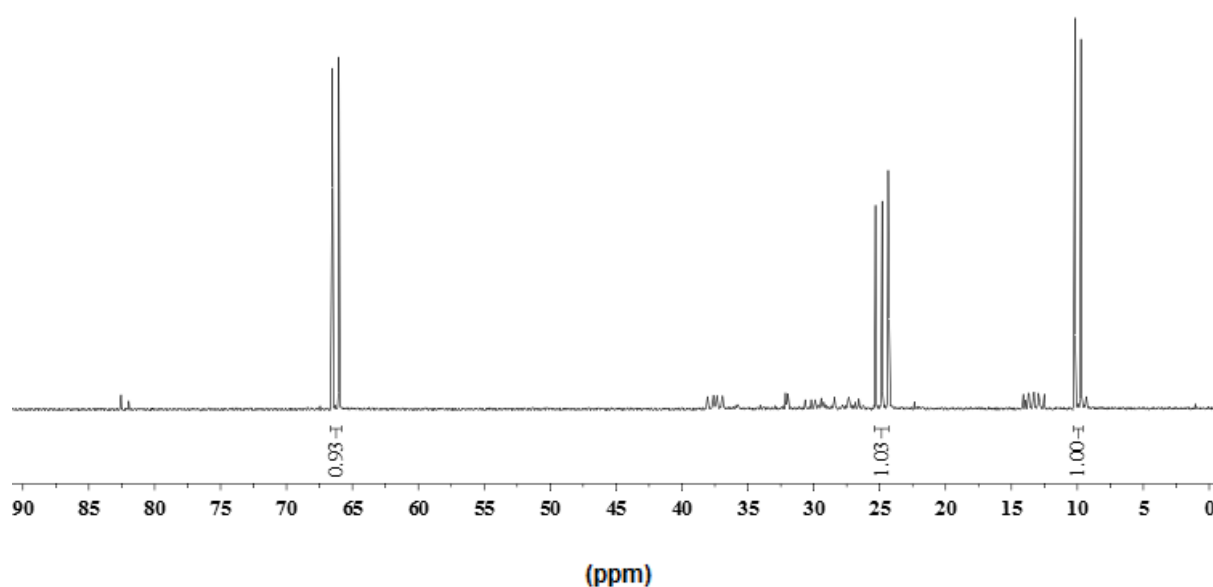


**Figure 5:** Spectre RMN  $^{13}\text{C}\{^1\text{H}\}$  à 75 MHz de la réaction entre  $^{13}\text{C}$ [(dcpp)nickelalactone] **IV-4**( $^{13}\text{C}$ ) et 3 eq. de pinacolborane **IV-8** à température ambiante. Par souci de clarté, le [d8]-THF a été remplacé par du  $\text{C}_6\text{D}_6$ .

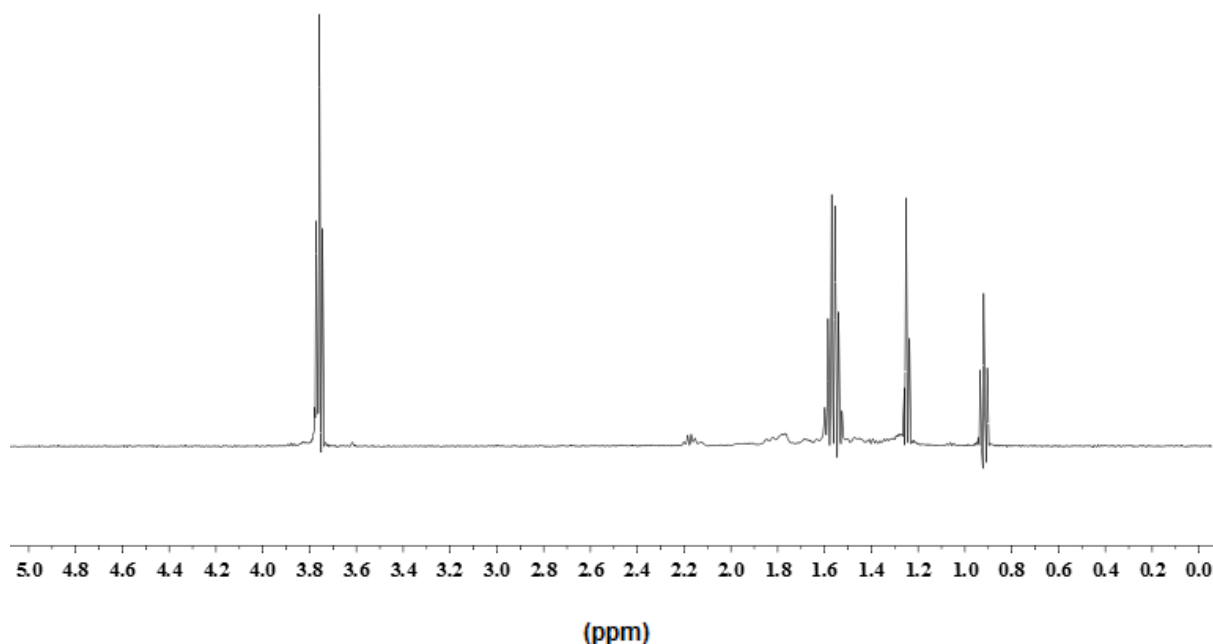


**Figure 6:** Spectre RMN  $^1\text{H}\{^{13}\text{C}\}$  1D HSQC à 500 MHz de la réaction entre  $^{13}\text{C}$ [(dcpp)nickelalactone] **IV-4**( $^{13}\text{C}$ ) et 3 eq. de pinacolborane **IV-8** à température ambiante dans du [d8]-THF.

Afin de bien confirmer la formation de propoxypinacolborane **IV-11**, une expérience de spiking a été réalisée. Le propoxypinacolborane **IV-11** peut être synthétisé indépendamment en 15 min. à partir de propanol et de pinacolborane **IV-8** à température ambiante. Ainsi, la réaction entre [(dcpp)nickelalactone] **IV-4** et pinacolborane **IV-8** est suivie par RMN  $^1\text{H}$  en utilisant le mésitylène comme standard interne. Une fois la réaction terminée, 5 eq. de propoxypinacolborane **IV-11** sont rajoutés au milieu réactionnel, qui est toujours suivi par RMN  $^1\text{H}$ . Les pics et les intégrations correspondants au propoxypinacolborane **IV-11** augmentent de manière conséquente, apportant une preuve supplémentaire à la formation de propoxypinacolborane **IV-11** au cours de la réaction. Les spectres RMN  $^1\text{H}$  associés à l'expérience de spiking peuvent être consultés dans la **Figure 7** ci-dessous.



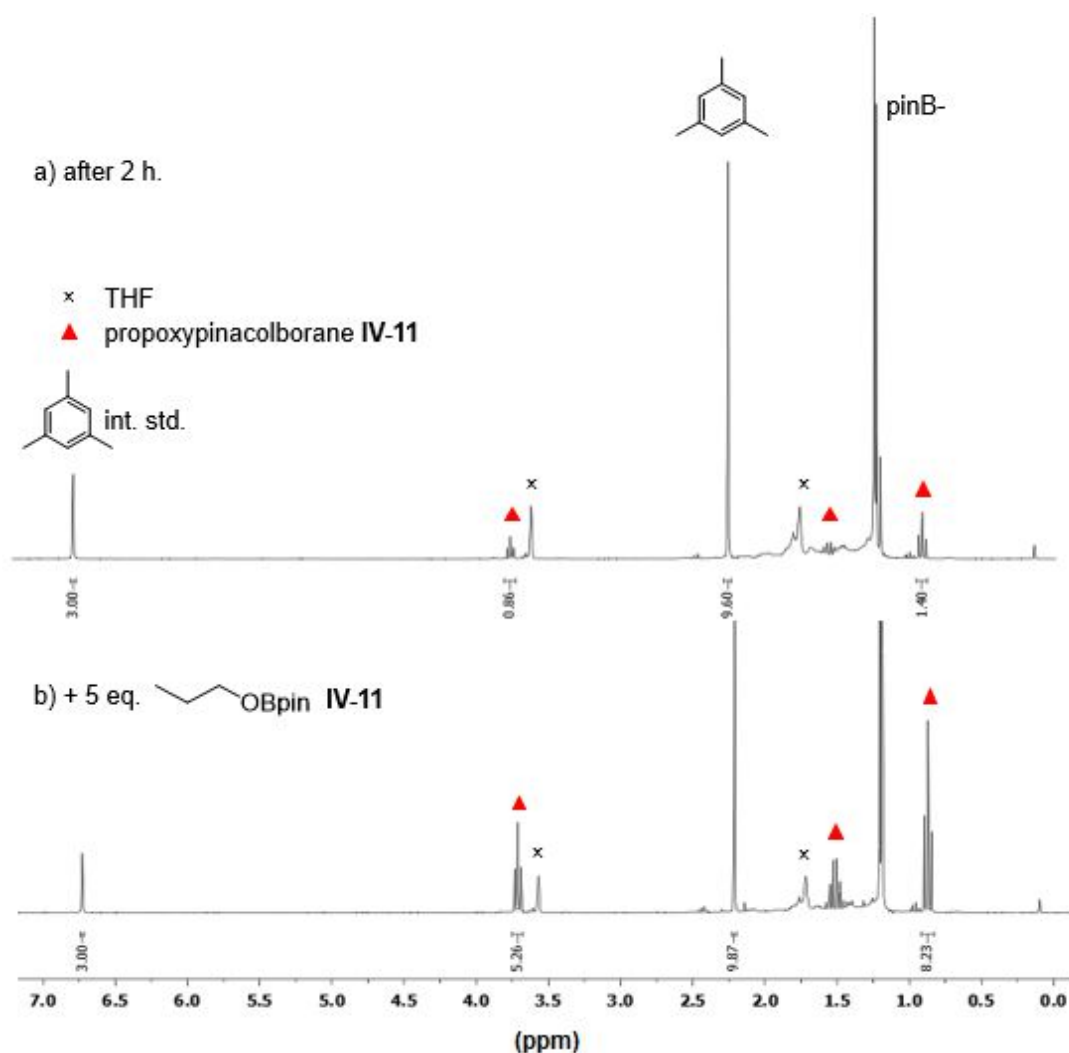


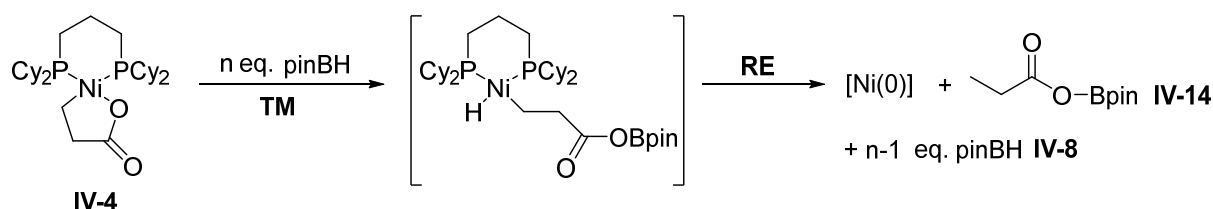
**Figure 7:** Spectre RMN  $^1\text{H}$  NMR de l'expérience de spiking. a) Réaction entre [(dcp)nickelalactone] **IV-4** et 3 eq. de pinacolborane **IV-8** après 2 h. à température ambiante. b) Après ajout de 5 eq. de propoxypinacolborane **IV-11**.

### 7.3.2.6 Etude mécanistique de la réaction

La réduction de [(dcp)nickelalactone] **IV-4** en propoxypinacolborane **IV-11** requiert au moins 3eq. de pinacolborane **IV-8**. La force motrice de la réaction est la formation de liaisons B-O fortes, comme le montre la formation du produit secondaire pinBOBpin **IV-12**. Le borane joue donc à la fois le rôle de réducteur et de piège à oxygène.

Le premier équivalent de pinacolborane **IV-8** est employé comme agent de transmétallation, qui permet de cliver la liaison Ni-O de [(dcp)nickelalactone] **IV-4**. Cela conduit à un complexe [(dcp)Ni(propanoate)(H)] intermédiaire, à partir duquel le dérivé d'acide propanoïque correspondant **IV-14** est libéré très facilement par élimination réductrice avec formation concomitante d'un complexe de Ni(0) hautement réactif, comme l'indique le **Schéma 10**.

Cette première étape a pu être vérifiée expérimentalement à partir du complexe de Ni(0) [(dcpp)Ni(naphthalène)], qui en présence du dérivé d'acide propanoïque **IV-14** et de pinacolborane **IV-8**, génère après 14 h. at 60 °C du propoxypinacolborane **IV-11** et du diboroxane **IV-12**. La réaction est plus lente que dans les conditions originales de la réaction, car le complexe de Ni(0) utilisé est stabilisé par la coordination du naphthalène.



**Scheme 10:** Première étape du mécanisme de la réaction entre [(dcpp)nickelalactone] **IV-4** et du pinacolborane **IV-8**.

Ensuite, le reste du mécanisme et notamment la réduction du dérivé d'acide propanoïque **IV-14** en présence de pinacolborane **IV-8** reste encore à élucider. Trois mécanismes sont cependant suggérés. Le premier, fortement inspiré de la réduction de CO<sub>2</sub> par des boranes en présence de complexes organométalliques, prévoit l'intervention de complexes de nickel hydrures.<sup>[27]</sup> Le second, envisage l'addition oxydante du dérivé d'acide propanoïque à l'espèce de Ni(0) libre générée, mais semble moins probable de part l'absence d'électrons π, qui facilitent ce processus. Enfin, le troisième, le plus probable, fait intervenir l'addition oxydante du pinacolborane sur le Ni(0), qui générerait des espèces [Ni(I)-boryles] promouvant la réduction du dérivé d'acide propanoïque **IV-14** en propoxypinacolborane **IV-11**. Des expériences supplémentaires vont être menées afin de départager ces trois mécanismes.

### 7.3.2.7 Vers un procédé catalytique

Un cycle catalytique, conduisant à la formation de propoxypinacolborane **IV-11** à partir du couplage oxydant entre de l'éthylène et du CO<sub>2</sub> en présence d'un complexe de nickel et de pinacolborane **IV-8**, a été construit étape par étape. Le cycle est représenté dans le **Schéma 11**.

A forte pression de CO<sub>2</sub>, il est possible de réaliser le couplage oxydant sur le complexe [(dcpp)Ni(C<sub>2</sub>H<sub>4</sub>)] **IV-3**, conduisant à la formation de [(dcpp)nickelalactone] **IV-4**. Ensuite, en présence d'au moins 3 eq. de pinacolborane **IV-8**, il est possible de convertir à température

ambiante [(dcpp)nickelalactone] **IV-4** en propoxypinacolborane **IV-11** et en diboroxane pinBOBpin **IV-12**, en passant par un intermédiaire de dérivé d'acide propanoïque **IV-14**. Au cours de cette étape, le complexe diamagnétique de Ni(0) [(dcpp)NiH]<sub>2</sub> **IV-9** est également produit. Celui-ci se laisse très facilement reconvertir en [(dcpp)Ni(C<sub>2</sub>H<sub>4</sub>)] **IV-3**, sous 1 bar d'éthylène à température ambiante en 20 min, fermant ainsi le cycle catalytique. L'étape cinétiquement déterminante de ce cycle est donc le couplage oxydant entre [(dcpp)Ni(C<sub>2</sub>H<sub>4</sub>)] **IV-3** et CO<sub>2</sub>.

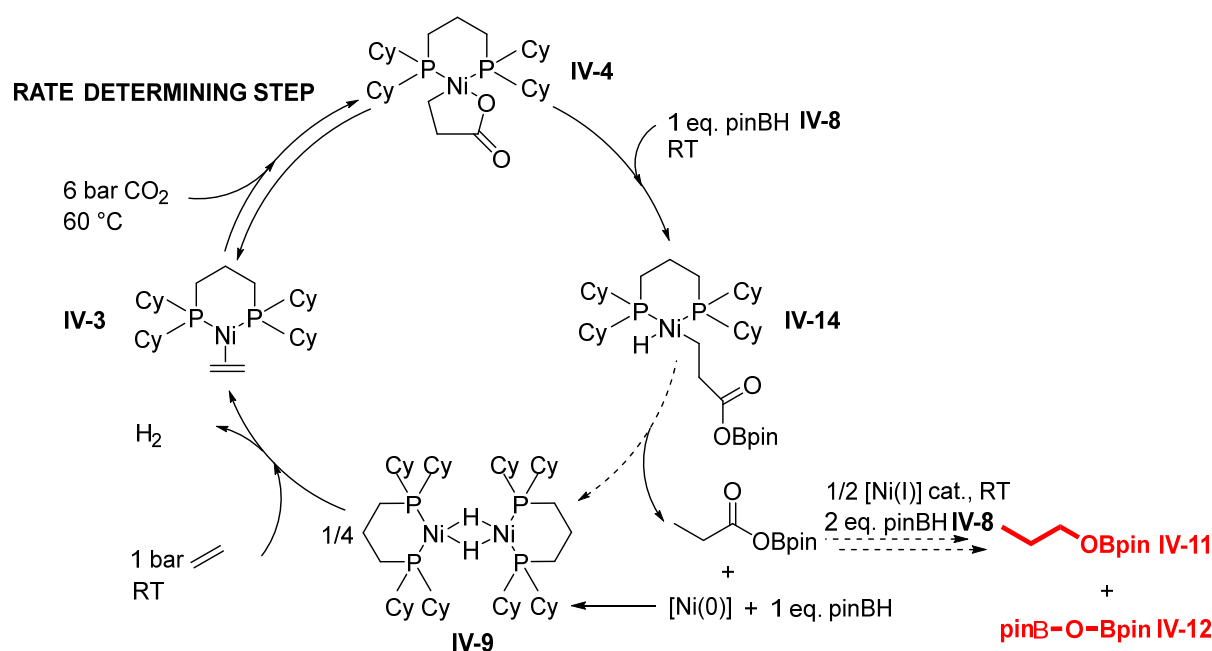


**Schéma 11:** Cycle catalytique proposé pour la réaction entre l'éthylène, le CO<sub>2</sub> et le pinacolborane **IV-8** en présence de complexes de nickel dcpp.

De premières réactions catalytiques ont été menées en autoclave à différentes pressions de CO<sub>2</sub> et d'éthylène avec divers catalyseurs, sans grand succès. Le produit principal de la réaction est le complexe [(dcpp)Ni(CO)<sub>2</sub>] **IV-23**, qui une fois généré, empoisonne toute la catalyse de part sa très grande stabilité thermodynamique. De nouvelles conditions expérimentales vont être testées, notamment en faisant varier le ratio de pression éthylène/CO<sub>2</sub>, le solvant de la réaction ou le catalyseur employé, afin de pouvoir rendre cette réaction catalytique.

### 7.3.3 Activation du CO<sub>2</sub> avec des complexes de nickel coordonnés par des ligands bis-NHC

#### 7.3.3.1 Introduction

De nombreuses recherches ont été menées sur le couplage oxydant entre l'éthylène et le CO<sub>2</sub> avec des complexes de nickel substitués par des ligands diamines et bis-phosphines. Cependant, il existe à ce jour une seule nickelalactone, coordonnée par un ligand carbène monodente de type NHC, reportée par Walther en 2006. <sup>[28]</sup> Le développement d'une chimie des bis-NHCs analogue à celle des bis-phosphines et à ce jour encore inexplorée revêt un grand intérêt.

Les ligands NHCs ont des propriétés analogues à celles des phosphines mais possèdent cependant un caractère  $\sigma$  donneur beaucoup plus important. Le remplacement des phosphines par des NHCs a permis des avancées majeures en catalyse et notamment le développement de réactions très efficaces telle que la métathèse des oléfines. <sup>[29]</sup> Cette substitution de ligand pourrait également permettre de résoudre certaines limitations cinétiques et thermodynamiques rencontrées lors de la fonctionnalisation du CO<sub>2</sub> en acrylates. En effet, il est tout d'abord primordial de trouver des conditions de couplage plus douces à faibles pressions de CO<sub>2</sub> et d'éthylène et ensuite de favoriser l'élimination des protons en  $\beta$  de la nickelalactone pour la production de dérivés acryliques.

Trois sels de bis-imidazoliums ont été sélectionnés pour cette étude: *Lt*BuH<sub>2</sub>Br<sub>2</sub> **VI-5**, LDippH<sub>2</sub>Br<sub>2</sub> **VI-6** et *Lt*Bu<sup>prop</sup>H<sub>2</sub>Br<sub>2</sub> **VI-7**. Dans un premier temps les complexes [(bis-NHC)Ni(C<sub>2</sub>H<sub>4</sub>)], encore inconnus à ce jour, ont été synthétisés et caractérisés. Ensuite, les nickelalactones correspondantes [(bis-NHC)nickelalactones] ont été obtenues par réactions de substitution de ligands ainsi que par couplage oxydant entre les complexes [(bis-NHC)Ni(C<sub>2</sub>H<sub>4</sub>)] et du CO<sub>2</sub>. Quelques expériences préliminaires ont testé la réactivité des [(bis-NHC)nickelalactones] synthétisées en vue de générer des acrylates.

#### 7.3.3.2 Synthèse de complexes [(bis-NHC)Ni(éthylène)] et [(bis-NHC)Ni(alcynes)]

Tout d'abord, les premiers complexes [(bis-NHC)Ni(C<sub>2</sub>H<sub>4</sub>)] ont été synthétisés par substitutions de ligands. Pour cela les sels de bis-imidazolium ont été déprotonés par 2 eq. de KO<sup>*t*</sup>Bu dans de l'éther sous atmosphère inerte afin de générer les bis-carbènes libres

correspondants, qui sont stables en solution pour plusieurs heures. Après avoir éliminé par filtration les sels de potassium (KBr) insolubles dans l'éther, les carbènes libres sont mis en présence de  $[\text{Ni}(\text{COD})_2]$  **VI-8** et d'éthylène. Le premier ligand COD est déplacé par le carbène libre alors que le second ligand COD est facilement substitué par l'éthylène. Ainsi les complexes  $[\text{L}t\text{Bu}]\text{Ni}(\text{C}_2\text{H}_4)$  **VI-9** et  $[(\text{LDipp})\text{Ni}(\text{C}_2\text{H}_4)]$  **VI-10** ont pu être obtenu avec 75 % et 71 % de rendement respectivement. Les conditions opératoires sont détaillées dans le **Schéma 12**.

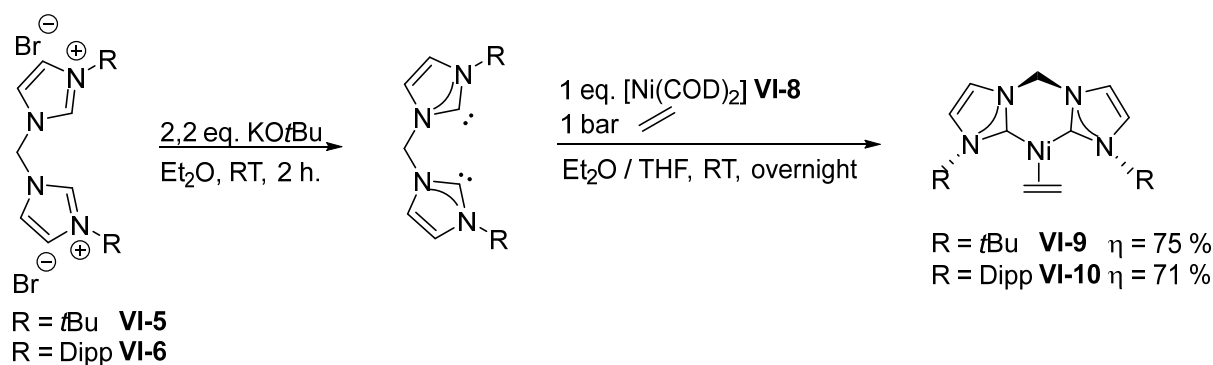


**Schéma 12:** Synthèse des complexes  $[(\text{L}t\text{Bu})\text{Ni}(\text{C}_2\text{H}_4)]$  **VI-9** et  $[(\text{LDipp})\text{Ni}(\text{C}_2\text{H}_4)]$  **VI-10**.

$[\text{L}t\text{Bu}]\text{Ni}(\text{C}_2\text{H}_4)$  **VI-9** et  $[(\text{LDipp})\text{Ni}(\text{C}_2\text{H}_4)]$  **VI-10** ont été caractérisés par spectroscopie RMN. La résonance des centres carbéniques à bas champ, à  $\delta = 203,7$  ppm et à  $\delta = 200,1$  ppm respectivement, prouve bien la coordination du ligand bis-NHC. Les déplacements chimiques des protons éthyléniques sont remarquablement déplacés vers la région des hauts champs. Les protons éthyléniques de  $[\text{L}t\text{Bu}]\text{Ni}(\text{C}_2\text{H}_4)$  **VI-9** résonnent comme un système AA'BB' à  $\delta = 1,06$  ppm et  $\delta = 1,20$  ppm ( $^3J_{\text{A},\text{A}'} = ^3J_{\text{B},\text{B}'} = 10,4$  Hz,  $^3J_{\text{A},\text{B}'} = 12,3$  Hz,  $^2J_{\text{A},\text{B}} = -2,9$  Hz) alors que les protons de  $[(\text{LDipp})\text{Ni}(\text{C}_2\text{H}_4)]$  **VI-10** sortent sous forme d'un singulet à  $\delta = 0,14$  ppm dans le [d8]-THF. Les déplacements chimiques des carbones associés sont également fortement décalés dans la région des alcanes ( $\delta = 27,7$  ppm et  $\delta = 25,2$  ppm respectivement). Ces déplacements chimiques inusuels pour des protons et carbones oléfiniques, démontrent la forte rétro-donation du fragment  $[(\text{bis-NHC})\text{Ni}]$  vers l'éthylène. Ces résultats sont corroborés par la structure du complexe  $[(\text{L}t\text{Bu})\text{Ni}(\text{C}_2\text{H}_4)]$  **VI-9** obtenue par DRX et présentée dans la **Figure 8**.  $[(\text{L}t\text{Bu})\text{Ni}(\text{C}_2\text{H}_4)]$  **VI-9** possède une géométrie plan carrée légèrement déformée et le cycle chélatant à six chaînons formé par l'atome de nickel et le ligand bis-NHC adopte une conformation bateau. L'angle de morsure  $\text{C}_3\text{-Ni}_1\text{-C}_4$  est de  $91,45(14)^\circ$  alors que la liaison

éthylénique C<sub>1</sub>-C<sub>2</sub> mesure 1,419(5) Å et se situe bien à mi- chemin entre une liaison C-C simple (1,54 Å) et une liaison C-C double (1,34 Å).

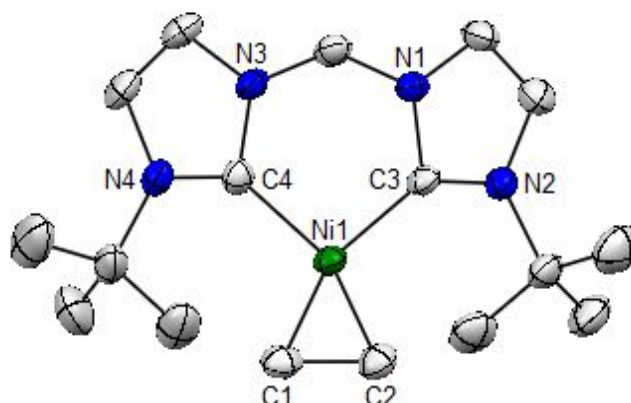


**Figure 8:** Structure moléculaire de  $[(L^tBu)Ni(C_2H_4)]$  **VI-9** déterminée par diffraction de rayons X sur monocristal. Les atomes d'hydrogène sont omis par souci de clarté. Longueurs de liaisons [Å] et angles [°] sélectionnés: Ni<sub>1</sub>-C<sub>1</sub> 1,953(4), Ni<sub>1</sub>-C<sub>2</sub> 1,947(3), Ni<sub>1</sub>-C<sub>3</sub> 1,923(3), Ni<sub>1</sub>-C<sub>4</sub> 1,903(3), C<sub>1</sub>-C<sub>2</sub> 1,419(5), C<sub>1</sub>-Ni<sub>1</sub>-C<sub>2</sub> 42,66(15), C<sub>3</sub>-Ni<sub>1</sub>-C<sub>4</sub> 91,45(14).

Par la suite, les complexes  $[(L^tBu)Ni(\text{diphénylacétylène})]$  **VI-13** et  $[(L^tBu)Ni(\text{phénylacétylène})]$  **VI-14** ont été obtenus de la même manière en remplaçant l'éthylène par du diphénylacétylène **VI-11** ou du phénylacétylène **VI-12** et ont été isolés avec 76 % et 73 % de rendement respectivement (**Schéma 13**). Ces complexes ont également été caractérisés par RMN et DRX.

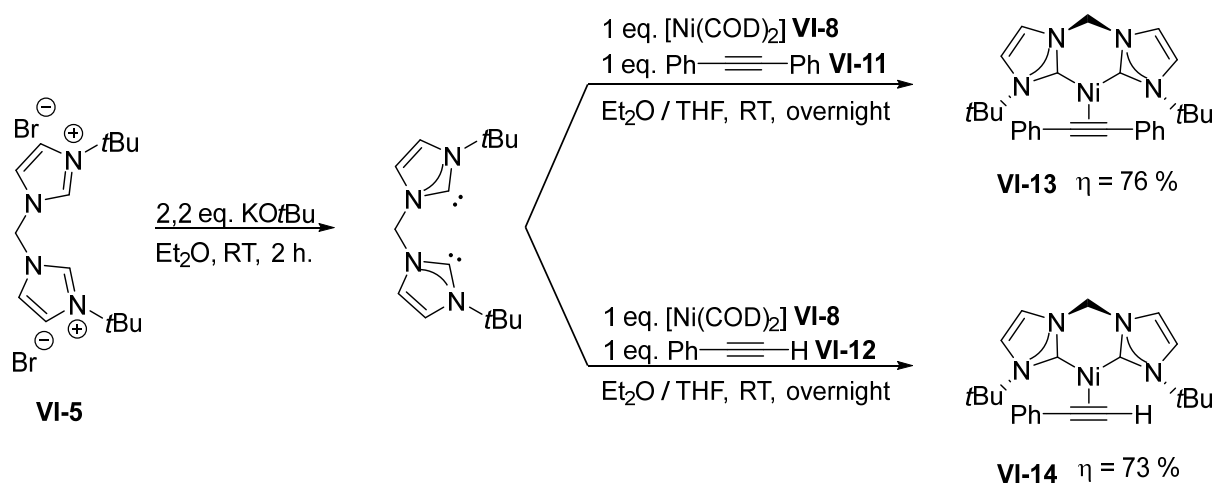


**Schéma 13:** Synthèse de  $[(L^tBu)Ni(\text{diphénylacétylène})]$  **VI-13** et  $[(L^tBu)Ni(\text{phénylacétylène})]$  **VI-14**.



NHC)Ni(alcènes)] et [(bis-NHC)Ni(alcynes)]. La déprotonation des sels de bis-imidazolium (bis-NHC)H<sub>2</sub>Br<sub>2</sub> par 2,2 eq. de KO<sup>t</sup>Bu, génère des bis-NHC libres, qui déplacent ensuite facilement la diamine dans le complexe préformé [(tmeda)nickelalactone] **VI-17**. Il est indispensable de réaliser la déprotonation dans de l'éther afin de pouvoir facilement éliminer par filtration le KBr formé. En effet comme les [(bis-NHC)nickelalactones] obtenues ont une solubilité très limitée dans presque tous les solvants organiques communs, il devient extrêmement difficiles de les séparer de KBr en fin de réaction. En suivant cette méthodologie de synthèse, [(*Lt*Bu)nickelalactone] **VI-18**, [(LDipp)nickelalactone] **VI-19** et [(*Lt*Bu)<sup>prop</sup>nickelalactone] **VI-20** ont pu être isolées avec de bons rendements, comme l'indique le **Schéma 15**, puis caractérisées. Ces complexes sont particulièrement stables et ne craignent ni l'eau ni l'air.

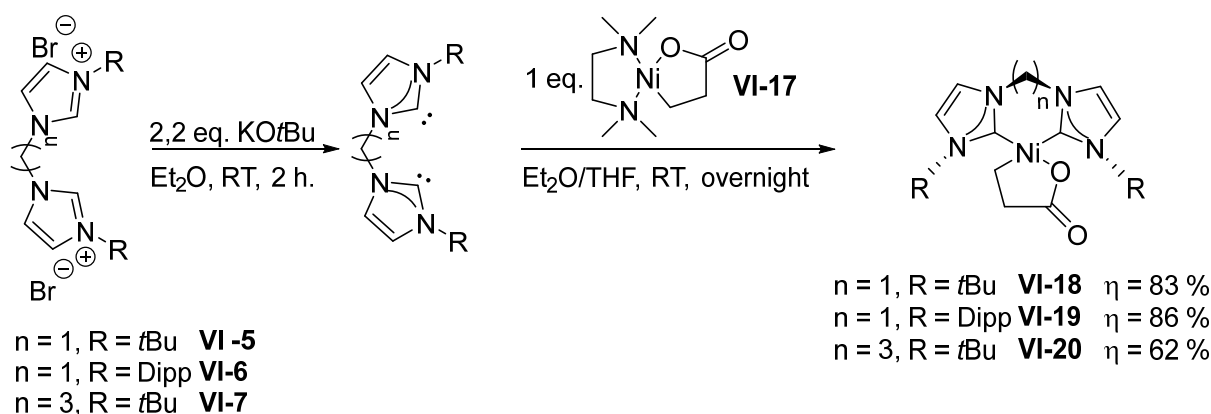


**Schéma 15:** Synthèse de [(*Lt*Bu)nickelalactone] **VI-18**, [(LDipp)nickelalactone] **VI-19** et [(*Lt*Bu)<sup>prop</sup>nickelalactone] **VI-20** par substitution de ligands à partir de [(tmeda)nickelalactone] **VI-17**.

En particulier, [(*Lt*Bu)nickelalactone] **VI-18** a été caractérisée par spectroscopie RMN, qui révèle deux protons Ni-CH<sub>2</sub> inéquivalents à  $\delta = 0,47$  ppm et à  $\delta = 0,74$  ppm et deux protons en  $\alpha$  de la fonction ester à  $\delta = 2,03$  ppm. La spectroscopie <sup>13</sup>C{<sup>1</sup>H} confirme la coordination du bis-carbène par l'apparition de deux pics associés à des carbones quaternaires à  $\delta = 180,6$  ppm et  $\delta = 186,1$  ppm ainsi que la présence d'un groupement acyl à  $\delta = 189,6$  ppm. En IR une bande d'absorption à 1619 cm<sup>-1</sup> donne une preuve supplémentaire pour la formation de la lactone. De plus, la structure RX de [(*Lt*Bu)nickelalactone] **VI-18** a été résolue et présente une géométrie plan carrée, avec un chélate à six chaînons en conformation bateau. L'angle de morsure de [(*Lt*Bu)nickelalactone] **VI-18** C<sub>4</sub>-Ni<sub>1</sub>-C<sub>5</sub> (86,89(17) °) est significativement plus petit de celui de [(dcpp)nickelalactone] **IV-4** (99,66(2) °). Les autres paramètres cristallographiques sont par



ailleurs comparables entre les deux nickelalactones. La structure de [(*Lt*Bu)nickelalactone] **VI-18** est présentée dans la **Figure 9**.

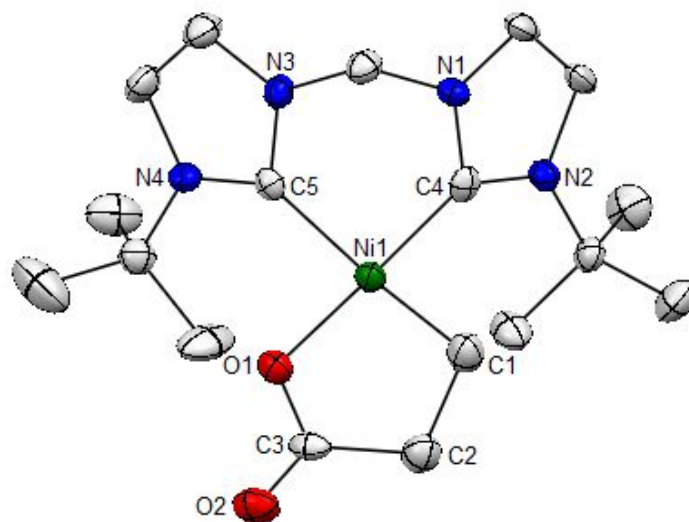


**Figure 9:** Structure moléculaire de [(*Lt*Bu)nickelalactone] **VI-18** déterminée par diffraction de rayons X sur monocristal. Les atomes d'hydrogènes sont omis par souci de clarté. Longueurs de liaisons [Å] et angles [°] sélectionnés: Ni<sub>1</sub>-O<sub>1</sub> 1,909(3), Ni<sub>1</sub>-C<sub>1</sub> 1,942(4), C<sub>3</sub>-O<sub>2</sub> 1,228(5), Ni<sub>1</sub>-C<sub>4</sub> 1,860(4), Ni<sub>1</sub>-C<sub>5</sub> 1,957(4), C<sub>4</sub>-Ni<sub>1</sub>-C<sub>5</sub> 86,89(17), C<sub>1</sub>-Ni<sub>1</sub>-O<sub>1</sub> 84,73(16).

### 7.3.3.5 Synthèse de [(bis-NHC)nickelalactones] par couplage oxydant avec des complexes [(bis-NHC)Ni(C<sub>2</sub>H<sub>4</sub>)]

Alternativement, les complexes [(bis-NHC)nickelalactones] peuvent aussi être obtenus directement par le couplage oxydant entre du CO<sub>2</sub> et des complexes [(bis-NHC)Ni(C<sub>2</sub>H<sub>4</sub>)]. De façon remarquable, il suffit d'1 bar de CO<sub>2</sub> pour réaliser le couplage oxydant à température ambiante, tel que le montre le **Schéma 16**. Ainsi, le couplage oxydant se fait dans des conditions beaucoup plus douces en présence des ligands bis-NHC, que pour les ligands analogues bis-phosphines étudiés précédemment. Par comparaison des données spectroscopiques avec celles des complexes synthétisés indépendamment auparavant, les [(bis-NHC)nickelalactones] ont pu être identifiées sans aucune ambiguïté. Cependant un produit secondaire encore non-identifié est également généré lors de la réaction de couplage.

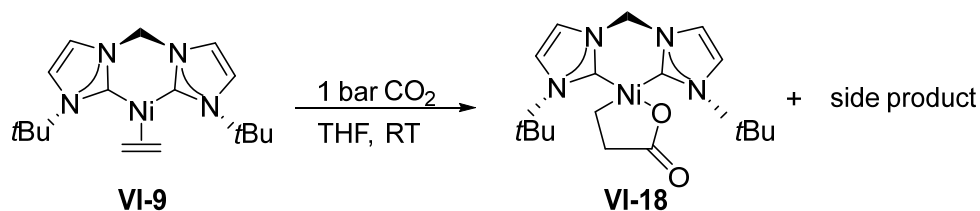


**Schéma 16:** Synthèse de [(*LtBu*)nickelalactone] **VI-18** par couplage oxydant entre 1 bar de CO<sub>2</sub> et [(*LtBu*)Ni(C<sub>2</sub>H<sub>4</sub>)] **VI-9** à température ambiante.

### 7.3.3.6 Réactivité des [(bis-NHC)nickelalactones]

La réactivité des [(bis-NHC)nickelalactones] synthétisées a ensuite été étudiée vis-à-vis de bases et d'agents de transmétallation afin de générer des dérivés d'acide acrylique. Cependant, dans les conditions catalytiques reportées par Limbach<sup>[22]</sup> et par Vogt,<sup>[21]</sup> [(*LtBu*)nickelalactone] **VI-18** n'a pas pu être convertie avec succès en produits chimiques valorisables et [(LDipp)nickelalactone] **VI-19** fournit des acrylates seulement en quantité stoechiométrique. De même la réactivité de [(*LtBu*)nickelalactone] **VI-18** avec divers boranes et zinciques n'est pas concluante pour l'instant. Les réactions sont limitées par le manque de solubilité des [(bis-NHC)nickelalactones] dans de nombreux solvants organiques ainsi que par leur stabilité thermodynamique. De plus l'absence de sonde phosphore rend le suivi des réactions beaucoup plus difficile. Pour pallier à ces difficultés [(*LtBu*)nickelalactone] **VI-18** a été marquée au <sup>13</sup>C, ce qui permet d'une part de mieux identifier les produits issus des réactions testées et d'autre part de comprendre les processus mis en jeu lors de ces différentes réactions.

### 7.3.4 Références

- [1] C. C. C. Johansson Seechurn, M. O. Kitching, T. J. Colacot, V. Snieckus, *Angew. Chem. Int. Ed.*, **2012**, *51*, 5062 - 5085.
- [2] R. Magano, J. R. Dunetz, *Chem. Rev.*, **2011**, *111*, 2177 - 2250.
- [3] L. Verheyen, P. Leysen, M.-P. Van Den Eede, N. Ceunen, T. Hardeman, G. Koeckelberghs, *Polymer*, **2017**, *108*, 521 - 546.
- [4] N.-H. Chang, M. Kinoshita, Y. Nishihara, *Lecture Notes in Chemistry*, **2013**, *80*, 111 - 135.
- [5] A. F. Littke, G. C. Fu, *Angew. Chem. Int. Ed.*, **2002**, *41*, 4176 - 4211.

- [6] A. Gavryushin, C. Kofink, G. Manolikakes, P. Knochel, *Org. Lett.*, **2005**, *7*, 4871 - 4874.
- [7] L. Wang, Z.-X. Wang, *Org. Lett.*, **2007**, *9*, 4335 - 4338.
- [8] R. Gerber, C. M. Frech, *Chem. Eur. J.*, **2011**, *17*, 11893 - 11904.
- [9] Matthieu Demange, Thèse de doct., Ecole polytechnique, Paris, **2013**.
- [10] T. T. Tsou, J. K. Kochi, *J. Am. Chem. Soc.*, **1979**, *101*, 7547 - 7560.
- [11] I. Colon, D. R. Kelsey, *J. Org. Chem.*, **1986**, *51*, 2627 - 2637.
- [12] M. M. Lin, *Appl. Catal. A: Gen.*, **2001**, *207*, 1 - 16.
- [13] H. Hoberg, D. Schaefer, *J. Organomet. Chem.*, **1983**, *251*, C51 - C53.
- [14] H. Hoberg, Y. Peres, C. Krüger, Y.-H. Tsay, *Angew. Chem.*, **1987**, *99*, 799 - 800.
- [15] D. C. Graham, C. Mitchell, M. I. Bruce, G. F. Metha, J. H. Bowie, M. A. Buntine, *Organomet.*, **2007**, *26*, 6784 - 6792.
- [16] C. Bruckmeier, M. W. Lehenmeier, R. Reichardt, S. Vagin, B. Rieger, *Organomet.*, **2010**, *29*, 2199 - 2202.
- [17] S. Y. T. Lee, M. Cokoja, M. Drees, Y. Li, J. Mink, W. A. Herrmann, F. E. Kühn, *ChemSusChem*, **2011**, *4*, 1275 - 1279.
- [18] S. Y. T. Lee, A. Abdul Ghani, V. D'Elia, M. Cokoja, W. A. Herrmann, J.-M. Basset, F. E. Kühn, *New. J. Chem.*, **2013**, *37*, 3512 - 3517.
- [19] D. Jin, T. J. Schmeier, P. G. Williard, N. Hazari, W. H. Bernskoetter, *Organomet.*, **2013**, *32*, 2152 - 2159.
- [20] M. L. Lejkowski, R. Lindner, T. Kageyama, G. É. Bódizs, P. N. Plessow, I. B. Müller, A. Schäfer, F. Rominger, P. Hofmann, C. Futter, S. A. Schunk, M. Limbach, *Chem. Eur. J.*, **2012**, *18*, 14017 - 14025.
- [21] C. Hendriksen, E. A. Pidko, G. Yang, B. Schöffner, D. Vogt, *Chem. Eur. J.*, **2014**, *20*, 12037 - 12040.
- [22] N. Huguet, I. Jevtovikj, A. Gordillo, M. L. Lejkowski, R. Lindner, M. Bru, A. Y. Khalimon, F. Rominger, S. A. Svhunk, P. Hofmann, M. Limbach, *Chem. Eur. J.*, **2014**, *20*, 16858 - 16862.
- [23] M. Takimoto, K. Shimizu, M. Mori, *Org. Lett.*, **2001**, *3*, 3345 - 3347.

- [24] M. Takimoto, M. Mori, *J. Am. Chem. Soc.*, **2001**, *123*, 2895 - 2896.
- [25] E. M. O'Brien, E. A. Bercot, T. Rovis, *J. Am. Chem. Soc.*, **2003**, *125*, 10498 - 10499.
- [26] R. Fischer, J. Langer, A. Malassa, D. Walther, H. Görls, G. Vaughan, *Chem. Commun.*, **2006**, *23*, 2510 - 2512.
- [27] S. Bontemps, *Coord. Chem. Rev.*, **2016**, *308*, 117 - 130.
- [28] J. Langer, D. Walther, H. Görls, *J. Organomet. Chem.*, **2006**, *691*, 4874 - 4881.
- [29] M. Scholl, S. Ding, C. W. Lee, R. H. Grubbs, *Org. Lett.*, **1999**, *1*, 953 - 956.



## *Nickel Mediated Negishi and Oxidative Couplings*

The aim of this research project is to promote the formation of new C-C bonds and the production of valuable chemicals by using chelated nickel complexes.

The first part of this thesis is dedicated to [nickel(bis-phosphine)] complexes employed as catalysts for Negishi cross coupling reactions. Designed Ni(0) precatalyst [(dcp)Ni( $\eta^2$ -toluene)] (dcp = 1,3-bis(dicyclohexylphosphino)propane) promotes efficiently the Negishi cross coupling between aryl chlorides and phenylzinc chloride derivatives at low catalyst loadings (down to 0.2 mol% - 1 mol%) under mild conditions (THF, 60°C). Mechanistic investigations relying on stoichiometric reactions and DFT calculations prove the involvement of Ni(0)/Ni(II) intermediates rather than Ni(I)/Ni(III) species during the catalysis.

The second part of this work deals with the oxidative coupling between ethylene and CO<sub>2</sub> at bis-phosphine and bis-NHC chelated nickel complexes for the production of value-added chemicals. The equilibrium between [(dcp)Ni(C<sub>2</sub>H<sub>4</sub>)] and [(dcp)nickelalactone] has been investigated by kinetic studies. The subsequent cleavage of [(dcp)nickelalactone] by pinacolborane leads to its reductive functionalization into a propanol derivative. Preliminary mechanistic and catalytic investigations have been undertaken. Moreover, new methodologies are provided for the synthesis of the first [(bis-NHC)Ni(C<sub>2</sub>H<sub>4</sub>)] and [(bis-NHC)nickelalactone] complexes.

### *Couplages de Negishi et Couplages Oxydants à Base de Complexes de Nickel*

Ce projet de recherche porte sur la formation de nouvelles liaisons C-C et la production de produits chimiques valorisables grâce à l'utilisation de complexes de nickel chélatés.

La première partie de cette thèse est dédiée à des complexes bis-phosphines de nickel employés comme catalyseurs pour le couplage croisé de Negishi. Le précatalyseur [(dcp)Ni( $\eta^2$ -toluene)] (dcp = 1,3-bis(dicyclohexylphosphino)propane) permet de coupler efficacement des chloro-arènes avec des organozinciques en utilisant de faibles charges catalytiques (0,2 mol% - 0,1 mol%) et des conditions douces (THF, 60 °C). Une étude mécanistique fondée sur des réactions stœchiométriques et des calculs DFT prouve la présence d'intermédiaires Ni(0)/Ni(II) au cours de la catalyse et exclut tout passage par un mécanisme de type Ni(I)/Ni(III).

La seconde partie de ce travail porte sur le couplage oxydant entre l'éthylène et le CO<sub>2</sub> sur des complexes de nickel chélatés par des bis-phosphines ou des bis-NHC. Une étude cinétique de l'équilibre entre [(dcp)Ni(C<sub>2</sub>H<sub>4</sub>)] et [(dcp)nickelalactone] a été réalisée. Le complexe [(dcp)nickelalactone] peut ensuite être réduit et fonctionnalisé en dérivé du propanol en présence de pinacolborane. Des études mécanistiques et catalytiques préliminaires ont été menées. De plus, de nouvelles méthodologies de synthèses ont été développées afin d'obtenir les premiers complexes [(bis-NHC)Ni(C<sub>2</sub>H<sub>4</sub>)] et [(bis-NHC)nickelalactone].







## *Nickel Mediated Negishi and Oxidative Couplings*

The aim of this research project is to promote the formation of new C-C bonds and the production of valuable chemicals by using chelated nickel complexes.

The first part of this thesis is dedicated to [nickel(bis-phosphine)] complexes employed as catalysts for Negishi cross coupling reactions. Designed Ni(0) precatalyst [(dcp)Ni( $\eta^2$ -toluene)] (dcp = 1,3-bis(dicyclohexylphosphino)propane) promotes efficiently the Negishi cross coupling between aryl chlorides and phenylzinc chloride derivatives at low catalyst loadings (down to 0.2 mol% - 1 mol%) under mild conditions (THF, 60°C). Mechanistic investigations relying on stoichiometric reactions and DFT calculations prove the involvement of Ni(0)/Ni(II) intermediates rather than Ni(I)/Ni(III) species during the catalysis.

The second part of this work deals with the oxidative coupling between ethylene and CO<sub>2</sub> at bis-phosphine and bis-NHC chelated nickel complexes for the production of value-added chemicals. The equilibrium between [(dcp)Ni(C<sub>2</sub>H<sub>4</sub>)] and [(dcp)nickelalactone] has been investigated by kinetic studies. The subsequent cleavage of [(dcp)nickelalactone] by pinacolborane leads to its reductive functionalization into a propanol derivative. Preliminary mechanistic and catalytic investigations have been undertaken. Moreover, new methodologies are provided for the synthesis of the first [(bis-NHC)Ni(C<sub>2</sub>H<sub>4</sub>)] and [(bis-NHC)nickelalactone] complexes.

### *Couplages de Negishi et Couplages Oxydants à Base de Complexes de Nickel*

Ce projet de recherche porte sur la formation de nouvelles liaisons C-C et la production de produits chimiques valorisables grâce à l'utilisation de complexes de nickel chélatés.

La première partie de cette thèse est dédiée à des complexes bis-phosphines de nickel employés comme catalyseurs pour le couplage croisé de Negishi. Le précatalyseur [(dcp)Ni( $\eta^2$ -toluene)] (dcp = 1,3-bis(dicyclohexylphosphino)propane) permet de coupler efficacement des chloro-arènes avec des organozinciques en utilisant de faibles charges catalytiques (0,2 mol% - 0,1 mol%) et des conditions douces (THF, 60 °C). Une étude mécanistique fondée sur des réactions stœchiométriques et des calculs DFT prouve la présence d'intermédiaires Ni(0)/Ni(II) au cours de la catalyse et exclut tout passage par un mécanisme de type Ni(I)/Ni(III).

La seconde partie de ce travail porte sur le couplage oxydant entre l'éthylène et le CO<sub>2</sub> sur des complexes de nickel chélatés par des bis-phosphines ou des bis-NHC. Une étude cinétique de l'équilibre entre [(dcp)Ni(C<sub>2</sub>H<sub>4</sub>)] et [(dcp)nickelalactone] a été réalisée. Le complexe [(dcp)nickelalactone] peut ensuite être réduit et fonctionnalisé en dérivé du propanol en présence de pinacolborane. Des études mécanistiques et catalytiques préliminaires ont été menées. De plus, de nouvelles méthodologies de synthèses ont été développées afin d'obtenir les premiers complexes [(bis-NHC)Ni(C<sub>2</sub>H<sub>4</sub>)] et [(bis-NHC)nickelalactone].